

# **ENGINEERING PROPERTIES OF RECYCLED MATERIALS FOR UNBOUND APPLICATIONS**

by

Principal Investigator: Tuncer B. Edil

Co-Investigators: Craig H. Benson and James M. Tinjum

Graduate Assistants: Gregory J. Scheartle, Ozlem Bozyurt, Kongrat Nokkaew, Jiannan Chen and Sabrina Bradshaw

Recycled Materials Resource Center  
University of Wisconsin-Madison  
Madison, WI 53706 USA

This report consists of several task reports prepared at the University of Wisconsin-Madison.

Task Reports include:

1. Literature Search and Report on Recycled Asphalt Pavement and Recycled Concrete Aggregate
2. The Usage, Storage and Testing of Recycled Materials – Results of Survey
3. Relationship Between Resilient Modulus and Composition of RCA or RAP
4. Scaling and Equivalency of Bench-Scale Tests to Field-Scale Conditions
5. Climate Effects (Freeze-Thaw Cycles)
6. Climate Effects (Hydraulic Properties of Recycled Asphalt Pavement and Recycled Concrete Aggregate)
7. Compaction Level and Assessment
8. Field Performance: Falling Weight Deflectometer Data Analysis
9. Materials Control
10. Leaching Characteristics: pH-dependent Leaching of Trace Elements from Recycled Concrete Aggregate

# **Literature Search and Report On Recycled Asphalt Pavement and Recycled Concrete Aggregate**

## **TPF-5 (129) Recycled Unbound Materials**

Mn/DOT Contract No. 89264 Work Order No. 2

CFMS Contract No. B14513

Task 1A: Literature Review

**Gregory J. Schaertl and Tuncer B. Edil  
University of Wisconsin- Madison**

**March 18, 2009**

## Introduction

The production of demolition and construction waste has been increasing at a gradual rate in recent years.<sup>(1)</sup> The amount of landfill available to contain this material has been decreasing, and the need to find appropriate disposal locations has been of increasing concern.<sup>(2)</sup> Recycling programs offer a viable solution. The use of these materials as recycled base course in new roadway construction has become more common in the last twenty years, with some municipalities reporting as much as 400,000 tons of recycled materials used in this manner.<sup>(3, 4)</sup>

Recycled roadway materials are typically generated and reused at the same construction site, providing increased savings in both money and time.<sup>(3)</sup> It has been speculated that in some municipalities recycled materials costs less to use than conventional crushed-stone base material by as much as 30%.<sup>(5)</sup> Despite the increased acceptance of recycled base materials, research concerning the mechanical properties and durability of such materials has been lacking.<sup>(3, 6)</sup>

The most widely used recycled materials are recycled asphalt pavement (RAP) and recycled concrete aggregate (RCA). RAP is produced by removing and reprocessing existing asphalt pavement<sup>(6,7)</sup>, and RCA is the product of the demolition of concrete structures such as buildings, roads and runways.<sup>(2)</sup> The production of RAP and RCA results in an aggregate that is well graded and of high quality.<sup>(7)</sup> The aggregates in RAP are coated with asphalt cement that reduces the water absorption qualities of the material.<sup>(6)</sup> In contrast, the aggregates in RCA are coated with a cementitious paste that increases the water absorption qualities of the material.<sup>(1)</sup>

## Production

There is some ambiguity regarding the nomenclature involved in the production of RAP. Based on the experience of the Geo Engineering Program at the University of Wisconsin-Madison, the following classification is recommended to remove ambiguity in nomenclature: RAP refers to the removal and reuse of the hot mix asphalt (HMA) layer of an existing roadway<sup>(7)</sup>; full depth reclamation (FDR) refers to the removal and reuse of the HMA and the entire base course layer; and recycled pavement material (RPM) refers to the removal and reuse of either the HMA and part of the base course layer or the HMA, the entire base course layer and part of the underlying subgrade implying a

mixture of pavement layer materials.<sup>(6)</sup> Unless specified, these three distinct recycled asphalt materials will be collectively referred to as RAP.

RAP is typically produced through milling operations, which involves the grinding and collection of the existing HMA<sup>(7)</sup>, and FDR and RPM are typically excavated using full-size reclaimers or portable asphalt recycling machines.<sup>(6)</sup> RAP can be stockpiled, but is most frequently reused immediately after processing at the site. Typical aggregate gradations of RAP are achieved through pulverization of the material, which is typically performed with a rubber tired grinder.<sup>(8)</sup>

The production of RCA involves crushing the material to a gradation comparable to that of typical roadway base aggregate. Fresh RCA typically contains a high amount of debris and reinforcing steel, and the RCA must be processed to remove this debris prior to placement. The material is first crushed in a jaw crusher that breaks the steel from the material and provides an initial crushing of the concrete.<sup>(7)</sup> The material is sent down a picking belt where the steel is removed from the material.<sup>(2)</sup> The remaining concrete material is further crushed and screened to a predetermined gradation.<sup>(7)</sup>

## **Material Properties**

The gradation of RAP can be compared to that of a crushed natural aggregate, although with a higher content of fines. The high fine content is the result of degradation of the material during milling and crushing operations. In RPM the inclusion of subgrade materials in the recycled material also contributes to a higher instance of fines. Finer gradations of RAP are produced through milling operations compared to crushing operations.<sup>(7)</sup> Table 1 provides a breakdown of typical physical and mechanical properties of RAP.

RCA is processed exclusively through crushing operations, and is very angular in shape.<sup>(7)</sup> Depending on the crushing methods, the particle size distribution of an RCA can have a wide variability, with a lower particle density and greater angularity than would normally be found in more traditional virgin base course aggregates. Residual mortar and cement paste are typically found on the surface of the RCA, as well as contaminants associated with construction and demolition debris.<sup>(2)</sup> The presence of this mortar contributes to a rougher surface texture, lower specific gravity, and higher water absorption than typical aggregates.<sup>(7)</sup>

The self-cementing capabilities of RCA are an interesting secondary property. The crushed material exposes un-hydrated concrete that can react with water, potentially increasing the materials strength and durability when used as unbound base

Table 1: Typical Physical Properties of RAP <sup>(7)</sup>

Physical Properties	
Unit Weight	1940 - 2300 kg/m <sup>3</sup> (120 - 140 pcf)
Moisture Content	Normal: Up to 5% Maximum: 7 - 8%
Asphalt Content	Normal: 4.5 – 6%
Asphalt Penetration	Normal: 10 – 80% at 25°C (77°F)
Absolute Viscosity or Recovered Asphalt Cement	Normal: 4000 – 25000 poises at 60°C (140°F)
Mechanical Properties	
Compacted Unit Weight	1600 – 2000 kg/m <sup>3</sup> (100 – 125 pcf)
California Bearing Ratio (CBR)	100% RAP: 20 – 25% 40% RAP and 60% Natural Aggregate: 150% or Higher

course for new roadway construction. It follows that service life could also be extended as a result of these properties. Although widely acknowledged, not much actual documentation has been published regarding this secondary hydration.<sup>(5)</sup> Although the cause of self-cementing properties has been studied, the actual effect of such parameters as age, grade, and mix-proportions of the RCA on the overall cementitious effect has yet to be determined.<sup>(1)</sup> This effect is outside the scope of this literature review. Table 2 provides a breakdown of typical physical and mechanical properties of RCA.

## Objective

The purpose of this literature review is to summarize the current state of knowledge regarding the mechanical behavior of RCA, RAP and blends of these recycled materials with traditional aggregate material. Laboratory and field investigations were considered in the scope of this review, and long-term performance issues were

noted. Of particular interest was the effect the recycled material had on resilient modulus values, stress state sensitivity, and overall material degradation.

Table 2: Typical Physical Properties of RCA <sup>(7)</sup>

Physical Properties	
Specific Gravity	2.2 to 2.5 (Coarse Particles) 2.0 to 2.3 (Fine Particles)
Absorption	2 to 6 (Coarse Particles) 4 to 8 (Fine Particles)
Mechanical Properties	
LA Abrasion Loss	20 – 45 (Coarse Particles)
Magnesium Sulfate Soundness Loss	4 or Less (Coarse Particles) Less than 9 (Fine Particles)
California Bearing Ratio (CBR)	94 – 148%

## Methods for Specification

When considering a recycled material for use as an unbound base course, the two most commonly used specifications are the gradation and the moisture-density relationship of the material. The gradation of a material can provide an indication of what the permeability, frost susceptibility, and shear strength of the material might be, and is determined through the use of material screening tests.<sup>(9)</sup> Screening tests are typically conducted through sieve analysis according to ASTM Standards C 117 and C 136, and AASHTO Standards T-27 and T-11. Some highway agencies and DOTs utilize their own screening test methods, such as Florida DOT FM1 T-027. Classification of soils is performed using the Unified Soil and AASHTO methods according to ASTM D 2487 and AASHTO M 145, respectively.

The determination of moisture-density relationships can help define the ideal density conditions that a material can achieve through compaction. Moisture-density relationships are established through compaction tests conducted according to the following standards: AASHTO T 99 Method C, AASHTO T-180 or ASTM D698, ASTM D 1557. Depending on the compaction effort to be used in the field, compaction tests can be performed in standard or modified variations. The information is used to determine

the optimum moisture content (OMC) and the maximum dry density (MDD) of a material. Through testing of specimens prepared based on this data, material properties such as strength, stiffness and moisture susceptibility can be determined.<sup>(6)</sup>

Other aggregate classification methods involve the determination of the specific gravity, absorption and Atterberg limits of the soils. The specific gravity and absorption characteristics of a given recycled aggregate are determined using ASTM D 854, and Atterberg limits of recycled aggregates are assessed using ASTM D 4318, AASHTO T 89 and T 90.<sup>(5, 6)</sup>

## Summary of Material Gradation

Tables 3 thru 5 represent the available estimated gradations of the RAP, RCA and RPM encountered in this literature review:

Table 3: Gradations of RAP \*

Material	% Passing											
	#200	#100	#50	#30	#16	#8	#4	3/8"	1/2"	3/4"	1	1.5
Bejarano Pulverized <sup>(8)</sup>	2	3	7	12	20	31	46	68	---	100	---	---
Guthrie R1 <sup>(6)</sup>	8	11	15	23	35	45	58	82	---	99	---	---
Guthrie R2 <sup>(6)</sup>	1	3	8	12	21	39	59	82	---	97	---	---
Bennert RAP <sup>(3)</sup>	1	2	3	5	10	20	39	68	---	90	---	---
Saeed RAP-LS-MS <sup>(9)</sup>	3	5	9	12	19	27	38	62	75	95	95	100
Saeed RAP-GR-CO <sup>(9)</sup>	1	2	5	12	18	25	39	63	75	92	97	100
Saeed RAP-GV-LA <sup>(9)</sup>	0	2	6	11	17	23	33	61	76	92	98	100
Average Value	2.3	4.0	7.6	12.4	20.0	30.0	44.6	69.4	75.3	95.0	96.7	100
Standard Deviation	2.7	3.3	3.8	5.3	7.5	9.0	10.2	9.0	0.6	3.8	1.5	0.0
Coefficient of Variance	1.2	0.8	0.5	0.4	0.4	0.3	0.2	0.1	0.0	0.0	0.0	0.0

\*Gradations estimated from existing gradation curves in literature. Actual percent passing values are within  $\pm 1\%$



Table 4: Gradations of RPM \*

Material	% Passing																		
	#200	#100	#60	#50	#40	#30	#20	#16	#10	#8	#4	1/4"	3/8"	1/2"	3/4"	7/8"	1"	1.5"	2"
Li RPM-1 <sup>(10)</sup>	16	19	24	---	33	---	50	---	66	---	85	---	---	---	---	---	---	---	---
Li RPM-2 <sup>(10)</sup>	12	15	18	---	24	---	35	---	49	---	66	---	---	---	---	---	---	---	---
Li RPM-3 <sup>(10)</sup>	3	5	7	---	13	---	26	---	41	---	59	---	---	---	---	---	---	---	---
Li RPM-4 <sup>(10)</sup>	9	9	13	---	20	---	33	---	50	---	67	---	---	---	---	---	---	---	---
Li RPM-5 <sup>(10)</sup>	11	12	17	---	25	---	40	---	57	---	76	---	---	---	---	---	---	---	---
Li RPM-6 <sup>(10)</sup>	6	8	10	---	16	---	27	---	41	---	59	---	---	---	---	---	---	---	---
Li RPM-7 <sup>(10)</sup>	5	7	9	---	14	---	25	---	38	---	53	---	---	---	---	---	---	---	---
Li RPM-8 <sup>(10)</sup>	7	9	12	---	20	---	34	---	52	---	70	---	---	---	---	---	---	---	---
Li RPM-9 <sup>(10)</sup>	9	11	14	---	24	---	39	---	52	---	65	---	---	---	---	---	---	---	---
Li RPM-10 <sup>(10)</sup>	10	12	16	---	25	---	41	---	55	---	70	---	---	---	---	---	---	---	---
Carmargo <sup>(11)</sup>	11	13	18	---	22	---	28	---	38	---	54	61	70	78	93	---	100	---	---
Wen & Edil <sup>(12)</sup>	6	6	---	9	---	16	---	26	39	38	60	---	69	77	96	---	99	---	100
Wen et al <sup>(13)</sup>	4	5	---	8	---	14	---	22	31	34	51	---	72	82	---	98	99	100	---
Wen et al <sup>(13)</sup>	3	5	7	---	13	---	22	---	35	---	55	62	74	84	95	97	99	---	100
Average Value	8.0	9.7	13.8	8.5	20.8	15	33.3	43.3	44.8	60.1	63.3	68.0	75.8	86.4	95.8	98.7	99.4	100	100
Standard Deviation	3.8	4.2	5.1	0.7	6.0	1.4	8.2	2.8	9.9	2.8	9.6	0.7	2.2	3.3	1.5	0.7	0.5	0	0
Coefficient of Variance	0.4	0.4	0.4	0.08	0.3	0.1	0.2	0.1	0.2	0.0	0.2	0.0	0.0	0.0	0.0	0.0	0.0	0.0	0.0

\*Gradations estimated from existing gradation curves in literature. Actual percent passing values are within  $\pm 1\%$

Tables 3 thru 5 show that the coefficient of variance of gradation for the RAP, RPM and RCA remains approximately 40% or lower for materials retained on the #8 sieve and larger. This trend continues for the RPM and RCA retained in the remaining finer sieves. However, it can be seen that for RAP aggregates finer than the #8 sieve, the coefficient of variance for the data noticeably increases. This is more than likely due to the large gradation values found in the sample Guthrie R1. <sup>(6)</sup>

Table 5: Gradations of RCA \*

Material	% Passing												
	#200	#100	#50	#30	#16	#10	#8	#4	3/8"	1/2"	3/4"	1	2"
Bennert RCA <sup>(3)</sup>	7	10	15	24	28	---	32	42	56	---	76	---	---
Blankenagel Demolition <sup>(5)</sup>	3	6	9	12	15	---	20	31	60	---	---	---	---
Blankenagel Haul-Back <sup>(5)</sup>	8	10	13	23	37	---	46	60	72	---	---	---	---
Saeed RCP-LS-IL <sup>(9)</sup>	4	8	15	26	36	---	48	60	89	---	99	100	---
Saeed RCP-GV-LA <sup>(9)</sup>	8	11	16	26	32	---	48	64	74	---	89	96	---
Saeed RCP-GR-SC <sup>(9)</sup>	3	5	9	13	19	---	27	38	62	76	95	98	---
Kuo District 1 <sup>(2)</sup>	4	---	12	---	---	30	---	45	52	---	76	99	100
Kuo District 2 <sup>(2)</sup>	5	---	17	---	---	30	---	40	53	---	76	99	100
Kuo District 4 <sup>(2)</sup>	5	---	11	---	---	28	---	40	56	---	81	99	100
Kuo District 5 <sup>(2)</sup>	4	---	18	---	---	45	---	56	80	---	100	100	100
Kuo District 6 <sup>(2)</sup>	5	---	20	---	---	30	---	33	37	---	50	86	99
Kuo District 7 <sup>(2)</sup>	5	---	20	---	---	40	---	50	63	---	82	99	100
Average Value	5.1	8.3	14.6	20.7	27.8	33.8	36.8	46.6	62.8	76.0	82.4	97.3	99.8
Standard Deviation	1.7	2.4	3.8	6.4	9.1	6.9	12.1	11.2	14.1	---	14.8	4.4	0.4
Coefficient of Variance	0.3	0.3	0.3	0.3	0.3	0.2	0.3	0.2	0.2	---	0.2	0.0	0.0

\*Gradations estimated from existing gradation curves in literature. Actual percent passing values are within  $\pm 1\%$ .

If the data for this sample is removed, the resulting variances fall within the same variance. The sample Guthrie R1 was a composite taken at different locations with different equipment, and therefore the actual source for the erratic gradation of the material could not be determined. <sup>(6)</sup> Gradation requirements for recycled materials vary from agency to agency. Unless indicated, the recycled materials referenced in this report passed the gradation requirements specified by the respective agencies.

Blankenagel et al <sup>(5)</sup> performed gradations on material taken from demolition sources as well as from relatively new materials sampled from batch-plant overruns and haul-back material sources. Batch plant overruns refer to excess concrete produced at a batch plant but never delivered to a job site, and haul-back material refers to excess concrete delivered to a job site but returned to the batch plant. The haul-back material was found to have more medium and fine materials than the demolition material. Although Blankenagel recognizes the source of the gradation differences could be due to crushing operations, the most likely reason is probably related to the mechanical breakdown tendencies of the materials. The haul-back material would have a higher porosity and lower strength due to being more properly consolidated and cured, resulting in a greater degree of pulverization regardless of crushing techniques.

In the study conducted by Kuo<sup>(2)</sup>, gradations of the RCA met Florida DOT specifications. However, for specifications regarding average gradation for each sieve, the standard deviations of the 3/4", 3/8", #4 and #10 sieves were all excessively high and each fell out of specification. The test would indicate that for recycled materials, these sieves might be considered more critical than the others.

## **Summary of Moisture-Density Characteristics**

Table 6 and 7 represent the available moisture-density relationships for the RAP, RPM and RCA encountered in this literature review. For various blends of RAP with pure aggregate, some trends were noted regarding the effect of RAP content on the MDD and OMC of a material. Guthrie et al found that an increase in RAP content led to a decrease in MDD and OMC values.<sup>(6)</sup> The aggregates particles in the RAP were partially encased in asphalt, which decreased the specific gravity. It was further assumed that the partial asphalt coating reduced the aggregate water absorption potential and inter-particle friction, leading to a reduction in the required water to achieve MDD.

Table 6: Maximum Dry Density and Optimum Moisture Content of RAP and RPM

Material	Proctor Effort	Maximum Dry Density, kg/m <sup>3</sup>	Optimum Moisture Content, %
Bejarano: Pulverized <sup>(8)</sup>	Caltrans CTM 216	2332	5.5
Bennert RAP <sup>(3)</sup>	Standard	1872	5
Guthrie R1 <sup>(6)</sup>	Modified	2083	5.6
Guthrie R2 <sup>(6)</sup>	Modified	1842	5.8
Saeed RAP-LS-MS <sup>(9)</sup>	Standard	1988	6.3
Saeed RAP-GR-CO <sup>(9)</sup>	Standard	2015	10.3
Saeed RAP-GV-LA <sup>(9)</sup>	Standard	1978	5.4
Carmargo RPM <sup>(11)</sup>	Standard	2161	7.5
Wen et al <sup>(13)</sup>	Modified	2162	6.5

Table 7: Dry Density and Optimum Moisture Content of RCA

Material	Proctor Effort	Maximum Dry Density, kg/m <sup>3</sup>	Optimum Moisture Content, %
Bennert RCA <sup>(3)</sup>	Standard	1984	7.5
Blankenagel Demolition <sup>(5)</sup>	Modified	1830	9.7
Blankenagel Haul Back <sup>(5)</sup>	Modified	2020	10.6
Saeed RCP-LS-IL <sup>(9)</sup>	Standard	1971	11
Saeed RCP-GV-LA <sup>(9)</sup>	Standard	1950	9
Saeed RCP-GR-SC <sup>(9)</sup>	Standard	1990	9.5
Kuo UCF <sup>(2)</sup>	Modified	1823	11.2
Kuo FDOT <sup>(2)</sup>	Modified	1839	12.1

For various blends of RAP with pure aggregate, some trends were noted regarding the effect of RAP content on the MDD and OMC of a material. Guthrie et al found that an increase in RAP content led to a decrease in MDD and OMC values.<sup>(6)</sup> The aggregates particles in the RAP were partially encased in asphalt, which decreased the

specific gravity. It was further assumed that the partial asphalt coating reduced the aggregate water absorption potential and inter-particle friction, leading to a reduction in the required water to achieve MDD.

An interesting variation in the study by Kim et al<sup>(14)</sup> was the use of a gyratory compaction test (GCT) instead of a proctor compaction test (PCT) to prepare RAP specimens. Comparisons with field density measurements indicated that MDD and OMC calculations determined from GCT methods were a better correlation than those determined by PCT testing. When compared to PCT results, GCT results showed a large change in MDD values and a small change in OMC values. Kim noted the effect of RAP content on the MDD and OMC of aggregate/RAP blends. As the RAP content of the material increased, the OMC of the material decreased for both the GCT and PCT prepared specimens. As with the study by Guthrie, the increase in asphalt content most likely reduced the absorption of the material, leading to the decrease in OMC. As the RAP content of the material increased, the MDD decreased for the PCT-prepared specimens and remained the same for GCT-prepared specimens.

Bennert et al<sup>(3)</sup> investigated the effect of recycled content on the MDD and OMC of samples containing both RAP and RCA. The study found that as the RAP and RCA content of a material increased, the MDD of the material decreased. As was found in the Guthrie<sup>(6)</sup> and Kim<sup>(14)</sup> studies, the OMC of the material decreased with increasing RAP content. However, as the RCA content of the material increased, the OMC also increased.

In the study conducted by Saeed et al<sup>(9)</sup>, it was found that in general virgin aggregates had a higher MDD than pure (100%) RAP and RCA samples. In agreement with the study by Kim<sup>(14)</sup>, the MDD of the material decreased as the RAP and RCA content of recycled material/aggregate mixtures increased.

Blankenagel et al<sup>(5)</sup> noted the effect of material source on the MDD and OMC of RCA. The demolition material used in his study had an OMC of 9.7% and a MDD of 1830 kg/m<sup>3</sup>, whereas the haul-back material had an OMC of 10.6% and a MDD of 2,020 kg/m<sup>3</sup>. The haul-back material had a higher fines content, which resulted in higher MDD and OMC values than those found in the demolition material. Pore spaces are more readily filled by the increased fines, resulting in a tighter aggregate matrix.

Investigations<sup>(11,13)</sup> on two RPM at the University of Wisconsin-Madison indicated an OMC of 6.5 to 7.5% and a MDD of 2162 kg/m<sup>3</sup>.

## Methods for Design and Performance Tests

The two most common tests used to determine strength parameters for unbound recycled materials are the Static Triaxial Test and the California Bearing Ratio test. The Static Triaxial Test is typically performed in accordance with ASTM D 2850 and AASHTO T 296, although some state DOTs have been known to use their own standards such as CalTRAN<sup>(8)</sup>. The California Bearing Ratio test is typically performed in accordance with ASTM D 1883 or AASHTO T 193. Kuo<sup>(2)</sup> uses the Limerock Bearing Ratio test which is indigenous to the Florida DOT, and is documented as standard FM5-515. T

The two most common tests used to determine the stiffness for unbound recycled materials are the resilient modulus test and the free-free resonant column test. The resilient modulus test is typically performed in accordance with AASHTO TP46-94, Strategic Highway Research Program Test Protocol P-46 (SHRP P-46), or National Cooperative Highway Research Program Protocol 1-28A (NCHRP 1-28A). The free-free resonant column test is typically performed according to ASTM D 4015. Permanent deflection is typically performed by use of a cyclic triaxial test. Moisture susceptibility is typically determined by use of the Tube Suction Test. There is no current standard for the use of the test; however Guthrie and Blankenagel use methods as outlined by Scullion and Saarenketo in 1997.<sup>(5, 6, 16)</sup>

Two typical tests used to assess the durability of a material are the LA abrasion test and the freeze-thaw cycling test. The LA abrasion test is typically performed in accordance with ASTM C 131, although other methods are sometimes used by different agencies, such as Australian test method AS 1141.23. The freeze-thaw cycling test is typically performed in accordance with ASTM D 560.

A method that follows ASTM D 6035 for specimen conditioning is used at the University of Wisconsin-Madison<sup>(11,13)</sup> for frost susceptibility. ASTM D 6035 describes a method to determine the freeze-thaw effects on hydraulic conductivity; in the UW procedure, resilient modulus tests are performed to determine the freeze-thaw effects instead of hydraulic conductivity. Test specimens are compacted in molds at the specified moisture content and density. Preliminary testing on specimens instrumented with a thermocouple showed that complete freezing occurred within 1 d at -19°C. Thus, all specimens are retained in their mold and wrapped with plastic sheet in the freezer for at least 1 d. After freezing, the height and weight are measured and the specimen is

allowed to thaw at room temperature. This process is repeated as many freeze-thaw cycles as desired but typically 5 cycles is used. After the last cycle, specimens are extruded frozen and thawed inside the resilient modulus cell prior to resilient modulus testing.

## **Summary of Strength and Stiffness Tests**

Bejarano et al<sup>(8)</sup> conducted static triaxial tests on one RAP and two different aggregate materials. Individual RAP and aggregate specimens were compacted at OMC and 95% and 100% of maximum wet density (MWD) according to CalTRANS specification CTM 216. Static triaxial tests were conducted at confining pressures of 0, 35, 70 and 105 kPa. After comparing the shear strengths of the RAP and aggregate, it was determined that the shear strength calculated for the RAP was comparable in magnitude to shear strengths calculated for the representative aggregate materials. This shear strength correlation was valid at both 95% and 100% MWD and each of the four confining pressures. Bejarano<sup>(8)</sup> also conducted stiffness tests for the three material according to SHRP test protocol P-46. Of the three tested materials, the RAP had a higher resilient modulus than the two aggregate materials tested at 95% and 100% MWD. When the compaction level was increased from 95% to 100%, the resilient modulus of the RAP and one of the aggregate materials increased. This change in compaction level had no affect on the resilient modulus of the second aggregate material. Lime stabilized RAP specimens cured for 7 days had a higher resilient modulus than the non-stabilized material in all cases.

Bennert et al<sup>(3)</sup> conducted a similar test in which the shear strength of pure (100%) RAP and RCA were evaluated against the shear strength of a dense graded aggregate base course (DGABC) typical of the area the recycled materials would be used. Static triaxial test results for the pure samples indicate that the aggregate alone had higher shear strength than either RAP or RCA alone. Stiffness tests were also conducted on blends of the materials used in the study. Specimens were prepared combining the aggregate with RAP and RCA percentages of 100%, 75%, 50%, 25% and 0% (100% aggregate). Contraray to the strength behavior, it was found that as the amount of recycled material in the blend increased, the resilient modulus of the blended material also increased. Pure (100%) specimens of RAP and RCA had higher resilient modulus values than pure specimens of the virgin aggregate.

Guthrie et al<sup>(6)</sup> evaluated the effects of RAP content on the shear strength of base course materials using the California Bearing Ratio test. Two RAP and two aggregate materials (one recycled and one virgin) were acquired for the test. Specimens were prepared at RAP percentages of 100%, 75%, 50%, 25% and 0% (100% aggregate) for each of the permutations of RAP and aggregate samples. The tests found that the shear strength decreased with an increase in RAP content supporting Bennert et al.'s results..

Blankenagel et al<sup>(5)</sup> conducted a study documenting the difference between RCA samples obtained from demolition projects with relatively new RCA samples obtained through batch-plant overruns and haul-backs. The strength of the material was determined immediately after compaction using the California Bearing Ratio test. The demolition RCA and the haul-back RCA had CBR test results of 22% and 55% respectively. Unconfined compressive strength tests conducted on the material were used to determine strength gain over time due to the residual hydration in the RCA. The strength of the demolition material increased 130% and 180% at 3 and 7 days after compaction, respectively. The strength of the haul back material increased 150% to 190% at 3 and 7 days after compaction, respectively. Higher strength gain in the haul back material is most likely due to a greater amount of unreacted cement in the material as well as a finer material gradation. The average 7-day strengths for the demolition and haul-back material were 1260 kPa and 1820 kPa, respectively.

Kuo et al<sup>(2)</sup> incorporated the use of the Limerock Bearing Ratio (LBR) in Florida to determine the strength of RCA to be used as potential base course. The overall LBR values for the materials tested were 181.71%, which is higher than the required minimum value of 100%.

Kim et al<sup>(14)</sup> studied the effect of RAP content on the resilient modulus of blended aggregate base course. An in-situ blend of FDR was taken during the reconstruction of an existing road along with pure samples of RAP and aggregate materials. The FDR and several blends of the pure RAP and aggregate base material were tested for material stiffness using the resilient modulus test in accordance with NCHRP 1-28A protocol. Blended mixtures of the pure materials were prepared at RAP to aggregate ratios (%/%) of 0/100, 25/75, 50/50 and 75/25. The study found that for an increase in RAP content, the resilient modulus of the blended material increased.<sup>(10)</sup> The effects of increased RAP content were more defined when the blends were exposed to higher confining pressures, however specimens also experienced higher permanent deformation at



higher confining pressures. Specimens tested at 65% optimum moisture content had higher resilient modulus values when compared to specimens prepared at 100% OMC. This trend was consistent for all confining pressures. At low confining pressures (~20kPa), specimens with RAP to aggregate ratios of 50% to 50% and specimens consisting of 100% aggregate had resilient modulus values that were approximately equivalent. As the confining pressures increased, the 50/50 and pure RAP blends became stiffer. The 50/50, 100% RAP and in-situ material tested at the corresponding site had similar resilient modulus values.

Nataatmadja et al<sup>(4)</sup> evaluated the resilient modulus of four RCAs. One commercial and three laboratory-produced RCAs were used in the study. The commercial RCA had an estimated compressive strength of 15 MPa, and the three laboratory manufactured RCAs had compressive strengths of 18.5, 49, and 75 MPa. The materials were tested individually and were not blended with any other material, although each material was prepared and mixed as to produce a particle size distribution comparable to typical road aggregate blends. The study found that the resilient modulus of each of the RCAs tested was comparable or better (higher) than the typical aggregates used for roadway base course; the resilient modulus seemed to increase with an increase in the compressive strength of the material. An increase in elongated particles also led to a decrease in resilient modulus, as these particles were more prone to degradation after extensive loading. Nataatmadja suggests that RCA with very high compressive strengths are more prone to break into elongated particles during crushing, resulting in a lower resilient modulus than would otherwise be expected. One exception in the test is that the specimen with a high flakiness index produced a lower strength value than would be expected.

Guthrie et al<sup>(6)</sup> used the free-free resonant column test to determine the stiffness of RAP and aggregate blends. At OMC, the stiffness of the material decreased with the addition of 25% RAP, and then increased with the addition of 50%, 75%, and 100% RAP. When the material was dried for 72 hours, the trend reversed: the stiffness of the material increased with the addition of 25% RAP and then decreased with the addition of 50%, 75% and 100% RAP. This decrease in stiffness can be attributed to the softening of the asphalt in the RAP during the drying process. Each specimen was then soaked for 24 hours prior to being tested for stiffness a third time. As with the oven-dried specimens, the soaked specimens displayed an increase in stiffness with the addition of 25% RAP followed by a decrease with increased RAP content. However, the soaked

materials displayed a 40% to 90% decrease in stiffness when compared to the oven-dried materials.

Blankenagel et al<sup>(5)</sup> also used the resonant column test on RCA samples procured from demolition and haul-back sources. During the first 12 hours in 100% relative humidity, the modulus increased 390% for the demolition material and 940% for the haul-back material. Again, a greater amount of unreacted cement in the haul-back material accounts for the larger stiffness. Average 7-days stiffness measurements for the demolition and haul-back materials were 100 MPa and 150 MPa, respectively.

The tests performed at the University of Wisconsin-Madison<sup>(11,13, 15)</sup> on two RPMs indicated results in general support of the investigations summarized above. The unsoaked CBR values of RPM varied from 9 to 38 and, as an indicator of strength, were lower than the CBR of aggregates with similar gradation. However, higher resilient moduli<sup>(11)</sup> (257-309 MPa) were measured consistently for RPM compared to different crushed aggregates qualified as base course material.

Addition of fly ash increased the modulus of RPM (at least a factor of 6, which is less than for a similarly stabilized natural aggregate), and the modulus increased as the fly ash content was increased<sup>(11)</sup>. Modulus also increased with curing time, with the rate of increase being largest between 7 and 28 d of curing. The moduli of RPM stabilized with fly ash were independent of bulk stress and could be described by a constant modulus.

## **Summary of Moisture Susceptibility Tests**

In the tube suction test, a specimen is oven dried for 72 hours before being allowed to soak in a shallow water bath for 10 days. Over the course of the soaking period, unbound water within the material rises through the aggregate matrix and collects at the surface. The dielectric value at the surface of the material increases with an increase in the amount of unbound water permeating the specimen, and thereby provides an estimate of the materials susceptibility to moisture permeation.

Guthrie et al<sup>(6)</sup> used the tube suction test to determine the effect of RAP content on the moisture susceptibility of RAP/aggregate blends. It was found that the moisture susceptibility of the material increased as RAP was added to the mixture. However, tests were only conducted with the addition of 25% and 50% RAP. Materials with RAP

contents above 75% were classified as non-moisture-susceptible and were not tested. Overall, the dry density of the blended material decreased as RAP content increased.

Blankenagel et al<sup>(5)</sup> used the tube suction test on demolition and haul-back RCA to help determine the moisture susceptibility characteristics of the material. The moisture susceptibility of the demolition material was classified as “good”, with a dialectic value of 6.4 and a gravimetric water content of 10.6%. The moisture susceptibility of the haul back material was classified as “marginal”, with a dialectic value of 15.0 and a gravimetric water content of 2.0%.

## Summary of Durability Tests

Blankenagel et al<sup>(5)</sup> incorporated the LA Abrasion and freeze-thaw cycling test into his study comparing demolition and haul-back materials. Results of the LA Abrasion tests indicated that the demolition and haul-back materials experienced average material losses of 31% and 18%, respectively. The primary cause of the degradation was thought to be the stripping of cement paste from the aggregate. This degradation caused an increase in fines that affected each of the two RCAs differently. The demolition material was initially low in fines content, and an increase in degradation fines would lead to an increase in MDD. The haul-back material was initially high in fines content, and the addition of degradation fines would decrease the structural stability and increase the moisture susceptibility of the material.

Nataatmadja et al<sup>(4)</sup> attempted to use the LA abrasion test to determine the relative hardness of the four RCAs. Commercial RCA had a lower hardness than laboratory manufactured RCAs, even though commercial RCA had the lowest (estimated) compressive strength. The relative hardness between the laboratory manufactured RCAs could not be differentiated by the LA Abrasion Test method, most likely due to test severity.

Blankenagel et al<sup>(5)</sup> used freeze-thaw cycling to measure the durability of the demolition and haul-back RCMs. Freeze thaw testing was performed after 7 days of curing. Specimens were submerged for 4 hours, frozen (-29 deg C) for 24 hours and thawed (+20 deg C) for 24 hours. Stiffness was measured after each freezing period and after each thawing period. The demolition RCM experienced a 30% stiffness loss within the first two cycles and thereafter stabilized at a stiffness of 70 MPa. The haul-back RCM experience a 90% stiffness loss over the first 9 cycles and thereafter stabilized at a stiffness of 30 MPa. Unconfined compressive strength tests for the materials after

freeze-thaw testing indicated strength losses of 52% and 28% for the demolition and haul-back material, respectively.

Freeze-thaw cycling tests performed at the University of Wisconsin-Madison showed that there was a small effect on resilient modulus (less than 15%) for RPM and also for natural aggregate with or without fly ash, with no consistent effect for materials stabilized with fly ash.

## Summary of Permanent Deflection Tests

Bennert et al<sup>(3)</sup> studied the effect of recycled material content on the permanent deflection experienced by base course materials. Specimens were created from blends of aggregate with either RAP or RCA. For cyclic loads of 100,000 cycles, specimens blended with RCA were found to have the lowest amount of permanent deformation, and specimens blended with RAP had the highest amount of permanent deformation.

RPMs tested at the University of Wisconsin-Madison<sup>(11)</sup> exhibited smaller plastic strains during resilient modulus testing than base course aggregate, i.e., the opposite of the resilient modulus trend. However, other data show that plastic strains for RPM may be higher or lower than those of conventional base aggregates, depending on the type of aggregate used. Plastic strains for RPM stabilized with fly ash were smaller than the plastic strains of the RPM alone.

## Conclusions

Several important findings were noted in the course of this literature review. Kim et al<sup>(14)</sup> compared the compaction properties of specimens prepared by typical proctor methods with specimens prepared with a gyratory compactor and found that the OMC and MDD of the specimens compacted via gyratory compactor were found to more closely correlate with field density measurements. Kim also found that at low confining pressures, pure aggregate and 50%/50% blends of RAP and aggregate had an equivalent stiffness, but at high confining pressures the 50%/50% blends had a higher stiffness than the pure aggregate. Bennert et al<sup>(3)</sup> found that pure specimens of RAP and

RCA had higher resilient moduli than pure virgin aggregate specimens. Bennert also found that specimens of pure aggregate had higher shear strength than pure RAP or RCA specimens. This trend is supported in a study by Guthrie et al<sup>(6)</sup> in which RAP/aggregate blends showed a decrease in shear strength as RAP content increased. In general, RPM seems to show a better response than natural aggregate for similar gradation and compaction in tests that induce relatively smaller strains such as resilient modulus tests than tests that induce large strains such as triaxial compression or CBR tests.

## References

1. Poon, C. S., Qiao, X. C. and Chan, D. X. (2006). "The Cause and Influence of Self-Cementing Properties of Fine Recycled Concrete Aggregates on the Properties of Unbound Sub-Base", *Waste Management*, Vol. 26, No. 10, pp. 1166-1172
2. Kuo S. S., Mahgoub, H. S. and Nazef, A. (2002). "Investigation of Recycled Concrete Made with Limestone Aggregate for a Base Course in Flexible Pavement", *Geomaterials*, No. 1787, pp. 99-108
3. Bennert, T., Papp Jr, W. J., Maher, A. and Gucunski, N. (2000). "Utilization of Construction and Demolition Debris Under Traffic-Type Loading in Base and Subbase Applications", *Transportation Research Record*, No. 1714, pp. 33-39
4. Nataatmadja, A. and Tan, Y. L. (2001) "Resilient Response of Concrete Road Aggregates", *Journal of Transportation Engineering*, Vol. 127, No. 5, pp 450-453
5. Blankenagel, B. J. and Guthrie, W. S. (2006). "Laboratory Characterization of Recycled Concrete for Use as Pavement Base Material", *Geomaterials*, No. 1952, pp. 21-27
6. Guthrie, W. S., Cooley, D. and Eggett, D. L. (2007). "Effects of Reclaimed Asphalt Pavement on Mechanical Properties of Base Materials", *Transportation Research Record*, No. 2006, pp. 44-52

7. "User Guidelines for Byproducts and Secondary Use Materials in Pavement Construction." FHWA Report FHWA-RD-97-148, Federal Highway Administration, McLean, Virginia (2008).
8. Bejarano, M.O., Harvey, J. T., Lane, L. (2003). "In-Situ Recycling of Asphalt Concrete as Base Material in California", *Proceedings of the 82<sup>nd</sup> Annual Meeting*, Transportation Research Board, Washington D.C .CD-Rom, 22 pp.
9. Saeed, A. (2008). "Performance-Related Tests of Recycled Aggregates for Use in Unbound Pavement Layers", *NCHRP Report 598*, Transportation Research Board, Washington, D.C., 53 pp.
10. Li, L., Benson, C. H., Edil, T. B., Hatipoglu, B., and Tastan, O. (2007). "Evaluation of Recycled Asphalt Pavement Material Stabilized with Fly Ash", *ASCE Geotechnical Special Publication*, CD-Rom, 10 pp.
11. Carmargo, F., Wen, H., Edil, T. B., and Son, Y. H. (2009). "Laboratory Evaluation of Sustainable Materials at MnRoad", *Proceedings of the 88<sup>th</sup> Annual Meeting*, Paper No. 09-3160, National Research Council, Washington D.C., CD-ROM.
12. Wen, H., and Edil, T. B. (2009). "Sustainable Reconstruction of Highways with In-Situ Reclamation of Materials Stabilized for Heavier Loads", *BCR2A Conference*, Champaign, Illinois
13. Wen, H., Baugh, J., and Edil, T.B. (2007). "Use of Cementitious High Carbon Fly Ash to Stabilize Recycled Pavement Materials as a Pavement Base Material", *Proceedings of the 86<sup>th</sup> Annual Meeting*, Paper No. 07-2051, National Research Council, Washington D.C., CD-ROM.
14. Kim, W., Labuz, J. F. and Dai, S. (2007). "Resilient Modulus of Base Course Containing Recycled Asphalt Pavement", *Transportation Research Record*, No. 2006, pp. 27-35
15. Wen, H., Warner, J., and Edil, T. B., (2008). "Laboratory Comparison of Crushed Aggregate and Recycled Pavement Material with and without High Carbon Fly

Ash”, *Proceedings of the 87<sup>th</sup> Annual Meeting*, Paper No. 08-3075, National Research Council, Washington D.C., CD-ROM

16. Scullion, T. and Saareneko, T. (1997). “Using Suction and Dielectric Measurements as Performance Indicators for Aggregate Base Materials”, *Transportation Research Record*, No. 1577, pp. 37-44

# **The Usage, Storage and Testing of Recycled Materials - Results of Survey**

## **TPF-5 (129) Recycled Unbound Materials**

Mn/DOT Contract No. 89264 Work Order No. 2

CFMS Contract No. B14513

Addendum to Task 1A: Literature Review

**Gregory J. Schaertl and Tuncer B. Edil**

**University of Wisconsin- Madison**

**March 28, 2009**



## **1. Introduction**

The use of recycled material as base course in roadway construction has steadily increased for the past twenty years. Over time the methods associated with these practices continue to evolve, and therefore the data regarding the usage of recycled materials can quickly become outdated.<sup>(1)</sup> The University of Wisconsin-Madison has conducted a survey to better define the current state of practices involving the use, storage, and testing of materials used as granular base course in roadway applications. The survey focused on three materials: recycled asphalt pavement (RAP), recycled pavement material (RPM), and recycled concrete aggregate (RCA).

### **1.1. Recycled Asphalt Pavement (RAP)**

The production of RAP material involves the removal and reprocessing of existing asphalt pavement from roadway structures. The top portion of the existing roadway is removed and either crushed on or off-site before being reused as a base course for the new roadway. The process of crushing and milling RAP material typically results in a high content of finer particles present within the recycled material. The aggregates in RAP materials typically display low water absorption properties due to a coating of asphalt cement preventing the water from reaching the individual particles of the material.<sup>(2,3)</sup>

### **1.2. Recycled Pavement Material (RPM)**

The production of RPM material is similar to the production of RAP material, except that RPM production involves the pulverization and blending of the part or entire existing roadway rather than only the top HMA portion. The RPM production process may reclaim the existing roadway HMA, base, and part of the existing subgrade to a typical depth of approximately 300 mm. This process of excavating the entire roadway profile is commonly referred to as Full Depth Reclamation (FDR). RPM material typically has a lower strength and stiffness than RAP material due to the larger amount of fines contributed by the subgrade material.<sup>(4)</sup>

### **1.3. Recycled Concrete Aggregate (RCA)**

Similar to the production of RAP and RPM materials, the production of RCA involves the removal and reprocessing of existing material. However, whereas the production of RAP involves the recycling of pavement almost exclusively, the production of RCA is expanded to include materials reclaimed from roadways as well as other demolition sources such as old buildings, airport runways, and the like. The RCA is initially crushed to break up the material and to allow any debris and steel reinforcement to be removed. Once the material is free from debris, the material is crushed again to a gradation typical of roadway base aggregate before being used in that capacity. Unlike the asphalt coating that retards water absorption in RAP material, the cementitious paste that coats the aggregate in RCA increases the water absorption of the material through hydration. In

addition, the hydration of residual cementitious paste present in the recycled material contributes to an increase in strength of the material.<sup>(3,5,6)</sup>

## 2. Survey Method

The University of Wisconsin-Madison conducted a survey to determine the extent of the use of recycled materials as a granular base course in roadway applications. The survey was conducted in the month of November, 2008, and was extended to individuals with a working connection to state and federal transportation agencies involved in roadway planning and construction. Those asked to take the survey were presented with thirteen (13) questions regarding the application, storage, and testing of recycled materials used as roadway base course.

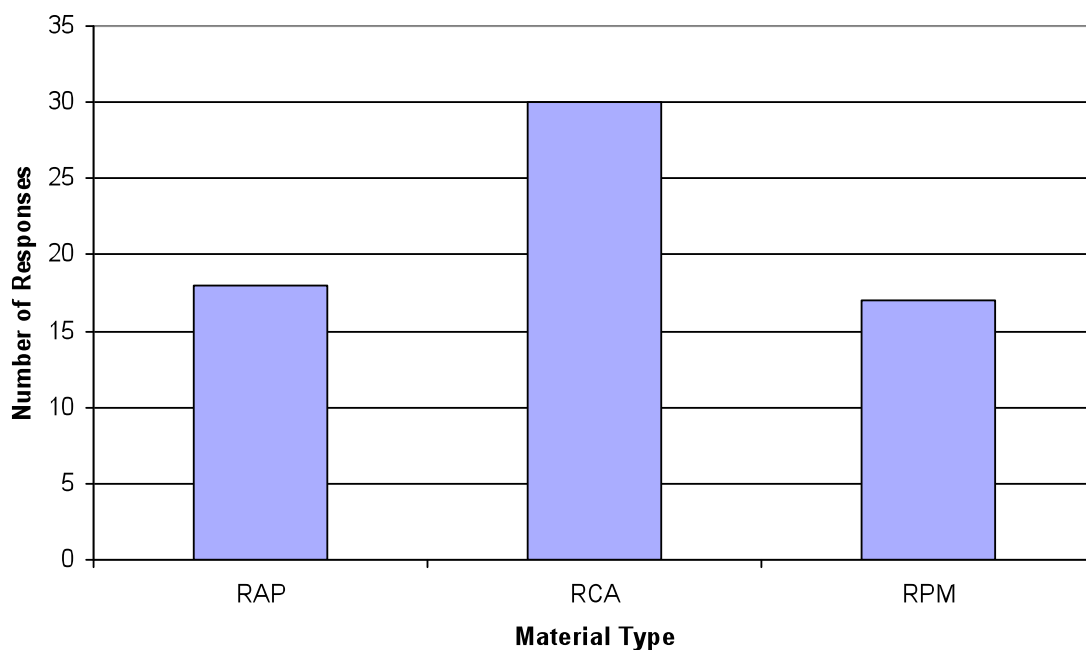
## 3. Survey Results and Discussion

### 3.1. Material Usage

#### Question 1

The first question asked in the survey was “Which of the following recycled materials do you use as a granular base course?” Each of the respondents had the opportunity to select one or more of the following options: Recycled Asphalt Pavement (RAP), Recycled Concrete Aggregate (RCA), and Recycled Pavement Material (RPM). There were 34 unique respondents to this question in the survey. The total responses to each option are represented in Figure 1.

**Figure 1: Recycled Materials Used as Granular Base Course**



Based on the survey information, the most commonly used recycled material type was RCA with 30 responses. RAP and RPM were the second and third most commonly used recycled material types with 18 and 17 responses, respectively. However, the combined RAP and RPM is 35% and slightly more than RCA.

#### Question #2

The second question presented in the survey was “When are the recycled materials used?” Each of the respondents had the opportunity to select one of the following options for each of the recycled material types: “Stockpiled and Used Later”, “Used in Place Immediately” or “Both”. There were 36 unique respondents to this question on the survey. The total distribution of responses to each option is represented in Figures 2 thru 4.

**Figure 2: Placement Transition Time: RAP (Recycled Asphalt Pavement)**

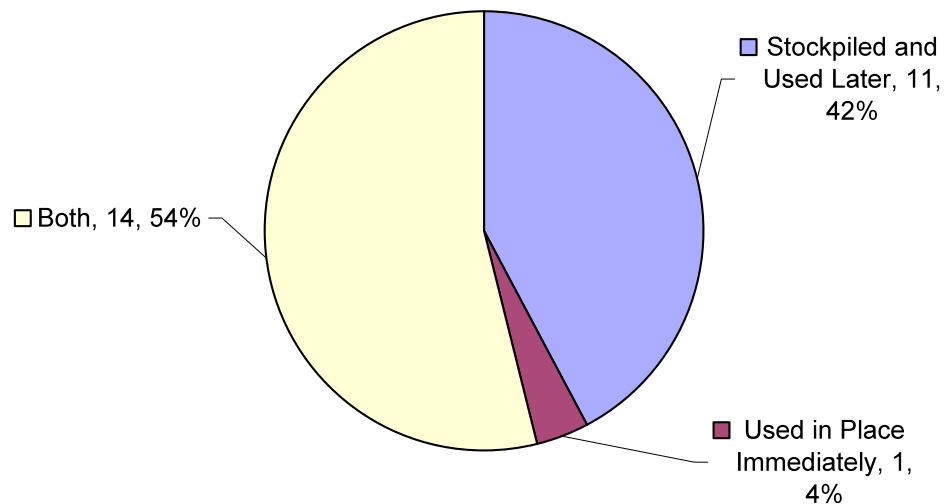


**Figure 3: Placement Transition Time: RCA (Recycled Concrete Aggregate)**

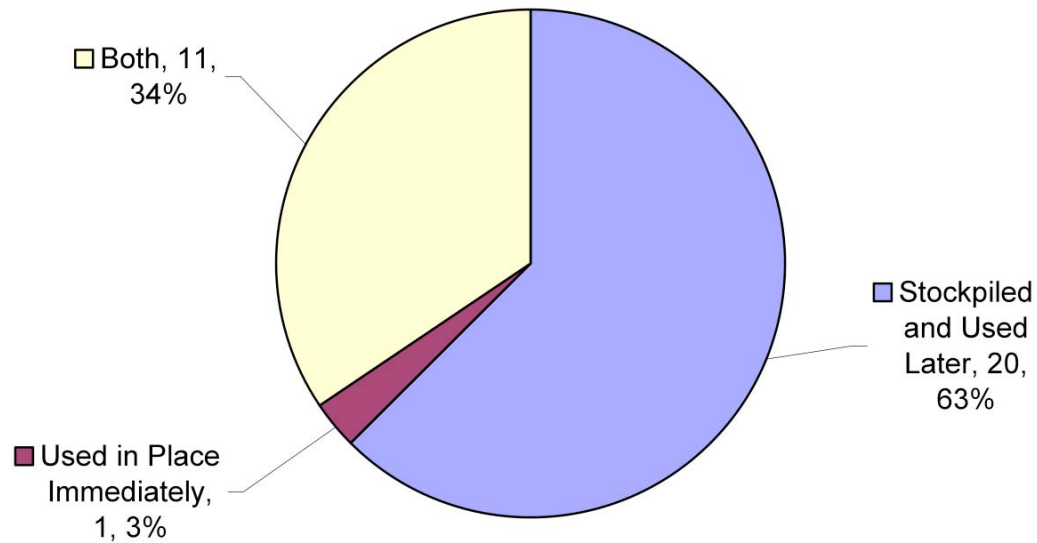
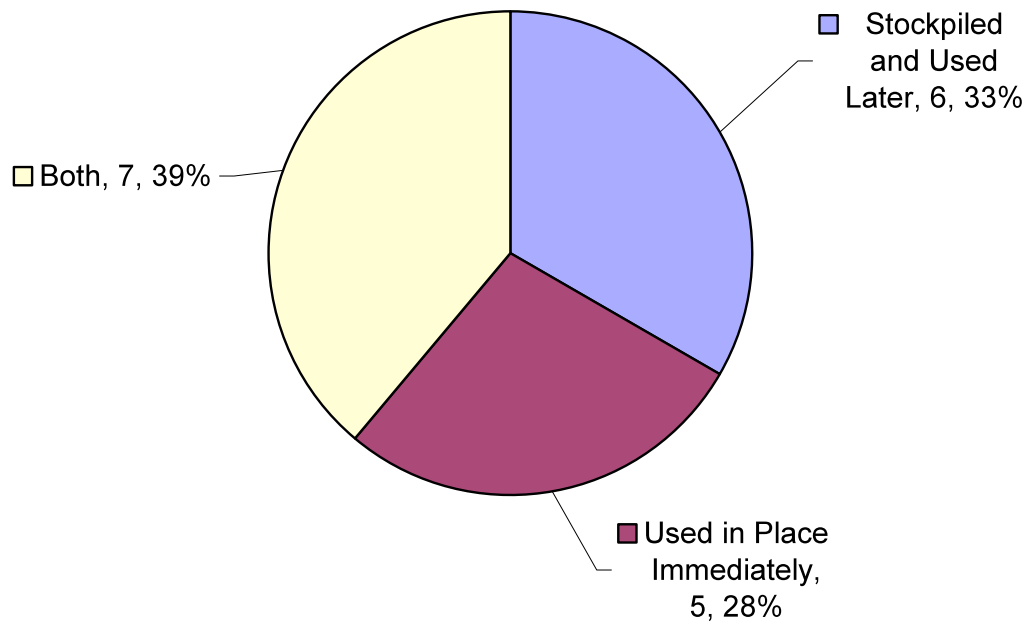


**Figure 4: Placement Transition Time: RPM (Recycled Pavement Material)**



Of the three materials considered in this report, RCA is most likely to be exclusively stockpiled for later use, followed by RAP and RPM. RAP is the most common material in situations where stockpiling and in-place use are both utilized, followed by RCA and RPM. With very little exception, RPM is the only material which is exclusively used-in-

place immediately after reclamation. This is most likely a reflection of construction practices associated with FDR techniques and the common use of RPM as aggregate in bituminous mixtures. The data would suggest that the practice of stockpiling materials is far more common than the practice of using the material in place immediately after reclamation.

### Question 3

The third question presented in the survey was “In a given year, how much of the recycled material do you use?” Each of the respondents had the opportunity to select one of the following options for each of the recycled material types: “Less than 1,000 Tons”, “1,000 to 5,000 Tons”, “5,000 to 10,000 Tons”, “10,000 to 25,000 Tons”, “25,000 to 50,000 Tons”, “50,000 to 75,000 Tons”, and “More than 75,000 Tons”. There were 33 unique respondents to this question on the survey. The distribution of responses to each option is represented in Figures 5 thru 7.

**Figure 5: Annual Quantity Used: RAP (Recycled Asphalt Pavement)**

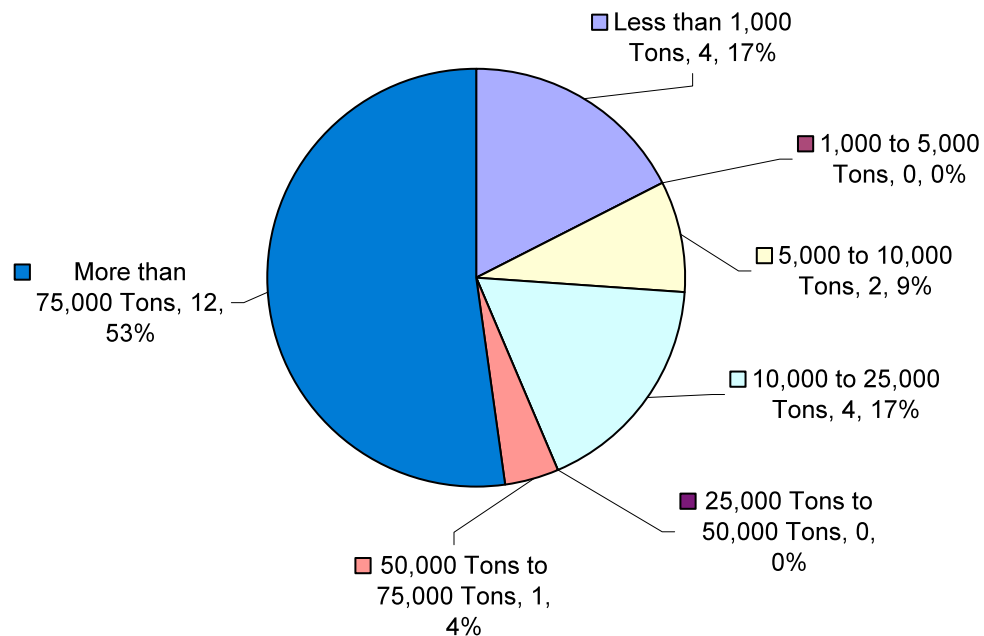


**Figure 6: Annual Quantity Used: RCA (Recycled Concrete Aggregate)**

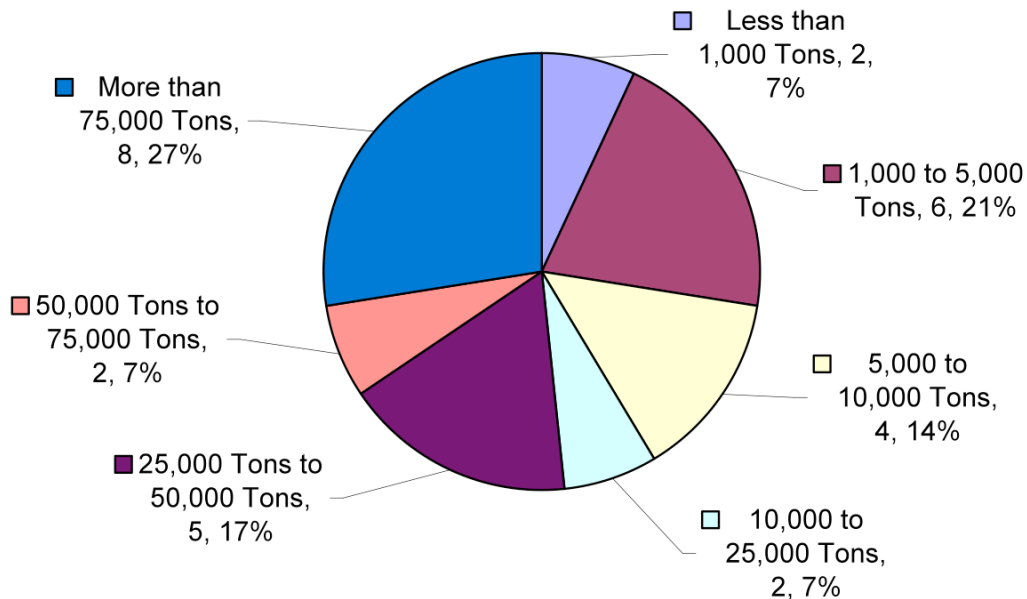
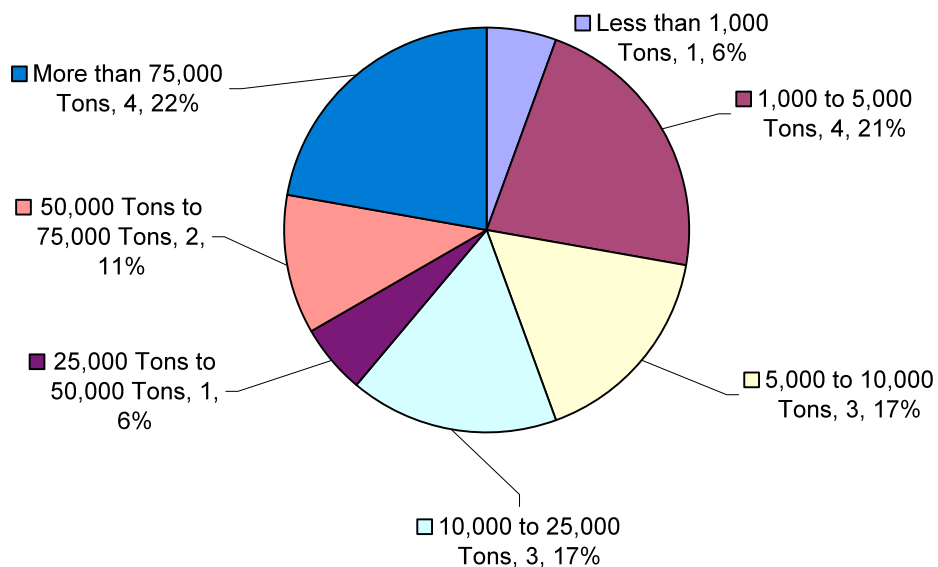


**Figure 7: Annual Quantity Used: RPM (Recycled Pavement Material)**

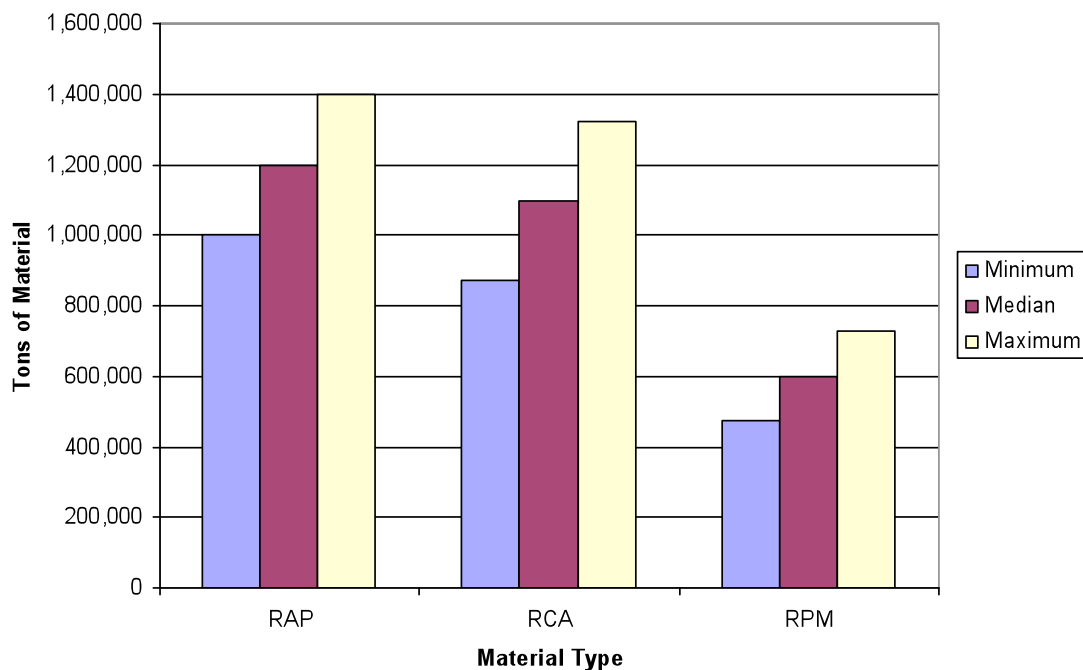


The most common response to the question for all three materials is “more than 75,000 tons” which would indicate that the use of recycled materials is significantly widespread. Of these materials, the use of RAP seems to be the most advanced in terms of quantity, with more than half of the respondents indicating that 75,000 tons of material or more was typically used. RCA is the second most advanced, with more than half the

respondents indicating that 25,000 tons of material or more was typically used. RPM seemed to be the least advanced; with more than half of the respondents indicating that 25,000 tons or less was typically used.

The data represented in Figures 5 thru 7 can be further understood if the total tonnage is considered. The total material used in each case was calculated and is represented in Figure 8. Three calculations were made for each material corresponding to the maximum, median, and maximum values of tons used for each of the quantity ranges. The maximum value for the “More than 75,000 Tons” option was assumed to be 100,000 tons.

**Figure 8: Quantity of Each Material Used**



The trends for all three materials represented in the survey can be seen to fall within a clearly visible trend, with RAP material being the most widely used in all three categories. The trend continues with RCA and RPM being the second and third most widely used, respectively. Contrasting this data with the data in Figure 1 seems to indicate that although more agencies are currently using RCA as a recycled fill, RAP material is being used in greater amounts. If RAP and RPM are combined, it appears flexible pavement recycling is far greater than RCA, which include rigid pavement recycling as well as building concrete. This is also reflective of the preponderance of flexible pavements compared to rigid pavements.

#### Question #4

The fourth question presented in the survey was “How long have you been using the recycled materials?” Each of the respondents had the opportunity to select one of the following options for each of the recycled material types: “Less than 1 Year”, “1 to 2

Years”, “2 to 5 Years”, “5 to 10 Years” or “More than 10 Years”. There were 34 unique respondents to this question on the survey. The distribution of responses to each option is represented in Figures 9 thru 11.

**Figure 9: Number of Years Used: RAP (Recycled Asphalt Pavement)**

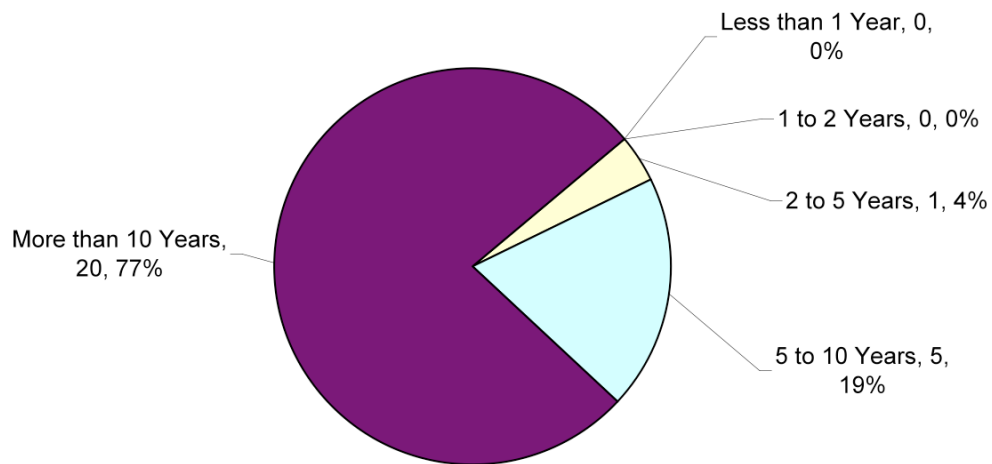


**Figure 10: Number of Years Used: RCA (Recycled Concrete Aggregate)**

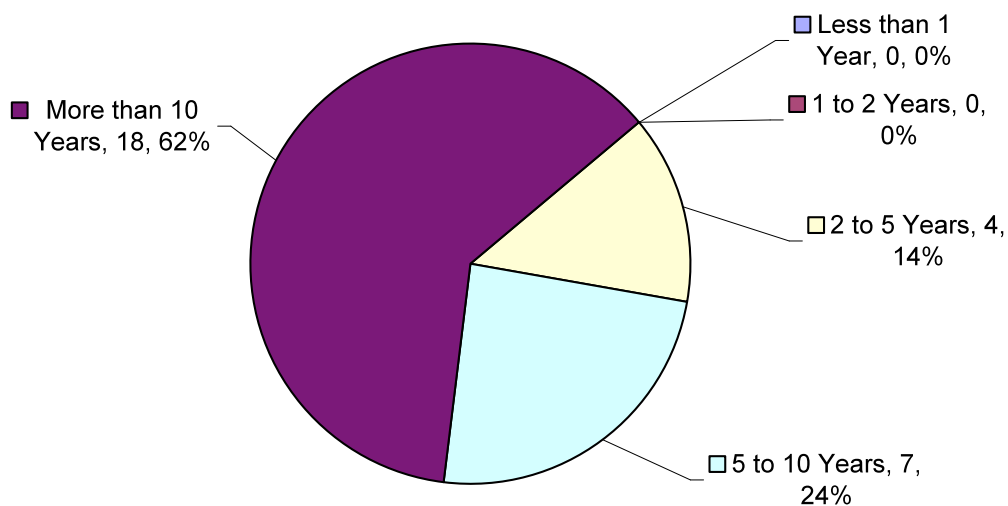
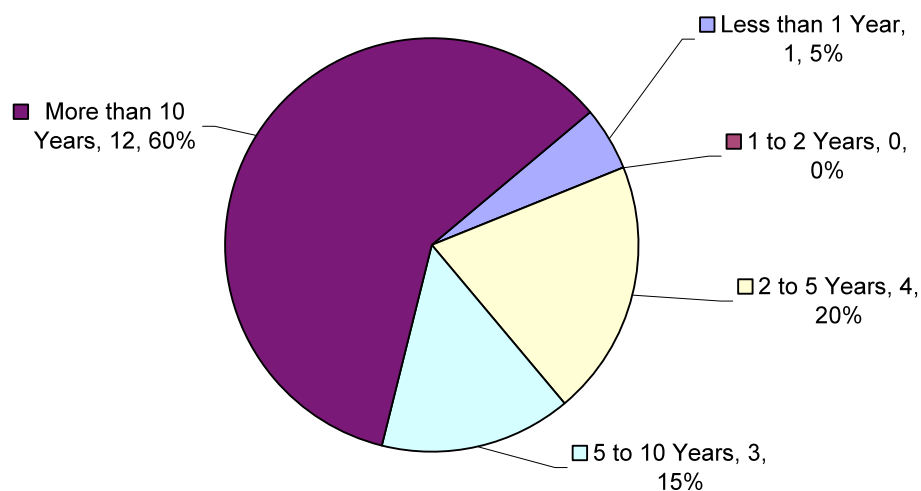




**Figure 11: Number of Years Used: RPM (Recycled Pavement Material)**



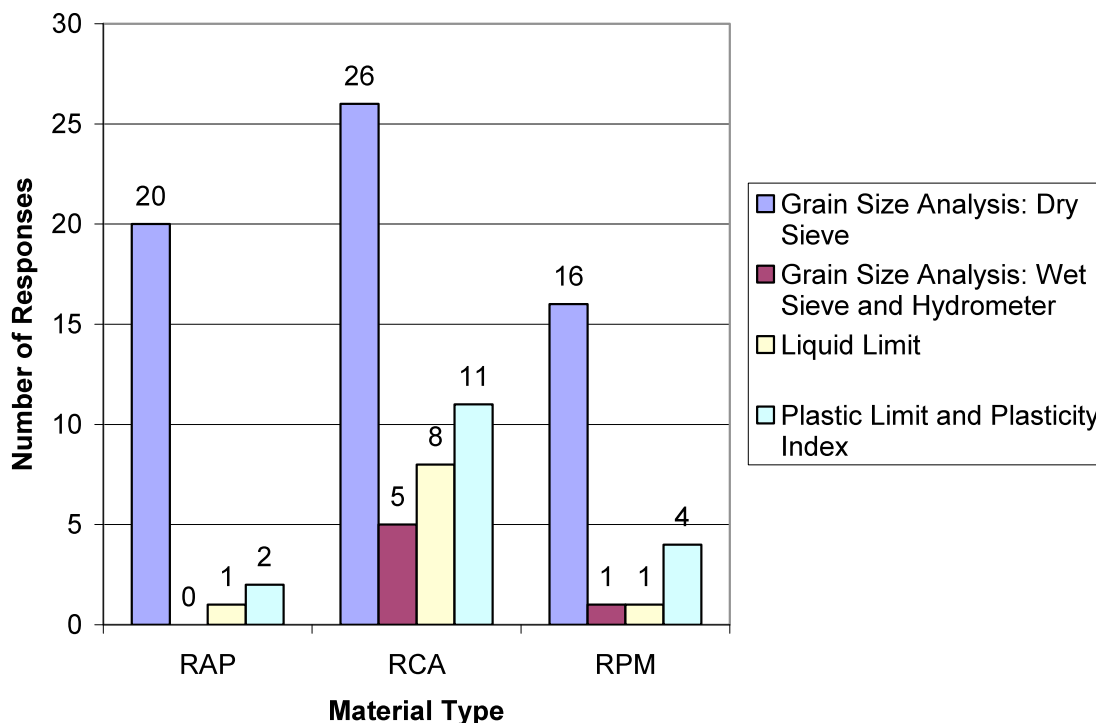
The overall results indicate that the use of recycled materials has been established for a considerable amount of time. For each of the given materials, more than half of the respondents indicated that the material had been used for more than 10 years. All but one response (for RPM) indicated that each responding agency had used the given material for more than 2 years.

### 3.2. Aggregate Specification and Quality

#### Question #5:

The fifth question presented in the survey was “Are any of the following tests used in specifications for the material?” Each of the respondents had the opportunity to select any of the following options for each of the recycled material types: “Grain Size Analysis: Dry Sieve”, “Grain Size Analysis: Wet Sieve and Hydrometer”, “Liquid Limit”, and “Plastic Limit and Plasticity Index”. There were 32 unique respondents to this question on the survey. The distribution of responses to each option is represented in Figure 12.

**Figure 12: Specification Tests Used by Material Type**

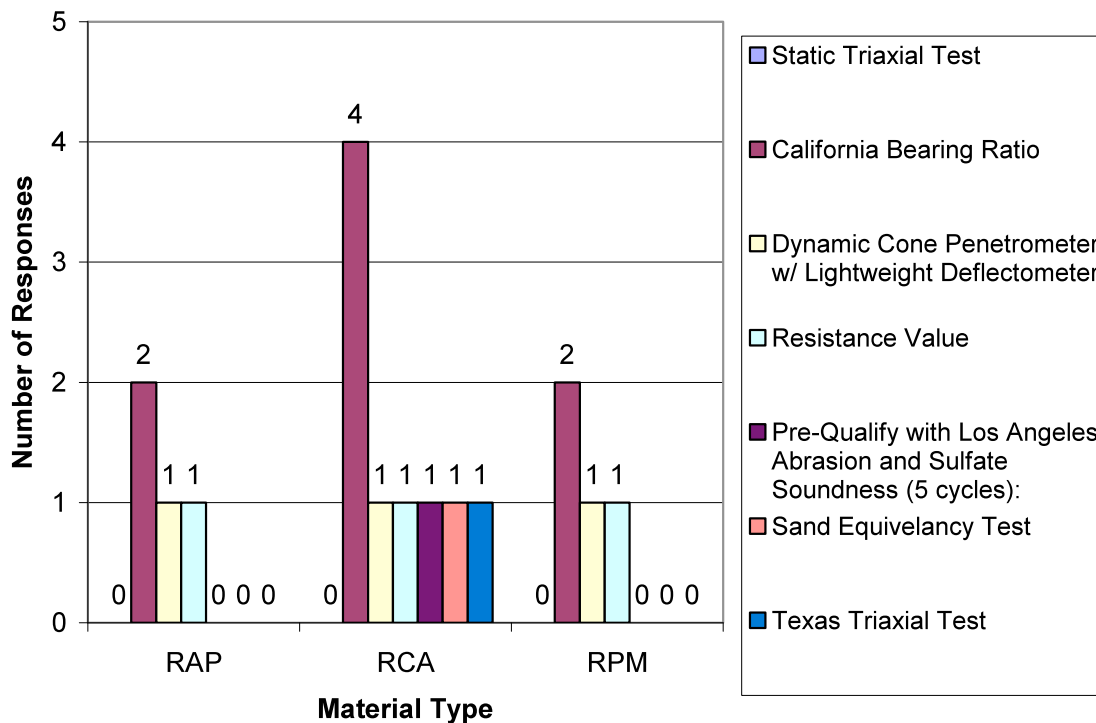


It can be seen from Figure 12 that the dry sieve method of grain size analysis is by far the most common test used to establish specification compliance for the given material, with plastic limit and plasticity index determinations ranking second by a wide margin. The wet sieve and hydrometer method of grain size analysis and the determination of liquid limits rank third and fourth most common, respectively. From Figure 12 it seems that the RCA material is the most rigorously tested of the three materials, with the greatest response totals for all three test methods.

#### Question #6

The sixth question presented in this survey was “Which of the following aggregate quality tests for shear strength do you perform on the material prior to placement?” Each of the respondents had the opportunity to select any of the following options for each of the recycled material types: “Static Triaxial Test (AASHTO T 296, ASTM D 2850)”, “California Bearing Ratio (AASHTO T 193, ASTM D 1883)”, “Dynamic Cone Penetrometer (ASTM D 6951)”, or “Other”. If “Other” was selected, the respondent was requested to indicate the optional test performed. There were 11 unique respondents to this question on the survey. The distribution of responses to each option is represented in Figure 13.

**Figure 13: Aggregate Quality Tests for Shear Strength**

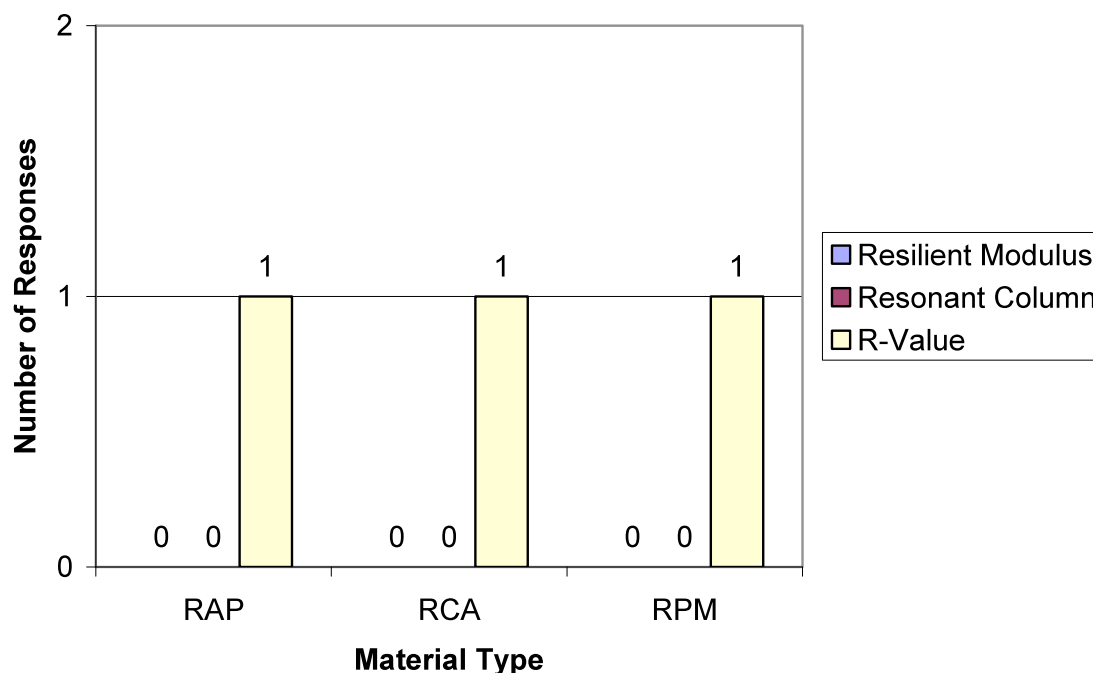


Despite the limited amount of response to the question, the California Bearing Ratio test stood out as the most commonly used test to determine shear strength for each of the recycled materials. Four of the respondents chose “other”, indicating that their particular agencies used additional tests for shear strength. The collected data indicated that one agency used the Resistance Value test for each of the three materials, and three separate agencies respectively used the following three tests for RCA: “LA Abrasion Test and Sulfate Soundness (Pre-Qualify)”, “Sand Equivalency Test”, and “Texas Triaxial Test”.

#### Question 7

The seventh question presented in the survey was “Which of the following aggregate quality tests for stiffness do you perform on the material prior to placement?” Each of the respondents had the opportunity to select any of the following options for each of the recycled material types: “Resilient Modulus (AASHTO T 307)”, “Resonant Column (ASTM D 4015)”, or “Other”. If “Other” was selected, the respondent was requested to indicate the optional test performed. There was only 1 unique respondent to this question on the survey. The distribution of responses to each option is represented in Figure 14.

**Figure 14: Aggregate Quality Tests for Stiffness**



There was only one response to the question, so the data is inconclusive. Neither of the provided options was chosen in response to the question. The sole respondents chose “other” and indicated that their particular agency used the R-Value test as an additional test for stiffness on all three material types. However, based on the data, it appears that the testing of materials for stiffness prior to placement is not common.

#### Question 8

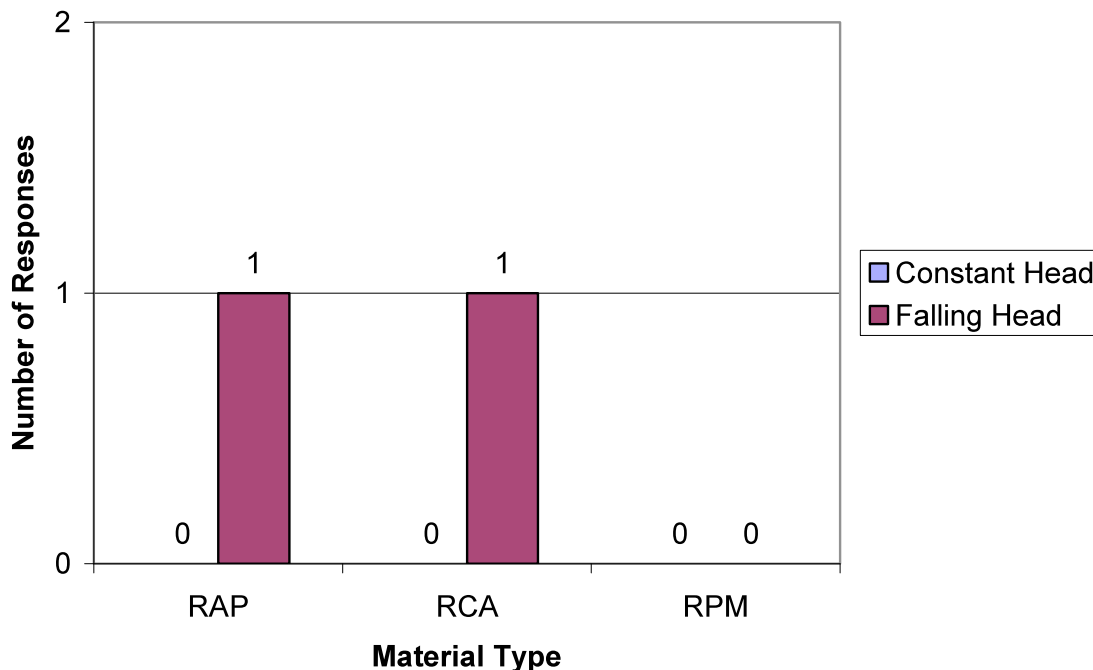
The eighth question presented in the survey was “Which of the following aggregate quality tests for frost susceptibility do you perform on the material prior to placement?” Each of the respondents had the opportunity to select any of the following options for each of the recycled material types: “Tube Suction Test (Texas Method 144E)”, or “Other”. If “Other” was selected, the respondent was requested to indicate the optional test performed. There were no respondents to this question on the survey, and therefore it appears that the testing of materials for frost susceptibility prior to placement is not common.

#### Question 9

The ninth question presented in the survey was “Which of the following aggregate quality tests for permeability do you perform on the material prior to placement?” Each of the respondents had the opportunity to select any of the following options for each of the recycled material types: “Constant Head (AASHTO T 215, ASTM D 2434)”, “Falling Head”, or “Other”. If “Other” was selected, the respondent was requested to indicate the

optional test performed. There was only 1 unique respondent to this question on the survey. The distribution of responses to each option is represented in Figure 15.

**Figure 15: Aggregate Quality Tests for Permeability**

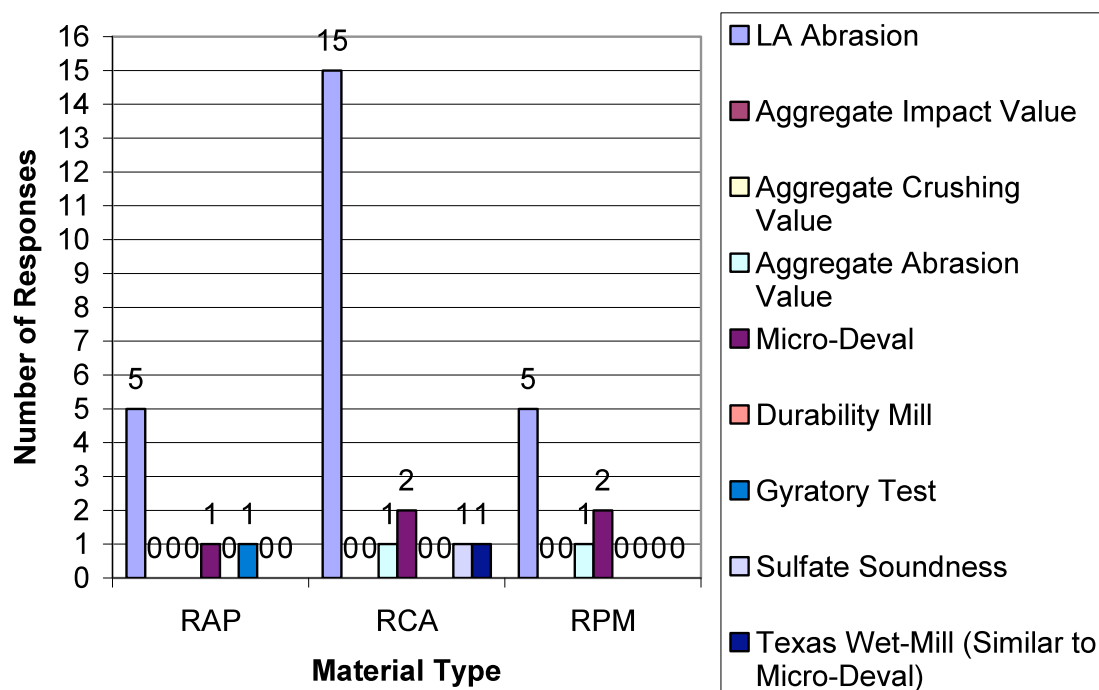


The only response to the question indicated that the Falling Head test was typically used for permeability determinations. However, the limited response to this question renders the data inconclusive. It appears that the testing of materials for permeability prior to placement is not common.

#### Question 10

The tenth question presented in the survey was “Which of the following aggregate quality tests for toughness do you perform on the material prior to placement?” Each of the respondents had the opportunity to select any of the following options for each of the recycled material types: “LA Abrasion (AASHTO T 96, ASTM C 131)”, “Aggregate Impact Value (BS 812)”, “Aggregate Crushing Value (BS 812)”, “Aggregate Abrasion Value”, “Micro-Deval (AASHTO TP 58 and T 327, ASTM D 6928)”, “Durability Mill (Sampson and Netterberg 1989)”, “Gyratory Test”, or “Other”. If “Other” was selected, the respondent was requested to indicate the optional test performed. There were 21 unique respondents to this question on the survey. The distribution of responses to each option is represented in Figure 16.

**Figure 16: Aggregate Quality Tests for Toughness**



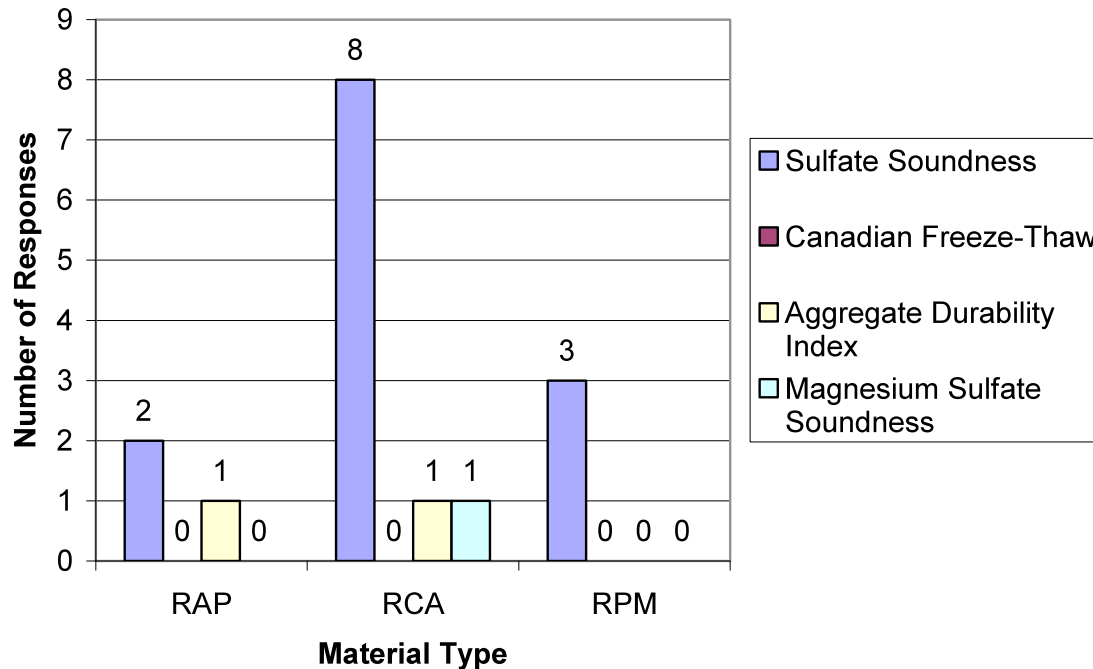
It is clear from Figure 16 that the LA Abrasion test is the most commonly used test for the toughness of a material prior to placement and is frequently used for all three material types, but most commonly when RCA material is considered. Despite the minimal data available for the other test methods, the Micro-Duvall test for all materials, the Aggregate Abrasion Value test for RCA and RPM, and the Gyratory Test for RAP were each indicated as being marginally used. None of the respondents indicated that the Aggregate Impact Value, Aggregate Crushing Value or Durability Mill Tests were used.

Two of the respondents chose “other”, indicating that their particular agencies used additional tests for toughness. The Sulfate Soundness test and Texas Wet-Mill test were respectively used by two different agencies for toughness testing on RCA material. The Texas Wet-Mill test was described as “similar to the idea of Micro-Deval.”

### Question 11

The eleventh question presented in the survey was “Which of the following aggregate quality tests for durability do you perform on the material prior to placement?” Each of the respondents had the opportunity to select any of the following options for each of the recycled material types: “Sulfate Soundness (AASHTO T 104, ASTM C 88)”, “Canadian Freeze-Thaw (MTO LS-614)”, “Aggregate Durability Index (AASHTO T 210 and T 176, ASTM D 3744)”, or “Other”. If “Other” was selected, the respondent was requested to indicate the optional test performed. There were 12 unique respondents to this question on the survey. The distribution of responses to each option is represented in Figure 17.

**Figure 17: Aggregate Quality Tests for Durability**

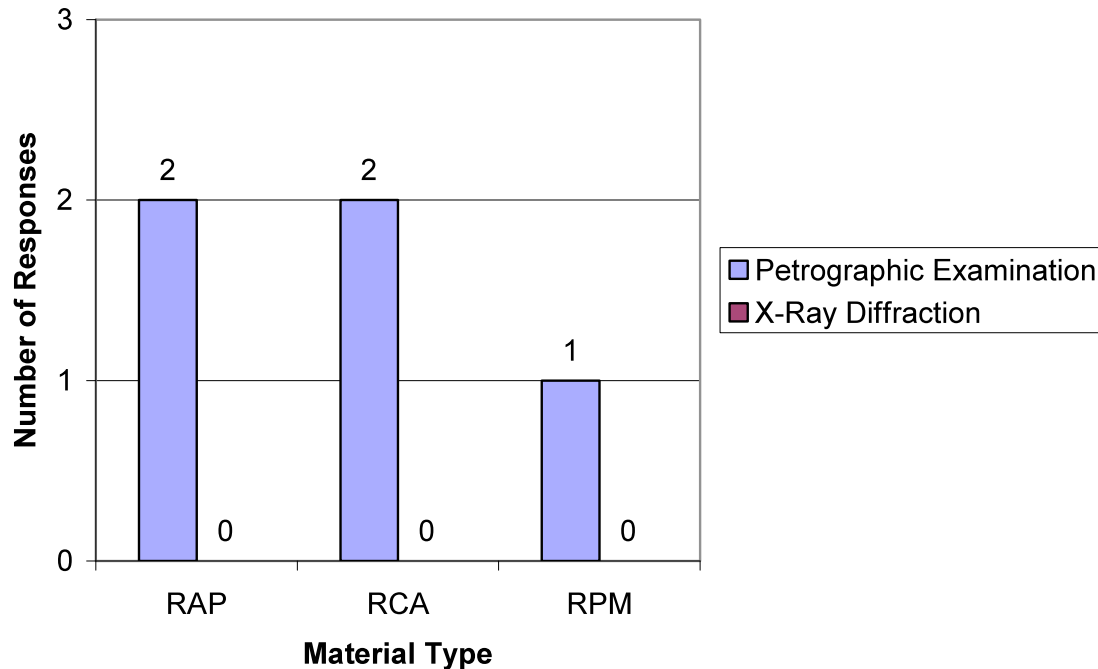


From Figure 17 it can be seen that the Sulfate Soundness test is the most commonly used test for the durability of a material prior to placement, and is frequently used for all three material types. Despite the minimal data available indicating other test methods, the Aggregate Durability Index test for RAP and RCA was indicated as being marginally used. None of the respondents indicated that the Canadian Freeze-Thaw test was used. One of the respondents chose “other”, indicating that their particular agency used the Magnesium Sulfate Soundness test as an additional durability test for RCA.

#### Question 12

The twelfth question presented on the survey was “Which of the following aggregate quality tests for mineralogical composition do you perform on the material prior to placement?” Each of the respondents had the opportunity to select any of the following options for each of the recycled material types: “Petrographic Examination (ASTM C 295)”, “X-Ray Diffraction”, or “Other”. If “Other” was selected, the respondent was requested to indicate the optional test performed. There were 4 unique respondents to this question on the survey. The distribution of responses to each option is represented in Figure 18.

**Figure 18: Aggregate Quality Tests for Mineralogical Composition**



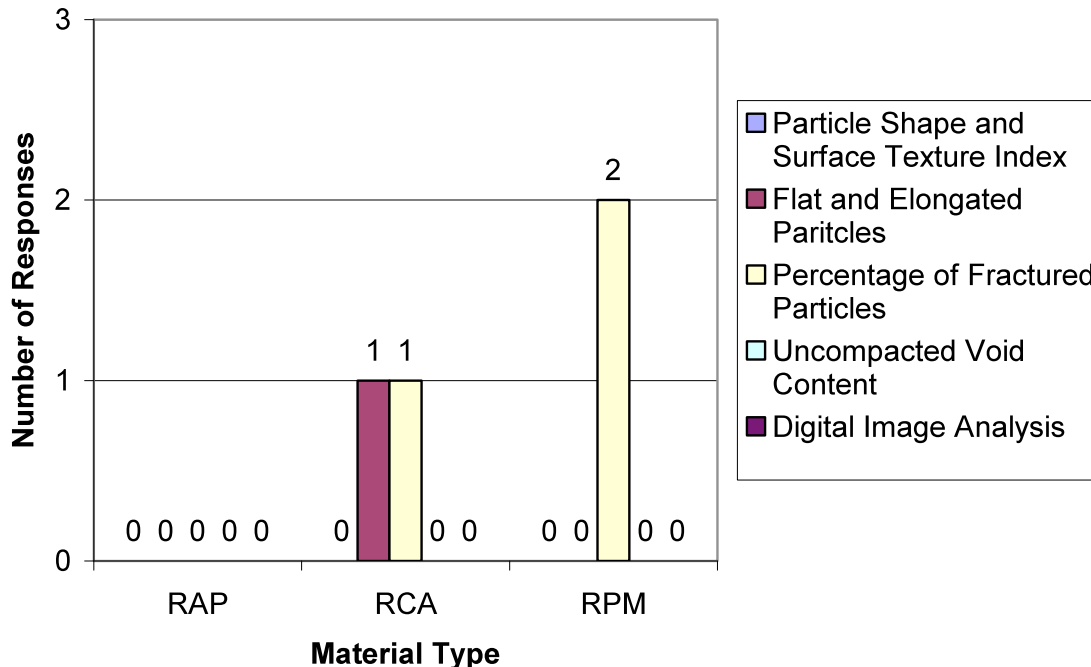
The only response to the question indicated that the Petrographic Examination test method was the only test typically used for the determination of mineralogical composition in recycled materials. However, the limited response would indicate that the data is inconclusive, and therefore it appears that the testing of materials for mineralogical composition prior to placement is not common.

### Question 13

The thirteenth and final question presented on the survey was “Which of the following aggregate quality tests for particle geometric properties do you perform on the material prior to placement?” Each of the respondents had the opportunity to select any of the following options for each of the recycled material types: “Particle Shape and Surface Texture Index (ASTM D 3398)”, “Flat and Elongated Particles (ASTM D 4791)”, “Percentage of Fractured Particles (ASTM 5821)”, “Uncompacted Void Content (AASHTO T 326, ASTM C 1252)”, “Digital Image Analysis”, or “Other”. If “Other” was selected, the respondent was requested to indicate the optional test performed. There were 4 unique respondents to this question on the survey. The distribution of responses to each option is represented in Figure 19.



**Figure 19: Aggregate Quality Tests for Particle Geometric Properties**



The minimal data available for question thirteen indicates that tests for Particle Geometric Properties are marginally used. The usage of the Percentages of Fractured Particles test was slightly more common than that of the Flat and Elongated Particles test, with the former used for RCA and RPM materials and the latter used for RCA materials only. None of the other three tests were selected for the survey. Based on the results of this survey, it appears that the testing of materials for particle geometric properties prior to placement is not common.

#### 4. Conclusion

A survey was conducted by the University of Wisconsin-Madison to determine the extent of use of recycled materials as granular base course in roadway applications. The survey found that of the three recycled materials considered, recycled concrete aggregate (RCA) was the most commonly used material, followed by recycled asphalt pavement (RAP) and recycled pavement material (RPM). However, if RAP and RPM are combined, recycling of flexible pavements is more common both in terms frequency and quantity. Following reclamation operations, it is more common for a recycled material to be stockpiled and used later than to be used immediately after reclamation. However, RPM materials, common to full-depth reclamation efforts, are more likely to be used immediately after reclamation than the other materials considered. In terms of quantity, RAP material represents the greatest total tonnage used, followed by RCA and RPM, respectively. Although RCA is the most common material used, RAP material is used in greater amounts.

The most common test used to determine specification compliance for a recycled material was Grain Size Analysis using dry sieve, followed by Plastic Limit and Liquid Limit determinations and Grain Size Analysis using a wet sieve and hydrometer. The survey indicated that the most common tests for aggregate quality are the California Bearing Ratio test for aggregate shear strength, the LA Abrasion test for aggregate toughness, and the Sulfate Soundness test for aggregate durability. Less common to uncommon tests for aggregate quality were found to be the R-Value test for stiffness, the Falling Head Method test for permeability, the Petrographic Examination test for mineralogical composition, and either the Percent of Fractured Particles test or Flat and Elongated Particles test for particle geometry. The results of the survey gave no indication that frost susceptibility tests were performed for summative quality. It is apparent from the survey that there is limited data for structural properties. For instance, resilient modulus needed for the Mechanistic-empirical design procedure is not performed. Developing a database of such properties for these recycled materials is needed.

## 5. Bibliography

1. Nataatmadja, A. and Tan, Y. L. (2001) "Resilient Response of Concrete Road Aggregates", *Journal of Transportation Engineering*, Vol. 127, No. 5, pp 450-453
2. Guthrie, W. S., Cooley, D. and Eggett, D. L. (2007). "Effects of Reclaimed Asphalt Pavement on Mechanical Properties of Base Materials", *Transportation Research Record*, No. 2006, pp. 44-52
3. "User Guidelines for Byproducts and Secondary Use Materials in Pavement Construction." FHWA Report FHWA-RD-97-148, Federal Highway Administration, McLean, Virginia (2008).
4. Li, L., Benson, C. H., Edil, T. B., Hatipoglu, B., and Tastan, E. (2007). "Evaluation of Recycled Asphalt Pavement Material Stabilized with Fly Ash", *ASCE Geotechnical Special Publication (CD-ROM)*, 169
5. Poon, C. S., Qiao, X. C. and Chan, D. X. (2006). "The Cause and Influence of Self-Cementing Properties of Fine Recycled Concrete Aggregates on the Properties of Unbound Sub-Base", *Waste Management*, Vol. 26, No. 10, pp. 1166-1172
6. Kuo S. S., Mahgoub, H. S. and Nazef, A. (2002). "Investigation of Recycled Concrete Made with Limestone Aggregate for a Base Course in Flexible Pavement", *Geomaterials*, No. 1787, pp. 99-108

APPENDIX  
SURVEY RESULTS

# WebSurvey@UW

Home	New Survey	Surveys	Libraries	Templates	Email Lists	Reports	Users	My Account	Help	Logout
------	------------	---------	-----------	-----------	-------------	---------	-------	------------	------	--------

## Survey Results -- Overview

<a href="#">Export Data</a>	<a href="#">Individual Responses</a>
-----------------------------	--------------------------------------

### Recycled Material

**Respondents:** 41 displayed, 41 total      **Status:** Open  
**Launched Date:** 11/06/2008      **Closed Date:** N/A

**Display:**

[Manage Filters](#) 0 filters

[Share Results](#) Disabled

### 1. Q1

		Response Total	Response Percent
Recycled Asphalt Pavement (RAP)		18	53%
Recycled Concrete Aggregate (RCA)		30	88%
Recycled Pavement Material (RPM) (Mixture of HMA and Base Course)		17	50%
<b>Total Respondents</b>		<b>34</b>	
(skipped this question)			7

### 2. When are the recycled materials used?

	Stockpiled and Used Later	Used in Place Immediately	Both	Response Total
Recycled Asphalt Pavement (RAP)	42% (11)	4% (1)	54% (14)	26
Recycled Concrete Aggregate (RCA)	65% (20)	3% (1)	35% (11)	31
Recycled Pavement Material (RPM)	33% (6)	28% (5)	39% (7)	18
<b>Total Respondents</b>				<b>36</b>
(skipped this question)				5

### 3. In a given year, how much of the recycled material do you use?

	Less than 1,000 Tons	1,000 to 5,000 Tons	5,000 to 10,000 Tons	10,000 to 25,000 Tons	25,000 to 50,000 Tons	50,000 to 75,000 Tons	More than 75,000 Tons	Response Total
Recycled Asphalt Pavement (RAP)	17% (4)	0% (0)	9% (2)	17% (4)	0% (0)	4% (1)	52% (12)	23
Recycled Concrete Aggregate (RCA)	7% (2)	21% (6)	14% (4)	7% (2)	17% (5)	7% (2)	28% (8)	29

Recycled Pavement Material (RPM)	6% (1)	22% (4)	17% (3)	17% (3)	6% (1)	11% (2)	22% (4)	<b>18</b>
	<b>Total Respondents</b>							<b>33</b>
	(skipped this question)							8

**4.** How long have you been using the recycled materials?

	Less than 1 year	1 to 2 years	3 to 5 years	5 to 10 years	More than 10 years	Response Total	
Recycled Asphalt Pavement (RAP)	0% (0)	0% (0)	4% (1)	19% (5)	77% (20)	<b>26</b>	
Recycled Concrete Aggregate (RCA)	0% (0)	0% (0)	14% (4)	24% (7)	62% (18)	<b>29</b>	
Recycled Pavement Material (RPM)	5% (1)	0% (0)	20% (4)	15% (3)	60% (12)	<b>20</b>	
	<b>Total Respondents</b>						<b>34</b>
	(skipped this question)						7

**5.** Are any of the following tests used in specifications for the material?

	Grain Size Analysis: Dry Sieve	Grain Size Analysis: Wet Sieve and Hydrometer	Liquid Limit	Plastic Limit and Plasticity Index	Response Total	
Recycled Asphalt Pavement (RAP)	87% (20)	0% (0)	4% (1)	9% (2)	<b>23</b>	
Recycled Concrete Aggregate (RCA)	76% (26)	15% (5)	24% (8)	32% (11)	<b>34</b>	
Recycled Pavement Material (RPM)	76% (16)	5% (1)	5% (1)	19% (4)	<b>21</b>	
	<b>Total Respondents</b>					<b>32</b>
	(skipped this question)					9

**6.** Which of the following aggregate quality tests for shear strength do you perform on the material prior to placement?

	Recycled Asphalt Pavement (RAP)	Recycled Concrete Aggregate (RCA)	Recycled Pavement Material (RPM)	Response Total	
Static Triaxial Test (AASHTO T 296, ASTM D 2850)	0% (0)	0% (0)	0% (0)	<b>0</b>	
California Bearing Ratio (AASHTO T 193, ASTM D 1883)	50% (2)	100% (4)	50% (2)	<b>4</b>	
Dynamic Cone Penetrometer (ASTM D 6951)	50% (1)	50% (1)	50% (1)	<b>2</b>	
Other	33% (3)	67% (6)	33% (3)	<b>9</b>	
	<b>Total Respondents</b>				<b>11</b>
	(skipped this question)				30

**7.** If "Other", please indicate what additional aggregate quality tests you perform for shear strength.

View responses to this question [view](#)

**Total Respondents** **11**

(skipped this question) 30

8. Which of the following aggregate quality tests for stiffness do you perform on the material prior to placement?

	Recycled Asphalt Pavement (RAP)	Recycled Concrete Aggregate (RCA)	Recycled Pavement Material (RPM)	Response Total
Resilient Modulus (AASHTO T 307)	0% (0)	0% (0)	0% (0)	0
Resonant Column (ASTM D 4015)	0% (0)	0% (0)	0% (0)	0
Other	75% (3)	75% (3)	75% (3)	4
			<b>Total Respondents</b>	<b>4</b>
			(skipped this question)	37

9. If "Other", please indicate what additional aggregate quality tests you perform for stiffness.

View responses to this question [view](#)

**Total Respondents** 12  
(skipped this question) 29

10. Which of the following aggregate quality tests for frost susceptibility do you perform on the material prior to placement?

	Recycled Asphalt Pavement (RAP)	Recycled Concrete Aggregate (RCA)	Recycled Pavement Material (RPM)	Response Total
Tube Suction Test (Texas Method 144 E)	0% (0)	0% (0)	0% (0)	0
Other	67% (2)	67% (2)	67% (2)	3
			<b>Total Respondents</b>	<b>3</b>
			(skipped this question)	38

11. If "Other", please indicate what additional aggregate quality tests you perform for frost susceptibility.

View responses to this question [view](#)

**Total Respondents** 11  
(skipped this question) 30

12. Which of the following aggregate quality tests for permeability do you perform on the material prior to placement?

	Recycled Asphalt Pavement (RAP)	Recycled Concrete Aggregate (RCA)	Recycled Pavement Material (RPM)	Response Total
Constant Head (AASHTO T 215, ASTM D 2434)	0% (0)	0% (0)	0% (0)	0
Falling Head	100% (1)	100% (1)	0% (0)	1
Other	67% (2)	67% (2)	67% (2)	3
			<b>Total Respondents</b>	<b>4</b>
			(skipped this question)	37

13. If "Other", please indicate what additional aggregate quality tests you perform for permeability.

View responses to this question [view](#)

**Total Respondents** 11  
(skipped this question) 30

**14.** Which of the following aggregate quality tests for toughness do you perform on the material prior to placement?

	<b>Recycled Asphalt Pavement (RAP)</b>	<b>Recycled Concrete Aggregate (RCA)</b>	<b>Recycled Pavement Material (RPM)</b>	<b>Response Total</b>
LA Abrasion (AASHTO T 96, ASTM C131)	26% (5)	79% (15)	26% (5)	<b>19</b>
Aggregate Impact Value (BS 812)	0% (0)	0% (0)	0% (0)	<b>0</b>
Aggregate Crushing Value (BS 812)	0% (0)	0% (0)	0% (0)	<b>0</b>
Aggregate Abrasion Value (BS 812)	0% (0)	50% (1)	50% (1)	<b>2</b>
Micro-Deval (AASHTO TP 58 and T 327, ASTM D6928)	25% (1)	50% (2)	50% (2)	<b>4</b>
Durability Mill (Sampson and Netterberg 1989)	0% (0)	0% (0)	0% (0)	<b>0</b>
Gyratory Test	100% (1)	0% (0)	0% (0)	<b>1</b>
Other	33% (1)	67% (2)	0% (0)	<b>3</b>
			<b>Total Respondents</b>	<b>21</b>
			(skipped this question)	20

**15.** If "Other", please indicate what additional aggregate quality tests you perform for toughness.

View responses to this question [view](#)

**Total Respondents** 9  
(skipped this question) 32

**16.** Which of the following aggregate quality tests for durability do you perform on the material prior to placement?

	<b>Recycled Asphalt Pavement (RAP)</b>	<b>Recycled Concrete Aggregate (RCA)</b>	<b>Recycled Pavement Material (RPM)</b>	<b>Response Total</b>
Sulfate Soundness (AASHTO T 104, ASTM C 88)	20% (2)	80% (8)	30% (3)	<b>10</b>
Canadian Freeze-Thaw (MTO LS-614)	0% (0)	0% (0)	0% (0)	<b>0</b>
Aggregate Durability Index (AASHTO T 210 and T 176, ASTM D 3744)	100% (1)	100% (1)	0% (0)	<b>1</b>
Other	67% (2)	67% (2)	67% (2)	<b>3</b>
			<b>Total Respondents</b>	<b>14</b>
			(skipped this question)	27

**17.** If "Other", please indicate what additional aggregate quality tests you perform for durability.

View responses to this question [view](#)

**Total Respondents** 8  
(skipped this question) 33

**18.** Which of the following aggregate quality tests for mineralogical composition do you perform on the material prior to placement?

	<b>Recycled Asphalt Pavement (RAP)</b>	<b>Recycled Concrete Aggregate (RCA)</b>	<b>Recycled Pavement Material (RPM)</b>	<b>Response Total</b>
Petrographic Examination (ASTM C295)	50% (2)	50% (2)	25% (1)	<b>4</b>
X-Ray Diffraction	0% (0)	0% (0)	0% (0)	<b>0</b>
Other	100% (2)	50% (1)	100% (2)	<b>2</b>
			<b>Total Respondents</b>	<b>6</b>
			(skipped this question)	35

**19.** If "Other", please indicate what additional aggregate quality tests you perform for mineralogical composition.

View responses to this question [view](#)

**Total Respondents** **8**  
(skipped this question) 33

**20.** Which of the following aggregate quality tests for particle geometric properties do you perform on the material prior to placement?

	<b>Recycled Asphalt Pavement (RAP)</b>	<b>Recycled Concrete Aggregate (RCA)</b>	<b>Recycled Pavement Material (RPM)</b>	<b>Response Total</b>
Particle Shape and Surface Texture Index (ASTM D 3398)	0% (0)	0% (0)	0% (0)	<b>0</b>
Flat and Elongated Particles (ASTM D 4791)	0% (0)	100% (1)	0% (0)	<b>1</b>
Percentage of Fractured Particles (ASTM 5821)	0% (0)	33% (1)	67% (2)	<b>3</b>
Uncompacted Void Content (AASHTO T 326, ASTM C 1252)	0% (0)	0% (0)	0% (0)	<b>0</b>
Digital Image Analysis	0% (0)	0% (0)	0% (0)	<b>0</b>
Other	100% (2)	50% (1)	100% (2)	<b>2</b>
			<b>Total Respondents</b>	<b>6</b>
			(skipped this question)	35

**21.** If "Other", please indicate what additional aggregate quality tests you perform for particle geometric properties.

View responses to this question [view](#)

**Total Respondents** **9**  
(skipped this question) 32

Contact the DoIT Help Desk at 264-HELP or helpdesk.doit.wisc.edu for WebSurvey@UW Support  
Portions Copyright © 2009, Board of Regents of the University of Wisconsin System



# **Recycled Unbound Materials**

## **TPF-5 (129) Recycled Unbound Materials**

Mn/DOT Contract No. 89264 Work Order No. 2

CFMS Contract No: B14513

### **Task IB: Relationship Between Resilient Modulus and Composition of RCA or RAP**

**Ozlem Bozyurt, Younghwan Son, Tuncer B. Edil, James Tinjum, and Craig H. Benson**  
**University of Wisconsin- Madison**

**August, 2011**

## 1. INTRODUCTION

The growth in the construction and rehabilitation of the roadway systems in the United States (US) increases the consumption of natural materials and energy (Lee et al. 2010). The United States Geological Survey (USGS 2010) estimated that 508 million tons of crushed stone (natural aggregate) was consumed in the US in 2010, and 82% as construction material. Natural aggregate is largely used for public infrastructure, mostly for highway and road construction and related maintenance (Langer 1988). Road base or road surfacing materials are the major uses of natural aggregate without binder (i.e., unbound aggregate) (USGS 2010). However, rapidly decreasing sources of natural aggregate, along with limits placed upon aggregate production by environmental regulation and land use policies, has caused the price of these materials to increase dramatically (ACPA 2009).

Construction and demolition (C&D) waste makes up 25% to 45% of the waste bound for landfills in the US, thus contributing to reduced landfill life and increased environmental impacts (Leigh and Patterson 2004). The production of C&D waste has increased while the amount of landfill available for disposal has decreased (Chini et al. 2001; Poon et al. 2006). Appropriate means for the final disposition of C&D waste is of increasing concern (Kuo et al. 2002). With increasing generation of C&D waste coupled with landfill space limits, beneficial reuse of C&D waste appears attractive. One accepted way to beneficially reuse these materials is to incorporate them into base/subbase applications in flexible pavement construction.

Using recycled materials in the base and subbase layers can result in reductions in global warming potential by reducing the greenhouse gas emissions, and hazardous waste generation, while extending the service life of the pavement (Lee et al. 2010). The use of recycled material as base and subbase course in new or rehabilitated roadway construction has become common with some municipalities in the US (Bennert et al. 2000). State departments of transportation (DOTs) have participated in the development of markets for recyclables by using recycled materials in highway construction (Pratt 1993). By establishing engineering properties, specifications, and markets for recycled content within infrastructure projects, state DOTs contribute to the demand that sustains the practice of beneficial reuse of recycled material (Pratt 1993).

The most common C&D materials used as unbound base course in pavement construction are recycled concrete aggregate (RCA), recycled asphalt pavement aggregate (RAP) and recycled pavement materials (RPM). RCA is the product of the demolition of concrete structures such as buildings, roads, and runways. RAP is produced by removing and reprocessing existing asphalt pavement (Kuo et al., 2002; Guthri et al., 2007; FHWA 2008). The material generated from FDR, comprised of existing HMA and underlying base and perhaps some subgrade material, is referred to as RPM (Li et al. 2007; Wen and Edil 2008; Ebrahimi et al. 2010). By beneficially reusing concrete and asphalt, a waste product is converted to a resource for pavement construction (Langer 1988). An increase in the amount of RCA used to replace natural aggregates in pavement construction has economic and environmental benefits, while extending the supply of traditional construction material (Saeed et al. 2006).

The objective of this study is to evaluate the stiffness of RCA and RAP sources used as unbound base course without treatment and to determine the relationship between the  $M_r$  and physical properties (e.g., particle shape, binder type, aggregate mineralogy and contamination) of RCA and RAP through statistical correlations. The  $M_r$  of RAP and RCA measured in this study are compared to results from conventional base course.

The effect of varying RAP/RCA content on the stiffness of natural aggregates used as conventional unbound road base/subbase layer was determined. This thesis describes the findings of this study.

## **2. BACKGROUND**

### **2.1. Resilient Modulus**

RAP and RCA compete with natural aggregates that are currently used in roadway base applications (Guthri et al. 2007; FHWA 2008). Despite the increased acceptance of recycled base material in construction, research concerning the mechanical properties and durability of such materials is limited (Bennert et al. 2000; Nataatmadja and Tan 2001; Guthri et al. 2007). Recycled materials should perform well under the intended use in pavement design; therefore, the mechanical properties of recycled materials need to be investigated thoroughly such that appropriate design procedures and specifications can be established.

Schaertl (2010) indicates that RCA and RAP used alone or in blends with natural aggregates can have different resilient modulus ( $M_r$ ), sensitivity to stress state, and rutting performance compared to natural aggregates. The durability and toughness of recycled materials can also be different than that of natural aggregates (Weyers et al. 2005).

Base and subgrade layers undergo deformation when subjected to repeated loads from moving vehicular traffic. The resilient response of granular material is important for the load-carrying capacity of the pavement and the permanent strain response, which characterizes the long-term performance of the pavement (Lekarp et al., 2000). The  $M_r$  is a linear-elastic modulus obtained from dynamic loading, defined as the ratio of the cyclic deviator stress,  $\sigma_d$ , to the resilient (recoverable) strain,  $\epsilon_r$ :

$$M_r = \sigma_d / \epsilon_r \quad (1)$$

Design for pavements and rehabilitation of layered pavement systems use  $M_r$  as an essential parameter in the design process (Heydinger et al., 2007). Generally, a higher  $M_r$  infers a stiffer base course layer, which increases pavement life.

RAP and RCA compete with natural aggregates that are currently used in roadway base applications (Guthrie et al. 2007; FHWA 2008). Recycled materials should perform well under the intended use in pavement design; therefore, the mechanical properties of recycled materials need to be investigated thoroughly such that appropriate design procedures and specifications can be established. Despite the increased acceptance of recycled material as base course, research concerning the mechanical behavior of such material is lacking (Guthrie et al., 2007).

### 3. MATERIALS

Sixteen recycled materials, one conventional base course, and one blended recycled/conventional material were used in this investigation. Seven of the recycled materials were recycled asphalt pavement (RAP), six were recycled concrete aggregate (RCA), and two were recycled pavement materials (RPM). The recycled materials used in this study were obtained from a wide geographical area, covering eight different states: California, Colorado, Michigan, Minnesota, New Jersey, Ohio, Texas and Wisconsin (Fig. 1). The materials named according to the origin of the materials. The reference base course was a gravel meeting the Class 5 aggregate specifications for base course in Minnesota per the Minnesota Department of Transportation (MnDOT). Class 5 aggregate is formed by quartz, granite and carbonates

(limestone and dolomite). The ratio of quartz/granite to carbonates is 2.1. The percentage of mineral type in Class 5 aggregate is 68 % for Quartz/Granite and 32 % for Carbonates. Percent quartz/granite (aggregate and concrete) and percent carbonate of gravel (aggregate and concrete) of gravel are 43% and 20%, respectively. The blend (MN) was a mix of approximately equal parts (by mass) RCA from MnDOT (50%) and Class 5 aggregate (50%). The Class 5 aggregate was used as the control in this study.

The material from MnDOT was obtained during construction of roadway cells at the MnROAD test facility in Maplewood, Minnesota for investigation of the field behavior. The RAP was milled from the surface of roadway cells that were previously constructed at the MnROAD test facility. The RCA was obtained from a stockpile maintained by the Knife River Corporation at their pit located at 7979 State Highway 25 NE in Monticello, Minnesota.

The RAP from the Ohio Department of Transportation (ODOT) came from an existing asphalt pavement, processed through a portable plant, and stored in approximately 2268 Mg stockpiles. The Ohio RCA is from a 1.2-m-high barrier wall that existed between the north- and south-bound lanes of State Route 315 in downtown Columbus, Ohio. The broken-up concrete was taken from the project to a portable processing plant, crushed, sized, and stockpiled. The material for this project came from stockpiles of approximately 9071 Mg. The RCA samples provided were 100% RCA.

The material received from the Colorado DOT was collected from over 500 demolition sites from curb, gutter, sidewalk, highways, high-rise buildings, and housing foundations. Although the concrete came from varied sources, the aggregates for the production of the concrete originated from rock in Colorado, most from the quarries in Morrison and Golden and some aggregates were sourced from the Platte River.

The material provided by the New Jersey DOT (NJ DOT) is from stockpiles for demolition projects, primarily in New Jersey. The material in the stockpiles is in flux since NJ DOT constantly adds new loads and removes content for different purposes.

The RAP from California DOT is a combination of roadway millings and waste from an HMA plant (discharge from warm up and cleaning processes). The RCA is broken concrete rubble from the demolition of structures. Stockpiling in California is usually done three times a year. These stockpiles are not added to throughout their life-cycle. If stockpiled material is still unavailable during visits from subcontractors, new material is used to create a new stockpile.

The RCA sent by the Texas DOT is from a commercial source; therefore, the individual sources of aggregate or material characteristics included in the RCA are not known. The Texas RAP is from a highway project where the contractor milled the "binder" course after approximately 1.5 years of service. The RAP 1 from Michigan was provided by the Michigan DOT and is from highway reconstruction projects.

A summary of the grain characteristics and classifications for the seventeen materials is shown in **Error! Reference source not found.** The materials used in this study are classified as non-plastic per the Unified Soil Classification System (USCS). The Class 5 aggregate is classified as well-graded gravel (GW-GM) per the USCS (ASTM D 2487) and A-1-b per the AASHTO Soil Classification System (ASTM D 3282). The blended RCA/Class 5 is classified as A-1-b according to ASTM D 3282 and as poorly graded sand (SP) according to ASTM D 2487. The samples of RCA range from an SP to a well-graded gravel (GW) classification via USCS and A-1-a or b for AASHTO. The various RAPs and RPMs classify as SP, SW, or GW, whereas their AASHTO classifications are A-1-a or b. All materials are coarse-grained granular materials with fines contents mostly less than 7% except Class 5 aggregate and one RCA sample.

The particle size distribution (PSD) curves were determined according to ASTM D 422. Samples were wet-sieved through a No. 200 (75- $\mu\text{m}$  opening) sieve to separate the fine particles attached to the coarser aggregates. The PSDs for the RCA and the RAP/RPM samples are shown in Fig. 2 and Fig. 3 respectively, along with the upper and lower bounds from the literature.

To evaluate the effects of RAP content in blends on  $M_r$ , RAP (CO) and RAP (CA) were selected. The materials were chosen according to the availability of materials obtained from DOTs for this study. Additionally, RCA (MN)-Class 5 aggregate blend as obtained from the field project was also tested and compared with pure component materials.

## **4. METHODS**

### **4.1. Compaction**

The modified Proctor compaction test was performed on each material in accordance with ASTM D 1557, and the optimum moisture content (OMC) and maximum dry unit weight

(MDU) were determined. Before running the compaction test, the samples were screened through a 25-mm sieve.

#### 4.2. Resilient Modulus Test

Resilient modulus tests were performed on compacted specimens according to NCHRP 1-28a Procedure Ia, which applies to base and subbase materials. The materials used in this study classify as Type I material in NCHRP 1-28A, which requires a 152-mm-diameter and 305-mm-high specimen for resilient modulus testing (NCHRP 2004). Specimens were prepared at OMC and compacted to 95% of maximum modified Proctor density. Specimens were compacted in six lifts of equal mass within 1% of the target dry unit weight and 0.5% of target moisture content to ensure uniform compaction (NCHRP 2004).

Resilient modulus tests were conducted with internal and external linear variable displacement transducers (LVDT). External LVDTs have an accuracy of  $\pm 0.005$  mm, and internal LVDTs have an accuracy of  $\pm 0.0015$  mm. Clamps for the internal LVDTs were built in accordance with NCHRP 1-28A specifications. Internal LVDTs were placed at quarter points of the specimen to measure the deformations over the half-length of the specimen, whereas external LVDT measured deformations of the entire specimen length. An MTS Systems Model 244.12 servo-hydraulic machine was used for loading the specimens. Loading sequences, confining pressures and data acquisition were controlled from a computer running LabView 8.5 software.

The loading sequence was applied using a haversine load pulse with a frequency 1Hz. The load was applied for 0.1sec at the beginning of each cycle, and was followed by a 0.9sec rest period. An MTS Systems Model 244.12 servo-hydraulic machine was used for loading the specimens. Loading sequences, confining pressure, and data acquisition were controlled by a PC equipped with Labview 8.5 software. Resilient moduli ( $M_r$ ) from the last 5 cycles of each test sequence were averaged to obtain the resilient modulus for each load sequence.

The  $M_r$  for each load sequence was obtained by averaging the  $M_r$  from the last 5 cycles of each test sequence. The  $M_r$  data were fitted with the power function model proposed by Moosazeh and Witczak (1981)

$$M_R = k_1 \times \theta^{k_2} \quad (2)$$

where  $M_r$  is resilient modulus,  $\theta$  is bulk stress and  $k_1$  and  $k_2$  are empirical fitting parameters. The constants  $k_1$  and  $k_2$  are unique to a given material and are independent of one another.  $k_1$  and  $k_2$

are material-dependent parameters. For a given material,  $k_2$  obtained from replicate tests were averaged and fixed for that material (Camargo 2008). Bulk stress is another means of quantifying confining pressure and deviator stress in a single term and is defined as the sum of the three principle stresses. Bulk stress is defined as

$$\theta = \sigma_1 + \sigma_2 + \sigma_3 \quad (3)$$

where  $\sigma_1$ ,  $\sigma_2$ , and  $\sigma_3$  are the principal stresses acting on the specimen.

The  $M_r$  data were also fitted with the NCHRP model( NCHRP 2004) defined

$$M_r = k_1 \cdot p_a \cdot \left( \frac{\theta - 3k_6}{p_a} \right)^{k_2} \cdot \left( \frac{\tau_{oct}}{p_a} + k_7 \right)^{k_3} \quad (4)$$

where  $M_r$  is resilient modulus,  $k_1$ ,  $k_2$ ,  $k_3$ ,  $k_6$ , and  $k_7$  are constants,  $p_a$  is atmospheric pressure (101.4 kPa),  $\tau_{oct}$  is octahedral shear stress, and  $\theta$  is bulk stress.

For base course, the summary resilient modulus (SRM) corresponds to the  $M_r$  at a bulk stress of 208 kPa and octahedral shear stress of 48.6 kPa, as suggested by Section 10.3.3.9 of NCHRP 1-28a.  $M_r$  is used to determine the layer coefficient, which is a required input in the AASHTO pavement design equation (Tian et al. 1998).

#### **4.2.1. Blended RAP/RCA Effect on Stiffness of Recycled Materials**

To investigate the behavior of RAP or RCA blended with Class 5 aggregate, specimens were prepared by blending RAP or RCA to Class 5 aggregate and tested for  $M_r$  along with pure RAP or RCA and pure Class 5 aggregate. The modified Proctor compaction test was performed on the blended materials (50%RAP or RCA-50%Class 5 aggregate) in accordance with ASTM D 1557 to determine the OMC and MDU of the blended materials. Resilient modulus tests were performed on the compacted specimens according to NCHRP 1-28a Procedure Ia.

### **5. RESULTS AND ANALYSIS**

#### **5.1. Compaction Characteristics**

Optimum moisture content (OMC) and maximum dry unit weight (MDU) for RCA, RAP/RPM, , RCA (MN)-Class 5 aggregate blend and Class 5 aggregate are summarized in Table 2 and the associated compaction curves are given in Fig. 4. The respective averages (AVG), standard deviations (SDT), and coefficients of variation (CV) for RCA and RAP/RPM are summarized in Table 3. The averages of MDU and OMC for RCA and RAP/RPM as obtained



from this study are compared with those from the literature in Table 4 (Blankenagel and Guthrie 2006; Bejarano et al. 2003; Saeed et al. 2008; Camargo 2008; Guthrie et al. 2007; Wen et al. 2008; Bennert, et al. 2000; Kuo et al. 2002).

The compaction characteristics (MDU and OMC) of RCA follow a similar trend to the compaction characteristics of RAP/RPM with higher MDU and lower OMC (Fig. 5). The high coefficient of variation ( $R^2=0.89$  for RAP/RPM and  $R^2=0.83$  for RCA) between the compaction characteristics of RCA and RAP/RPM from different sources indicates that the values are statically significant. MDU is within a narrow range of 19.4 to 21.5  $\text{kN/m}^3$  for RAP/RPM at lower OMC (5.2 to 8.8%) and 19.4 to 20.8  $\text{kN/m}^3$  for RCA at high OMC (8.7 to 11.8%). The OMC of RAP/RPM was lower than RCA since asphalt coatings reduce the amount of water required to achieve MDU by preventing the water from reaching the individual particles of the material (Kim et al. 2007). RCA has high absorption capacity due to the porous nature of the cement paste portion (Arm 2001). Therefore, the amount of water required to achieve the MDU is higher than for natural aggregate and RAP (Juan and Gutierrez 2009).

## 5.2. Resilient Modulus

The resilient modulus presented is based on deformation measured with internal and external LVDTs. Variability in determining  $M_r$  was assessed by performing triplicate tests. The SRM for Class 5 aggregate, RCA, and RAP/RPM, computed in accordance with Procedure Ia of NCHRP 1-28A, are summarized in Table 5, along with parameters ( $k_1$  and  $k_2$ ) for the power function model (Eq. 2) and the parameters ( $k_1, k_2, k_3, k_6,$  and  $k_7$ ) for NCHRP model (Eqn.3) in Table 6. These SRM and parameters correspond to compaction at OMC and 95% modified Proctor MDU.

The estimated SRM by both models were compared with the measured modulus for RCA (Fig. 6) and RAP/RPM (Fig. 7). These comparisons are based on internally measured axial deformations. Statistical analysis indicated that results using both models are significant at a 95% confidence level, and both models represent the data reasonably well for RCA ( $R^2=0.85$  from power function model and  $R^2=0.96$  from NCHRP model) and for RAP ( $R^2=0.91$  from power function model and  $R^2=0.97$  from NCHRP model). The NCHRP model has less dispersion of the data than the power function for RCA and RAP. The power function model assumes constant Poisson's ratio and considers only the sum of the principal stresses (the bulk stress) as the effect

of stress on  $M_r$  (Lekarp et al., 2000). However, the NCHRP model considers the bulk stress and the magnitude of the shear strain influenced mainly by shear or deviator stress (Lekarp et al., 2000).

The relationship between internal SRM and external SRM (from the power function model) for unbound recycled materials, blend, and Class 5 aggregate is shown in Fig. 8. The SRM based on internal LVDT measurements of deformation were found to be consistently higher than those based on external LVDT measurements of deformation for all specimens. Camargo et al. (2009) reported that deformation measured with internal LVDTs more accurately described deformation of the specimens for computation of resilient modulus. Since the external LVDT measurements are affected by bedding errors, specimen end effects, and machine compliance, results tend towards larger deformation measurements and, consequently, lower modulus for a given applied cyclic stress (Ping et al. 2003; Bejarano et al. 2002; Camargo 2008). This ratio, however, should be considered typical but not universal as it is likely to depend on the equipment and the material being tested.

The measured  $M_r$  of the recycled materials was compared to the conventional base course based on deformations measured with internal LVDTs fitted to the power function model (Fig. 9 and Fig. 10). RAP/RPM has the highest SRM (ranging from 627 to 989 MPa) of the recycled materials evaluated. RCA has slightly the lower SRM (ranging from 549 to 715 MPa) in comparison to RAP/RPM, while Class 5 aggregate has the lowest SRM (525 MPa).

Previous research has reported that the stiffness of road base or subbase layers containing RCA or RAP has equal or higher  $M_r$  in comparison to natural aggregates (Kim et al., 2007; Bejarano et al., 2003; Wen et al., 2008). Wen et al. (2008) evaluated untreated RPM and crushed aggregates used at MnROAD test facility in terms of  $M_r$  and found that RPM has higher modulus than crushed aggregate. Bejarano et al. (2003) evaluated the stiffness of RAP compared to typical base course using  $M_r$  testing in accordance with Strategic Highway Research program test protocol. The stiffness of RAP was greater than that of the typical base course. Kim et al. (2007) performed  $M_r$  tests on an aggregate base blended with varying RAP contents (0-75%), with pure aggregate used as base course. All blends of aggregate base and RAP had  $M_r$  higher than the aggregate base alone, which explains the high SRM for RAP when compared to materials of similar USCS classification.

### 5.3. Plastic Strain

Plastic strains were determined for base materials from  $M_r$  testing by using the measured permanent deformations from the internal LVDTs with the power function model (Table 5). Plastic strains were calculated as the sum of the plastic strains for each loading sequence during resilient modulus test by excluding the plastic strains in the conditioning phase (Sequence 0). RCA showed average plastic strains of 0.7 %, whereas RAP, RPM and Class 5 showed plastic strain of 1.4 %, 1.5 % and 1.6 %, respectively. These results are different from those in Camargo (2009), but similar to those in Kim et al. (2007); Wen and Edil (2008, 2009) and Schaertl (2010). Camargo (2009) reported that RPM showed a plastic strain of 1.9 %, whereas Class 5 aggregate showed a plastic strain of 3.3 %. However, Kim et al. (2007) indicated that specimens with RAP exhibited higher plastic strains than the typical aggregate base material. Wen and Edil (2009) performed  $M_r$  tests on RPM and conventional crushed aggregate (Class 6sp) in accordance with NCHRP 1-28A test protocol. RPM had higher internal modulus (257 MPa) compare to Class 6sp (220 MPa). However, RPM showed higher plastic strains (2.8%) than Class 6sp (0.7%) indicating higher potential for rutting.

Schaertl (2010) determined the plastic deformation of RAP, RCA, Class 5 aggregate and blend (50%RCA and 50%Class 5 aggregate) by using Large-Scale Model Experiments (LSME) for two layer thickness (0.3 m and 0.2 m). The plastic deformation of RAP (211% and 102% in two experiments) was found to be greater than that experienced by Class 5 aggregate and RCA at the end of 10,000 cycles of load. LSME is a prototype pavement experiment and allows many cycles of loading thus its data are considered to be more representative.

### 5.4. Correlations

Stepwise regression was performed by using multiple linear regressions to develop correlations (models) to predict the SRM and compaction characteristics (OMC and MDU) of RCA and RAP based on their gradation characteristics. Regression methods estimate the predictive equation and compute a correlation coefficient to describe how strongly the value of one variable is associated with another. Regression was preferred because of the simplicity to ensure statistical significance of each independent variable and the clarity to evaluate the physical significance between the dependent and independent variables (Bareither et al., 2008).

A multiple regression model was developed between the compaction characteristics ( $w_{opt}$  and  $\gamma_{dmax}$ ) and index properties ( i.e.  $C_u$ ,  $C_c$ , sand%, gravel%, fines%,  $D_{10}$ ,  $D_{30}$ ,  $D_{50}$ ,  $D_{60}$ , absorption, asphalt content, specific gravity and deleterious materials) (given in Table 1) for RCA and RAP is summarized in Table 7. The models of compaction characteristics for RAP have relatively high  $R^2$  values (0.92 for  $w_{opt}$  and 0.70 for  $\gamma_{dmax}$ ) from the regression analysis in comparison to those for RCA (0.65 for  $w_{opt}$  and 0.67 for  $\gamma_{dmax}$ ). The variability in the source of RCA materials is more significant than RAP materials.

A multiple linear regression model was developed between internal SRM (given in Table 5) and index properties (given in **Error! Reference source not found.**) for RCA and RAP are summarized in Table 8. The model has relatively high  $R^2$  value of the regression analysis for internal SRM for RCA (0.89), and all the independent variables used in the model have p-values smaller than 0.05. The coefficients of the models have also physical significance. The negative coefficient on  $D_{30}$  indicate that internal SRM decreases with increasing fines content (Tutumluer and Seyhan 1998) and the negative coefficient on  $w_{opt}$  (%) indicates that internal SRM decreases with increasing  $w_{opt}$  (%) (Pan et al. 2006; Attia and Abdelrahman 2010). The change in  $D_{30}$  may affect the gradation of the materials as the increase in fines is likely to increase the water holding capacity of RCA (Saeed et al. 2008; Alam et al. 2010), which may reduce the resilient modulus (Tutumluer and Seyhan 1998).

The model for internal SRM for RAP has an  $R^2=0.99$ , and all the independent variables used in the model have p-values smaller than 0.05. The coefficients have also physical significance. The negative coefficient of fines content indicate that internal SRM decreases with increasing fines and the negative coefficients on absorption indicate that internal SRM decreases with increasing water holding capacity of the specimen. The positive coefficient on  $D_{60}$  and asphalt content (%) indicates that SRM increases with increasing  $D_{60}$  and asphalt coating. The increase in asphalt coating may increase the water drainage during compaction while reducing the absorption capacity of the material (Attia and Abdelrahman 2010). The decrease in water content may increase the  $M_r$  of the materials (Pan et al. 2006).  $D_{60}$  reflects the influence of gradation on the materials. This strong relationship between SRM and index properties suggests that the internal SRM of RCA and RAP could be estimated from the index properties.

## 5.5. Blended RAP/RCA Effect on Stiffness of Recycled Material

The effect of the amount of RAP blended with natural aggregate on the stiffness was investigated by blending 50% of RAP (CO) and RAP (CA) with Class 5 aggregate. Modified Proctor compaction test was conducted on the blend to obtain the OMC and MDU. Fig. 10 and Fig. 11 show the compaction curves of RAP (CA) and RAP (CO) blended with Class 5 aggregate, respectively along with the compaction curves of the blending components. Adding RAP to Class 5 aggregate causes a shift in compaction curve. The type of shift depends on the type of the recycled material used (Kim et al. 2007). Increasing RAP content is associated with decreasing OMC and MDU values, since the presence of asphalt coating does reduce the amount of water required to achieve the MDU probably due to reduced water absorption capacity (Alam et al. 2010).

Previous studies showed that the increase in the percentage of RAP in base materials increased the resilient modulus (Bennert et al. 2000; Guthrie et al. 2007). The results of the effect of RAP content on Class 5 aggregate are summarized in Table 9. Samples containing 100% RAP has a higher SRM compared to samples containing 50% RAP, and 0% RAP (Class 5 aggregate) as presented in Fig. 12. The 50% increase in the RAP (CO) and RAP (CA) increased the stiffness of the Class 5 aggregate, 11% and 39%, respectively.

The effect of RCA amount on the stiffness of unbound base layer was investigated by using the field blended materials (50% RCA (MN) and 50% Class 5 aggregate) obtained from MnDOT. Modified Proctor compaction test conducted on the 50% RCA (MN) blended with Class 5 aggregate to obtain the OMC and MDU are already given in Fig. 4. Adding RCA (MN) to Class 5 aggregate causes a shift in compaction curve and that the type of shift. Increasing RCA content is associated with increasing OMC and decreasing MDU due to the high water absorption capacity of RCA (FHWA 2008). The 50% increase in the RCA (MN) increased the stiffness of the Class 5 aggregate by 20 % (Fig. 12).

Fig.13 shows normalized SRM of the RAP and RCA blends (relative to SRM of Class 5 aggregate) as a function of blending percentage. Even though the rate of increase in SRM varied with the type of RAP, the trend in the increase in SRM for Class 5 aggregate is similar. Some recent studies also reported that an increase in RAP content improves the stiffness of unbound base course. Kim et al. (2007) investigated the stiffness of base course containing different ratios of RAP and natural aggregate. Resilient modulus tests were conducted on the recycled material

in accordance with NCHRP 1-28a. The 50% aggregate-50% RAP specimens developed stiffness equivalent to the 100% aggregate specimens at lower confining pressures (~ 20 kPa); at higher confinement (~ 120 kPa), the RAP specimens were stiffer. Alam et al. (2010) also blended natural aggregates with different percentages of RAP and significant amount of increase observed in Mr. Even though the rate of increase in SRM varied upon recycled materials, the trend in the increase in SRM for Class 5 aggregate is similar.

## **6. SUMMARY AND CONCLUSIONS**

This laboratory investigation dealt with the characterization of the engineering properties of the recycled materials (recycled asphalt pavement (RAP), recycled pavement material (RPM) and recycled concrete aggregate (RCA), as well as one field blended materials consisting of 50% RCA and 50% conventional base material used as unbound base/subbase layer without treatment. These recycled materials were collected from a wide geographical area, covering eight states in the U.S: California, Colorado, Michigan, Minnesota, New Jersey, Ohio, Texas and Wisconsin. A conventional base material meeting the gradation standard of Minnesota Department of Transportation Class 5 aggregate used as a reference material. The investigation also dealt with the determination of the influence of compaction effort and compaction moisture content, and freeze-thaw cycling on the engineering properties of unbound recycled materials, and the behavior of RAP or RCA blended to Class 5 aggregate used as unbound base/subbase layer.

The objectives were to investigate the mechanical properties of the recycled materials as unbound base or subbase material without treatment or stabilization under laboratory conditions. The objectives were met by determining the resilient modulus of the recycled materials in accordance with NCHRP 1-28a protocol measuring deflections both externally and internally on the specimens.

RAP/RPM had higher SRM than Class 5 aggregate and RCA. RAP/RPM exhibited slightly smaller plastic strain than Class 5, whereas RCA (0.7%) showed lowest plastic strain during Mr testing. There were quantitative differences in the stiffness of recycled materials from different sources. However, considering the wide geographic area they were obtained from, the

differences were not extraordinary. Two commonly used resilient modulus functions (Power Function and NCHRP models) for unbound base aggregates both captured the stress dependency of  $M_r$  satisfactorily. The multiple linear regression models were developed to estimate summary resilient modulus (SRM) from compaction parameters and materials parameters that exhibited high coefficient of determination for RAP and for RCA.

Blending recycled materials with natural aggregate result in intermediate modulus between the moduli of the two materials. Recycled materials had higher moduli than natural aggregate in this study. Therefore, no benefit is seen for blending as long as sufficient recycled materials are available.

## 7. REFERENCES

- ACPA (2009). "Recycling Concrete Pavements." *Bulletin B043P*, American Concrete Pavement Association. Skokie, IL.
- Alam, T. B., Abdelrahman, M. and Schram, S. A. (2010). "Laboratory Characterisation of Recycled Asphalt Pavement as a Base Layer." *International Journal of Pavement Engineering*, No.2, 123-131.
- Arm, M. (2001). "Self-cementing Properties of Crushed Demolished Concrete in Unbound Layers: Results from Triaxial Tests and Field Tests." *Waste Management*, 235-239.
- Attia, M. and Abdelrahman, M. (2010). "Modeling the Effect of Moisture on Resilient Modulus of Untreated Reclaimed Asphalt Pavement." *Transportation Research Record: Journal of the Transportation Research Board*, No.1981, 30-40.
- Bareither, C. A., Edil, T. B., Benson, C. H. and Mickelson, D. M. (2008). "Geological and Physical Factors Affecting the Friction Angle of Compacted Soils." *Journal of Geotechnical and Geoenvironmental Engineering*, No.10, 1476-1489.
- Bejarano, M. O., Harvey, J. T. and Lane, L. (2003). "In-Situ Recycling of Asphalt Concrete as Base Material in California." *Proc. 82nd Annual Meeting*, Transportation Research Board, Washington, D.C., 22.
- Bennert, T., Papp Jr. W., Maher, A. and Gucunski, N. (2000). "Utilization of Construction and Demolition Debris Under Traffic-Type Loading in Base and Subbase Applications." *Transportation Research Record*, No. 1714, Washington, D.C., 33-39.

- Blankenagel, B. J. and Guthrie, W. S. (2006). "Laboratory Characterization of Recycled Concrete for Use as Pavement Base Material." *Geomaterials 2006*, No.1952, 21-27.
- Camargo, F. F. (2008). "Strength and Stiffness of Recycled Base Materials Blended with Fly Ash." MS Thesis, University of Wisconsin-Madison, WI
- Camargo, F. F., Edil, T. B. and Benson, C. H. (2009). "Strength and Stiffness of Recycled Base Materials Blended with Fly Ash." *Transportation Research Board 88th Annual Meeting*. Washington, D.C.
- Chini, A. R., Kuo, S.-S., Armaghani, J. M. and Duxbury, J. P. (2001). "Test of Recycled Concrete Aggregatenin Accelerated Test Track." *Journal of Transportation Engineering*, No.127, Washington, D.C., 486-492.
- FHWA. (2008). "User Guideline for Byproducts and Secondary Use Materials in Pavement Construction". *FHWA Report FHWA-RD-97-148*, FHWA, VA.
- Guthri, S. W., Cooley, D., and Eggett, D. L. (2007). "Effects of Reclaimed Asphalt Pavement on Mechanical Properties of Base Materials." *Journal of the Transportation Research Board*, No.2005, Washington, D.C., 44-52.
- Heydinger, A. G., Xie, Q. L., Randolph, B. W. and Gupta, J. D. (1996). "Analysis of Resilient Modulus od dense and Open-graded Aggregates." *Transportation Research Board*, Washington, D.C., No.1547, 1-6.
- Juan, M. S. and Gutierrez, P. A. (2009). "Study on the Influence of Attached Mortar Content on the Properties of Recycled Concrete Aggregate." *Construction and Building Materials*, No.23, Washington, D.C., 872-877.
- Kim, W., Labuz, J. F. and Dai, S. (2007). "Resilient Modulus of Base Course Containing Recycled Asphalt Pavement." *Journal of the Transportation Research Board* , No.2005, Washington, D.C., 27-35.
- Kuo, S.-S., Mahgoub, H. S., & Nazef, A. (2002). "Investigation of recycled concrete made with limestone aggregate for a base course in flexible pavement." *Transportation Research Record*, No.1787, Washington, D.C., 99-108.
- Langer, W. H. (1988). "Natural aggregates of the conterminous, United States:" *Geological Survey Bulletin*, No.1594, 33.
- Lee, J., Edil, T. B., Benson, C. H. and Tinjum, J. M. (2010). "Use of BE<sup>2</sup>ST in Highways for Green Highway Construction Rating in Wisconsin." *Proceeding of The 1<sup>st</sup> T&DI Green Streets and Highway Conference*, Denver, CO.



- Leigh, N. G. and Patterson, L. M. (2004). "Construction Demolition Debris Recycling for Environmental Protection and Economic Development." Southeast Regional Environmental Finance Center
- Moosazedh, J. and Witczak, M. (1981). "Prediction of Subgrade Moduli for Soil that Exhibits Nonlinear Behavior." *Journal of Transportation Research Board*, No.810, Washington, D.C., 10-17.
- Nataatmadja, A. and Tan, Y. L. (2001). "Resilient Reponse of Recycled Concrete Road Aggregates." *Journal of Transportation Engineering*, No.127, Washington, D.C., 450-453.
- NCHRP. (2004). "Laboratory Determination of Resilient Modulus for Flexible Pavement Design." NCHRP Research Results Digest.
- Pan, T., Tutumluer, E. and Anochie-Boateng, J. (2006). "Aggregate Morphology Affecting Resilient Behavior of Unbound Granular Materials." *Transportation Research Record: Journal of the Transportation Research Board*, No.1952, Washington, D.C., 12-20.
- Poon, C.-S., Qiao, X., and Chan, D. (2006). "The Cause and Influence of Self-Cementing Properties of Fine Recycled Concrete Aggregates on the Properties of Unbound Sub-Base" *Waste Management*, No.26, 1166-1172.
- Pratt, E. (1993). "Current Uses and Evaluation of Recycled Materials in Highway Construction: Overview of the Northeastern States." Northeast Recycling Council.
- Saeed, A. (2008). "Performance-Related Tests of Recycled Aggregates for Use in Unbound Pavement Layers." Transportation Research Board of the National Academies. Washington, D.C.
- Saeed, A., Hammons, M. I., Feldman, D. R. and Poole, T. (2006). "Evaluation, Design and Construction Techniques for Airfield Concrete Pavement Used as Recycled Material for Base". Innovative Pavement Research Dpindation Airport Concrete Pavement Technology Program, Skokie, IL:.
- Schaertl, G. J. (2010). "*Scaling and Equivalency of Bench-scale Tests to Field Scale Conditions.*" MS Thesis, University of Wisconsin-Madison, WI
- Tian, P., Zaman, M. M. and Laguros, J. G. (1998). "Gradation and Moisture Effects on Resilient Moduli of Aggregate Bases." *Transportation Research Record*, No.1619, Washington, D.C., 75-84.
- Tutumluer, E. and Seyhan, U. (1998). "Neural Network Modeling of Anisotropic Aggregate Behavior from Repeated Load Triaxial Testa." *Transportation Research Record*, No.1615, Washington, D.C., 86-93.

USGS. (2010). "Crushed Stone: Statistical Compendium U.S. Geological Survey." Reston, VA.

Wen, H. and Edil, T. B. (2009). "Sustainable Reconstruction of Highways with In-Situ Reclamation of Materials Stabilized for Heavier Loads." *BCR2A Conference*, Champaign, IL, 1011-1017.

Wen, H., Warner, J., Edil, T. and Wang, G. (2008). "Laboratory Comparison of Crushed Aggregate and Recycled Pavement Material With and Without High Carbon Fly Ash." *Geotechnical and Geological Engineering* , No.28, 405-411.

## **TABLES**

Table 1. Index properties for Recycled Materials and Class 5 aggregate

Material	States	D <sub>10</sub> (mm)	D <sub>30</sub> (mm)	D <sub>50</sub> (mm)	D <sub>60</sub> (mm)	C <sub>u</sub>	C <sub>c</sub>	G <sub>s</sub>	Absorption (%)	Asphalt Content /Mortar Content (%)	Impurities (%)	Gravel (%)	Sand (%)	Fines (%)	USCS	AASHTO
Class 5 Aggregate	MN	0.1	0.4	1.0	1.7	21	1.4	2.57	—	—	0.25	22.9	67.6	9.5	GW-GM	A-1-b
Blend	MN	0.2	0.6	1.5	2.8	13	0.5	—	—	—	0.36	32.7	63.8	3.4	SP	A-1-b
RCA	MN	0.1	0.4	1.0	1.7	21	1.4	2.39	5.0	55	0.87	31.8	64.9	3.3	SW	A-1-a
	MI	0.4	4.1	9.7	12.3	35	3.9	2.37	5.4	—	0.35	68.5	28.3	3.2	GP	A-1-a
	CO	0.1	0.6	2.8	4.9	66	1.1	2.28	5.8	47	0.26	40.9	46.3	12.8	SC	A-1-b
	CA	0.3	1.7	4.8	6.8	22	1.4	2.32	5.0	37	0.26	50.6	47.1	2.3	GW	A-1-a
	TX	0.4	6.5	13.3	16.3	38	6.0	2.27	5.5	45	0.86	76.3	21.6	2.1	GW	A-1-a
	OH	0.2	1.2	3.4	5.3	34	1.7	2.24	6.5	65	0.16	43.2	49.5	7.3	SW-SM	A-1-a
	NJ	0.2	0.5	2.0	5.1	28	0.3	2.31	5.4	—	1.67	41.2	54.6	4.3	SP	A-1-b
RAP	MN	0.3	0.7	1.6	2.3	7	0.7	2.41	1.8	7.1	0.06	26.3	71.2	2.5	SP	A-1-a
	CO	0.4	0.9	2.2	3.3	9	0.7	2.23	3.0	5.9	0.09	31.7	67.7	0.7	SP	A-1-a
	CA	0.3	1.3	3.0	4.2	13	1.2	2.56	2.0	5.7	0.33	36.8	61.4	1.8	SW	A-1-a
	TX	0.7	2.5	5.4	7.9	11	1.1	2.34	1.3	4.7	0.05	41.0	44.9	1.0	SW	A-1-a
	OH	0.5	1.6	2.9	3.8	7	1.3	2.43	0.6	6.2	0.06	32.1	66.2	1.7	SW	A-1-a
	NJ	1.0	2.8	4.9	5.9	6	1.3	2.37	2.1	5.2	0.48	50.9	48.4	0.7	GW	A-1-a
	WI	0.6	1.4	2.7	3.6	6	0.9	2.37	1.5	6.2	0.08	30.9	68.5	0.5	SP	A-1-b
RPM	NJ	0.5	2.1	5.8	8.7	18	1.0	2.35	2.6	4.3	0.04	55.7	43.6	0.6	GW	A-1-b
	MI	0.4	1.7	4.6	6.5	17	1.1	2.39	1.7	5.3	0.13	49.3	50.4	0.4	SW	A-1-b

Note: Asphalt Content determined for RAP/RPM and Mortar Content determined for available RCA

D<sub>10</sub> = effective size, D<sub>30</sub> = particle size for 30% finer, D<sub>50</sub> = median particle size, D<sub>60</sub> = particle size for 60% finer, C<sub>u</sub> = coefficient of uniformity, C<sub>c</sub> = coefficient of curvature, G<sub>s</sub> = Specific Gravity, AC = Asphalt Content, Abs = Absorption, Note: Particle size analysis conducted following ASTM D 422, G<sub>s</sub> determined by ASTM D 854, Absorption of coarse aggregate were determined by ASTM C127-07, USCS classification determined by ASTM D 2487, AASHTO classification determined by ASTM D 3282, asphalt content determined by ASTM D 6307

Table 2. Maximum dry unit weight and optimum water content for material used in this study

Specimens	States	Optimum Water Content $W_{opt}$ (%)	Maximum Dry Unit Weight $\gamma_{dmax}$ (kN/m <sup>3</sup> )
Class 5 Aggregate	MN	8.9	20.1
Blend*	MN	8	21.3
RCA	MN	11.2	19.5
	MI	8.7	20.8
	CO	11.9	18.9
	CA	10.4	19.9
	TX	9.2	19.7
	OH	11.8	19.4
	NJ	9.5	19.8
RAP	MN	6.7	20.8
	CO	5.7	20.7
	CA	6.1	20.7
	TX	8	20.3
	OH	8.8	19.8
	NJ	6.5	20.4
	WI	7.3	20
RPM	MI	5.2	21.5
	NJ	6.3	20.6

Note:\*Blend consists of 50% RCA (MN) and 50% Class 5 aggregate obtained at MNROAD

field site

Table 3. Summary of maximum dry unit weight and optimum water content of RCA and RAP/RPM

Specimens	Optimum Water Content $W_{opt}$ (%)				Maximum Dry Unit Weight $\gamma_{dmax}$ (kN/m <sup>3</sup> )			
	AVG	STD	CV	Range	AVG	STD	CV	Range
RCA	10.4	1.29	12%	3.2	19.7	0.59	3%	1.9
RAP/RPM	6.7	1.13	17%	3.6	20.5	0.49	3%	1.7

Note: AVG=Average, SDT=Standard deviations, CV=Coefficients of variation

Table 4. Compaction characteristics of recycled pavements from the literature

Specimens		Optimum Water Content $W_{opt}$ (%)	Maximum Dry Unit Weight $\gamma_{dmax}$ (kN/m <sup>3</sup> )
		Average	Average
		(range)	(range)
RCA	UW-Madison	10.4	19.7
		(8.7~11.9)	(18.9~20.8)
	Literature	10.1	18.9
		(7.5~12.1)	(17.9~19.8)
RAP/RPM	UW-Madison	6.7	20.6
		(5.2~8.8)	(19.8~21.5)
	Literature	6.4	20.1
		(5.0~10.3)	(18.1~22.9)

Table 5. Summary resilient modulus (SRM), power function model fitting parameters  $k_1$  and  $k_2$  (Eq. 3.1), and Plastic strain for base materials

Material	States	External			Internal			Plastic Strain (%)	SRM <sub>INT</sub> / SRM <sub>EXT</sub>
		$k_1$	$k_2$	SRM (Mpa)	$k_1$	$k_2$	SRM(Mpa)		
Class 5 Aggregate	MN	14.9	0.43	152	43.2	0.47	525	1.60	3.5
Blend*	MN	18.2	0.43	182	50.2	0.49	675	1.05	3.7
RCA	MN	18.5	0.44	189	38.3	0.54	680	0.63	3.6
	MI	14.3	0.46	171	40.7	0.54	715	0.80	4.2
	CO	17.4	0.43	175	41.5	0.49	580	0.73	3.3
	CA	15.2	0.46	178	33.0	0.54	627	0.70	3.5
	TX	9.1	0.54	164	17.6	0.64	549	0.83	3.3
	OH	12.6	0.48	163	27.7	0.56	554	0.57	3.4
	NJ	22.0	0.42	208	49.6	0.50	735	0.55	3.5
RAP	MN	23.0	0.39	180	26.3	0.61	674	1.35	3.7
	CO	25.6	0.37	184	75.0	0.41	673	1.47	3.7
	CA	12.3	0.49	173	36.4	0.53	627	1.16	3.6
	TX	21.6	0.42	198	52.4	0.52	776	1.38	3.9
	OH	15.6	0.48	197	42.7	0.52	699	1.32	3.6
	NJ	23.5	0.41	209	54.6	0.48	715	2.13	3.4
	WI	29.5	0.41	266	65.0	0.51	968	0.89	3.6
RPM	MI	14.7	0.46	168	43.5	0.50	631	1.49	3.8
	NJ	26.3	0.43	264	61.6	0.52	989	1.26	3.8

Note: \*Blend consists of 50% RCA (MN) and 50% Class 5 aggregate obtained at MNROAD field site

Table 6. Summary resilient modulus (SRM), NCHRP model fitting parameters  $k_1$ ,  $k_2$ ,  $k_3$ ,  $k_6$  and  $k_7$  (Eq. 3.3)

Material	States	External						Internal					
		$k_1$	$k_2$	$k_3$	$k_6$	$k_7$	SRM (Mpa)	$k_1$	$k_2$	$k_3$	$k_6$	$k_7$	SRM (Mpa)
Class 5 Aggregate	MN	1791	0.7	-0.8	-0.4	2.2	144	4416	1.0	-0.9	-28.9	1.8	484
Blend*	MN	15697	1.5	-2.3	-137.8	6.1	191	48303	1.6	-2.2	-95.9	4.4	683
RCA	MN	4164	1.3	-1.7	-110.6	4.4	190	49316	1.7	-2.2	-114.5	5.1	648
	MI	2122	0.8	-1.0	-0.3	1.8	171	9201	0.8	-0.9	-0.5	2.1	715
	CO	1059	1.1	-1.0	-25.8	1.2	162	5358	1.1	-1.2	-8.9	1.5	520
	CA	2199	0.9	-1.2	-0.3	1.7	166	8023	1.0	-1.4	-0.3	1.7	563
	TX	2044	0.9	-1.2	-0.4	1.8	151	6179	1.5	-1.7	-31.1	2.3	490
	OH	1971	0.7	-0.8	-0.1	2.1	158	6819	0.9	-0.9	-0.5	2.6	522
	NJ	2639	0.8	-1.2	-0.6	1.6	203	7080	1.2	-1.4	-17.5	1.4	683
RAP	MN	2190	0.6	-0.8	-0.4	2.2	174	5444	1.2	-0.4	-97.6	4.5	665
	CO	2093	0.6	-0.9	-0.2	1.5	177	7720	0.7	-1.0	-0.2	1.6	629
	CA	2043	0.8	-1.0	-0.3	1.8	166	7935	1.0	-1.2	-0.3	1.8	589
	TX	1749	0.7	-0.7	-11.9	1.3	188	8451	0.5	-0.2	0.0	13.4	779
	OH	2368	0.8	-1.0	-0.2	1.7	192	8727	0.9	-1.2	-0.3	1.7	674
	NJ	2450	0.6	-0.7	-0.2	1.9	207	8680	0.7	-0.8	-0.4	1.9	715
	WI	3251	0.6	-0.7	-0.3	2.0	274	12594	0.7	-0.9	-0.3	1.9	1013
RPM	MI	2019	0.7	-0.9	-0.3	2.0	161	7843	0.7	-0.8	-0.2	2.1	614
	NJ	3207	0.7	-0.9	-0.1	1.8	264	8719	1.1	-1.1	-24.2	1.5	995

Note: \*Blend consists of 50% RCA (MN) and 50% Class 5 aggregate obtained at MNROAD field site

Table 7. Relationship between compaction characteristics and soil properties for recycled materials

Materials	Compaction Characteristics	Correlation Equations	R <sup>2</sup>
RCA	W <sub>opt</sub> (%)	$-0.064 * Cu + 0.763 * Absorption(\%) + 7.75$	0.65
	γ <sub>dmax</sub> (kN/m <sup>3</sup> )	$-0.374 * W_{opt}(\%) + 23.6$	0.83
RAP	W <sub>opt</sub> (%)	$-0.0626 * Cu - 1.349 * Absorption(\%) + 9.84$	0.92
	γ <sub>dmax</sub> (kN/m <sup>3</sup> )	$-0.289 * W_{opt}(\%) + 22.42$	0.83



Table 8. Relationship between resilient modulus, compaction characteristics, and soil properties for recycled materials

Materials	Resilient Modulus (MPa)	Correlation Equations	R <sup>2</sup>
RCA	SMR <sub>INT</sub>	$14683.478-(36.764*D_{30})-(72.719*w_{opt})$	0.89
RAP	SMR <sub>INT</sub>	$-2268.783-(285.884*Fines\ \%)+(628.742*AC\ \%)+$ $(201.107*D_{60})-(483.158*G_s)-(58.243*Absorption\ \%)$	0.99

AC: asphalt content

Table 9. Summary resilient modulus (SRM) and power model fitting parameters  $k_1$  and  $k_2$  (Eq. 4.1) for base materials for blended RAP with Class 5 aggregate

Specimens	External			Internal			SRM <sub>Class 5</sub> / SRM <sub>Blend</sub>
	$k_1$	$k_2$	SRM (MPa)	$k_1$	$k_2$	SRM (MPa)	
Class 5 aggregate	66.2	0.20	191	129.2	0.15	281	1.0
Blend (CO-MN)	94.5	0.18	244	44.3	0.37	313	1.1
RAP (CO)	129.3	0.16	297	122.6	0.20	362	1.3
Class 5 aggregate	66.2	0.20	191	129.2	0.15	281	1.0
Blend (CA-MN)	76.4	0.22	245	209.7	0.12	391	1.4
RAP (CA)	122.5	0.14	256	348.8	0.06	473	1.7
Class 5 aggregate	66.2	0.20	191	129.2	0.15	281	1.0
Blend (MN)	90.7	0.17	230	116.8	0.21	350	1.2
RCA (MN)	122.5	0.14	256	348.8	0.06	473	1.7

## FIGURES

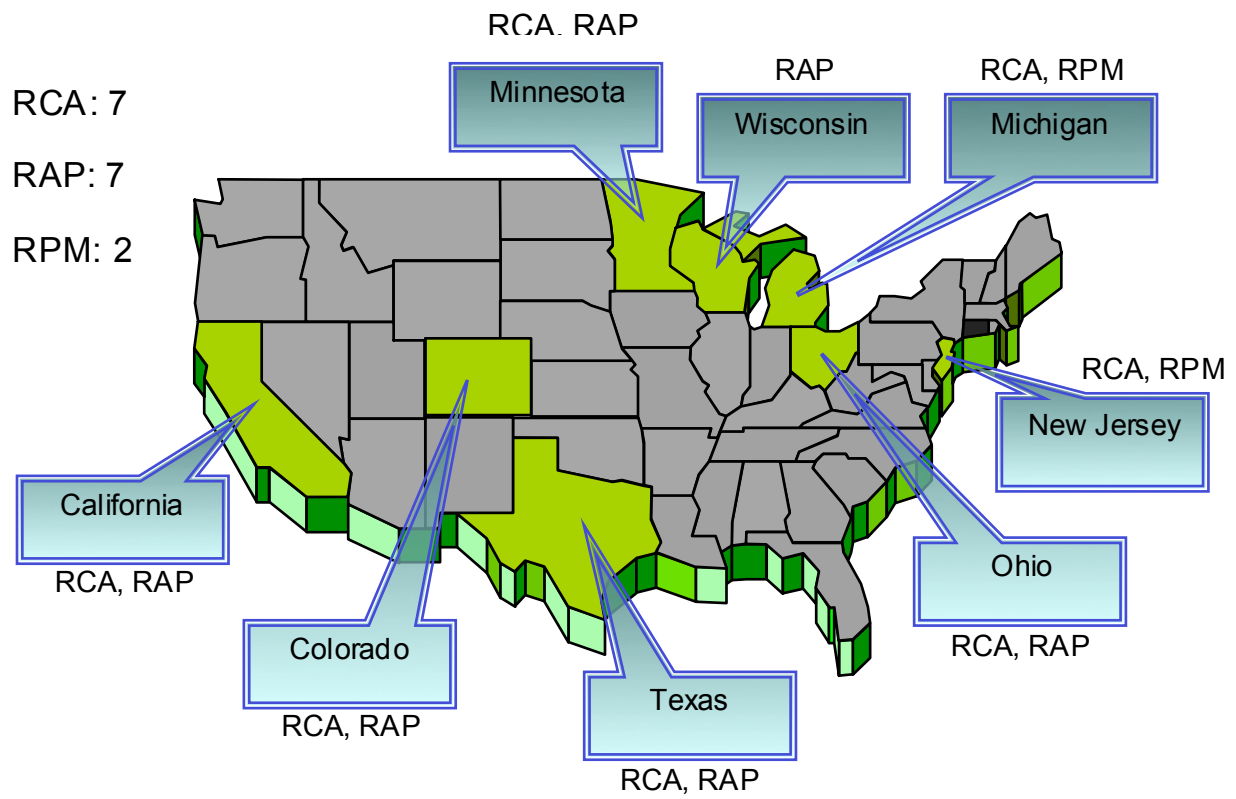


Fig. 1. Locations of recycled material used in this study

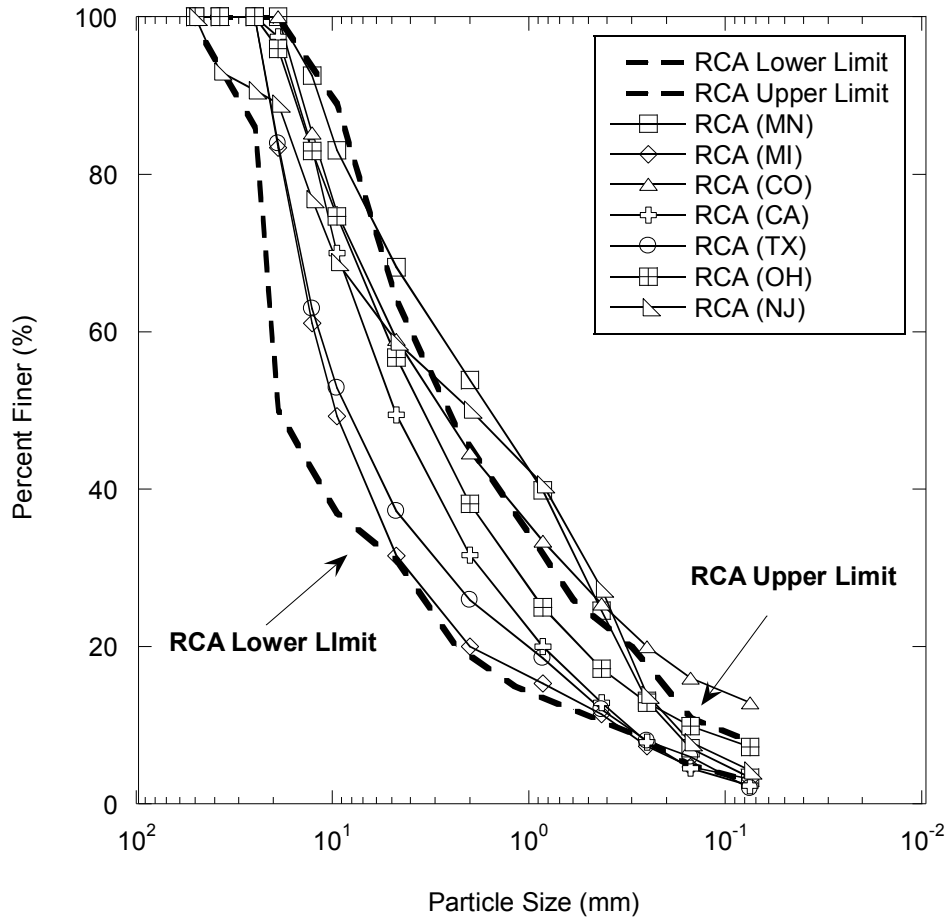


Fig. 2. Particle Size Distribution for RCA and RCAs reported lower and upper limits from literature

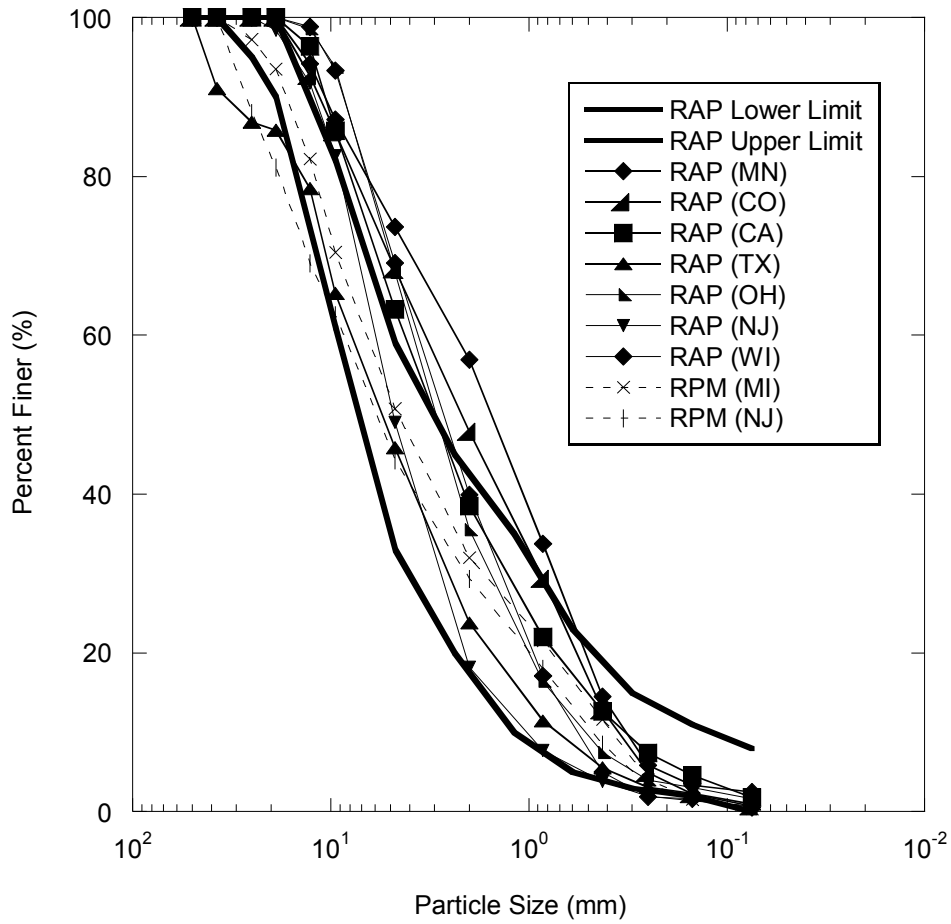


Fig. 3. Particle Size Distribution for RAP/RPM and RAPs reported lower and upper limits from literature

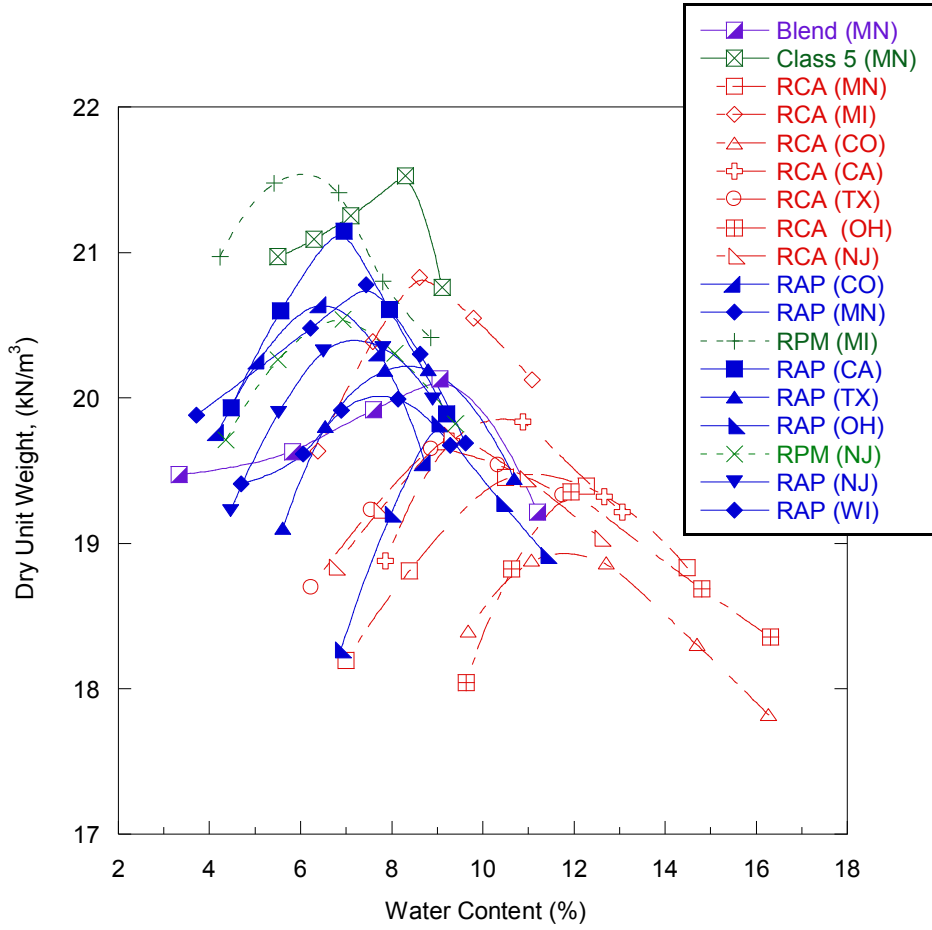


Fig. 4. Compaction Curves for recycled materials and Class 5 aggregate used in this study

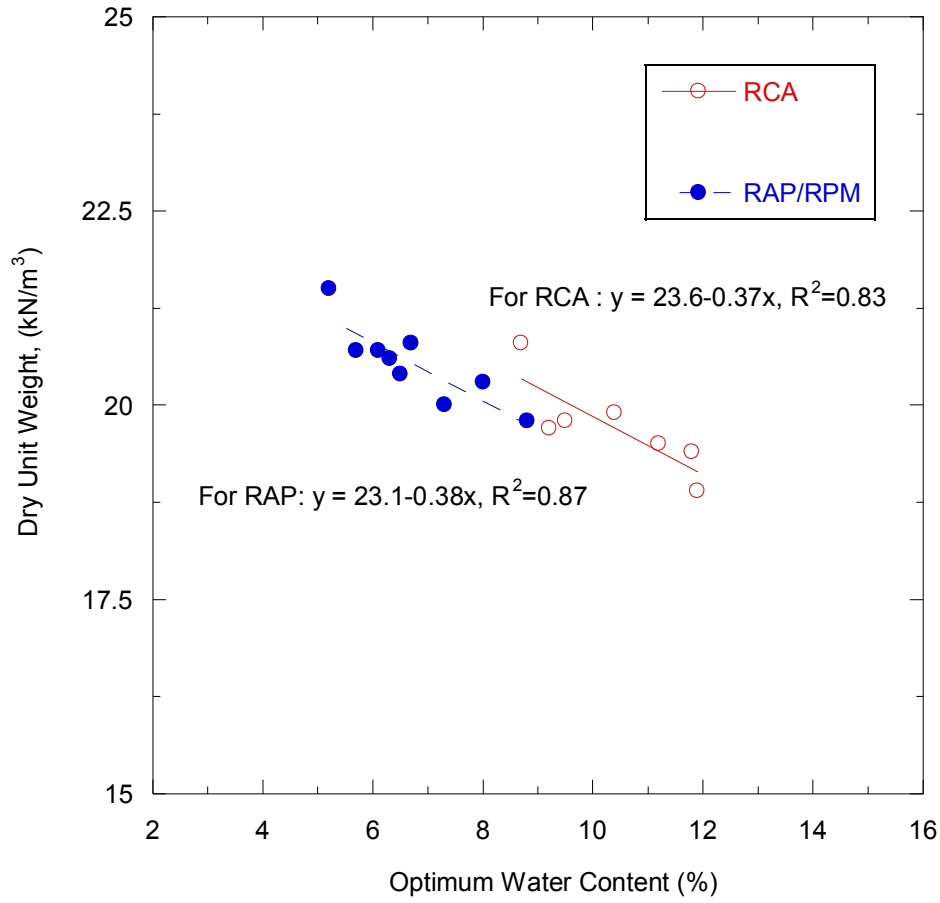


Fig. 5. Maximum dry unit weight and optimum water content for RCA and RAP.



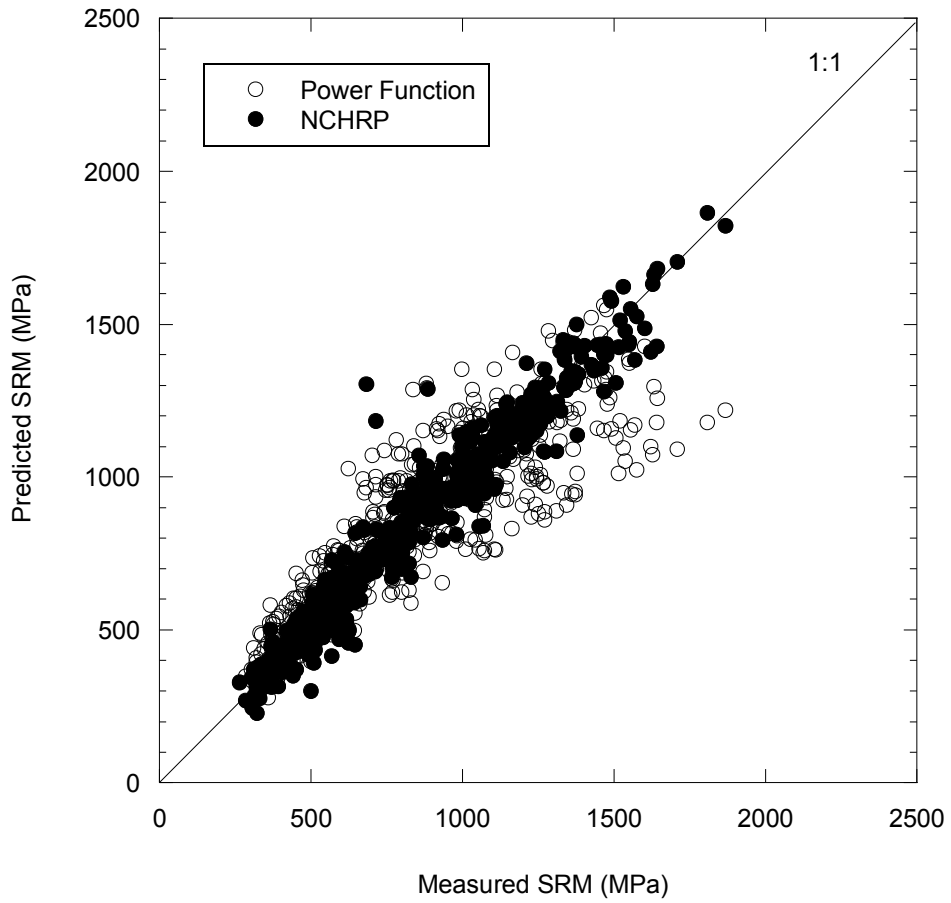


Fig. 6. Relationship between measured SRM and predicted SRM using the Power Function and NCHRP models for RCA (Internal)

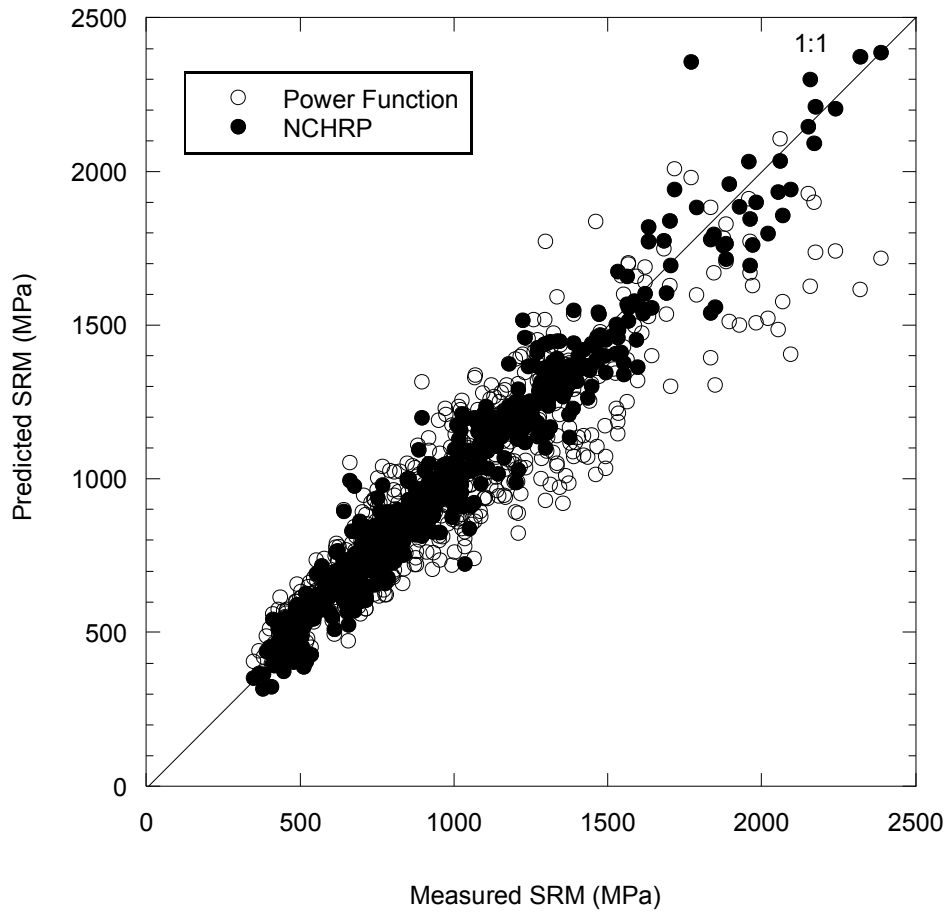


Fig. 7. Relationship between measured SRM and predicted SRM using the Power Function and NCHRP models for RAP/RPM (Internal)

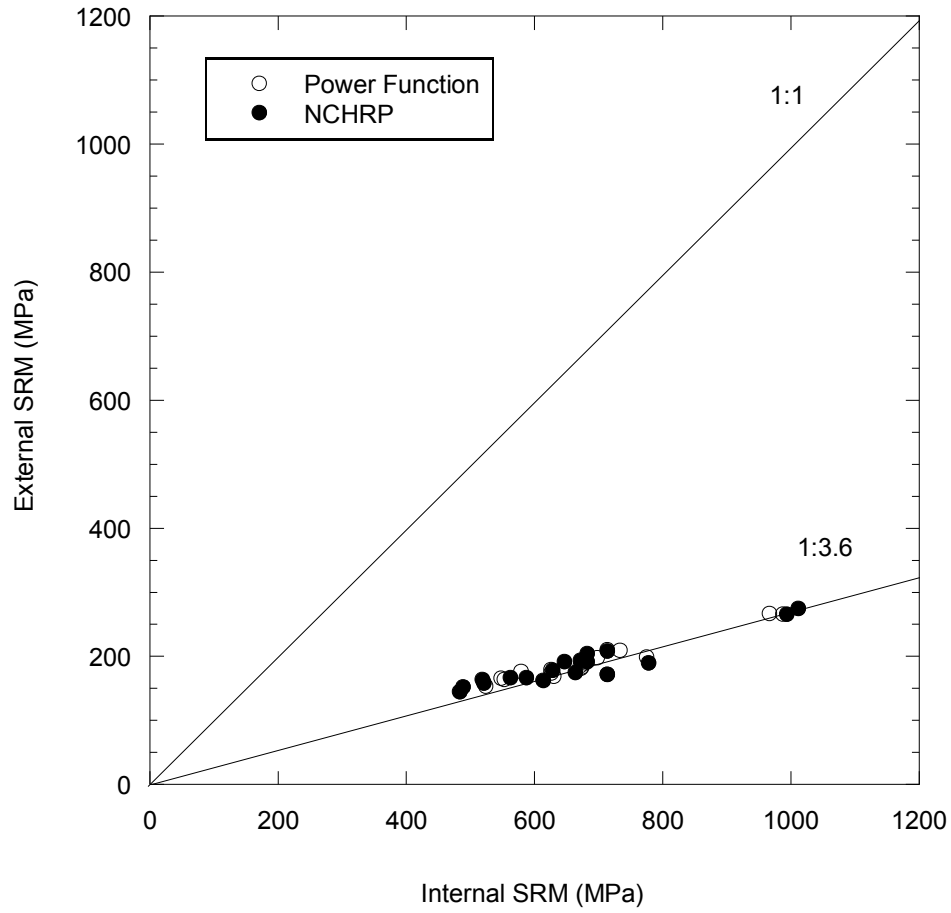


Fig. 8. Ratio of internal to external SRM versus internal SRM using the power function and NCHRP models for recycled materials

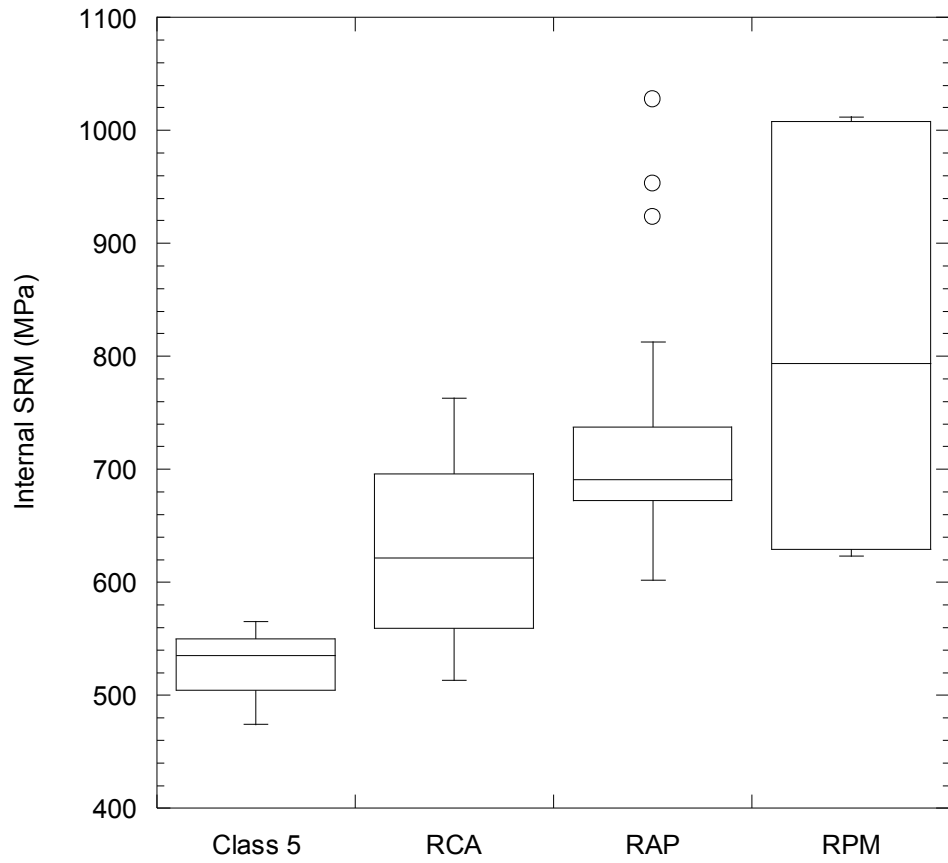


Fig. 9. Summary resilient modulus (SRM) measured by Internal LVDTs for Class 5 aggregate, RCA, RAP, and RPM

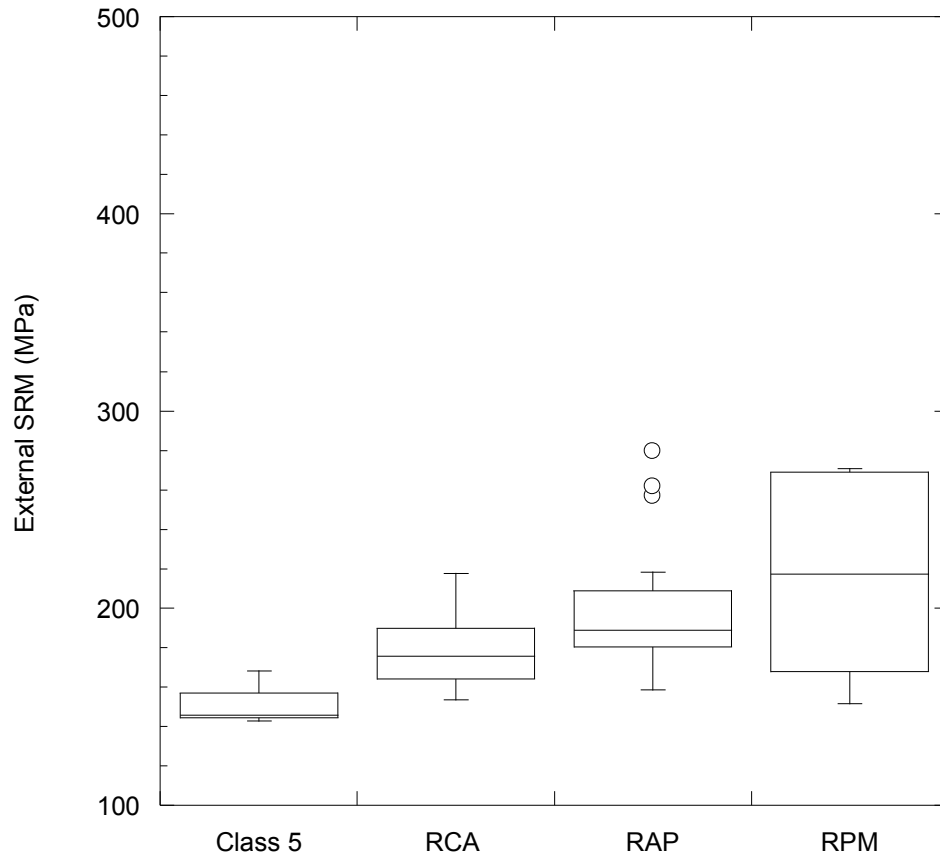


Fig. 10. Summary resilient modulus (SRM) measured by External LVDTs for Class 5 aggregate, RCA, RAP, and RPM

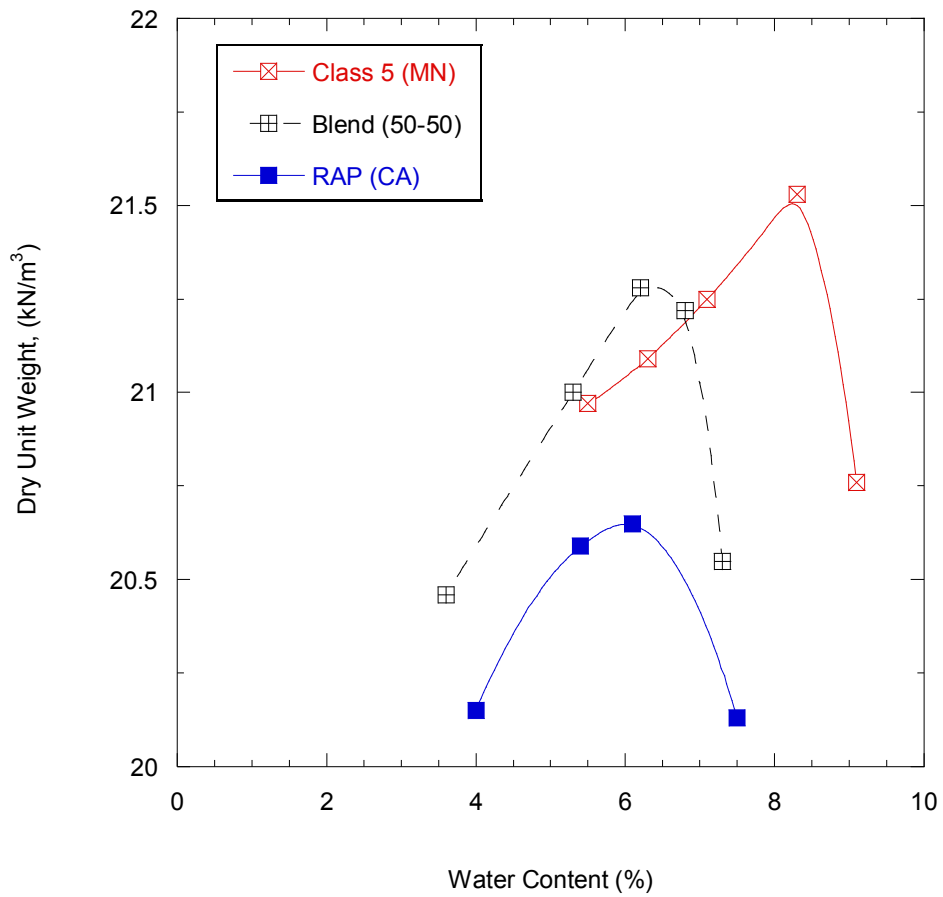


Fig. 11. Compaction curves for RAP (CA) and RAP (CA) blended with 50 % of Class 5 aggregate

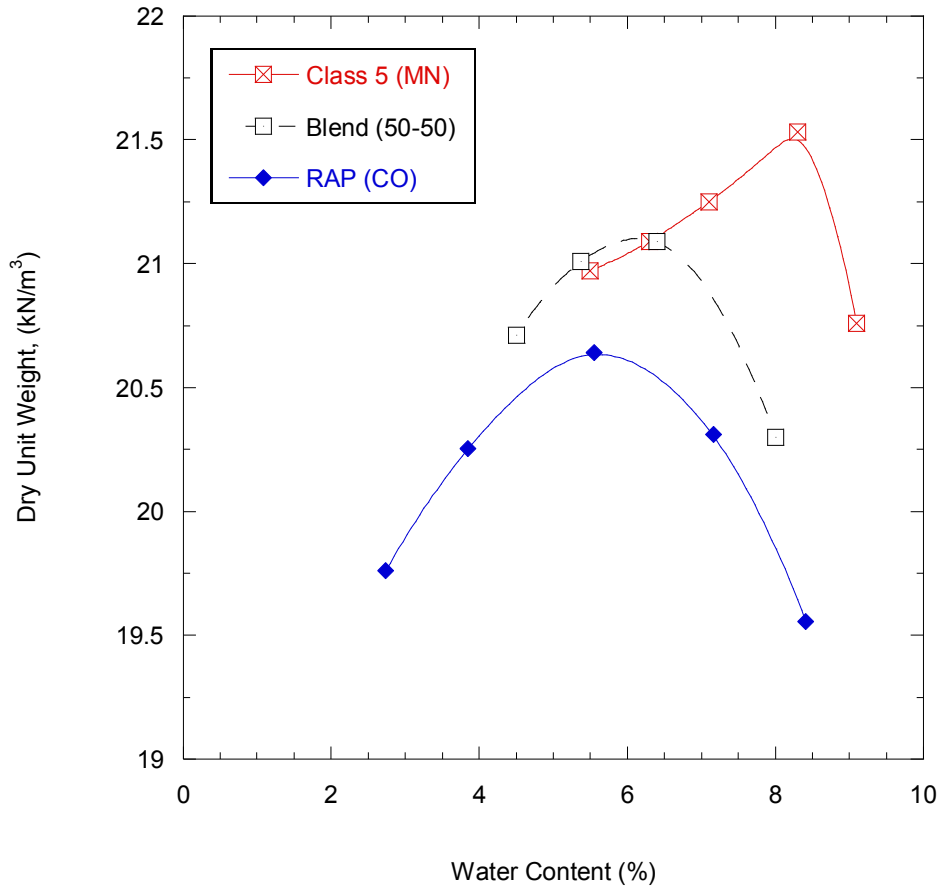


Fig. 12. Compaction curves for RAP (CO) and RAP (CO) blended with 50 % of Class 5 aggregate

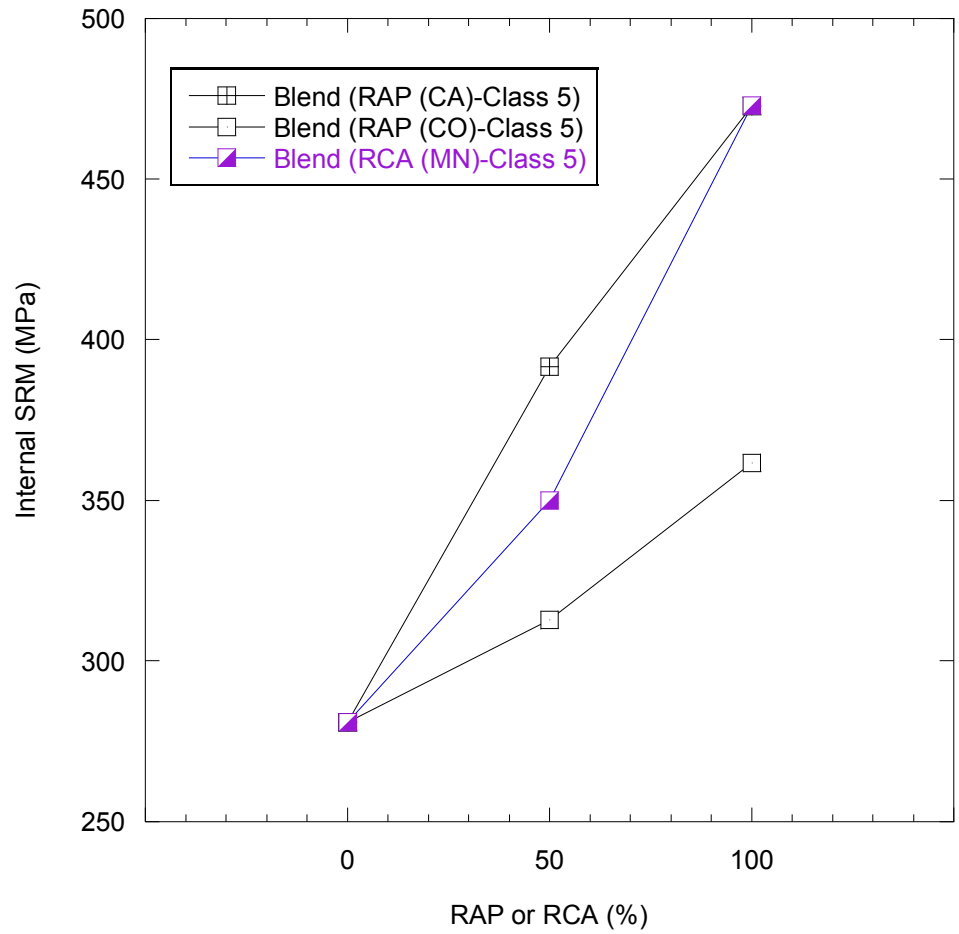


Fig. 13. Internal Summary Resilient Modulus (SRM) for Class 5 aggregate blended with RAP (CO), RAP (CA) and RCA (MN) at different percentages (0%, 50%, 100%).



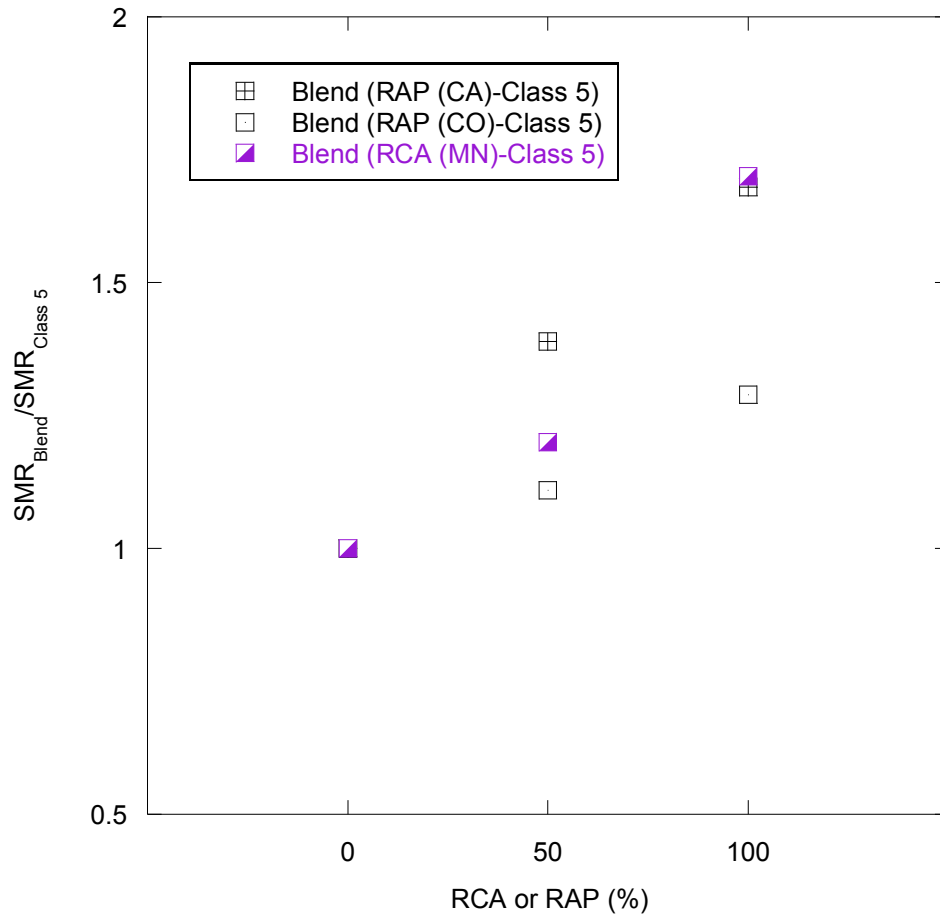


Fig. 14. Normalized Summary Resilient Modulus (SRM) for Class 5 aggregate blended with RAP (CO) and RAP (CA) at different percentages

**SCALING AND EQUIVALENCY  
OF  
BENCH-SCALE TESTS  
TO  
FIELD SCALE CONDITIONS**

**Recycled Asphalt Pavement and  
Recycled Concrete Aggregate**

**TPF-5 (129) Recycled Unbound Materials**

Mn/DOT Contract No. 89264 Work Order No. 2

CFMS Contract No. B14513

Task 1C: Scaling and Equivalency: Specimen Tests to Field-Scale  
Conditions

**Gregory J. Schaertl, Tuncer B. Edil, and Craig H. Benson  
University of Wisconsin- Madison**

**August 21, 2010**

## EXECUTIVE SUMMARY

The objectives of this study were to determine the resilient modulus for recycled materials using Large-Scale Model Experiments (LSME) to replicate field conditions. Tests were conducted on two recycled materials; recycled asphalt pavement (RAP) and recycled concrete aggregate (RCA), as well as on one blended material consisting of 50% RCA and 50% conventional base material (Class 5). The results of LSME testing were compared to the resilient modulus determined using laboratory methods in accordance with NCHRP 1-28a and field scale methods using falling weight deflectometer (FWD). The scalability of the laboratory results to field conditions was addressed by adjusting the resilient modulus to reflect a comparable stress-state and strain level. The plastic deformation of materials tested in the LSME was also assessed. A conventional base course meeting the gradation standard of a Minnesota Department of Transportation Class 5 aggregate was used as a reference material in this study.

The plastic deformation of RAP was 211% and 102% greater than that experienced by Class 5 for layer thicknesses of 0.3 m and 0.2 m, respectively, whereas the plastic deformation of RCA was 69% smaller than the plastic deformation experienced by the Class 5 for both layer thicknesses. The amount of deformation experienced by the Class 5 for both layer thicknesses. The amount of deformation experienced by the blended RCA/Class 5 was 39% and 19% smaller for the 0.2-m and 0.3-m thick layers, respectively, indicating that the amount of deformation experienced in the base decreases with an increase in RCA. The amount of plastic deformation experienced by the RAP, RCA and Class 5 decreased with an increase in layer thickness. The plastic deformation of RAP and RCA

decreased 44% and 10%, respectively, for an increase in layer thickness from 0.2 m to 0.3 m. Class 5 experienced a reduction in plastic deformation of about 14% for an increase in layer thickness from 0.2 m to 0.3 m, which was slightly larger than the plastic deformation experienced by RCA, but significantly smaller than the plastic deformation experienced by RAP.

The summary resilient modulus (SRM) of RCA was 24% to 77% greater than that of Class 5, while the SRM of RAP was 18 to 33% greater. The SRM of the blended RCA/Class 5 was 17% to 29% greater than that of Class 5, which was comparable in magnitude to the SRM of RAP. The SRM of specimens increased with an increase in RCA content, although not in a linear manner. The cause of this non-linear behavior may be that the blended material is not a perfect 50%/50% blend. The SRM of all materials increased with an increase in layer thickness. The magnitude of this increase was common between the materials, and was between 130 MPa and 176 MPa.

The recycled granular material tested in the LSME is sensitive to layer thickness, indicating that the resilient modulus of the material is sensitive to varying strain levels. The resilient modulus was normalized to the low-strain (maximum) modulus, and plotted as a function of shear strain. The resulting plot suggests a backbone curve which describes the stress-strain dependency of resilient modulus for a given material. After applying corrections for stress-state and strain level, the resulting low-strain moduli for FWD, LSME and bench-scale tests were determined and found to be of the same magnitude within a reasonable amount of variance thus indicating the scalability of laboratory modulus to operating field modulus.

## ACKNOWLEDGEMENTS

Thank you to my advisors, Professors Tuncer B. Edil and Craig H. Benson, for their guidance and support during my studies at the University of Wisconsin-Madison. Special thanks are extended to Professor James M. Tinjum for serving on my committee and to Professors Dante Fratta and James A. Schneider for providing scholarly insight. Much appreciation is extended to Ali Ebrahimi, Brian R. Kootstra, William G. Lang, and Xiaodong “Buff” Wang for helping to get the project started, and to Young-Hwan Son, Kyu Sun Kim, Timothy Alex Boecher, Logan Bailey, Jeff Casmer, Ozlem Bozyurt and Apisak Jutasiriwong for helping to keep the project going.

The past year and a half has been one of the most important and enriching periods of my life, and I owe it all to the friends and acquaintances I have made during that time. Their energy and support have kept me positive throughout my academic tenure, and will no doubt continue to inspire me as I embark on my professional career. This thesis is dedicated to all of them.

## TABLE OF CONTENTS

EXECUTIVE SUMMARY .....	i
TABLE OF CONTENTS .....	iv
LIST OF TABLES .....	vi
LIST OF FIGURES .....	vii
1. Introduction .....	1
2. Background .....	3
2.1. Production of Recycled Materials .....	3
2.2. Recycled Materials Used as Unbound Base Course .....	4
2.3. Resilient Modulus .....	8
2.3.1. Definition of Resilient Modulus .....	8
2.3.2. Factors that affect the Resilient Modulus of Unbound Aggregate .....	9
2.3.3. Small-Scale Determination of Resilient Modulus of Unbound Aggregate .....	11
2.3.4. Large-Scale Model Experiments for Determination of Resilient Modulus of Unbound Aggregate .....	12
3. Materials and Methods .....	15
3.1. Materials .....	15
3.2. Small Specimen-Scale Testing .....	17
3.3. Large-Scale Model Experiment .....	20
3.3.1. Apparatus and Loading Methodology .....	20
3.3.2. Deflection Measurements .....	25
3.3.3. Data Inversion .....	25
3.3.4. Base Course Compaction .....	26
3.3.5. Field-Scale Falling Weight Deflectometer Testing .....	26
4. Results .....	29
4.1. Deflection of LSME .....	29
4.2. Comparison of Large and Small-Scale Resilient Moduli .....	50
4.3. Scaling Laboratory Results to Field Conditions .....	61
4.3.1. Background .....	61
4.3.2. Measurement of Low-strain Modulus .....	62

4.3.3. Development of Backbone Curve.....	65
4.3.4. Scaling Specimen Tests to Field-Scale Conditions .....	67
5. Summary and Conclusions .....	78
REFERENCES .....	81
APPENDIX A .....	86
APPENDIX B .....	92

## LIST OF TABLES

Table 3.1. Index properties for RAP, Class 5, RCA, and Blended RCA/Class 5.

Table 3.2. Inputs used for MICHPAVE for determining stress on base layer. (Adapted from Kootstra 2009)

Table 4.1. Summary Resilient Modulus (SRM) and power model fitting parameters  $k_1$  and  $k_2$  (Eq. 2.2) for base materials.

Table 4.2. Summary Resilient Modulus (SRM) and power model fitting parameters  $k_1$  and  $k_2$  (Eq. 2.2) for base materials.

Table 4.3. Bulk stress, resilient modulus, low-strain modulus and normalized resilient modulus for FWD, LSME and bench-scale tests.

Table 4.4. Resilient modulus and low-strain modulus at field bulk stress.

Table 4.5. Variance of low-strain elastic modulus obtained at field bulk stress.

Table B. 1. Layer coefficients and structural numbers for different LSME thicknesses.



## LIST OF FIGURES

- Fig. 3.1. Particle size distributions for RAP, RCA, Blended RCA/Class 5 and Class 5 with MnDOT specifications.
- Fig. 3.2. Modified compaction curves for RAP, RCA, Blended RCA/Class 5 base, and Class 5.
- Fig. 3.3. Schematic of LSME testing setup.
- Fig. 3.4. Vertical stress on surface of base course vs. radial distance from center of traffic loading predicted by MICHPAVE.
- Fig. 3.5. Pavement profiles of cells tested using FWD at MnROAD testing facility. (Adapted from Johnson et al. 2009)
- Fig. 4.1. Total and plastic deflection of surface and subgrade layers vs. number of loading cycles for RAP.
- Fig. 4.2. Total and plastic deflection of surface and subgrade layers vs. number of loading cycles for RCA.
- Fig. 4.3. Total and plastic deflection of surface and subgrade layers vs. number of loading cycles for blended RCA/Class 5.
- Fig. 4.4. Total and plastic deflection of surface and subgrade layers vs. number of loading cycles for Class 5.
- Fig. 4.5. Surface (total), subgrade, and net elastic deflection vs. number of loading cycles for RAP.
- Fig. 4.6. Surface (total), subgrade, and net elastic deflection vs. number of loading cycles for RCA.
- Fig. 4.7. Surface (total), subgrade, and net elastic deflection vs. number of loading cycles for blended RCA/Class 5.
- Fig. 4.8. Surface (total), subgrade, and net elastic deflection vs. number of loading cycles for Class 5.
- Fig. 4.9. Comparison of surface and subgrade deflections for RAP, RCA, blended RCA/Class 5, and Class 5.
- Fig. 4.10. Comparison of (a) net elastic and (b) net plastic deflections for RAP, RCA, blended RCA/Class 5, and Class 5.
- Fig. 4.11. Comparison of net base elastic and net base plastic deflections vs. RCA content for RCA, blended RCA/Class 5, and Class 5.
- Fig. 4.12. Plastic strain vs. loading cycle for RAP.
- Fig. 4.13. Plastic strain vs. loading cycle for RCA.

- Fig. 4.14. Plastic strain vs. loading cycle for blended RCA/Class 5.
- Fig. 4.15. Plastic strain vs. loading cycle for Class 5.
- Fig. 4.16. Resilient modulus vs. bulk stress for bench-scale and LSME test methods for RAP.
- Fig. 4.17. Resilient modulus vs. bulk stress for bench-scale and LSME test methods for RCA.
- Fig. 4.18. Resilient modulus vs. bulk stress for bench-scale and LSME test methods for blended RCA/Class 5.
- Fig. 4.19. Resilient modulus vs. bulk stress for bench-scale and LSME test methods for Class 5.
- Fig. 4.20. Comparison of summary resilient modulus for RAP, RCA, blended RCA/Class 5, and Class 5.
- Fig. 4.21. Summary Resilient Modulus vs. layer thickness for RAP, RCA, blended RCA/Class 5, and Class 5.
- Fig. 4.22. Summary Resilient Modulus vs. RCA content for RCA, blended RCA/Class 5, and Class 5.
- Fig. 4.23. Simplified test setup to determine low-strain constraint modulus with applied stress near the surface. (Adapted from Edil and Fratta 2009)
- Fig. 4.24. Low-strain elastic modulus as a function of applied vertical stress.
- Fig. 4.25. Backbone curve fit to FWD, LSME and bench-scale data for RAP.
- Fig. 4.26. Backbone curve fit to FWD, LSME and bench-scale data for RCA.
- Fig. 4.27. Backbone curve fit to FWD, LSME and bench-scale data for blended RCA/Class5.
- Fig. 4.28. Backbone curve fit to FWD, LSME and bench-scale data for Class 5.
- Fig. 4.29. Resilient modulus at field bulk stress ( $\theta_f$ ) for RAP, RCA, blended RCA/Class 5, and Class 5.
- Fig. 4.30. Low-strain elastic modulus at field bulk stress ( $\theta_f$ ) for RAP, RCA, blended RCA/Class 5, and Class 5 as estimated from different test methods.
- Fig. A.1. Overview of abbreviated test pit area prior to material placement.
- Fig. A. 2. Placement of RPM within abbreviated test pit area.
- Fig. A.3. Comparison of resilient modulus of RPM obtained for full and abbreviated test pit areas with RCA, RAP, blended RCA/Class 5 and Class 5 obtained for abbreviated test pit area.
- Fig. B. 1. Layer coefficient vs. base layer thickness for RAP, RCA, blended RCA/Class 5, and Class 5.

## 1. Introduction

The production of crushed stone aggregate in the United States was estimated at 2.2 billion metric tons in 1996, of which the U.S. highway system accounts for over 40 percent of the total demand (Grogan 1996). However, rapidly decreasing sources of virgin aggregate, along with limits placed upon aggregate production by environmental regulation and land use policies, has caused the price of these materials to increase dramatically (ACPA 2009). Conversely, the production of demolition and construction waste has increased as the amount of landfill available to contain this material has decreased (Poon et al. 2006, Chini et al. 2001). The need to find appropriate disposal locations for this material has been of increasing concern (Kuo et al. 2002). Recycling programs offer a viable solution to both problems.

The use of recycled materials as recycled base course in new or rehabilitated roadway construction has become more common in the last twenty years, with some municipalities reporting as much as 400,000 tons of recycled materials used in this manner (Bennert et al. 2000, Nataatmadja and Tan 2001). Recycled roadway materials are typically generated and used at the same construction site, providing increased savings in both money and time (Bennert et al. 2000). It has been speculated that in some municipalities recycled materials cost less to use than conventional crushed-stone base material by as much as 30% (Blankenagel and Guthrie 2006).

Recycled asphalt pavement (RAP) and recycled concrete aggregate (RCA) are materials commonly used as unbound base course in the construction of

roadway pavement. RAP is produced by removing and reprocessing existing asphalt pavement, and RCA is the product of the demolition of concrete structures such as buildings, roads and runways (Kuo et al. 2002, Guthrie et al. 2007, FHWA 2008). The production of RAP and RCA results in an aggregate that is well graded and of high quality, and the costs of recycled materials have been estimated to be 25% to 50% cheaper than traditional aggregates (Guthrie et al. 2007, FHWA 2008). Despite the increased acceptance of recycled base materials in construction, research concerning the mechanical properties and durability of such materials has been lacking (Bennert et al. 2000, Nataatmadja and Tan 2001, Guthrie et al. 2007).

The objectives of this study were to determine the resilient modulus and permanent deformations of RAP and RCA in the laboratory using Large-Scale Model Experiments (LSME) to simulate field conditions, and to determine the effect of varying RCA content and layer thickness on material stiffness. Scaling between LSME, typical bench-scale laboratory, and falling weight deflectometer (FWD) testing in a road section constructed of these materials is also discussed. This thesis describes the findings of the study.

## **2. Background**

### **2.1. Production of Recycled Materials**

Recycled asphalt pavement (RAP) and recycled concrete aggregate (RCA) are two materials commonly used as an alternative to virgin aggregate in roadway construction and rehabilitation. There is some ambiguity regarding the nomenclature involved in the production of RAP. RAP refers to the removal and reuse of the hot mix asphalt (HMA) layer of an existing roadway. Recycled pavement material (RPM) is a term used by some investigators to describe pavement materials reclaimed through a less precise process in which the HMA with either part of the base course layer or the entire base course layer with part of the underlying subgrade is reclaimed for use (Li et al. 2007, Wen and Edil 2009). Unless specified, these two distinct recycled asphalt materials will be collectively referred to as RAP.

RAP is typically produced through milling operations, which involve the grinding and collection of the existing HMA. RPM is typically excavated using full-size reclaimers or portable asphalt recycling machines (Guthrie et al. 2007, FHWA 2008). RAP can be stockpiled, but is most frequently processed immediately and reused on-site. Grading of RAP is typically achieved through pulverization with a rubber tired grinder (Bejarano et al. 2003). Typical RAP gradations resemble a crushed natural aggregate, with a higher content of fines resulting from degradation of the material during milling and crushing operations. The inclusion of subgrade materials in RPM can also contribute to higher fines content. Milling produces a finer gradation of RAP when compared to crushing (FHWA 2008).

RCA production involves crushing to achieve gradations comparable to typical roadway aggregate. Fresh RCA contains a high amount of debris and reinforcing steel that must be removed prior to placement. A jaw crusher breaks any debris from the RCA and provides an initial crushing. Debris is removed along a picking belt, and the remaining concrete is further crushed and screened to a specified gradation (Kuo et al. 2002). RCA is very angular in shape with a lower particle density and greater angularity than would normally be found in traditional virgin base course aggregates. Residual mortar and cement paste found on the surface of RCA contributes to a rougher surface texture, lower specific gravity, and higher water absorption compared to typical roadway aggregates (Kuo et al 2002, FHWA 2008).

## **2.2. Recycled Materials Used as Unbound Base Course**

Several studies have been conducted comparing the mechanical properties of pure RAP and RCA with those of typical roadway base course aggregates. Bejarano et al. (2003) investigated the strength and stiffness of pure RAP compared to typical base course aggregate. Testing was performed on one RAP and two virgin base course aggregates. Individual specimens for each material were compacted at optimum moisture content (OMC) and at 95% and 100% of maximum wet density (MWD) according to CalTRANS specification CTM 216. Static triaxial tests were performed at confining pressures of 0, 35, 70 and 105 kPa. Stiffness tests were conducted according to AASHTO TP-46. Regardless of compaction effort, the shear strength of RAP and virgin aggregate were of comparable

magnitude, and the stiffness of RAP was greater than that of virgin aggregate. An increase in compaction effort increased the stiffness of RAP and one of the aggregate specimens, but had no effect on the second aggregate specimen.

Guthrie et al. (2007) evaluated the effects of RAP content on the shear strength and stiffness of roadway base course aggregate. Two RAP and two aggregates were chosen for the investigation. Specimens were prepared at RAP percentages of 100%, 75%, 50%, 25% and 0% (100% aggregate) for each of the possible RAP/aggregate permutations using modified compaction effort (ASTM D 1557). Specimen strength was determined by the California Bearing Ratio test (ASTM D 1883). Specimen stiffness was determined by free-free resonant column after compaction, after 72 hours of heating at 60°C to simulate summer conditions, and after an 11-day soaking/submerging period to simulate field saturation.

Specimen strength decreased with an increase in RAP content. The stiffness of specimens tested immediately after compaction decreased with the addition of 25% RAP, and then increased for RAP contents of 50%, 75%, and 100%. This trend reversed after 72 hours of heating: the stiffness of the material increased with the addition of 25% RAP, and then decreased for increased RAP content. Guthrie attributes this decrease in stiffness to the softening of asphalt during the heating process. After 11 days of soaking, the material maintained the same decrease-increase behavior as the heated specimen. However, the soaked materials displayed a 40% to 90% decrease in stiffness when compared to the heated material.

Kim et al. (2007) studied the effect of RAP content on the stiffness of blended aggregate base course. Stiffness tests were performed on pure RAP and aggregate samples and an in-situ blend of full-depth reclamation (FDR) material in accordance with National Highway Research Program testing protocol 1-28A (NCHRP 1-28a). Specimens were prepared at RAP percentages of 75%, 50%, 25% and 0% (i.e., 100% aggregate) and at moisture contents corresponding to 65% and 100% of OMC under standard compaction effort (AASHTO T 99). Stiffness increased for both an increase in RAP content and an increase in confining pressure. At higher confining pressures, the stiffness increased faster for specimens with higher RAP content. Specimens tested at 65% OMC had higher stiffness when compared to specimens prepared at 100% OMC at all confining pressures.

Bennert et al. (2000) investigated the shear strength of pure RAP and RCA compared to typical aggregate, and evaluated the effect of RAP and RCA content on the stiffness of blended aggregate base course. Strength tests were performed on one RAP, one RCA, and one aggregate sample. Specimens were compacted at maximum dry density (MDD) and OMC using standard compaction effort in accordance with methods described in AASHTO TP46-94, and loaded under drained static triaxial conditions at a common confining load of 103.42 kPa. Shear strength was higher for RCA than RAP; however shear strength was higher for pure aggregate than either RAP or RCA.

Stiffness tests were conducted according to AASHTO TP46-94. Specimens were prepared with RAP and RCA percentages of 100%, 75%, 50%, 25% and 0% (100% aggregate). Stiffness was higher for RAP and RCA than pure aggregate, and



increased with an increase in RAP or RCA content. RCA experienced lower permanent strain than pure aggregate; however RAP experienced higher permanent strain than RCA or pure aggregate. Bennert et al. (2000) suggest that the high permanent strains experienced by RAP may be due to either the breakdown of asphalt binder under loading or deficiencies inherent in the testing sequence itself.

Nataatmadja and Tan (2001) evaluated the relationship between the pre-crushing compressive strength and post-crushing stiffness of RCA. Four RCA with pre-crushing compressive strengths of 15, 18.5, 49 and 75 MPA were tested for stiffness according to methods proposed by Nataatmadja (1992). Each material was crushed and mixed to a particle size distribution comparable to typical roadway aggregate. Specimens were compacted at 89% of OMC using modified compaction effort (AS 1289.5.2.1). The stiffness of RCA increased with an increase in compressive strength from 15 MPa to 18.5 MPa, and again from 18.5 MPa to 49 MPa. However an increase in compressive strength from 49 MPa to 75 MPa resulted in a decrease in stiffness. Nataatmadja and Tan suggest that RCA with very high compressive strengths are more prone to break into elongated particles during crushing. Elongated particles were more prone to degradation after extensive loading, resulting in a lower stiffness than would otherwise be expected.

Camargo et al. (2009) compared the strength and stiffness of two recycled materials, RPM and recycled road surface gravel (RSG), to the strength and stiffness of an aggregate graded to the specifications for the Minnesota Department of Transportation (MnDOT) Class 5 base course. Specimen strength was determined by the California Bearing Ratio (CBR) test according to ASTM D 183,

and stiffness was determined by NCHRP 1-28a. The RPM and RSG each had a higher CBR than the typical base course aggregate, although all three materials had CBR values that were lower than the typically desired base course CBR value of 50. The RPM and RSG had a higher and lower stiffness, respectively, when compared to the Class 5 aggregate. The plastic strain experienced by the specimens during stiffness testing was lowest for RPM and highest for RSG and Class 5, which shared a plastic strain that was similar in magnitude.

Burrego et al. (2009) tested four RAP materials to quantify the variability of stockpiles in terms of gradation, asphalt content, and sand equivalency. An evident variation in gradation was noted for the RAP taken directly from stockpiles, although the variation was small after the material was subjected to ignition oven testing. The content of gravel, coarse sand, and fine sand were similar for each of the RAP samples. Burrego found that the asphalt content of RAP, which varied from 4.5% to 8.5%, had a significant effect on the gradation of the material. The sand equivalencies of the RAP samples were between 50 and 91.

## **2.3. Resilient Modulus**

### **2.3.1. Definition of Resilient Modulus**

Resilient modulus is a measure of a material's ability to deform elastically under cyclic compressive loading, and relates material stiffness to the mechanistic-empirical design method of pavements (NCHRP 1-37a). The performance of flexible pavement is dependent on the stiffness of the associated base course. Base course layers with higher resilient moduli are stiffer, incur less elastic deformation, and

transfer less stress to the overlying asphalt concrete and underlying subgrade. The reduction in fatigue cracking and rutting associated with this decrease in stress can have a positive effect on pavement life (Bejarano et al. 2003).

Resilient modulus testing involves cyclic loading of a specimen to simulate a moving wheel load. The elastic response of the specimen is recorded for various deviator and confining stresses. Elastic response is initially non-linear and the specimen experiences both plastic and elastic strains. When the applied deviator stress is small compared to the strength of the specimen, the plastic strain gradually dissipates and the remaining strain becomes almost entirely elastic and recoverable (Huang 2004). The linear-elastic modulus based on the recoverable strain is defined as resilient modulus, and is defined mathematically by Eqn. 2.1:

$$M_r = \frac{\sigma_d}{\varepsilon_r} \quad (2.1)$$

in which  $\varepsilon_r$  is the recoverable elastic strain and  $\sigma_d$  is the applied deviator stress.

### **2.3.2. Factors that affect the Resilient Modulus of Unbound Aggregate**

Several factors can influence the resilient behavior of a granular base course material, with stress-state having the greatest overall effect (Lekarp et al. 2000). Resilient modulus increases significantly with an increase in confining stress and decreases with an increase in deviator stress (Monismith et al. 1967, Hicks 1970). The effects of deviator stress are minimal to negligible for purely granular materials, depending on the amount of plastic deformation (Morgan 1966, Hicks and Monismith 1971). Moisture content can affect the stiffness of a granular material, but the extent to which this occurs depends on the degree of saturation. The stiffness of typical

granular specimens will stay nearly constant at lower saturation levels, but will decrease significantly as the saturation level rises (Hicks and Monismith 1971, Barksdale and Itani 1989). Lekarp et al. (2000) suggests that excess pore water pressures develop during cyclical loading for high degree of saturation, which decrease the strength and stiffness of the material.

Density, gradation and particle shape have been shown to have a small effect on the resilient modulus of granular material. Increased density contributes to an increased stiffness for granular material; however, increased fines content and increased crushing efforts appear to diminish these effects (Hicks and Monismith, 1971 Kolisojah 1997). Uniformly-graded specimens are stiffer than well-graded materials (Thom and Brown 1988); however the effects of moisture, fines content and particle angularity can increase the stiffness of well-graded aggregate to a degree equal-to or greater-than uniformly-graded aggregate (Plaistow 1994, Van Niekerk et al. 1998). Granular materials with angular to sub-angular particles have been found to have a higher resilient modulus than materials with rounded to sub-rounded particles (Hicks 1970, Thom and Brown 1989).

Research suggests that these influence factors also affect the resilient modulus of recycled aggregates. The resilient modulus of RAP and RCA has been shown to increase under the influence of increasing confining stress (Bennert et al. 2000, Molenaar and Van Niekerk 2002, Bejarano et al. 2003, Kim et al. 2007). Kim further found that increasing deviator stress decreased the resilient modulus of RAP, but had less of an effect than the confining stress. Tanyu et al. (2003) noted that

state of stress and strain amplitude had a significant effect on resilient moduli of various granular materials determined in both small and large-scale tests.

Kim et al. (2007) noted that RAP compacted at moisture contents less than optimum showed an increase in stiffness. Guthrie et al. (2007) found that RAP specimen stiffness decreased after extensive periods of saturation. Molenaar and Van Niekerk (2002) and Bejarano et al. (2003) found that increasing density increased the stiffness of RAP and RCA specimens, respectively. Molenaar and Van Niekerk (2002) also note that the gradation of RCA has limited influence on resilient modulus. Guthrie et al. (2007) found that the strength in RAP increased with particle angularity, although a correlation between angularity and stiffness could not be made.

### **2.3.3. Small-Scale Determination of Resilient Modulus of Unbound Aggregate**

The linear-elastic response of unbound aggregate vary with different stress-states, with an increase in confining stress contributing to an increase in resilient modulus. Bench-scale laboratory tests subject a specimen to a sequence of deviator stresses and confining pressures and the resilient modulus of the specimen is determined by the elastic response. These sequences reflect typical field loading situations, and are defined by standards published by AASHTO or NCHRP guides.

One common power-function relating resilient modulus to bulk stress in granular materials is known as the  $K-\theta$  model, and was proposed by Seed et al (1967), Brown and Pell (1967), and Hicks (1970). The  $K-\theta$  model is presented in Eqn. 2.2:

$$M_r = k_1 \left( \frac{\theta}{p_o} \right)^{k_2} \quad (2.2)$$

in which  $\theta$  is the bulk stress,  $p_o$  is a reference stress (1 kPa), and  $k_1$  and  $k_2$  are empirically fitted constants for a given material. The bulk stress is expressed as the sum of the three principle stresses as defined in Eqn. 2.3:

$$\theta = \sigma_1 + \sigma_2 + \sigma_3 \quad (2.3)$$

The reference stress is an atmospheric constant used to eliminate the influence of pressure units on the calculated resilient modulus.

#### **2.3.4. Large-Scale Model Experiments for Determination of Resilient Modulus of Unbound Aggregate**

The Large-Scale Modeling Experiment (LSME) is a large prototype-scale test developed for simulating the performance of pavement sections in a laboratory setting. The advantage of the LSME testing is that it allows field conditions to be more accurately modeled than typical bench-scale testing methods. The pavement sections, or parts of them, are loaded cyclically to simulate field traffic loads and the resilient modulus is back calculated from the recorded response.

Falling weight deflectometer (FWD) is a non-destructive test used to determine the elastic modulus of pavement sections in the field. A weight of known mass is dropped from a designated height, and the deflection of the pavement at radial distances from the load location is recorded. The elastic modulus is back calculated from these measurements.

Tanyu et al. (2003) used LSME testing to determine the resilient modulus of typical base course material and two granular industrial by-products used as subbase materials. LSME test results were compared to resilient moduli determined from FWD and bench-scale tests. The summary resilient modulus is based on a bulk stress of 208 kPa as suggested for base course materials by NCHRP 1-28a sec 10.3.3.9, and calculated according to Eq. 2.2. The summary resilient modulus determined from the LSME and FWD tests were found to be similar in magnitude; however the summary resilient modulus determined from the bench-scale tests were found to be lower than those determined from LSME and FWD. Tanyu suggests that the LSME is a good indicator of the resilient modulus of field pavement sections, but that use of laboratory resilient modulus tests should be considered conservative at best. The resilient modulus measured in the LSME was also shown to be sensitive to thickness, with thicker layers having a higher stiffness. The modulus is dependent on strain amplitude: thicker layers contribute to wider stress distributions which lead to lower vertical strains (Seed 1970).

Kootstra et al. (2010) and Ebrahimi et al. (2010) used LSME testing to determine the deflection behavior and resilient modulus of a typical base course material and two recycled road materials, RPM and road surface gravel (RSG), used as base course material. The typical base course material was graded to MnDOT Class 5 aggregate specifications. Plastic strain and resilient modulus for each material were found to increase monotonically with the number of loading cycles. The plastic strain experienced by the Class 5 exhibited plastic shakedown, in which the plastic deformation ceased after an initial deformation period, and the plastic

strain experienced by the RPM and RSG experienced creep shakedown, in which the plastic deformation continued constantly during cyclic loading. Kootstra et al. (2010) suggest that the reason for the continuous plastic deformation was respectively due to the viscous deformation of the asphalt in RPM and the amount of plastic fines present in RSG. RPM and RSG were found to have a greater overall susceptibility to plastic deformation than Class 5. Summary resilient moduli determined by LSME testing was compared to bench-scale tests on the same materials conducted by Camargo et al. (2009); however, no clear correlation between the two methods could be made. Ebrahimi suggests that the difference between the summary resilient moduli determined by these two methods could be due to either a scale effect related to the volume of material involved, or to a difference in the strain amplitude experienced by each specimen.

Bejarano et al. (2003) used FWD testing to investigate the performance of RAP used in roadway rehabilitation. Tests were performed prior to rehabilitation on pavement consisting of asphalt concrete over typical unbound aggregate base course. The asphalt concrete was then pulverized and used as unbound base course for new roadway construction. Additional testing on the rehabilitated roadway indicated that the new pulverized RAP base course had a higher resilient modulus and resistance to shear strength compared to the original base course.



### **3. Materials and Methods**

#### **3.1. Materials**

Two recycled materials, one conventional base material, and one blended recycled/conventional material were used in this investigation. The two recycled materials were a recycled asphalt pavement (RAP) and a recycled concrete aggregate (RCA), the conventional base material was a gravel meeting the MnDOT Class-5 specifications, and the blended material was a mix of approximately equal parts RCA and Class-5. The Class-5 material was used as the control material in this study. These materials are the same materials used in the roadway cells previously constructed at the MnROAD test facility in Maplewood, Minnesota and were obtained during construction. The Class-5 was salvaged from the base course of a previously constructed roadway cell. The RAP was milled from the surface of roadway cells also previously constructed at the MnROAD test facility. The RCA was obtained from a stockpile maintained by the Knife River Corporation at their pit located at 7979 State Highway 25 NE in Monticello, Minnesota. The blended material was mixed on site with the blade of a bulldozer prior to placement in the roadway cell.

A summary of the index properties, compaction test data and soil classifications for the four recycled materials is presented in Table 3.1. The RAP and Class-5 are classified as SP and A-1-b in the Unified Soil Classification System (USCS) (ASTM D 2487) and AASHTO Soil Classification System (AASHTO M 145), respectively. The blended RCA/Class 5 and RCA are classified as A-1-a according, and respectively as SP and GP according to USCS. Each of the materials used in

Table 3.1. Index properties for RAP, Class 5, RCA, and Blended RCA/Class 5.

Sample	D <sub>50</sub> (mm)	C <sub>u</sub>	C <sub>c</sub>	w <sub>opt</sub> (%)	γ <sub>d max</sub> (kN/m <sup>3</sup> )	Asphalt Content (%)	LL (%)	PL (%)	Gravel Content (%)	Sand Content (%)	Fine Content (%)	USCS Symbol	AASHTO Symbol
RAP	1.51	6.9	0.7	6.7	20.8	4.8	NP	NP	26.3	71.2	2.5	SP	A-1-b
Class-5	1.63	9.9	0.6	8.0	20.7	-	NP	NP	32.8	65.4	1.8	SP	A-1-b
RCA	5.90	20.6	0.9	11.2	19.5	-	NP	NP	54.9	43.5	1.6	GP	A-1-a
Blend	3.35	18.8	0.4	8.9	20.1	-	NP	NP	44.6	53.4	2.0	SP	A-1-a

D<sub>50</sub> = median particle size, C<sub>u</sub> = coefficient of uniformity, C<sub>c</sub> = coefficient of curvature, w<sub>opt</sub> = optimum water content, γ<sub>d max</sub> = maximum dry density, LL = liquid limit, PL = plastic limit, NP = nonplastic.

Note: Particle size analysis conducted following ASTM D 422, γ<sub>d max</sub> and w<sub>opt</sub> determined by ASTM D 1557 (AASHTO T-180), USCS classification determined by ASTM D 2487, AASHTO classification determined by AASHTO M 145 (ASTM D 3282), asphalt content determined by ASTM D 6307 (AASHTO TP-53), and Atterberg limits determined by AASHTO T-89 and T-90 (ASTM D 4318).

this study are classified as non-plastic. The particle size distribution curves for the four investigated materials as determined according to ASTM D 422 are shown in Fig. 3.1, along with the MnDOT specification for Class-5 used as a base course. Compaction tests were performed on each material using the modified compaction effort according to ASTM D 1557. Optimum water contents and maximum dry unit weights are summarized in Table 3.1, with associated compaction curves presented in Fig 3.2.

### **3.2. Small Specimen-Scale Testing**

Small laboratory bench-scale resilient modulus tests were performed on compacted specimens according to NCHRP test protocol 1-28a (NCHRP 1-28a). Cylindrical specimens measuring 152 millimeters in diameter by 305 millimeters in length were prepared from each material. Specimens were prepared at optimum moisture content and compacted to 95% maximum dry density under modified compaction effort. Compaction of specimens was performed in six lifts of equal mass and stiffness to ensure uniform compaction.

Resilient modulus testing was carried out according to NCHRP 1-28a Procedure 1a, which applies to base and subbase materials. Deflections were measured via LVDTs positioned both internally and externally, with each LVDT having an accuracy of  $\pm 0.005$  mm. The specimens were loaded with an MTS Systems Model 244.12 servo-hydraulic machine. Loading sequences, confining pressures and data acquisition were controlled from a computer running LabView 8.5 software.

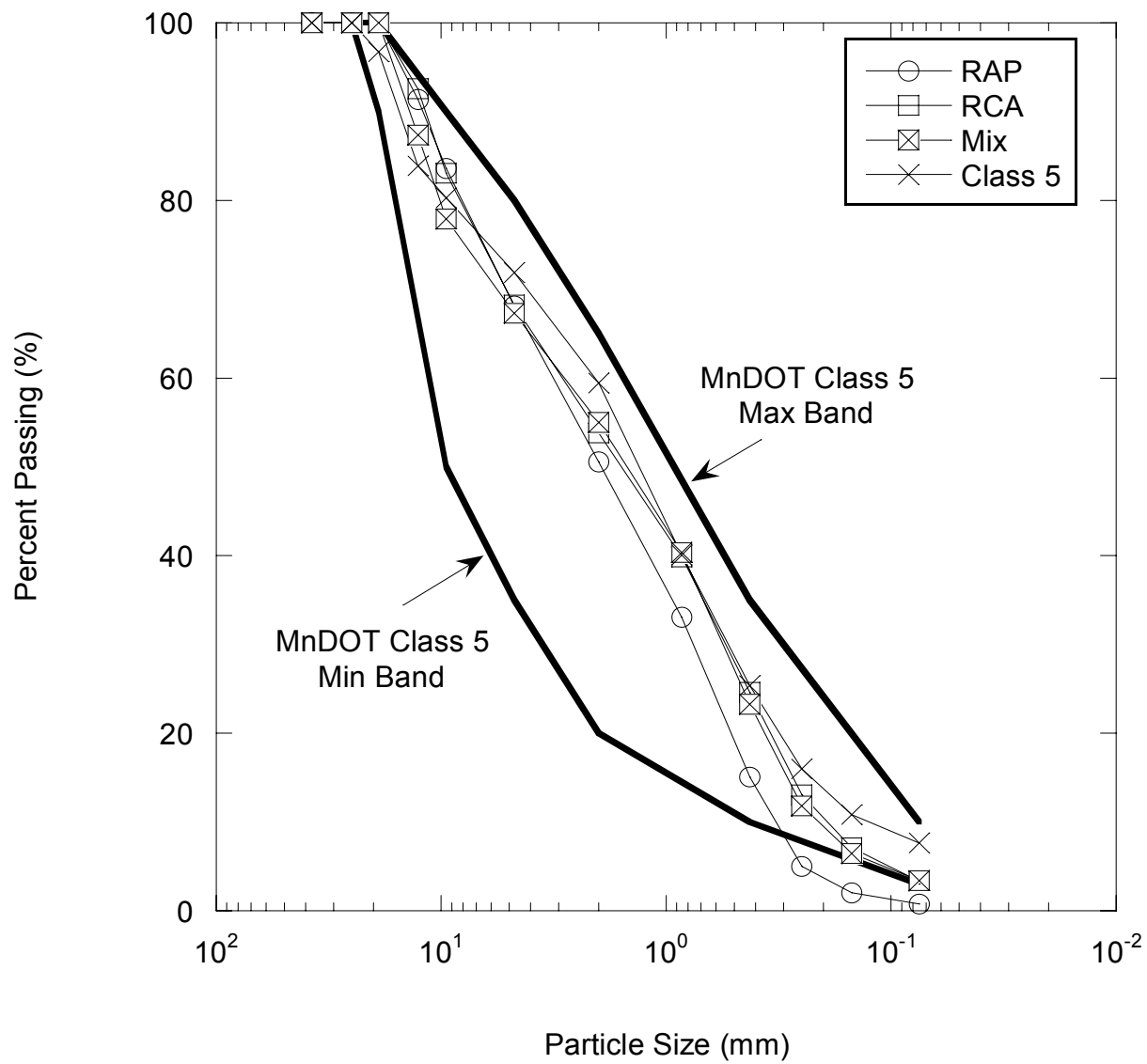


Fig. 3.1. Particle size distributions for RAP, RCA, Blended RCA/Class 5 and Class 5 with MnDOT specifications.

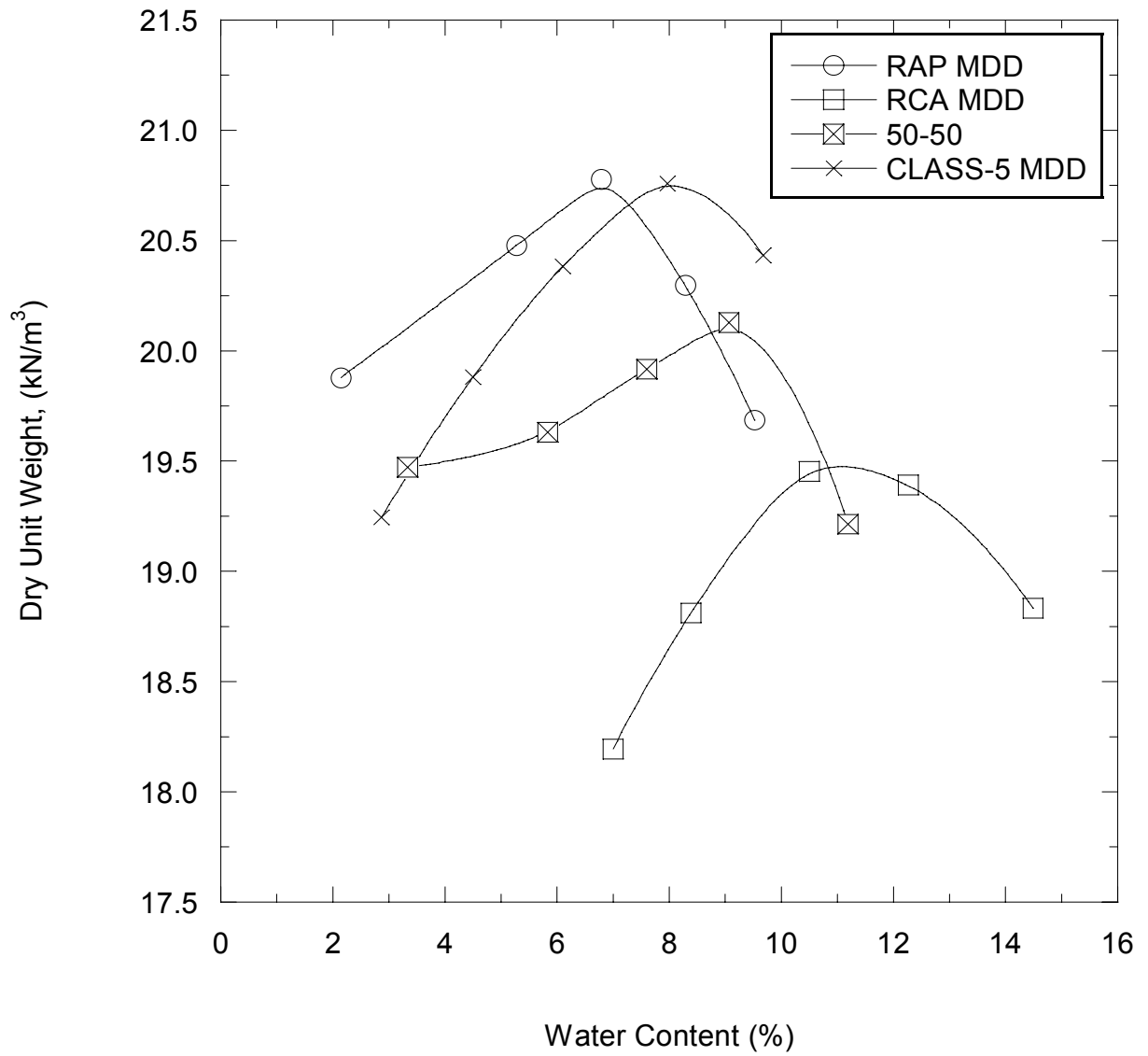


Fig. 3.2. Modified compaction curves for RAP, RCA, Blended RCA/Class 5 base, and Class 5.

The resilient modulus for each load sequence was obtained by averaging the resilient modulus from the last 5 cycles of each test sequence. The resilient modulus data were fit to the power function described by Eqn. 2.2. A summary resilient modulus was computed for each test at a bulk stress of 208 kPa, as suggested by Section 10.3.3.9 of NCHRP 1-28a. Further details of the specimen-scale laboratory testing methods are described by Son (2010) who performed the tests for unstabilized recycled materials.

### **3.3. Large-Scale Model Experiment**

#### **3.3.1. Apparatus and Loading Methodology**

LSME is a modeling method used to determine the deflection of a pavement structure at prototype scale in a manner that replicates field conditions as closely as practical (Tanyu et al. 2003). A schematic of the LSME is shown in Fig. 3.3. Pavement profiles are constructed in a test pit with dimensions 3 m x 3 m x 3 m, and are subjected to 10,000 cycles of simulated traffic loading. The simulated loading is representative of a 4-axle truck applying a tire pressure of 700 kPa to a contact area of 0.05 m<sup>2</sup>. Loads are generated by a MTS 280-L/m hydraulic actuator with a 100 kN force rating and 168 mm of stroke. Loads are applied to the pavement surface using a 25 mm thick circular steel plate with a radius of 125 mm. The pulse of the loading varies as a haversine function consisting of a 0.1 second load period followed by a 0.9 second rest period (Benson et al. 2009, Ebrahimi et al. 2010, Kootstra et al. 2010).

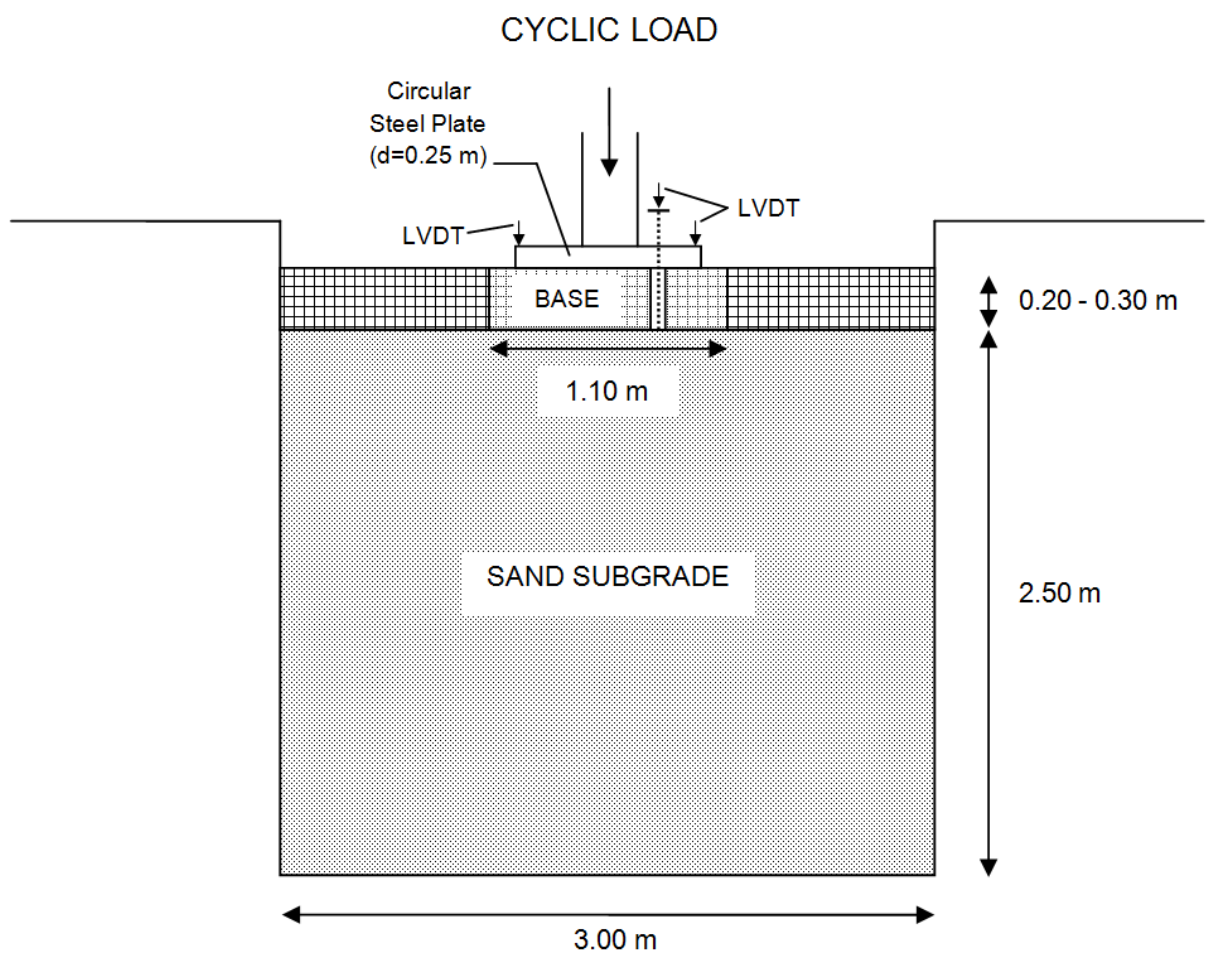


Fig. 3.3. Schematic of LSME testing setup.

The equivalent stress to be applied to the surface of the base course material in the absence of an asphalt layer was determined by non-linear finite-element analysis using the MICHPAVE program to model the performance of the proposed pavement profile (Benson et al. 2009, Kootstra et al. 2009). The base course was assumed to behave as non-linear elastic, and the asphalt surface and subgrade were assumed to behave as linear elastic. Loading and material properties used as inputs into the MICHPAVE program (Harichandran 1989) were determined from typical values (Huang 2004), and are presented in Table 3.2. The vertical stress distribution predicted by MICHPAVE is shown in Fig. 3.4. The vertical stress on the surface of the base layer is maximized directly below the center of loading, and decreases with an increase in radial distance. Based on a maximum stress of 133 kPa, a force of 6.7 kN was applied to base layer in the LSME with the loading plate. Previous LSME testing used the entire 3.0 m x 3.0 m test area to evaluate pavement performance (Tanyu et al. 2003, Benson et al. 2009, Kootstra et al. 2010). However, limited amounts of available base course materials made it necessary to reduce the evaluated test area to 1.0 m x 1.0 m. The remainder of the 3.0 m x 3.0 m test area was made up of recycled pavement material (RPM) to maintain the boundary stress that would otherwise be lost by a reduction in test area. The equivalency of this abbreviated test area and method of preparation are described in Appendix A. Pavement profiles consisted of 0.2 m to 0.3 m-thick of base course material over 2.5 m of dense, uniform sand subgrade. The performance of an asphalt layer was not central to the research, and therefore was not included in the LSME analysis.



Table 3.2. Inputs used for MICHPAVE for determining stress on base layer.  
(Adapted from Kootstra 2009)

<b>Material Property of Load Condition</b>	<b>Asphalt</b>	<b>Base</b>	<b>Subgrade</b>
Applied Load (kN)	35.0	6.7	NA*
Loading Radius (cm)	12.7	12.7	NA*
Thickness (cm)	12.7	20.3	NA*
Modulus (kPa)	3,300,000	398,000	48,000
$k_1, k_2$ (Eqn. 2.2)	NA*	27,600 kPa 0.5	NA*
Poisson's Ratio	0.35	0.35	0.45
Unit Weight (kN/m <sup>3</sup> )	22.8	20.4	18.8

\*NA = non-applicable

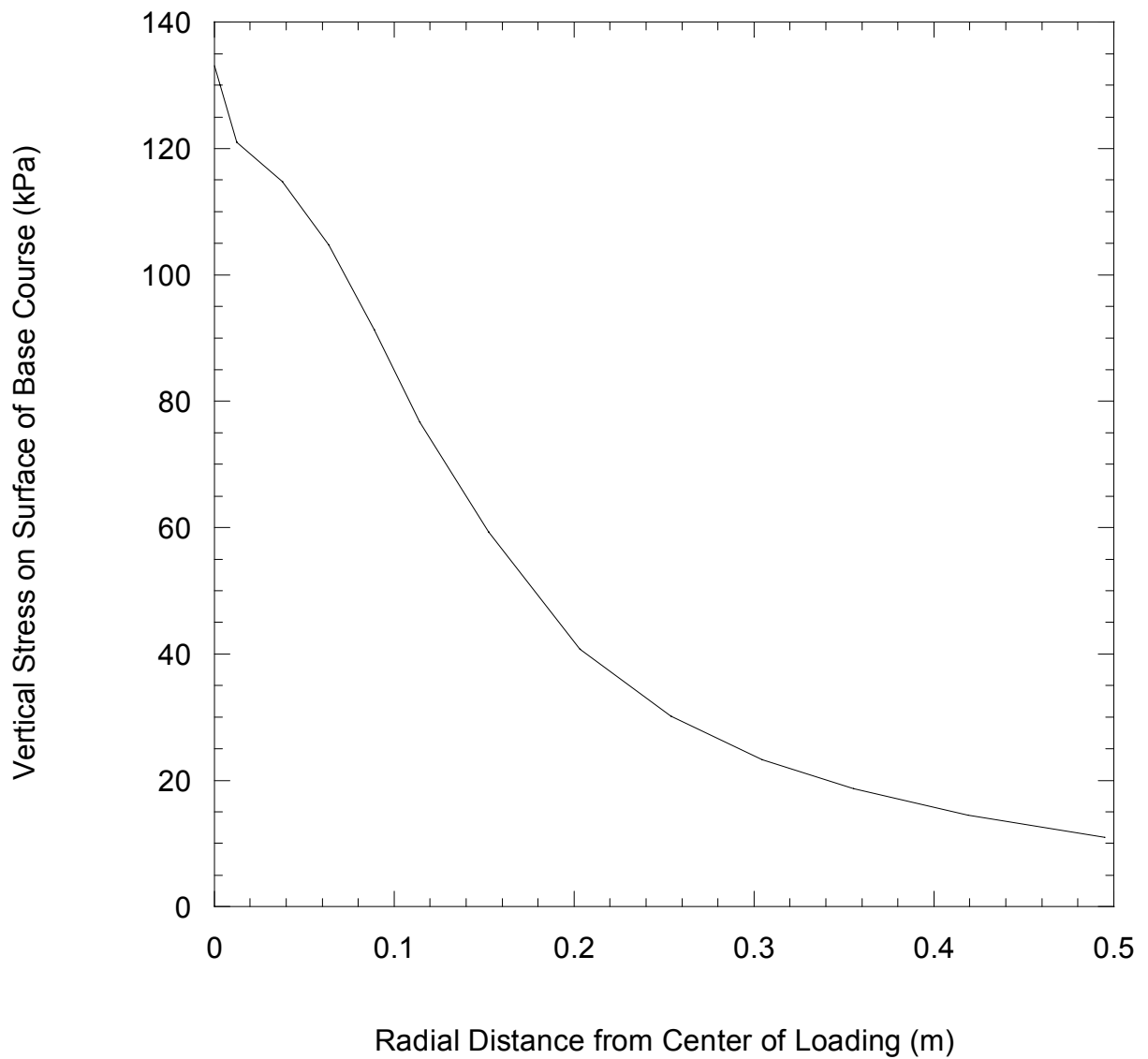


Fig. 3.4. Vertical stress on surface of base course vs. radial distance from center of traffic loading predicted by MICHPAVE.

### 3.3.2. Deflection Measurements

Vertical deflections at the surface of the base course and subgrade were measured during each loading cycle. Linear variable differential transducers (LVDT) were used to measure the deflections to a precision of  $\pm 0.005$  mm. Deflection of the base course was measured from the top of the loading plate, which was assumed rigid and able to translate the base course deflection. Subgrade deflections were measured by attaching small plates to either end of a thin rod extending through a tube extending through the loading plate and base course. One plate was laid flush with the subgrade surface while the other plate supported the LVDT located above the base course. Deflection of the subgrade was translated by the thin rod and measured by the LVDT. Deflections measured by the LVDTs were recorded using LabView 8.5 software.

### 3.3.3. Data Inversion

The resilient modulus of the base courses tested in the LSME was determined by performing a data inversion approach using MICHPAVE (Harichandran 1989). The elastic deflection of the base course was determined by subtracting the elastic deflection of the subgrade from the total elastic deflection of the profile as measured at the top of the base course. The LSME pavement profile was modeled as a two layer system in MICHPAVE. The elastic behavior of the base course and subgrade layers were modeled as non-linear and linear, respectively. The base course  $k_2$  was determined from small-scale laboratory experiments in accordance with NCHRP 1-28a. The base course  $k_1$  and subgrade elastic modulus

were varied until the elastic deflections predicted by MICHPAVE were within  $\pm 0.005$  of those measured in the LSME. This method assumes that  $k_2$  varies within a narrow range for a given material (Huang 2004) and follows the methods described by Tanyu et al. (2003) and Kootstra et al. (2009).

#### **3.3.4. Base Course Compaction**

Base course was compacted in lifts of approximately 0.10 m to efficiently and evenly distribute the modified compaction effort. Base course materials were prepared at optimum moisture content, and compacted to 95% of the modified maximum dry unit weight using a jumping-jack style compactor. A nuclear density gauge was employed to measure the in-situ dry unit weight and moisture content of each lift.

#### **3.3.5. Field-Scale Falling Weight Deflectometer Testing**

Field-scale in situ modulus of the materials was obtained from the Falling Weight Deflectometer (FWD) tests that were performed at the MnROAD testing facility in the roadway cells with the same materials tested in the small laboratory specimen tests and the LSME. Testing was performed using a trailer-mounted Dynatest model 1000 FWD. The FWD was controlled by an on-site computer which also recorded and stored load and deflection data. Three loads of 26.7, 40.0 and 53.4 kN were applied by the FWD to a 300-mm-diameter plate in contact with the pavement surface. Surface deflections were measured by nine load transducers

located at distances of 0, 0.30, 0.61, 0.91, 1.22, 1.52, and 1.83 meters from the center of the load.

The measured deflections were used to back-calculate the elastic modulus of the pavement layers using the MODULUS program developed at the Texas Transportation Institute. MODULUS uses linear-elastic theory to back-calculate elastic moduli from FWD data. The back-calculation was based on a three-layer model consisting of asphalt concrete, base course, and subgrade layers. Pavement profile and deflection data were provided by the MnDOT. The pavement profiles for the four test cells are presented in Fig. 3.5. The asphalt surface and base course layers were assigned a Poisson's ratio of 0.35, and the subgrade layer was assigned a Poisson's ratio of 0.40 (Huang 2004). The depth to the rigid layer was assumed to be at least 6 m and have little effect on the elastic moduli (Bush and Alexander 1985). The range of bulk stresses and vertical strains in the field was estimated using MICHPAVE. Surface loads taken from the FWD data and moduli from the MODULUS back-calculation were used as inputs. Structural layer coefficients were determined from the back-calculated moduli for use in pavement thickness design, as presented in Appendix B.

<b>Cell 16: Recycled Concrete Aggregate (RCA)</b>	<b>Cell 17: Blended 50% / 50% RCA/Class 5 (Blend)</b>	<b>Cell 18: Recycled Asphalt Pavement (RAP)</b>	<b>Cell 19: Mn/DOT Class 5 Aggregate (Class 5)</b>
<b>127 mm Asphalt Concrete</b>	<b>127 mm Asphalt Concrete</b>	<b>127 mm Asphalt Concrete</b>	<b>127 mm Asphalt Concrete</b>
<b>305 mm RCA</b>	<b>305 mm Blend</b>	<b>305 mm RAP</b>	<b>305 mm Class 5</b>
<b>305 mm Class 3 Aggregate</b>	<b>305 mm Class 3 Aggregate</b>	<b>305 mm Class 3 Aggregate</b>	<b>305 mm Class 3 Aggregate</b>
<b>178 mm Select Granular Material</b>	<b>178 mm Select Granular Material</b>	<b>178 mm Select Granular Material</b>	<b>178 mm Select Granular Material</b>
<b>Clay</b>	<b>Clay</b>	<b>Clay</b>	<b>Clay</b>

Fig. 3.5. Pavement profiles of cells tested using FWD at MnROAD testing facility.  
(Adapted from Johnson et al. 2009)

## **4. Results**

### **4.1. Deflections in LSME**

The total and plastic deflections at the surface of the base course and subgrade in the LSME as a function of loading cycle for RAP, RCA, blended RCA/Class 5, and Class 5 are presented in Figs. 4.1 thru 4.4. Deflections measured on the surface of the base course with thicknesses of 0.2 m and 0.3 m and subgrade are based on the haversine loading pulse. The total deflection is the peak deflection experienced during the 0.1-sec loading pulse, and the plastic deformation of each layer is the unrecovered deflection remaining during the 0.9-sec “at-rest” period. The amount of plastic deformation increases monotonically as the test progresses, with the greatest accumulation occurring during the first 50 loading cycles in all cases. The elastic deflection is the difference between the total and plastic deflections for each loading cycle. The net deflection represents the elastic deflection of the given base course layer and is the difference between the total elastic deflection measured at the surface and the elastic deflection of the subgrade. The elastic deflections at the surface and subgrade are presented as a function of loading cycle in Figs. 4.5 thru 4.8.

The net base elastic deflection for each of the materials slightly decreases as the cyclic loading progresses, which is caused by the gradual compaction of the particles into a denser matrix. The magnitude of the net elastic deflection for RAP and RCA were approximately equal for both layer thicknesses. The magnitude of the net elastic deflection for blended RCA/Class 5 and Class 5 is higher for the 0.2 m layer thickness than for the 0.3 m layer thickness. The thicker layer distributes the

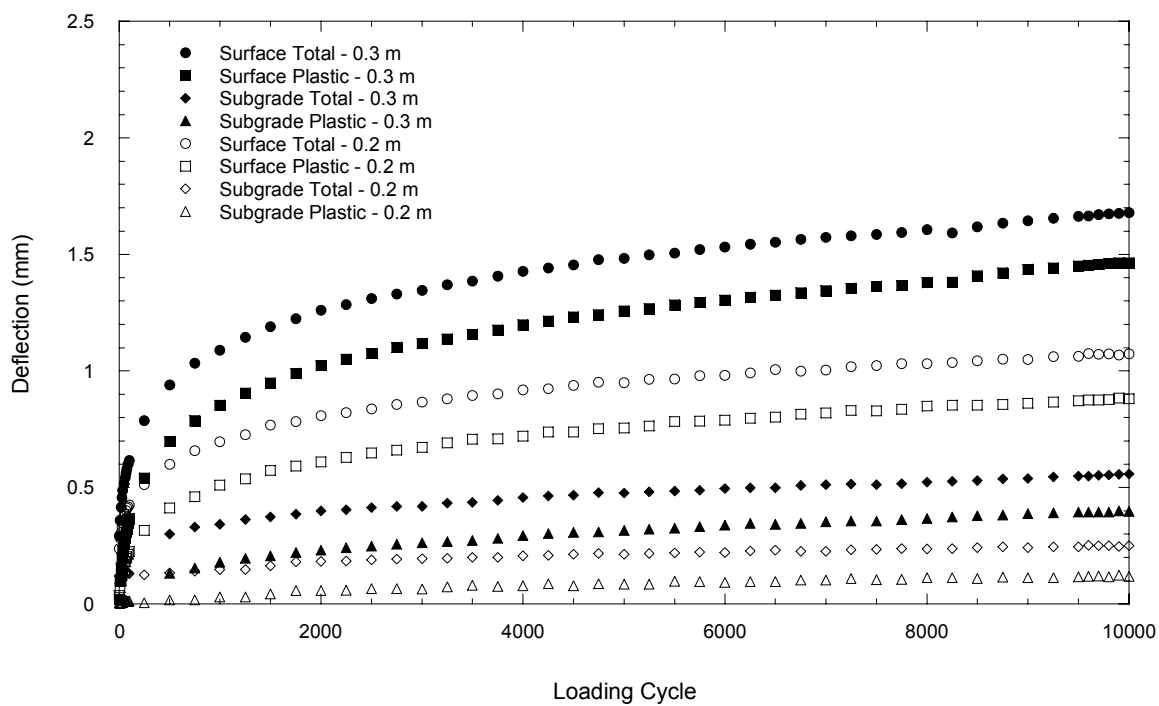


Fig. 4.1. Total and plastic deflection of surface and subgrade layers vs. number of loading cycles for RAP.



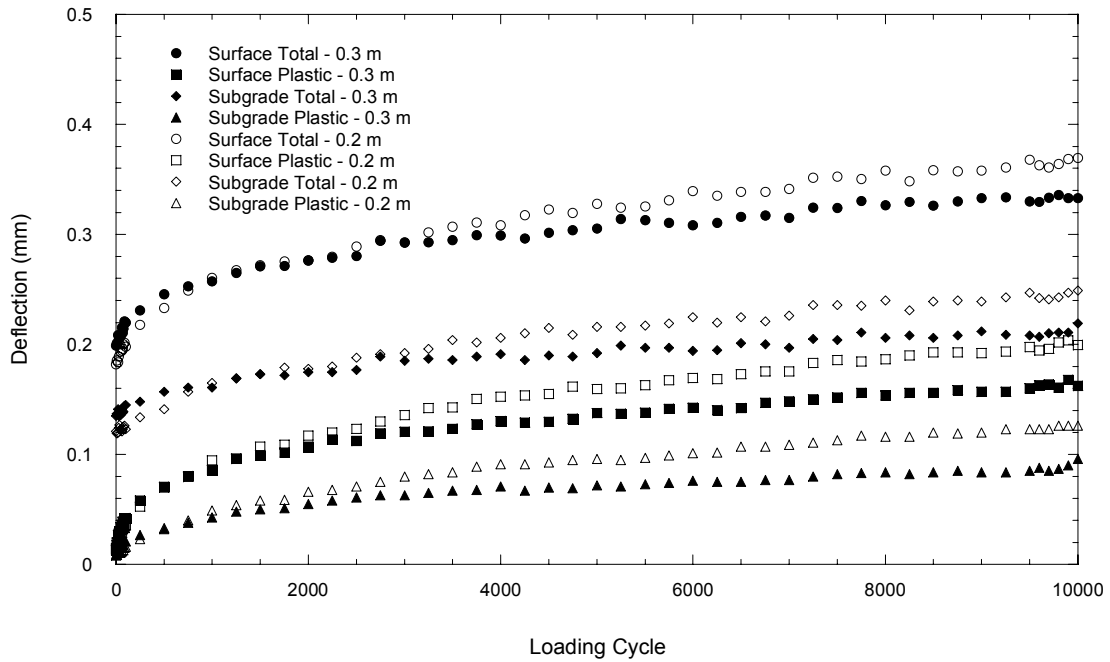


Fig. 4.2. Total and plastic deflection of surface and subgrade layers vs. number of loading cycles for RCA.

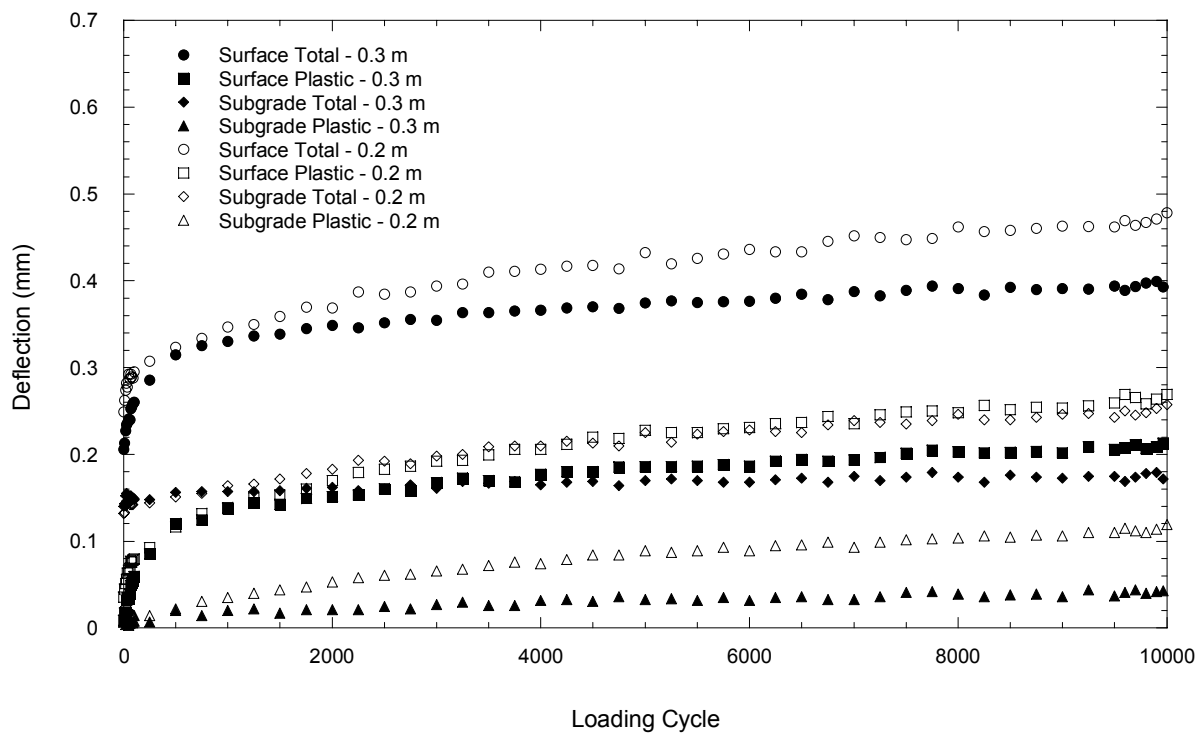


Fig. 4.3. Total and plastic deflection of surface and subgrade layers vs. number of loading cycles for blended RCA/Class 5.

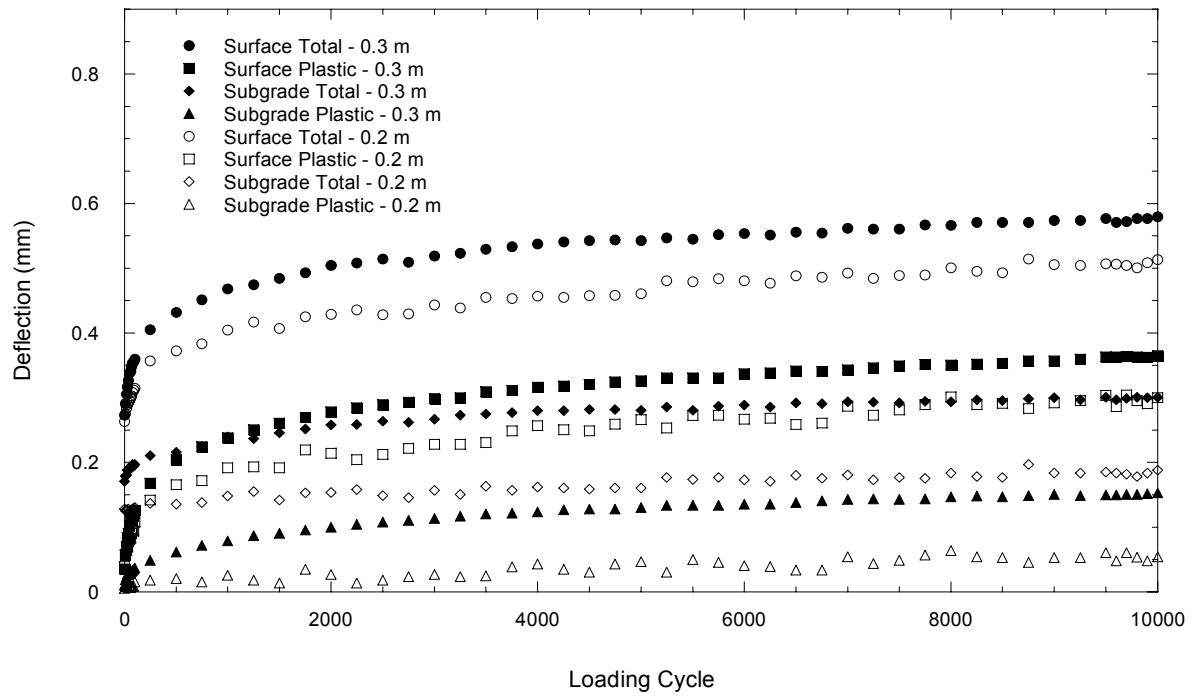


Fig. 4.4. Total and plastic deflection of surface and subgrade layers vs. number of loading cycles for Class 5.

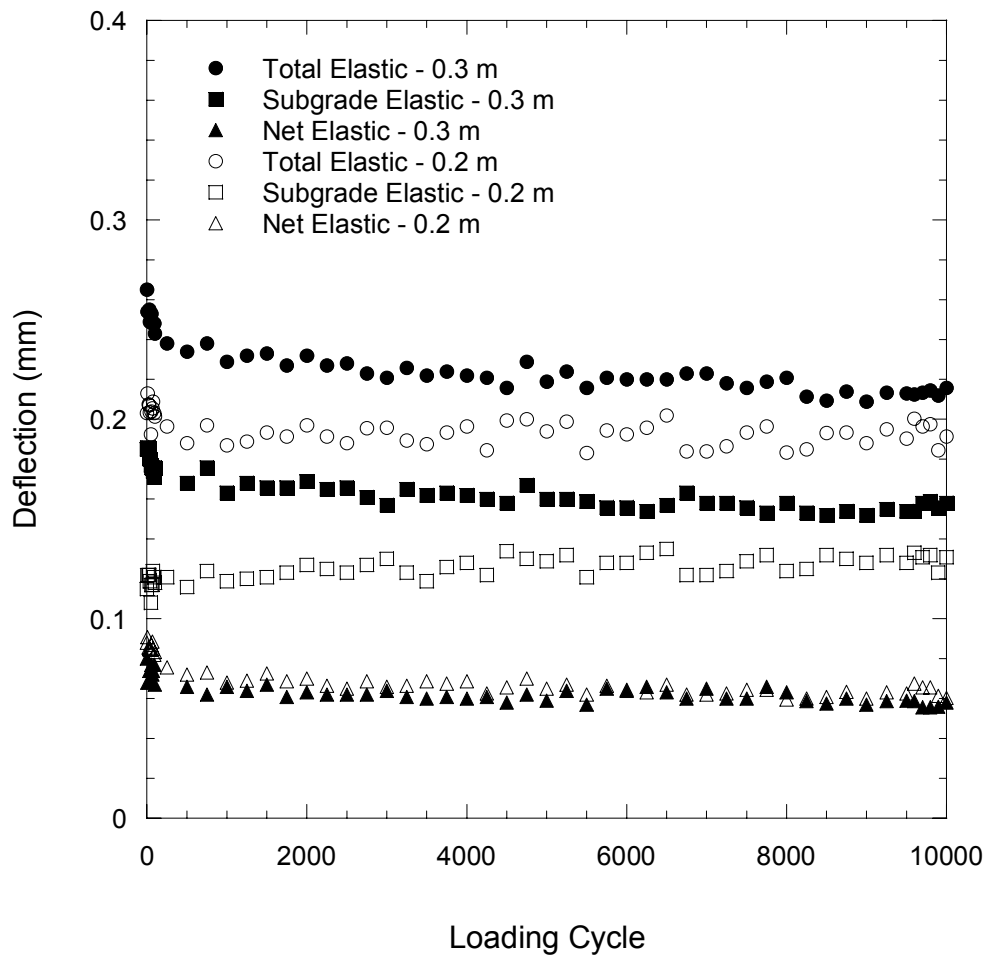


Fig. 4.5. Surface (total), subgrade, and net elastic deflection vs. number of loading cycles for RAP.

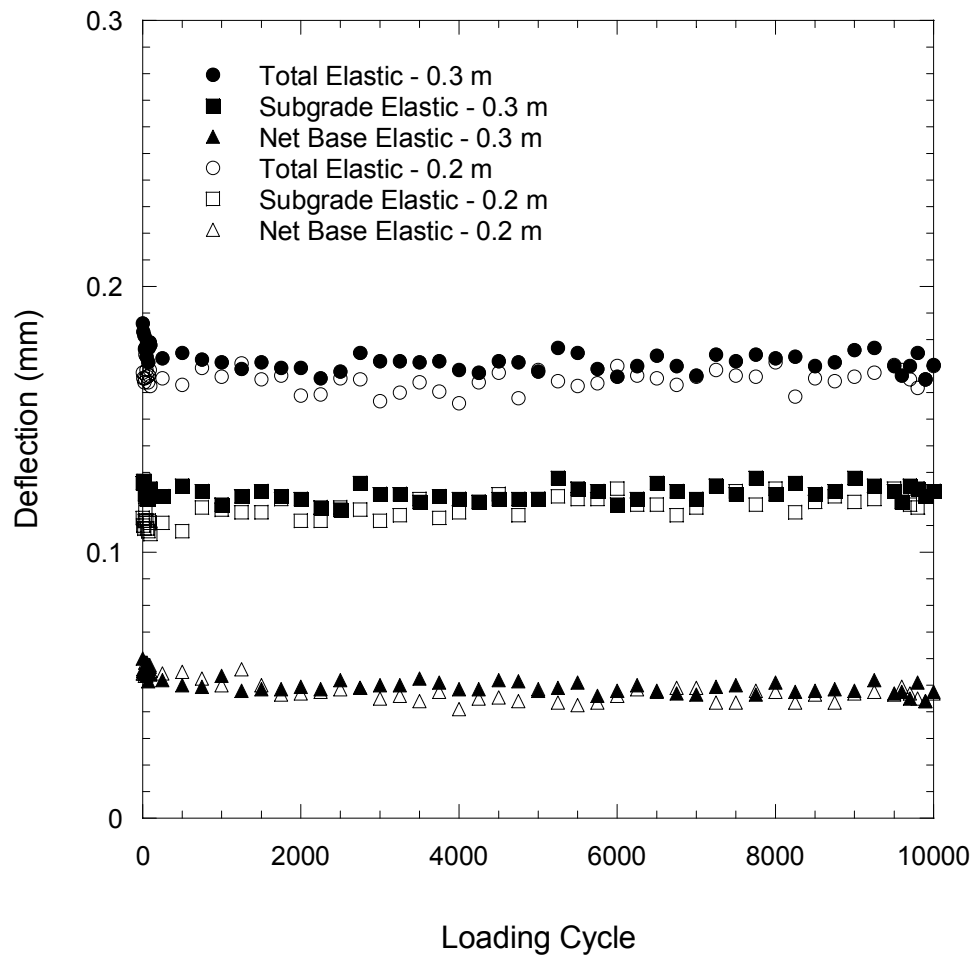


Fig. 4.6. Surface (total), subgrade, and net elastic deflection vs. number of loading cycles for RCA.

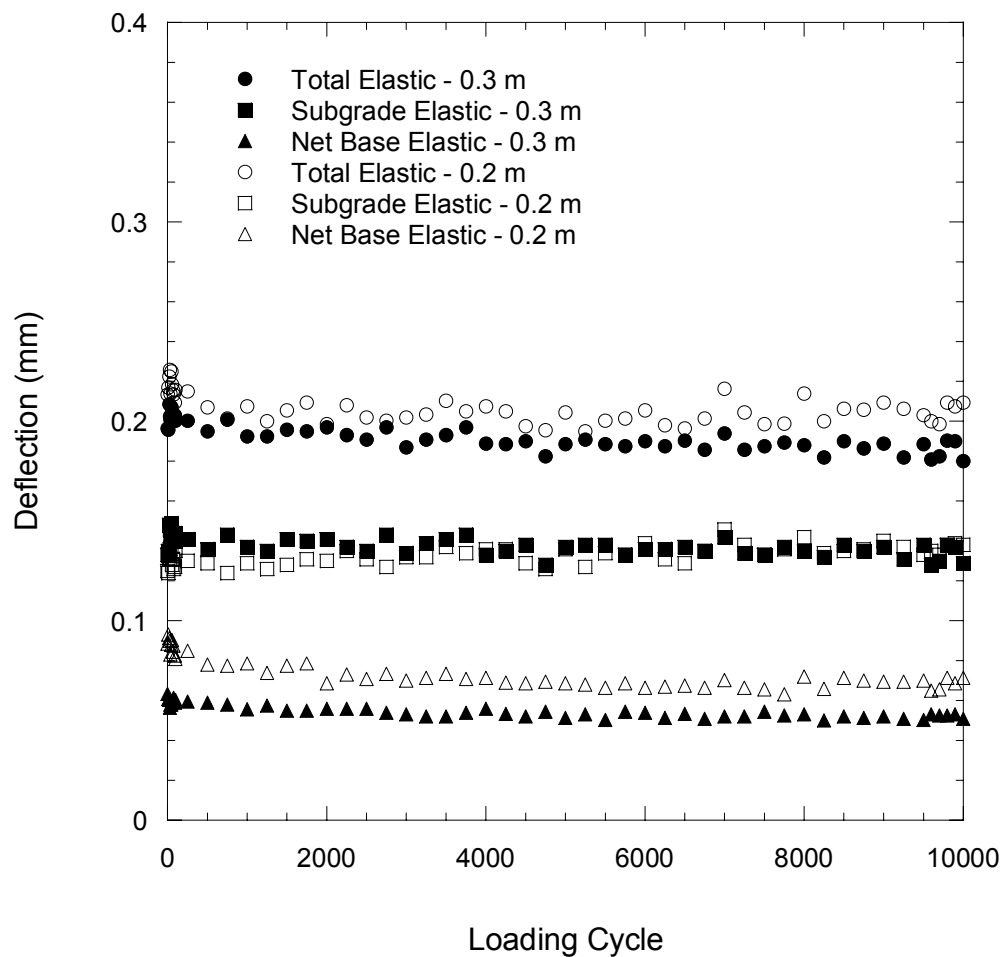


Fig. 4.7. Surface (total), subgrade, and net elastic deflection vs. number of loading cycles for blended RCA/Class 5.

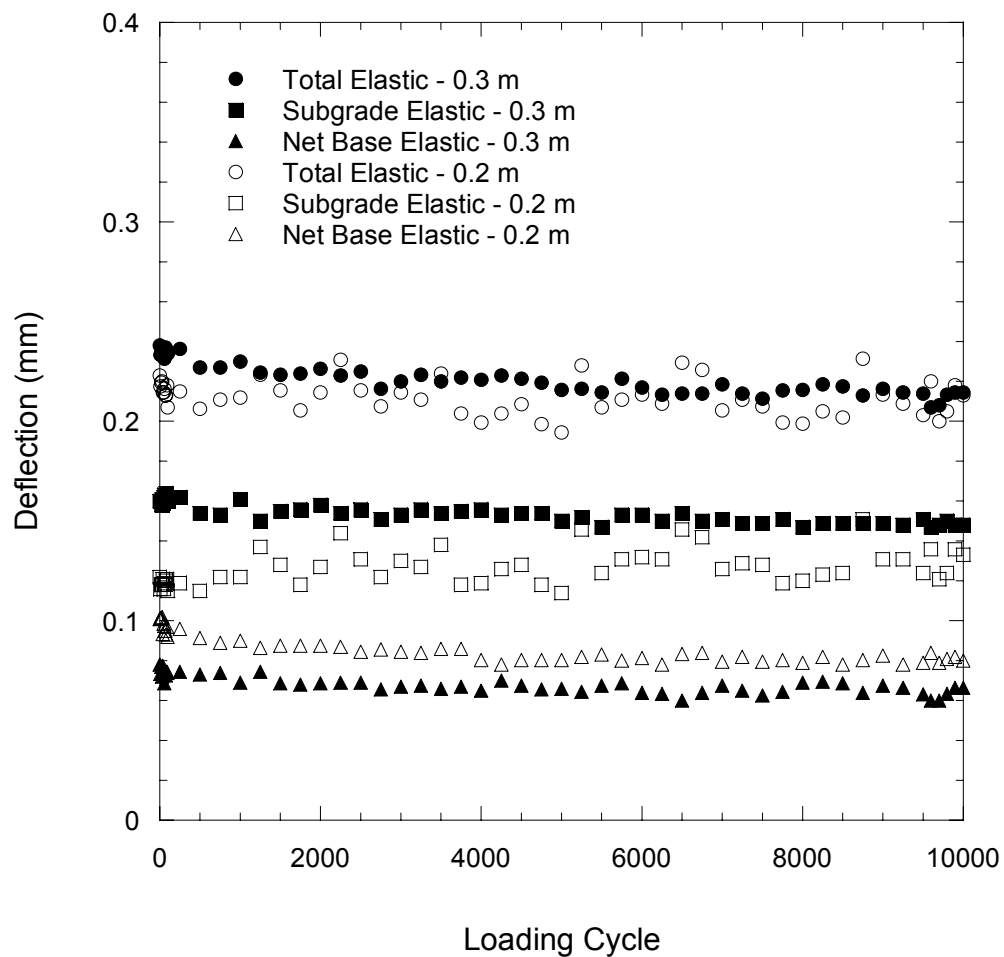


Fig. 4.8. Surface (total), subgrade, and net elastic deflection vs. number of loading cycles for Class 5.

stress within the layer more thoroughly, and therefore the amount of strain experienced in the material can be expected to be reduced. The subgrade elastic deflection was nearly constant during the loading of both layer thicknesses for each base course material.

A comparison of the surface and subgrade deflections after 10,000 loading cycles for 0.2-m and 0.3-m thick layers of RAP, RCA, blended RCA/Class 5 and Class 5 is presented in Fig. 4.9. The net plastic deflection is the difference between the total plastic deflection measured at the surface and the plastic deflection measured at the subgrade. The sum of the deflections represented in Fig. 4.9 is equal to the total deflection measured at the surface of the LSME at the end of loading. RAP and RCA had the largest and smallest amount of both total and net base plastic deflection, respectively, with Class 5 and blended RCA/Class 5 having the second and third largest amounts of both total and net base plastic deflections, respectively. The plastic deflection experienced by the RAP was approximately 211% and 402% greater than that of Class 5 for 0.2 m and 0.3 m layer thicknesses, respectively, whereas the plastic deflection experienced by the RCA was approximately 69% smaller than the plastic deflection experienced by the Class 5 for both layer thicknesses. The blended RCA/Class 5 material experienced plastic deflections that were 39% and 20% smaller than Class 5 for layer thicknesses of 0.2 m and 0.3 m, respectively. The net elastic and plastic deflections for 0.2 m and 0.3-m layer thicknesses of RAP, RCA, blended RCA/Class 5, and Class 5 can be compared in Fig. 4.10.



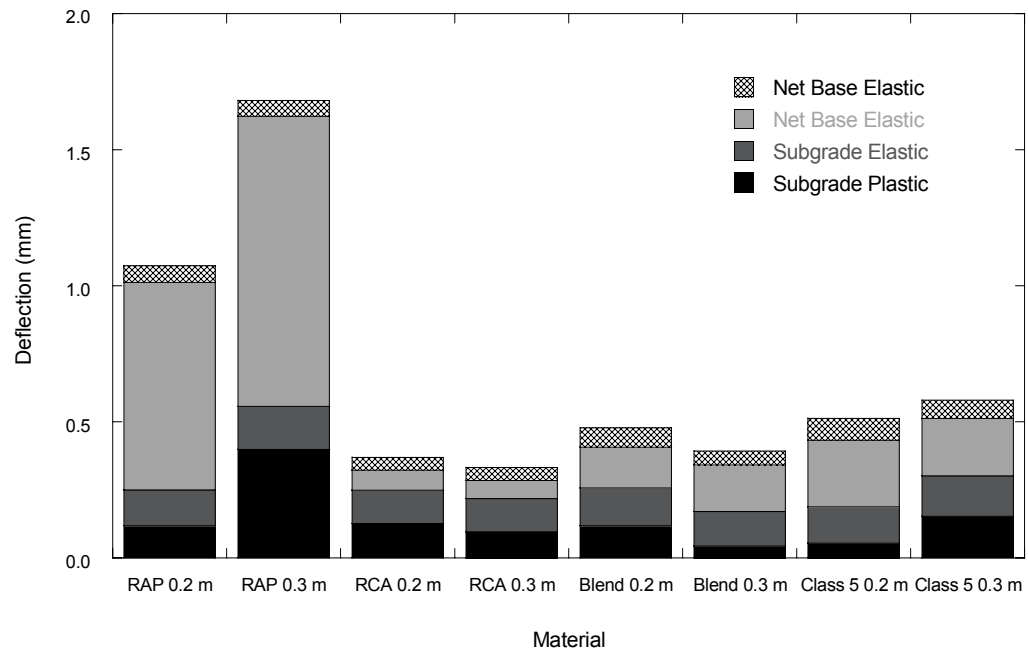


Fig. 4.9. Comparison of surface and subgrade deflections for RAP, RCA, blended RCA/Class 5, and Class 5.

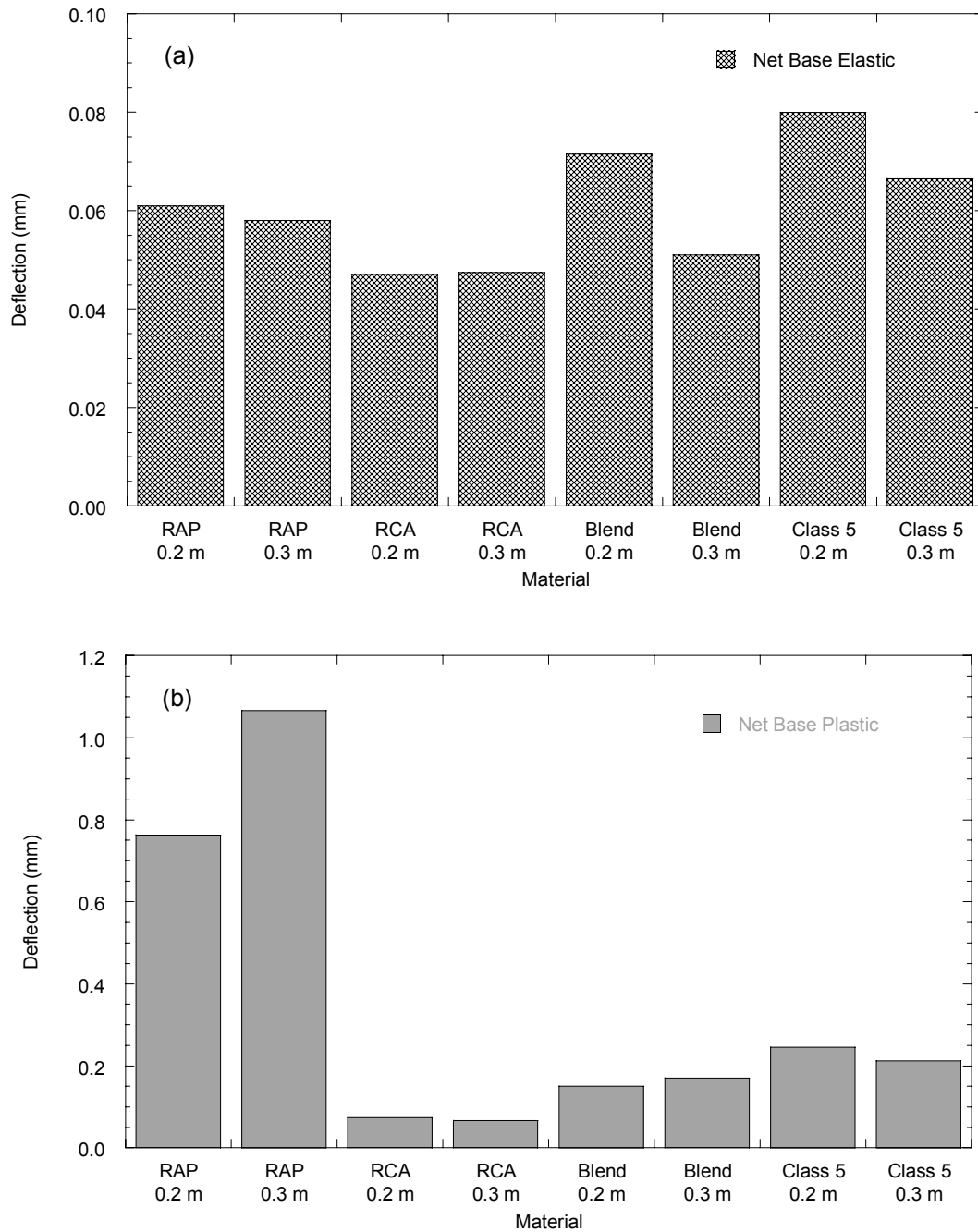


Fig. 4.10. Comparison of (a) net elastic and (b) net plastic deflections for RAP, RCA, blended RCA/Class 5, and Class 5.

The base plastic deflection of RCA and Class 5 was larger for the 0.2 m layer thickness compared to the 0.3 m layer thickness. Stress is better distributed within a layer of larger thickness, and the corresponding reduction in strain correlates to a reduction in plastic deflection. The plastic deflection of RCA and Class 5 decreased 10% and 13%, respectively, for an increase in layer thickness from 0.2 m to 0.3 m.

The plastic deflection experienced by the 0.3-m layer thickness of blended RCA/Class 5 is 13% larger than the plastic deflection experienced by the 0.2 m layer thickness, which contradicts the deflection that would be expected considering the deflections experienced by RCA and Class 5 alone. The most likely cause for this seemingly contradictory behavior is experimental error. Although LSME compaction was checked with a nuclear density gauge prior to testing, there is a possibility that the material directly under the loading plate was undercompacted. Undercompacted material would experience excess plastic deflection during the 10,000 cycles of loading, which would contribute to the total overall deflection. The effect of this undercompaction would be minimal for elastic deflection, however, as the compaction level required for the material to perform as linear-elastic would remain the same and would be achieved before the termination of loading.

The plastic deflection of RAP is 40% larger for the 0.3-m layer thickness compared to the 0.2-m layer thickness. This is attributed to the viscous nature of the asphalt coating on the RAP particles that contributes to increased amount of deflection of the layer despite the reduction of stress in the larger layer thickness.

The elastic and plastic net base deflection as a function of RCA content is presented in Fig. 4.11 for 0.2 m and 0.3 m layer thicknesses of RCA, blended

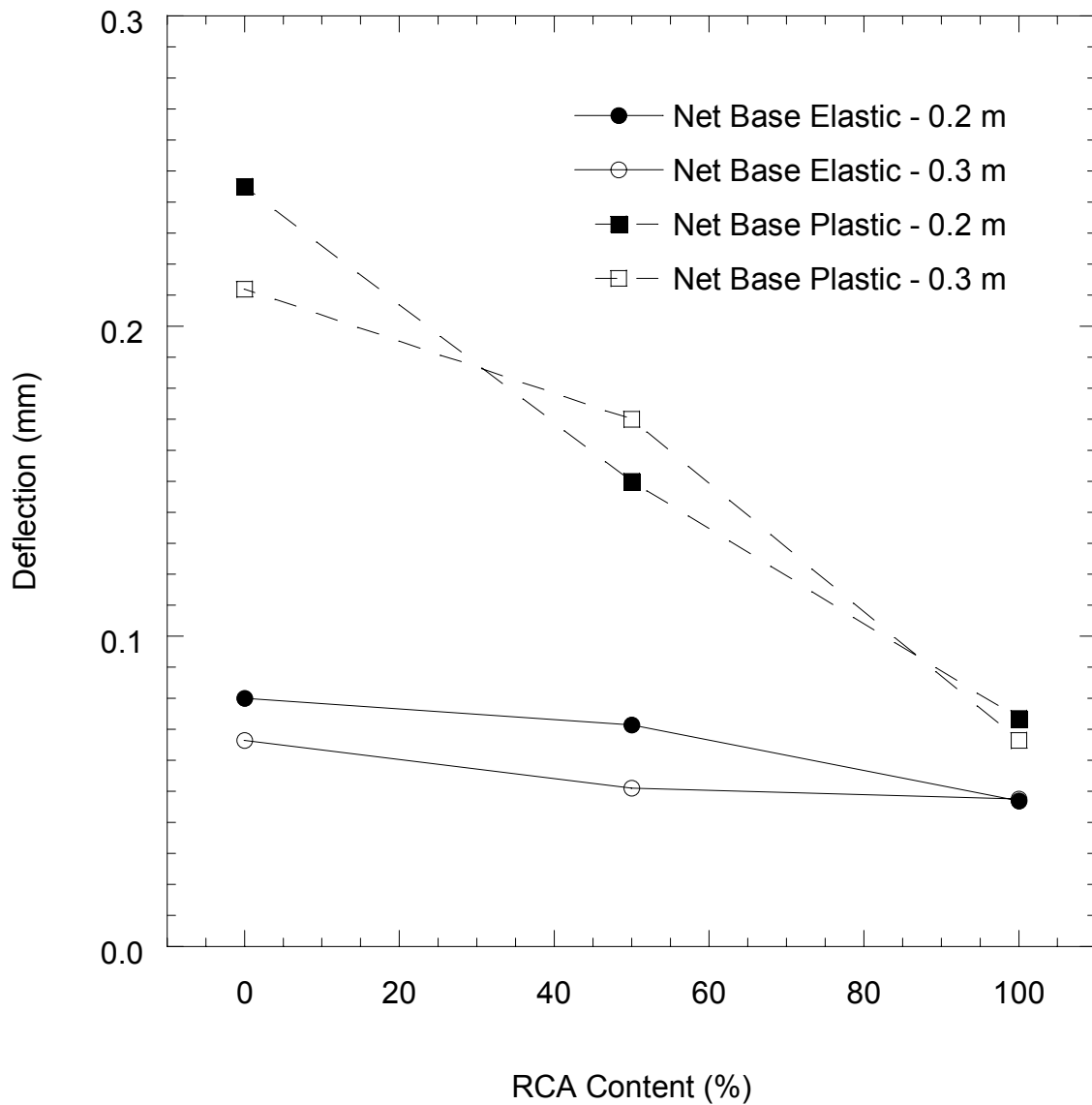


Fig. 4.11. Comparison of net base elastic and net base plastic deflections vs. RCA content for RCA, blended RCA/Class 5, and Class 5.

RCA/Class 5, and Class 5. The elastic deflection decreased slightly with an increase in RCA content, i.e., the 0.2-m and 0.3-m thick layers showed an overall decrease in the elastic deflections, i.e., approximately 0.03 mm and 0.02 mm, respectively. The plastic deflection also decreased with an increase in RCA content, although at a much higher rate. The 0.2-m and 0.3-m thick layers showed an overall decrease in plastic deflection of approximately 0.17 mm and 0.15 mm, respectively. As the RCA content increases, the elastic and plastic deflections of the different layer thicknesses seem to converge on common values, i.e., the elastic and plastic deflection of 100% RCA is approximately 0.05 mm and 0.07 mm, respectively, for both 0.2 m and 0.3 m layer thicknesses.

The average plastic strain ( $\epsilon_p$ ) in each base layer can be defined as:

$$\epsilon_p = \frac{d_p}{t} \times 100 \quad (4.1)$$

where  $d_p$  is the plastic deflection within the base layer and  $t$  is the layer thickness. The plastic strain of the base course as a function of loading cycle is presented in Figs. 4.12 thru 4.15 for 0.2-m and 0.3-m layer thicknesses of RAP, RCA, blended RCA/Class 5, and Class 5. The average plastic strain experienced by the 0.3-m thick base layer is greater than that experienced by the 0.2-m thick base layer for each of the tested materials. In addition, each material reaches a steady state condition within 500 cycles for both layer thicknesses.

The steady state condition achieved for RCA, blended RCA/Class 5, and Class 5 maintains a constant plastic strain rate of approximately zero, corresponding to a behavior, which is in accordance with plastic shakedown (Khogali et al. 2004,

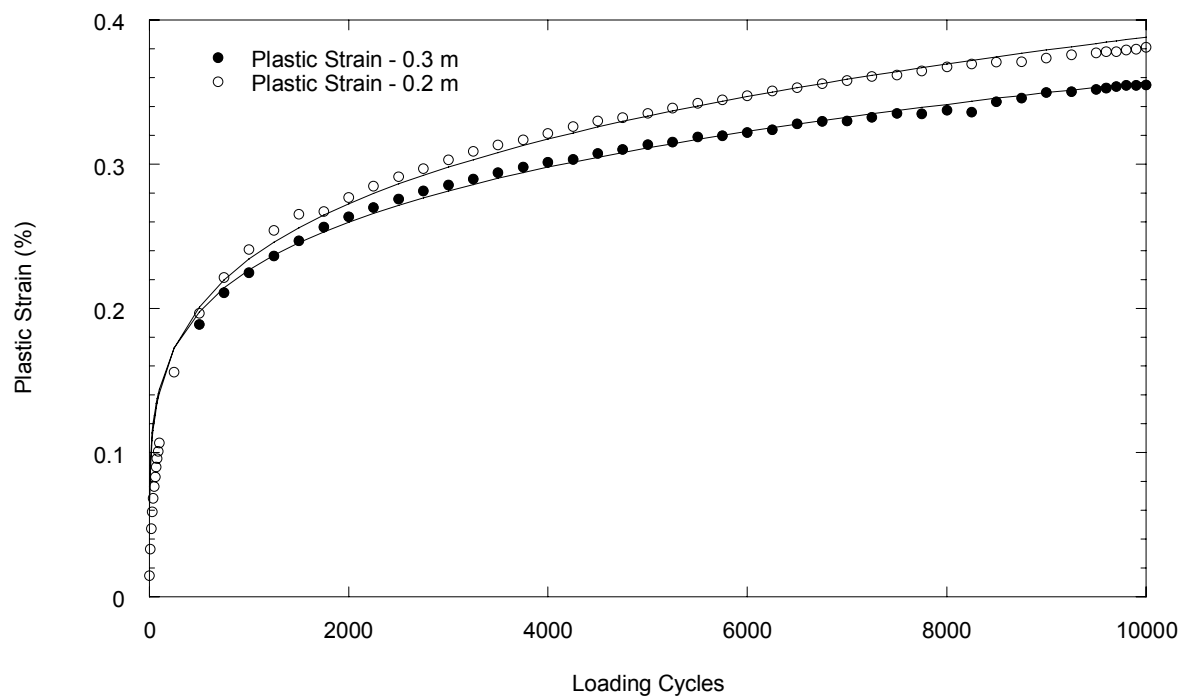


Fig. 4.12. Plastic strain vs. loading cycle for RAP.

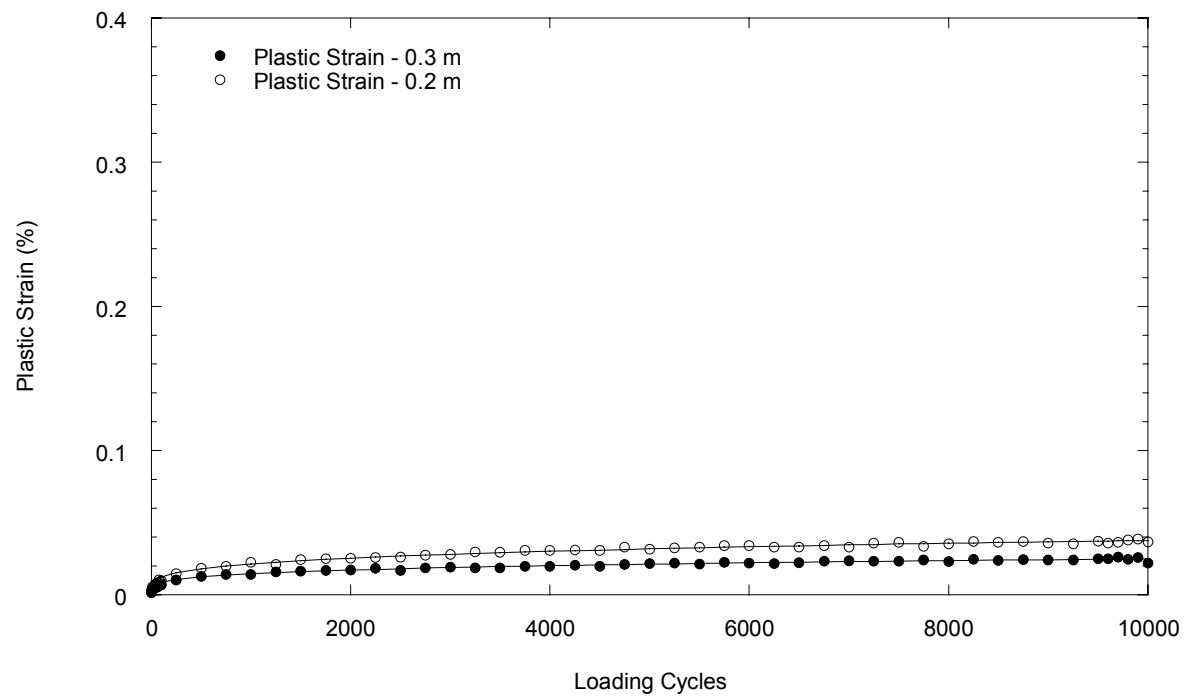


Fig. 4.13. Plastic strain vs. loading cycle for RCA.

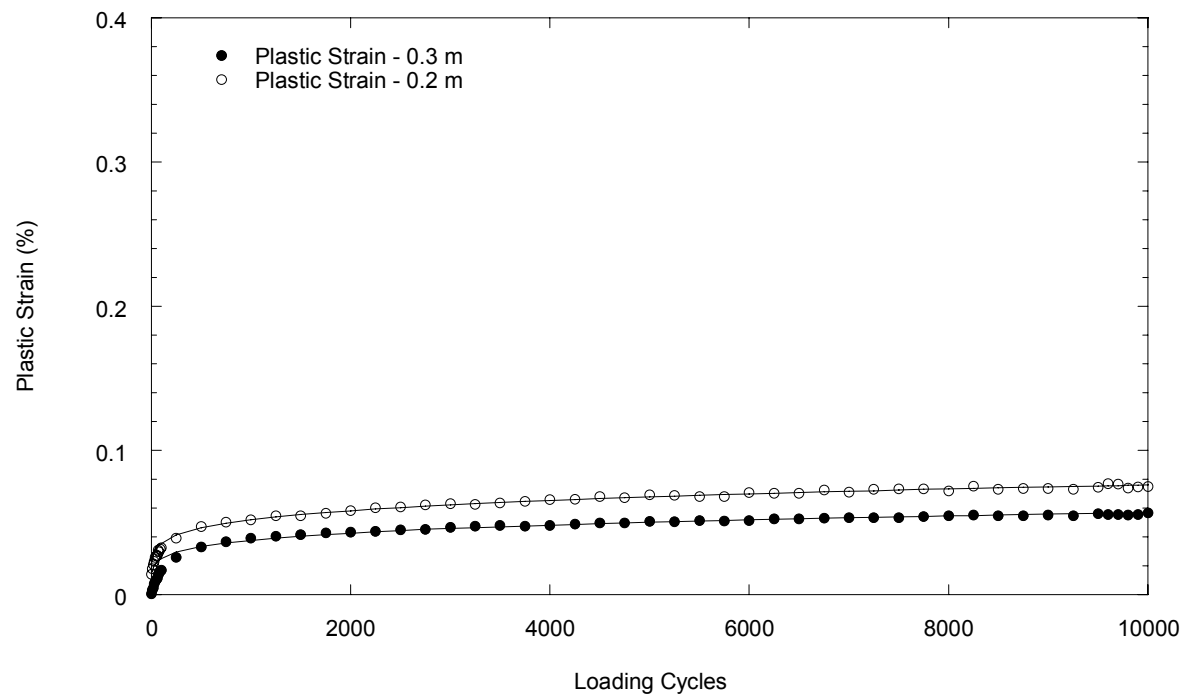


Fig. 4.14. Plastic strain vs. loading cycle for blended RCA/Class 5.



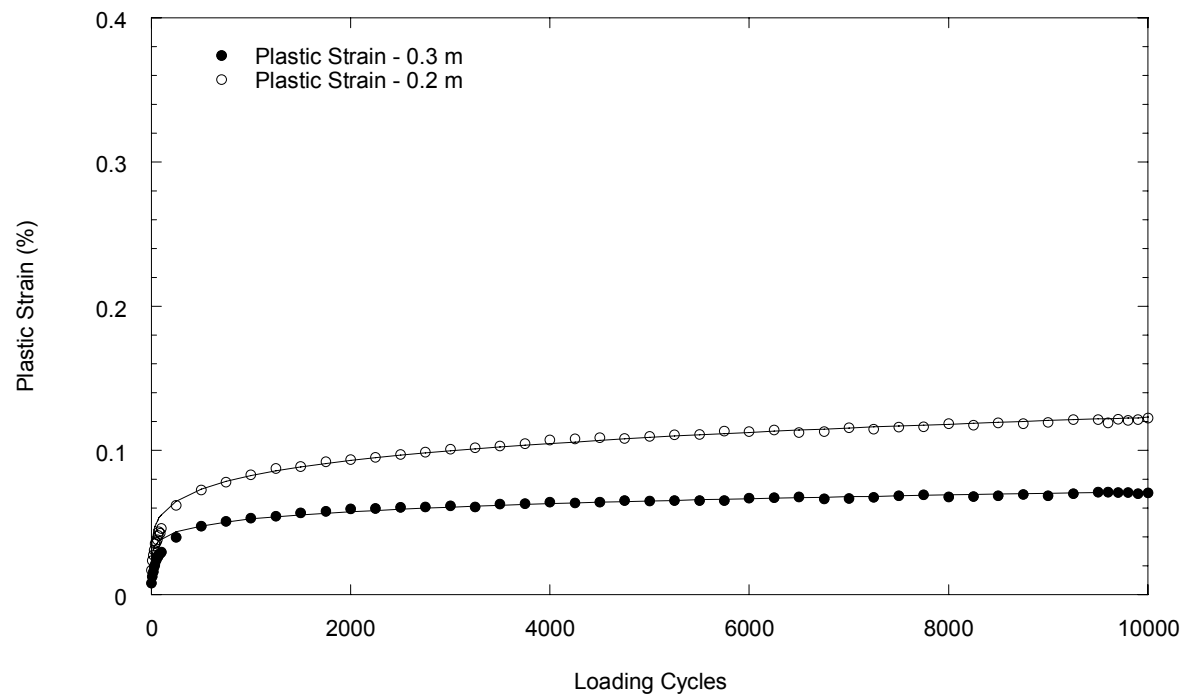


Fig. 4.15. Plastic strain vs. loading cycle for Class 5.

Yang et al. 2008, Kootstra et al. 2010). The steady state condition achieved for RAP also maintains a constant plastic strain rate; however the strain rate is non-zero and continues to accumulate with increased cyclical loading. The non-zero plastic strain rate in RAP can be attributed to the viscous nature of the asphalt that coats the RAP aggregate, and corresponds to behavior in accordance with creep shakedown (Mohammad et al. 2006, Kootstra et al. 2010).

The strain data from the LSME tests was fitted to the VESYS power function model (FHWA 1978) to estimate rutting potential. The VESYS power function is defined by:

$$\epsilon_p = aN^b \quad (4.2)$$

where  $a$  represents the initial densification after the first pass of traffic,  $b$  represents the rate at which permanent strain accumulates, and  $N$  is the number of load repetitions. Parameters  $a$  and  $b$  are dimensionless. The fitting parameters used in Eq. 4.2 are summarized in Table 4.1. The cumulative plastic strain in each of the base courses after  $3 \times 10^7$  loading cycles (i.e. 4000 daily truck loads over 20 years) was estimated using Eq. 4.2. Rutting depths based on the estimated plastic strain are also summarized in Table 4.1.

An acceptable limit to the rutting of flexible pavements has been suggested to be 13 mm (Huang, 2004). Based on LSME data, conventional granular base course (Class 5) can be expected to contribute 4 to 8% of the permissible rut depth. RCA and blended RCA/Class 5 can be expected to contribute 3 to 6% of the permissible rut depth, which is comparable to that of Class 5. Conversely, RAP can be expected

Table 4.1. Summary Resilient Modulus (SRM) and power model fitting parameters  $k_1$  and  $k_2$  Eq. 2.2) for base materials.

Material	Thickness (m)	Eq. 4.x		$\epsilon_p$ (%) due to cyclic load for $N=3 \times 10^7$	Rutting depth due to plastic strain in base (mm)
		a	b		
RAP	0.2	0.051	0.220	2.25	4.5
	0.3	0.058	0.197	1.72	5.2
RCA	0.2	0.004	0.243	0.26	0.5
	0.3	0.003	0.230	0.16	0.5
Blend	0.2	0.017	0.165	0.29	0.6
	0.3	0.011	0.178	0.24	0.7
Class 5	0.2	0.025	0.173	0.49	1.0
	0.3	0.021	0.134	0.21	0.6

to contribute between 30 and 40% of the acceptable rut depth, which is appreciable compared to that contributed by Class 5. Flexible pavements that incorporate RAP as a base course layer can be expected to encounter excessive rutting, whereas flexible pavements that incorporate RCA and RCA/natural aggregate blends will experience rutting comparable to pavements incorporating conventional base course aggregate.

#### **4.2. Comparison of Large and Small-Scale Resilient Moduli**

The resilient modulus as a function of bulk stress for RAP, RCA, blended RCA/Class 5, and Class 5 are presented in Figs. 4.16 thru 4.19, respectively. This relationship is presented for both the 0.2 m and 0.3 m thick layers tested in the LSME, as well as for the bench-scale specimen tests performed according to NCHRP 1-28a on the same materials by Son (2010). Bench-scale tests were evaluated for deflections measured externally, relative to the test cell, and internally at the upper and lower quarter points along the specimen length. Fitting parameters  $k_1$  and  $k_2$  determined from the bench-scale tests were used to calculate the resilient modulus as a function of bulk stress as defined by the power function model suggested by Eq. 2.2. The parameter  $k_2$  determined from the bench-scale tests was used in the back analysis of the LSME data to determine the parameter  $k_1$  that allowed the matching of the measured deflections in the LSME using the MICHPAVE code with the modulus function according to Eq. 2.2. The power-function relationship illustrates the concept that increased bulk stress contributes to an increase in resilient modulus for granular materials. A summary of the  $k_1$  and  $k_2$

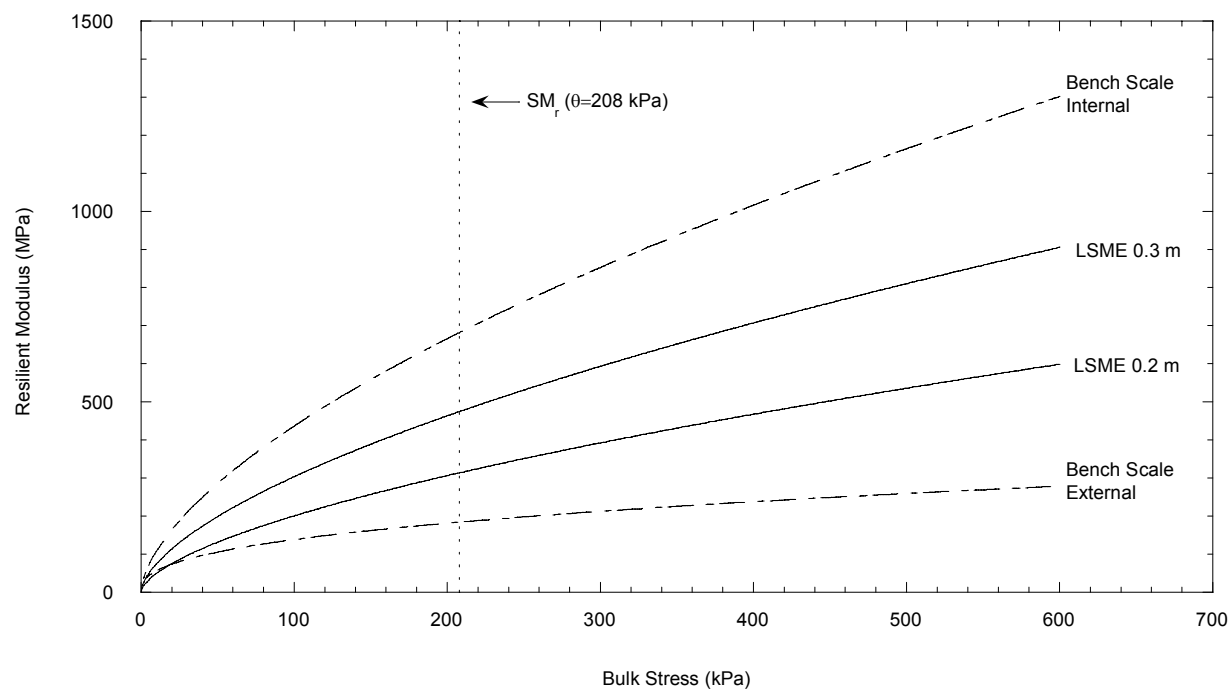


Fig. 4.16. Resilient modulus vs. bulk stress for bench-scale and LSME test methods for RAP.

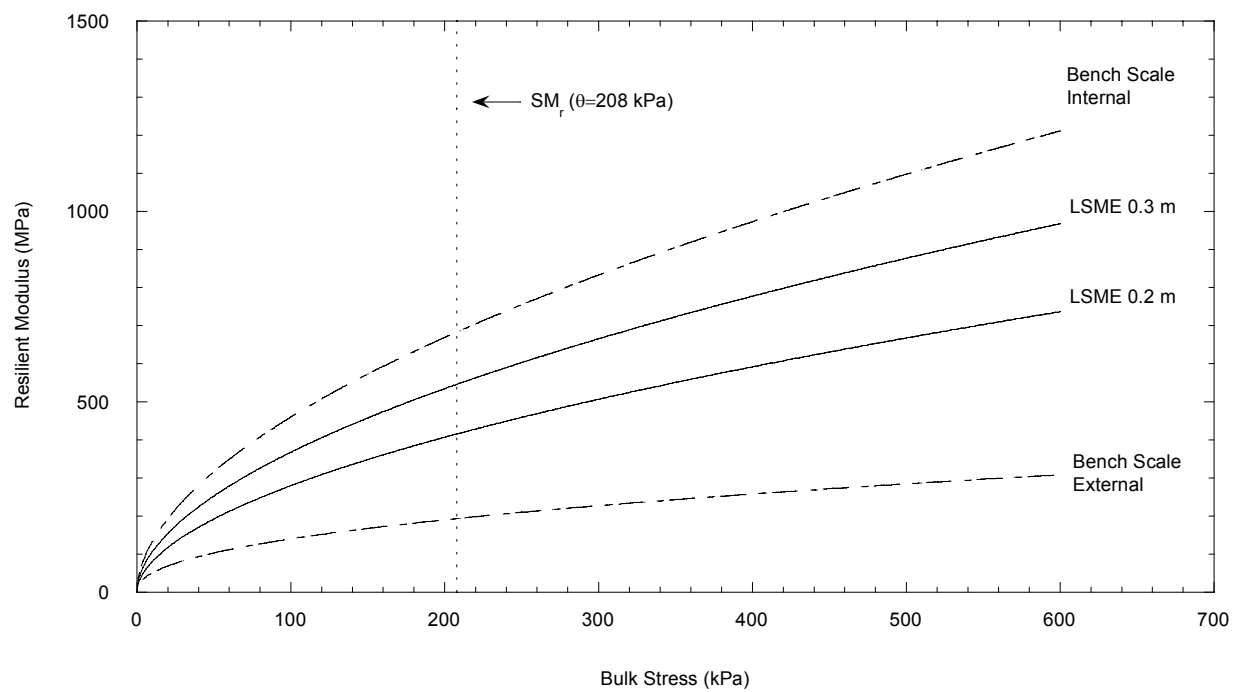


Fig. 4.17. Resilient modulus vs. bulk stress for bench-scale and LSME test methods for RCA.

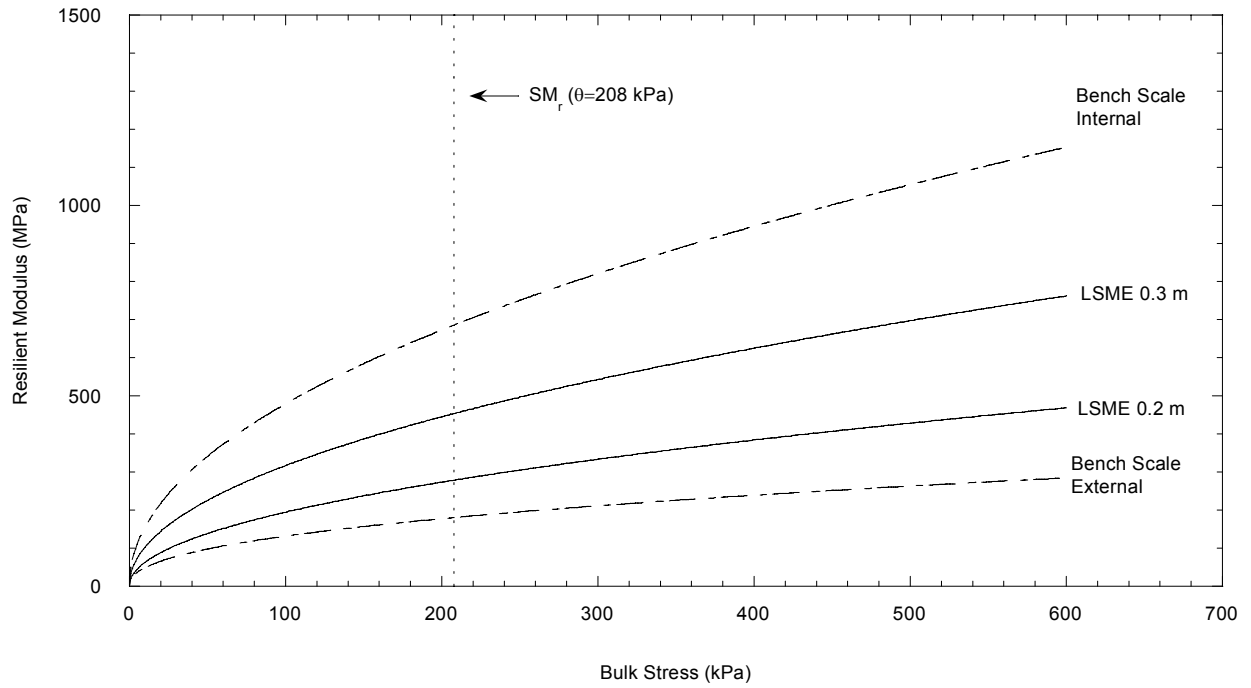


Fig. 4.18. Resilient modulus vs. bulk stress for bench-scale and LSME test methods for blended RCA/Class 5.

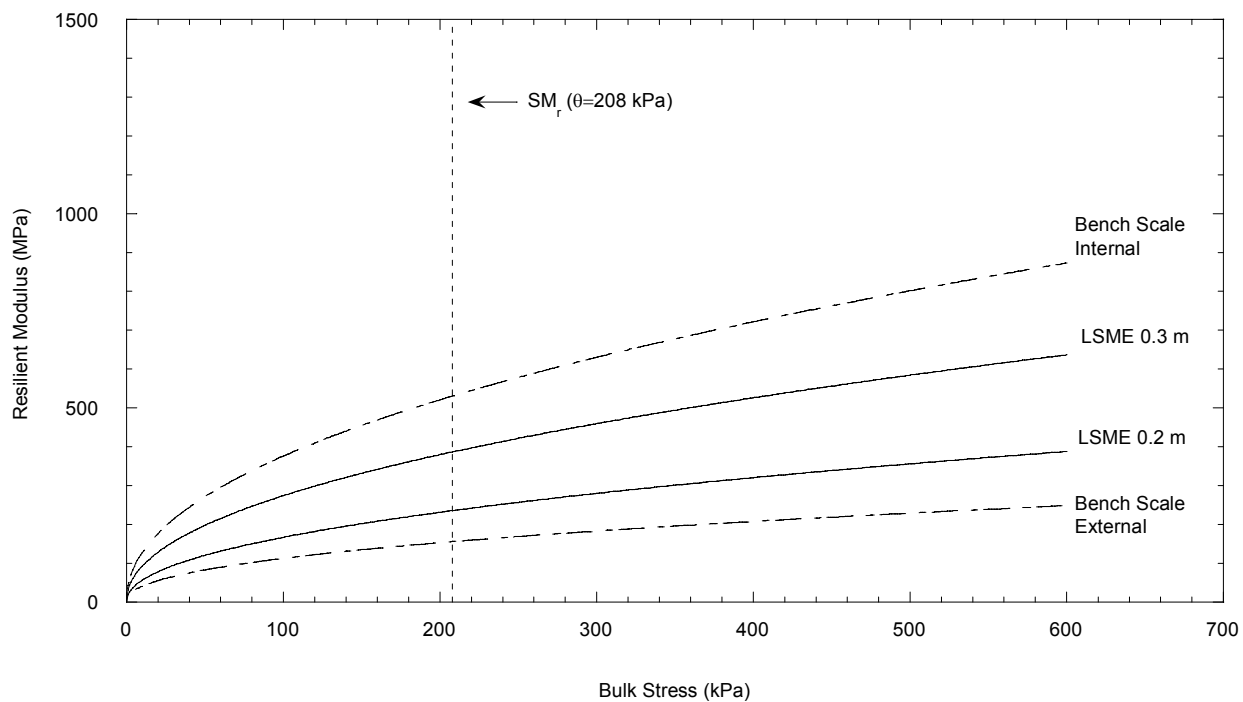


Fig. 4.19. Resilient modulus vs. bulk stress for bench-scale and LSME test methods for Class 5.



obtained in the tests is presented in Table 4.2.

The internal and external bench-scale tests had the highest and lowest resilient modulus, respectively, and the LSME tests for 0.3 m and 0.2 m layer thicknesses had the second and third highest resilient modulus, respectively, for each of the four materials (Figs. 4.16-4.19). No direct correlation can be made between the resilient moduli measured for bench-scale tests and the resilient modulus back-calculated from the LSME. The magnitudes of the four tests appear to be evenly spaced when referenced between the maximum and minimum values defined by the bench-scale tests. The moduli of both LSME tests seem to trend closer to the internal bench-scale test for the RCA case, and to the external bench-scale test for the blended RCA/Class 5 case; however these trends are slight and should not be considered direct correlations.

A comparison of the summary resilient moduli (SRM) determined for RAP, RCA, blended RCA/Class 5 and Class 5 are presented in Fig. 4.20. The SRM is based on a bulk stress of 208 kPa as suggested for base course materials by NCHRP 1-28a sec 10.3.3.9, and calculated according to Eq. 2.2 using the  $k_1$  and  $k_2$  presented in Table 4.2. The SRM calculated for each test method is also presented in Table 4.2.

RCA and Class 5 had the highest and lowest SRM, respectively, for each of the four testing methods. The SRMs of the RAP and blended RCA/Class 5 are approximately equal in magnitude for bench-scale testing, with RAP having a marginally higher SRM for both LSME tests. The SRM of RCA was 42% to 77% greater than that of Class 5, while the SRM of RAP was 23% to 33% greater. The

Table 4.2. Summary Resilient Modulus (SRM) and power model fitting parameters k1 and k2 Eq. 2.2) for base materials.

Material	Test Method	Thickness (m)	Measured Parameters		
			k1	k2	SRM (MPa)
RAP	Bench-Scale – Internal	0.30	26.3	0.61	674
	Bench-Scale – External	0.30	23.0	0.39	180
	LSME	0.20	12.1	0.61	314
		0.30	18.3	0.61	474
Class 5	Bench-Scale – Internal	0.30	43.2	0.47	525
	Bench-Scale – External	0.30	14.9	0.44	152
	LSME	0.20	19.2	0.47	236
		0.30	31.5	0.47	386
Blend	Bench-Scale – Internal	0.30	50.2	0.49	675
	Bench-Scale – External	0.30	18.2	0.43	182
	LSME	0.20	20.4	0.49	278
		0.30	33.2	0.49	454
RCA	Bench-Scale – Internal	0.30	38.3	0.54	680
	Bench-Scale – External	0.30	18.5	0.44	189
	LSME	0.20	23.3	0.54	417
		0.30	30.6	0.54	547

Note: SRM calculated at a bulk stress of 208 kPa.

\* Bench-scale SRM reported by Son (2010).

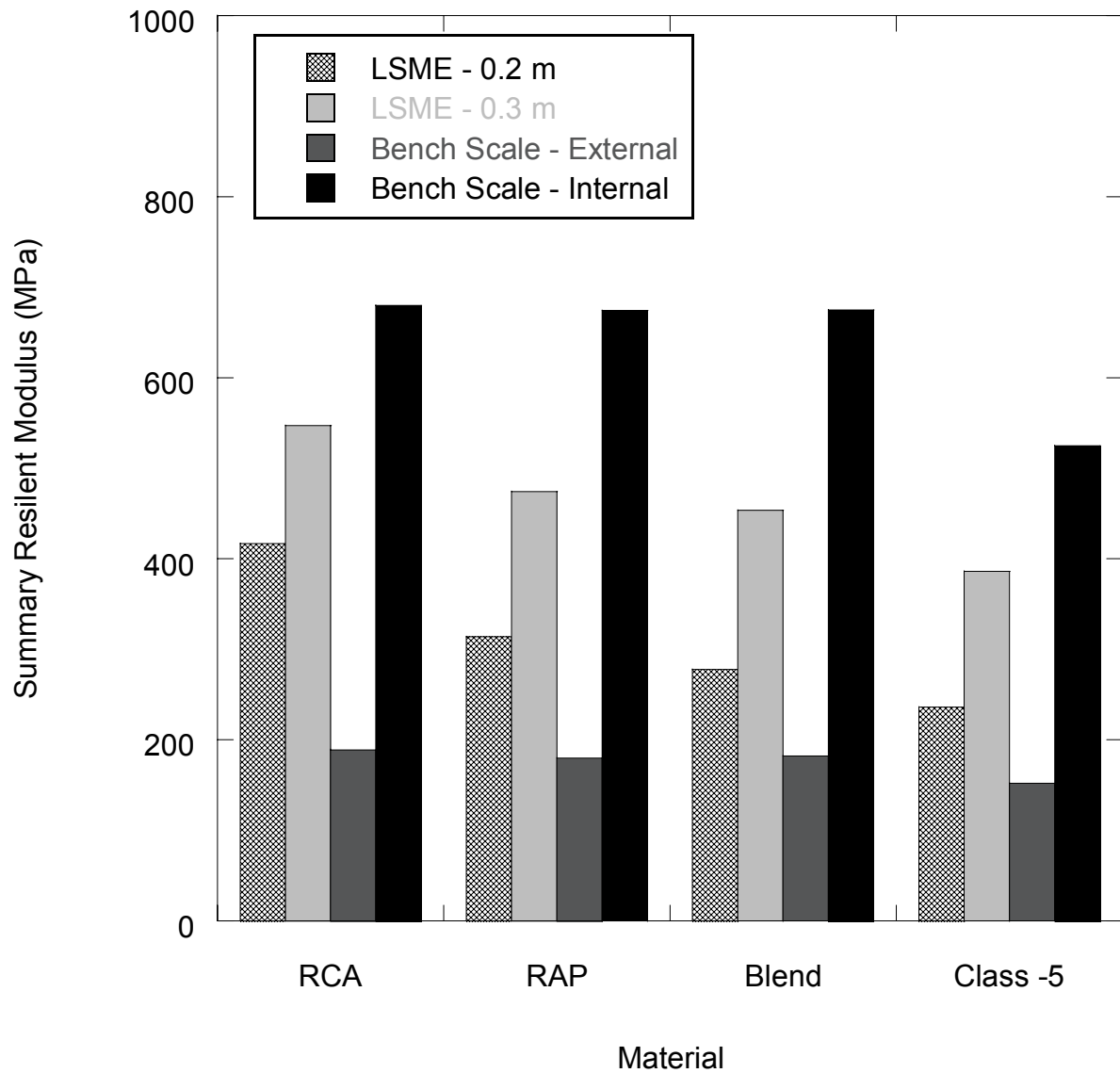


Fig. 4.20. Comparison of summary resilient modulus for RAP, RCA, blended RCA/Class 5, and Class 5.

SRM of the blended RCA/Class 5 was 18% greater than that of Class 5, which was comparable in magnitude to the SRM of RAP.

The SRM as a function of layer thickness is presented in Fig. 4.21 for RAP, RCA, blended RCA/Class 5, and Class 5. The resilient modulus of each material increases with a corresponding increase in layer thickness. The magnitude of this increase, which lies between 130 MPa and 176 MPa, appears relatively consistent for all materials and does not appear to trend differently for any individual material.

The SRM as a function of RCA content is presented in Fig. 4.22 for RCA, blended RCA/Class 5, and Class 5. The SRM of the materials increases with an increase in RCA content. The magnitude of the increase seems to increase at the same rate regardless of layer thickness. The blended RCA/Class 5 defines a downward “spike” for both the 0.2 m and 0.3 m layer thicknesses, which interrupts an otherwise linear trend. One possible reason for this spike is that there is some form of particle interaction that is reducing the stiffness of the blended material as a whole. A second, more probable reason for the spike is that the blended material is not a perfect blend of 50% RCA and 50% Class 5. Measuring the mass of materials in the field relies on approximations to a certain extent, and the actual amounts blended together might vary depending on the experience of the field engineer. Also, the material was mixed in the field using the blade of a bulldozer. Such mixing methods are not thorough, and samples taken from such mixtures could vary depending on sample location. Based on these assumptions and the SRM calculated for the blended material, a blend incorporating an RCA content of between 20% and 40% would better fit a linear trend between SRMs calculated for 0% and 100% RCA.

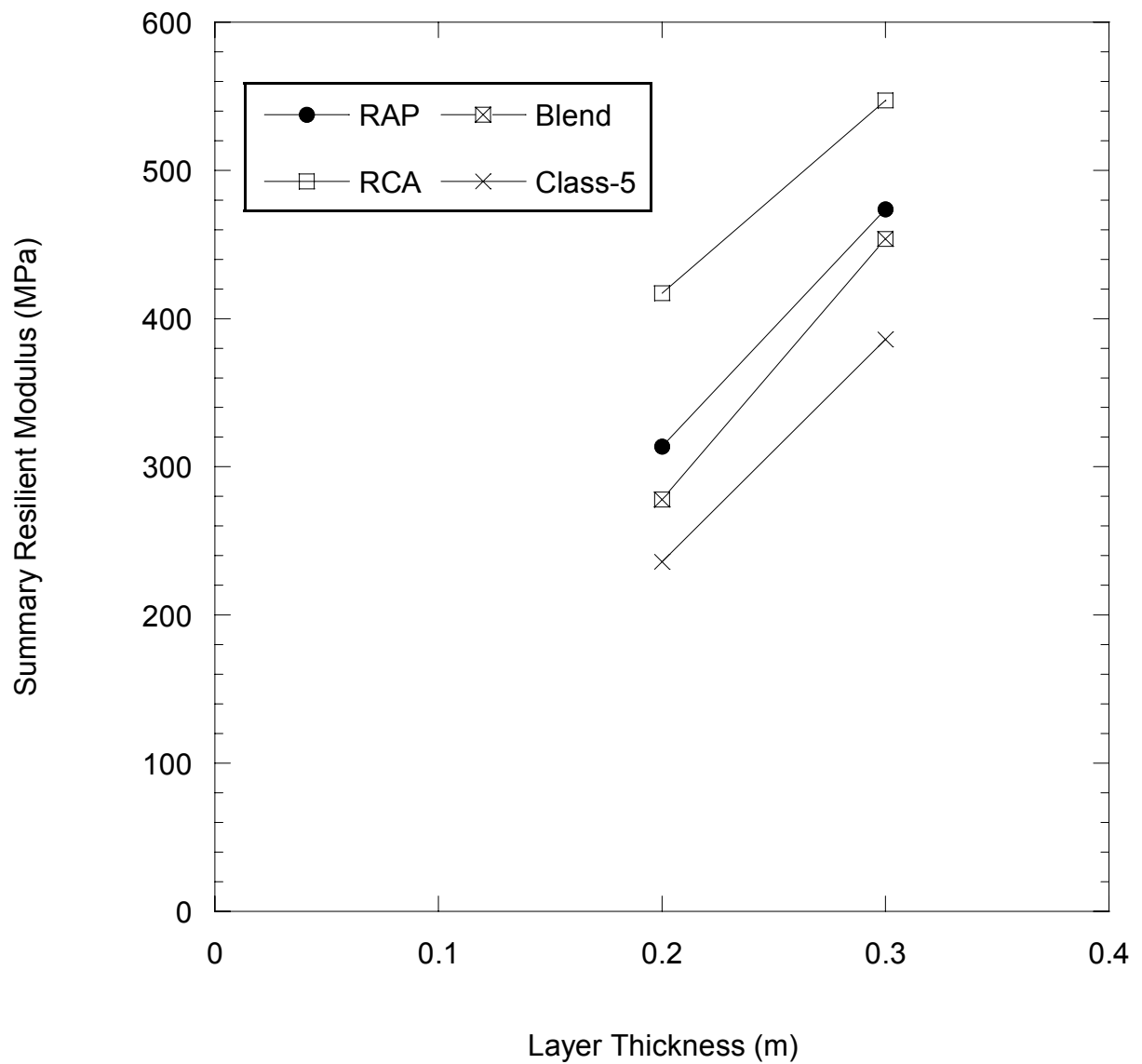


Fig. 4.21. Summary Resilient Modulus vs. layer thickness for RAP, RCA, blended RCA/Class 5, and Class 5.

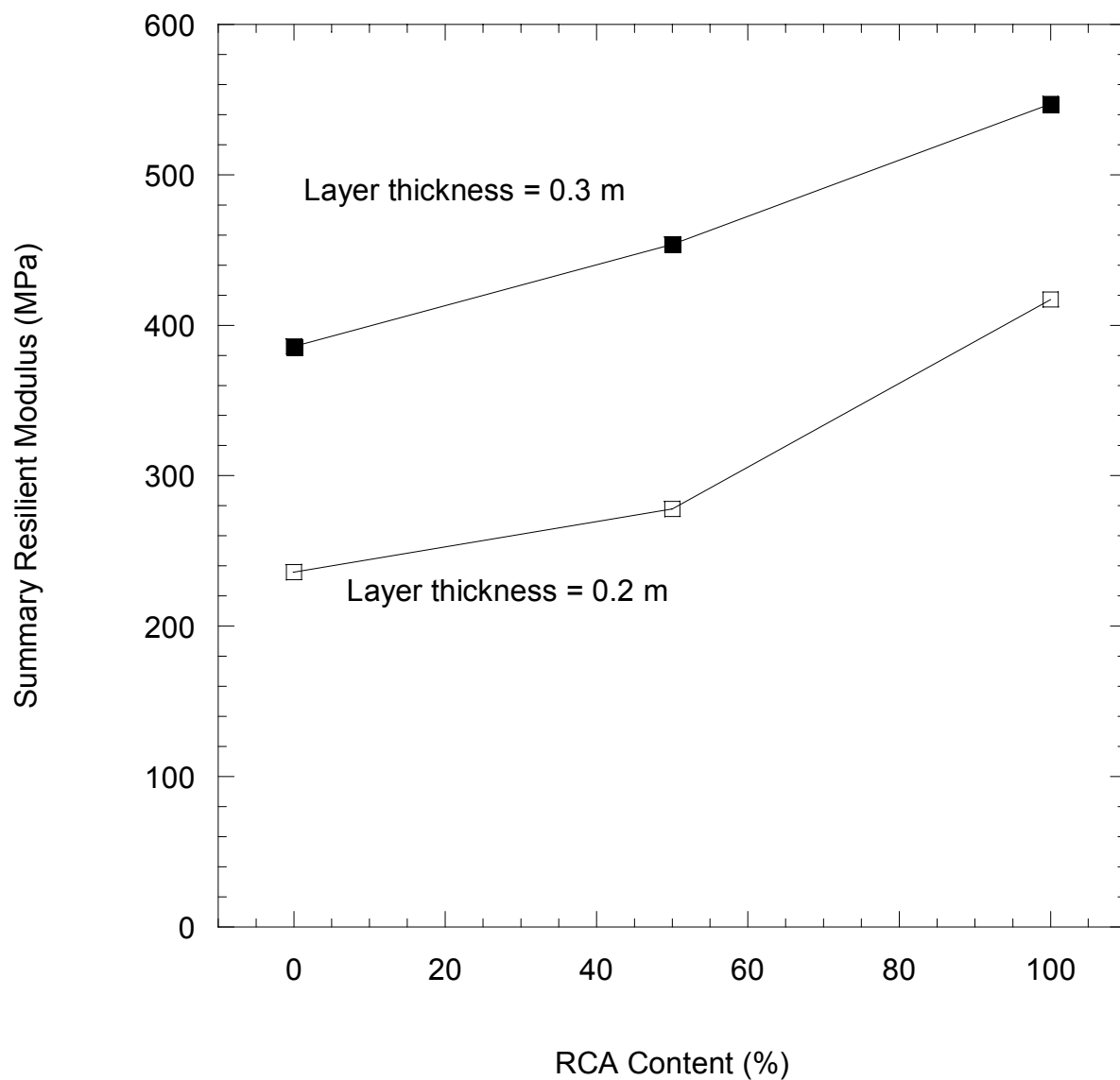


Fig. 4.22. Summary Resilient Modulus vs. RCA content for RCA, blended RCA/Class 5, and Class 5.

### 4.3. Scaling Laboratory Results to Field Conditions

#### 4.3.1. Background

The elastic modulus of granular material has been shown to be sensitive to strain amplitude (Seed and Idriss 1970, Hardin and Drnevich 1972, Edil and Luh 1978). Thicker layers distribute stress more efficiently and reduce the amount of strain experienced by the material. The resilient modulus of a material evaluated at a given bulk stress can vary in magnitude depending on which testing method is being used (Fig. 4.20). These differences in magnitude are assumed to be due to differences in stress state and strain level (Tanyu et al. 2003, Schuettpeiz et al. 2008, Benson et al. 2009). A more accurate comparison between the various testing methods can be established by adjusting the resilient modulus to account for these differences in stress and strain level.

A backbone curve can be used to describe the stress-strain dependency of resilient modulus (Seed and Idriss 1970, Hardin and Drnevich 1972). Backbone curves represent the ratio of shear modulus ( $G_V$ ) at a given shear strain to the low-strain shear modulus ( $G_{max}$ ) as a function of shear strain amplitude for a given state of stress. The relation between shear modulus and shear strain can be approximated by the following relationship suggested by Hardin and Drnevich:

$$\frac{G_V}{G_{max}} = \frac{M_r}{E_s} = \frac{1}{1+\gamma_h} \quad (4.3)$$

where  $\gamma_h$  is defined as the hyperbolic strain. The hyperbolic strain is the strain normalized with respect to the reference strain ( $\gamma_r$ ):

$$\gamma_h = \frac{\gamma}{\gamma_r} \left[ 1 + a e^{-b \left( \frac{\gamma}{\gamma_r} \right)} \right] \quad (4.4)$$

where  $a$  and  $b$  describe the shape of the backbone curve. The reference strain is defined as the strain at the intersection of maximum shear stress and shear modulus (Hardin and Drnevich 1972). These relationships can be used for resilient modulus dependency on strain amplitude by assuming that the ratio  $G_v/G_{\max}$  is equal to the ratio of resilient modulus at a given shear strain to the low-strain Young's modulus (maximum modulus) ( $M_r/E_s$ ),

#### **4.3.2. Measurement of Low-strain Modulus**

The low-strain modulus of the materials was determined using the small-scale simple seismic test method suggested by Schuettpelez (2009). The method is based on the propagation of surface waves and is intended to be a much simpler method of data acquisition when compared to methods involving larger testing schemes. Material was compacted to 95% of the maximum dry density under modified compaction effort within a 5-gallon bucket to a volume of approximately  $11 \times 10^{-3} \text{ m}^3$ . Approximately 0.23 kN of material was used for each test (Fig. 4.23). Material was compacted with a tamper in four lifts of equal measure to ensure uniform density. A 150 mm diameter load plate was placed central to the surface of the material, and a small amount of material was removed from opposing sides of the plate. Two accelerometers were placed adjacent to the plate and buried approximately 10 mm below the soil surface. The accelerometers were aligned with one axis parallel to the ground surface, and 500 gram masses were used to seat the accelerometers into the soil and make the first arrivals of elastic waves more distinguishable. The



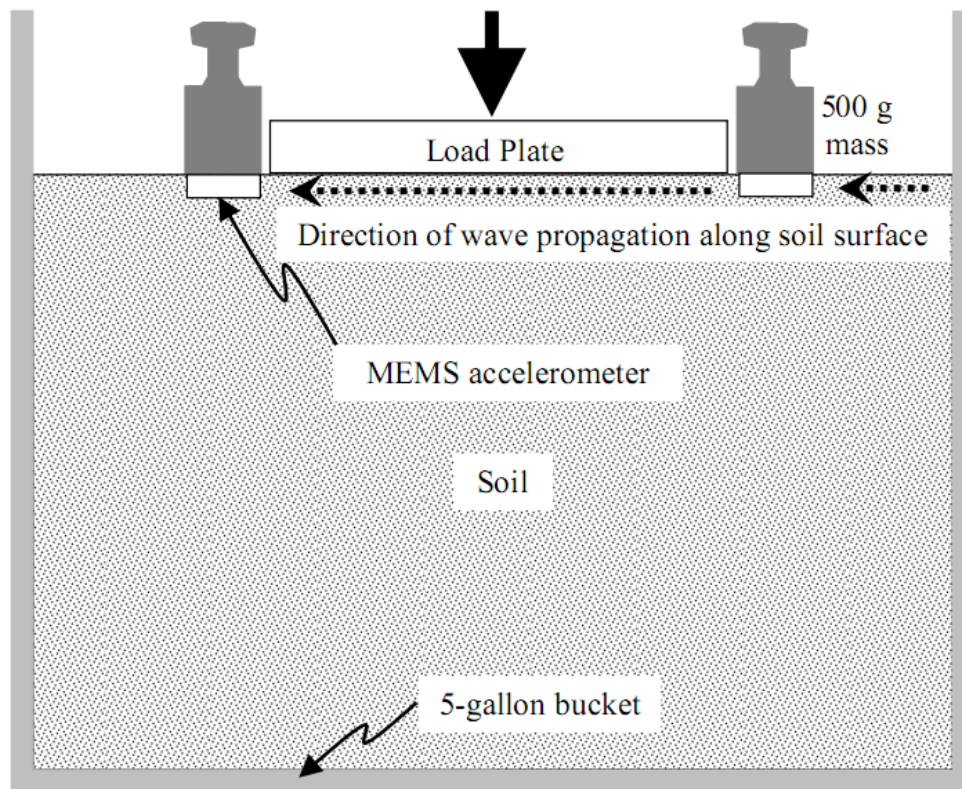


Fig. 4.23. Simplified test setup to determine low-strain constraint modulus with applied stress near the surface. (Adapted from Edil and Fratta 2009)

final distance between the accelerometers was recorded for each test. The actuator from the LSME was used to apply varying static loads to the material during testing.

The side of the 5-gallon bucket was tapped with a rubber mallet and the travel time of the surface wave between the two accelerometers was recorded. The P-wave velocity ( $V_p$ ) was determined by multiplying the surface velocity ( $V_r$ ) by a conversion factor based on the Poisson's ratio ( $\nu$ ) (Santamarina et al. 2001, Kramer 1996):

$$V_p = V_r \frac{(1+\nu) \sqrt{\frac{2(1-\nu)}{1-2\nu}}}{0.874+1.117\nu} \quad (4.5)$$

$V_p$  in particulate media is dependent on elastic modulus ( $E$ ), Poisson's ratio ( $\nu$ ), and density ( $\rho$ ) (Santamarina et al. 2001, Richart et al. 1970):

$$V_p = \sqrt{\frac{E(1-\nu)}{\rho(1+\nu)(1-2\nu)}} \quad (4.6)$$

The velocity of wave propagation increases with increasing applied load and soil stiffness.

The low-strain elastic modulus can be calculated from the  $V_p$ ,  $\rho$ , and  $\nu$  of the material by rearranging Eqn. 4.6:

$$E_s = \frac{V_p^2(1+\nu)(1-2\nu)}{(1-\nu)} \quad (4.7)$$

where  $\nu$  was taken to be 0.35 for the granular material. The low-strain elastic modulus was plotted as a function of the stress applied to the surface of the soil by the loading plate. The low-strain elastic modulus was assumed to increase with the applied stress according to the power function described by Eqn. 2.2. The fitting parameters  $k_{1,s}$  and  $k_{2,s}$  were varied until a best-fit was found for the plotted data.

The relationship between  $E_s$  and the applied stress for the evaluated base course materials is presented in Fig. 4.24. The low-strain modulus determined for the RCA and blended material were of approximately the same magnitude, with the Class 5 having a low-strain modulus approximately two-thirds the magnitude of RCA and blended material. The low-strain modulus for the RAP was significantly higher of a magnitude approximately 3.5 to 5 times greater than the other materials. The asphalt coating the RAP is most likely self-adhering, and under small strains and the effects of this adhesion are not as easily overcome as the typical particle friction common in non-bituminous materials. This resistance to strain at the particle level would increase the low-strain modulus of the RAP accordingly.

#### 4.3.3. Development of Backbone Curve

The backbone curve was developed from the resilient modulus and shear strain data collected from the bench-scale, LSME and FWD testing. Vertical strains and bulk stresses were determined for the bench-scale tests using NCHRP 1-28a, and for the LSME and FWD tests using MICHPAVE at varying depths within the base course layers. The shear strain was determined from the vertical strain (Kim and Stokoe 1992, Tanyu et al. 2003):

$$\gamma = \varepsilon(1 + \nu) \quad (4.8)$$

where  $\gamma$  is the shear strain,  $\varepsilon$  is the vertical strain, and  $\nu$  is the Poisson's ratio. The normalized resilient modulus was determined using Eqn. 4.9:

$$\text{Normalized resilient modulus} = \frac{M_r}{E_s} \quad (4.9)$$

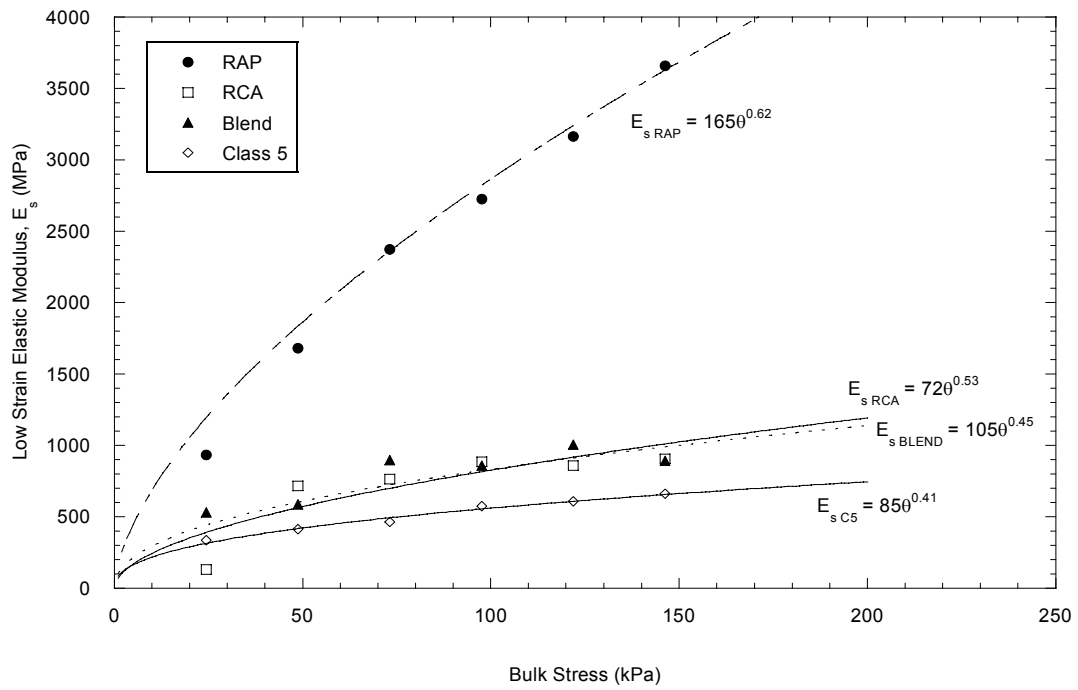


Fig. 4.24. Low-strain elastic modulus as a function of applied vertical stress.

where  $M_r$  and  $E_s$  are the resilient modulus and low-strain Young's modulus for a particular bulk stress, respectively. Parameters  $a$  and  $b$  in Eqn. 4.4 were adjusted to obtain a best-fit to the calculated points. The bulk stress, resilient modulus, low-strain Young's modulus, and normalized resilient modulus for each test method are presented in Table 4.3.

The backbone curves showing normalized modulus as a function of shear strain are shown in Figs. 4.25 thru 4.28 for RAP, RCA, Blended RCA/Class 5 and Class 5. The backbone shape describes the stress-strain behavior of the evaluated base course and is unique for a given material. The bench-scale tests with internally and externally measured deflections produce the lowest and highest strain levels, respectively. The 0.3-m and 0.2- m thick LSME tests produce the second and third lowest strains, respectively, with the FWD producing strains between those produced by the 0.2-m thick LSME and the external bench-scale test. The normalized resilient moduli of the RAP are considerably smaller compared to the normalized resilient modulus of the other tested materials. The bitumen coating the RAP causes the particles to adhere to each other, which leads to an increase in strain resistance at low stresses.

#### **4.3.4. Scaling Specimen Tests to Field-Scale Conditions**

A comparison of the resilient modulus calculated at field bulk stress is presented in Fig. 4.29 for RAP, RCA, blended RCA/Class 5, and Class 5. The field bulk stress is the bulk stress experienced under FWD loading as calculated at the

Table 4.3. Bulk stress, resilient modulus, low-strain modulus and normalized resilient modulus for FWD, LSME and bench-scale tests.

Test Method	Bulk Stress (kPa)	Resilient Modulus (MPa)	Low-strain Modulus (MPa)	Normalized Resilient Modulus
Recycled Asphalt Pavement				
FWD	112	195	3076	0.06
LSME (0.20 m)	169	276	3969	0.07
LSME (0.30 m)	117	335	3161	0.11
Bench-Scale – External	110 – 858	128 – 345	3,042 – 10,867	0.04*
Bench-Scale – Internal	110 – 858	435 – 2,071	3,042 – 10,867	0.15*
Recycled Concrete Aggregate				
FWD	137	265	977	0.27
LSME (0.20 m)	159	360	1,058	0.34
LSME (0.30 m)	116	398	893	0.45
Bench-Scale – External	113 – 857	141 – 403	882 – 2,582	0.15*
Bench-Scale – Internal	113 – 857	484 – 1,644	882 – 2,582	0.56*
Blended RCA/Class 5				
FWD	117	225	895	0.25
LSME (0.20 m)	166	248	1,047	0.24
LSME (0.30 m)	116	341	893	0.38
Bench-Scale – External	109 – 867	142 – 428	868 – 2,204	0.17*
Bench-Scale – Internal	113 – 867	492 – 1,857	881 – 2,204	0.64*
Class 5				
FWD	127	97	619	0.16
LSME (0.20 m)	170	215	698	0.31
LSME (0.30 m)	118	297	601	0.49
Bench-Scale – External	95 – 839	94 – 326	550 – 1,344	0.20*
Bench-Scale – Internal	95 – 839	309 – 1,291	550 – 1,344	0.71*

\* - Average value

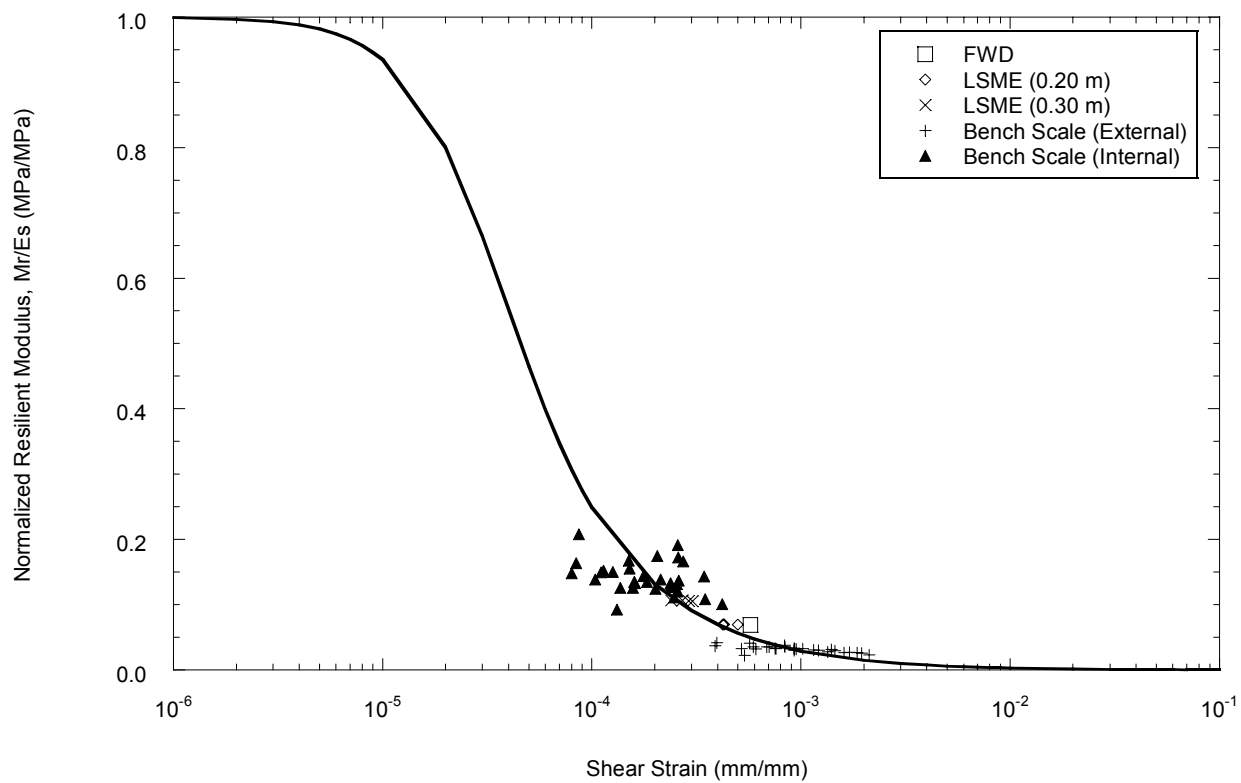


Fig. 4.25. Backbone curve fit to FWD, LSME and bench-scale data for RAP.

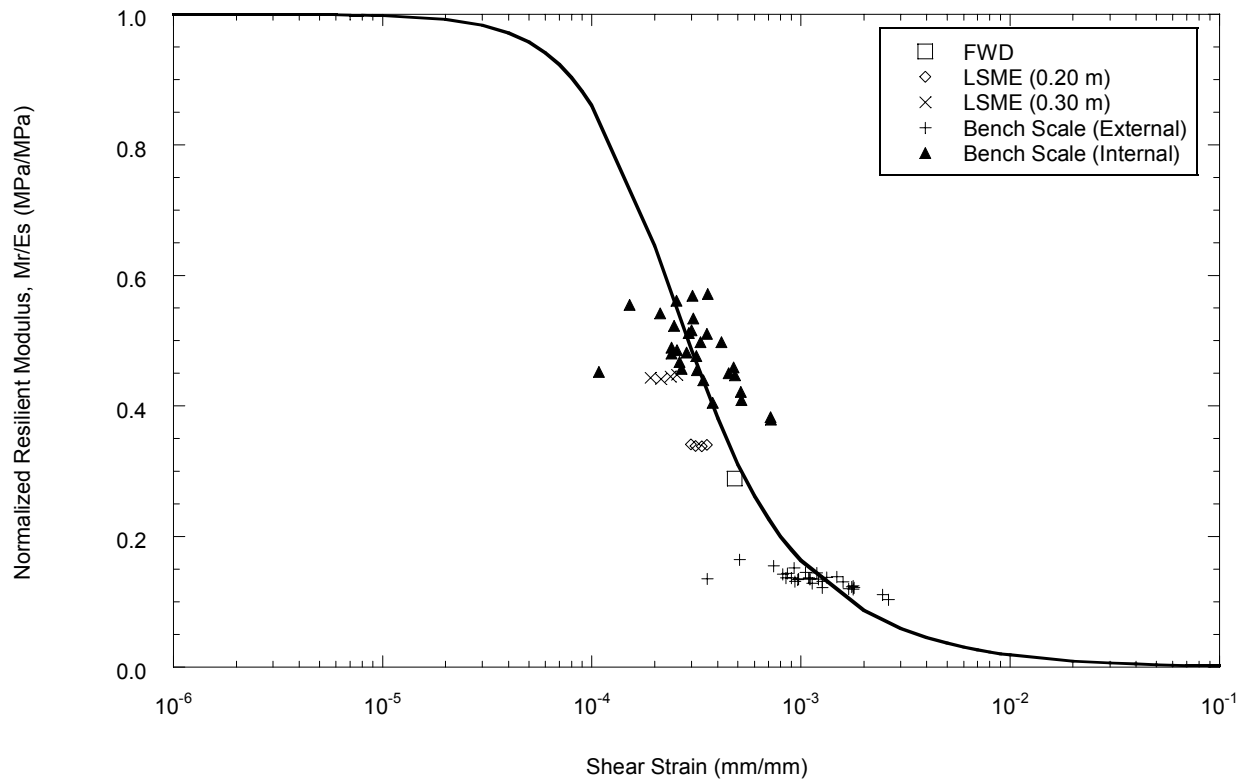


Fig. 4.26. Backbone curve fit to FWD, LSME and bench-scale data for RCA.



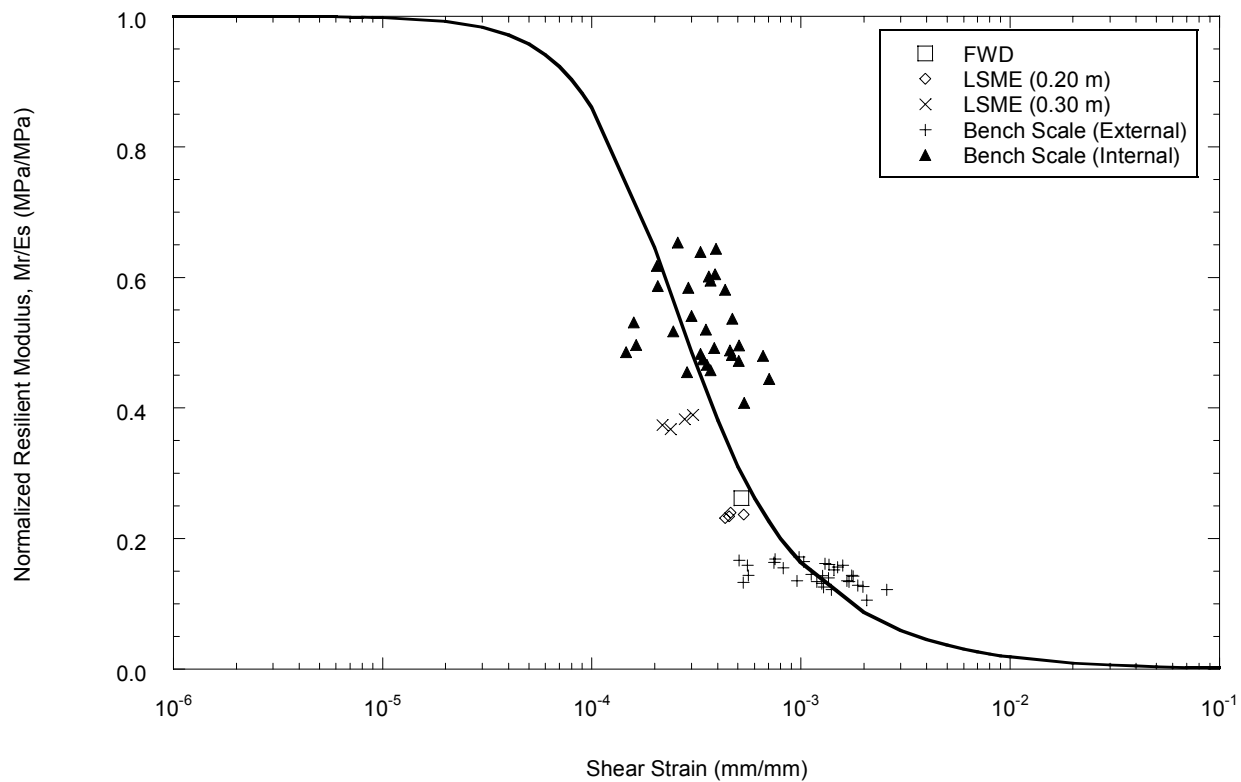


Fig. 4.27. Backbone curve fit to FWD, LSME and bench-scale data for blended RCA/Class5.

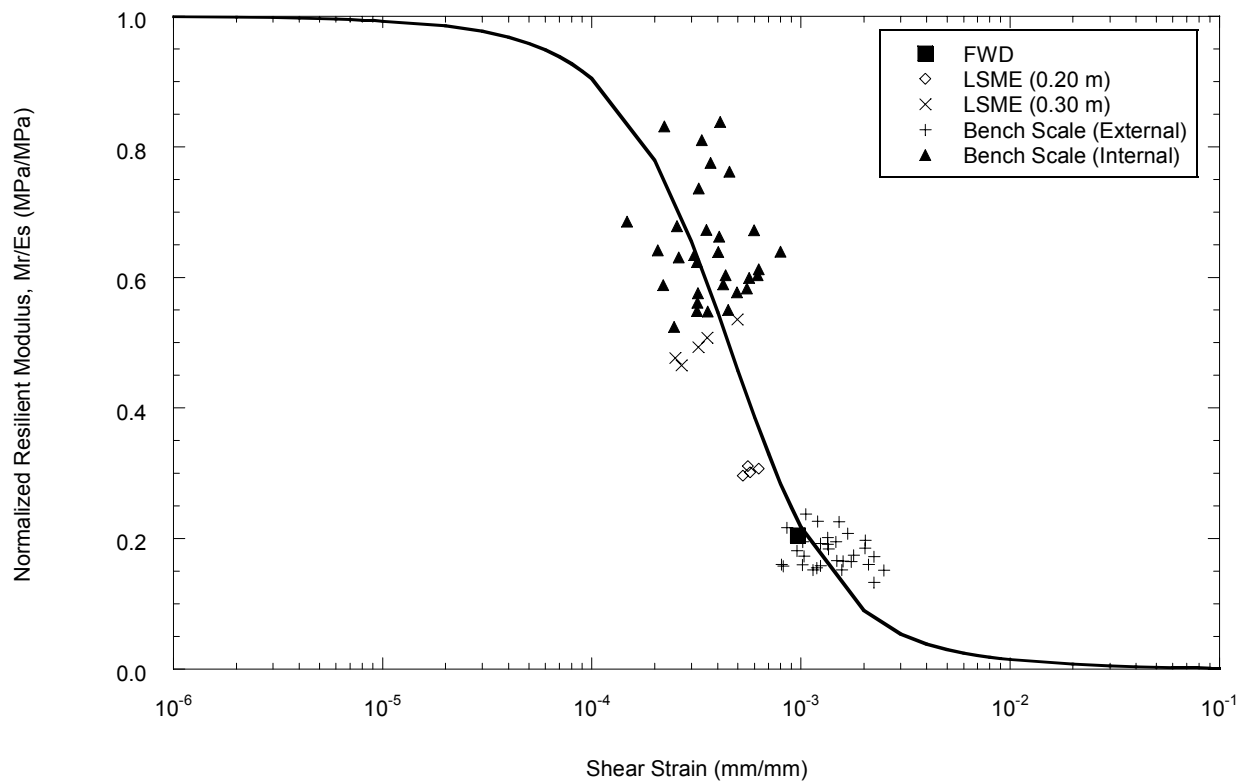


Fig. 4.28. Backbone curve fit to FWD, LSME and bench-scale data for Class 5.

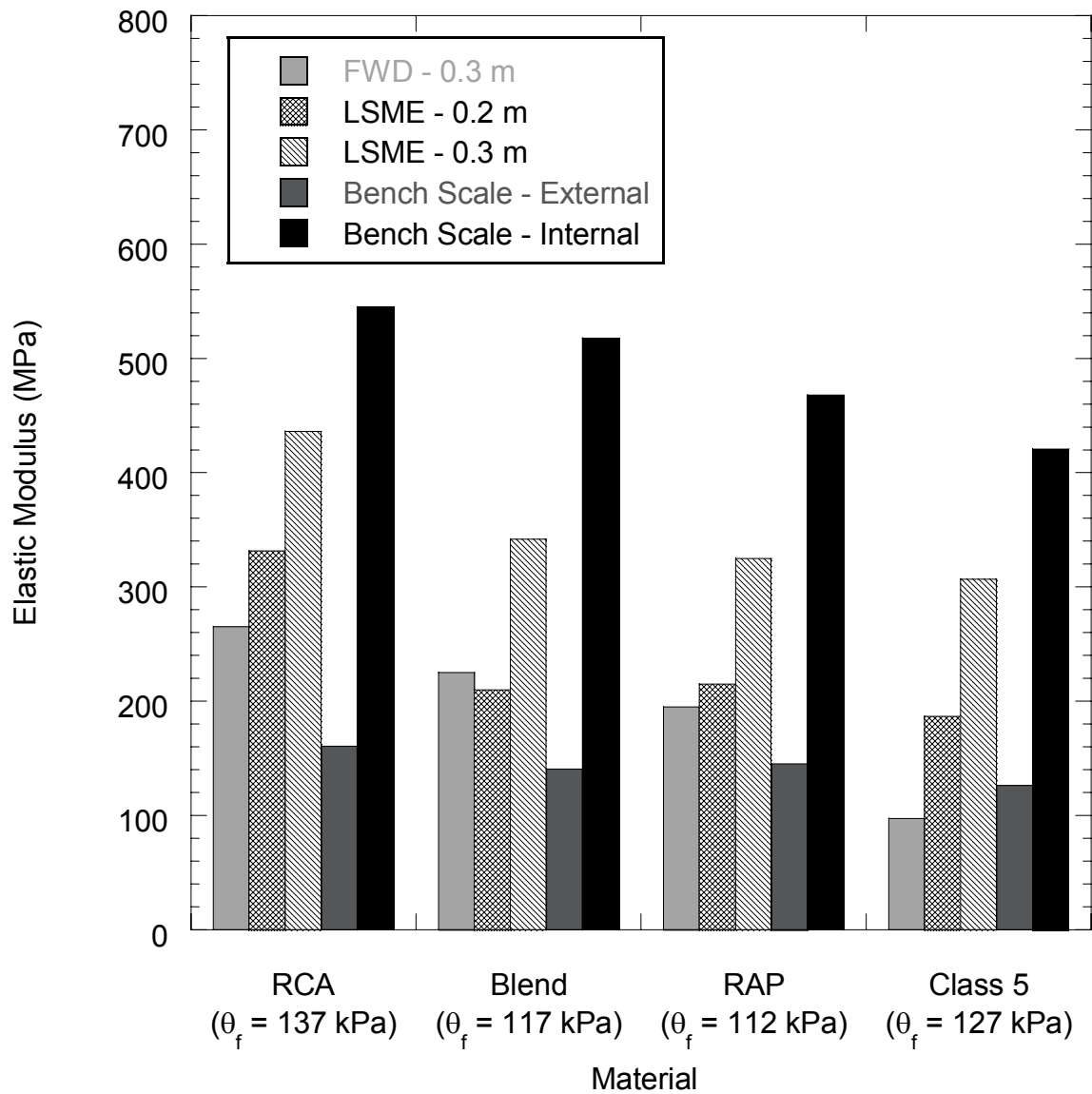


Fig. 4.29. Resilient modulus at field bulk stress ( $\theta_f$ ) for RAP, RCA, blended RCA/Class 5, and Class 5.

mid-depth of the layer using MICHPAVE. The resilient moduli of the LSME and bench-scale tests were recalculated for the field bulk stress using Eqn. 2.2. Table 4.3 summarizes the field bulk stress and resilient moduli determined for each loading test.

The low-strain modulus for each material at field bulk stress was calculated by multiplying the resilient modulus by the normalized resilient modulus. The low-strain resilient modulus at field bulk stress for each test method is presented in Fig. 4.30 and also summarized in Table 4.4. The variance of the low-strain (maximum) modulus determined for each test method is presented in Table 4.5. The coefficient of variance (c.o.v.) for RAP was the highest at 7.6%. The c.o.v. for RCA and blended material were approximately equal at 4.1% and 4.4%, respectively. The c.o.v. of the Class 5 was the smallest at 2.3%. For all materials, the coefficient of variance was 7.6% or less, indicating a reasonable amount of similarity between the test methods when properly scaled to the same bulk stress and strain level. It is also clear that different strain levels are induced in different tests resulting in varying resilient modulus depending on the test procedure even if at the same bulk stress. Bench-scale resilient modulus tests result in lower moduli based on externally measured deflections and in markedly higher moduli based on internally measured deflections in comparison to FWD or LSME moduli. LSME with 0.3-m thick layer (the same as in the field) resulted in higher moduli than the field moduli obtained from the FWD test. LSME moduli with 0.2-m thick layer were the closest to the field FWD moduli.

Table 4.4. Resilient modulus and low-strain modulus at field bulk stress.

Test Method	Resilient Modulus @ Field Bulk Stress (MPa)	Normalized Resilient Modulus	Low-strain Modulus (MPa)
Recycled Asphalt Pavement, Bulk Stress = 112 kPa			
FWD	195	0.06	3076
LSME (0.20 m)	215	0.07	3071
LSME (0.30 m)	325	0.11	2954
Bench-Scale – External	145	0.04	3625
Bench-Scale – Internal	468	0.15	3120
Recycled Concrete Aggregate, Bulk Stress = 137 kPa			
FWD	265	0.27	977
LSME (0.20 m)	332	0.34	976
LSME (0.30 m)	436	0.45	968
Bench-Scale – External	161	0.15	1073
Bench-Scale – Internal	545	0.56	973
Blended RCA/Class 5, Bulk Stress = 117 kPa			
FWD	225	0.25	895
LSME (0.20 m)	210	0.24	875
LSME (0.30 m)	342	0.38	900
Bench-Scale – External	141	0.17	829
Bench-Scale – Internal	518	0.64	809
Class 5, Bulk Stress = 127 kPa			
FWD	97	0.16	619
LSME (0.20 m)	187	0.31	603
LSME (0.30 m)	307	0.49	626
Bench-Scale – External	126	0.20	630
Bench-Scale – Internal	421	0.71	592

Table 4.5. Variance of low-strain elastic modulus obtained at field bulk stress.

Method	Low-strain Modulus at Field Bulk Stress (MPa)			
	RCA	RAP	Blend	Class 5
FWD	977	3076	895	619
LSME (0.20 m)	976	3071	875	603
LSME (0.30 m)	968	2954	900	626
Bench-Scale – External	1073	3625	829	630
Bench-Scale – Internal	973	3120	809	592
Mean Average	992	3160	863	614
Standard Deviation	40	239	38	14
Coefficient of Variance	4.1%	7.6%	4.4%	2.3%

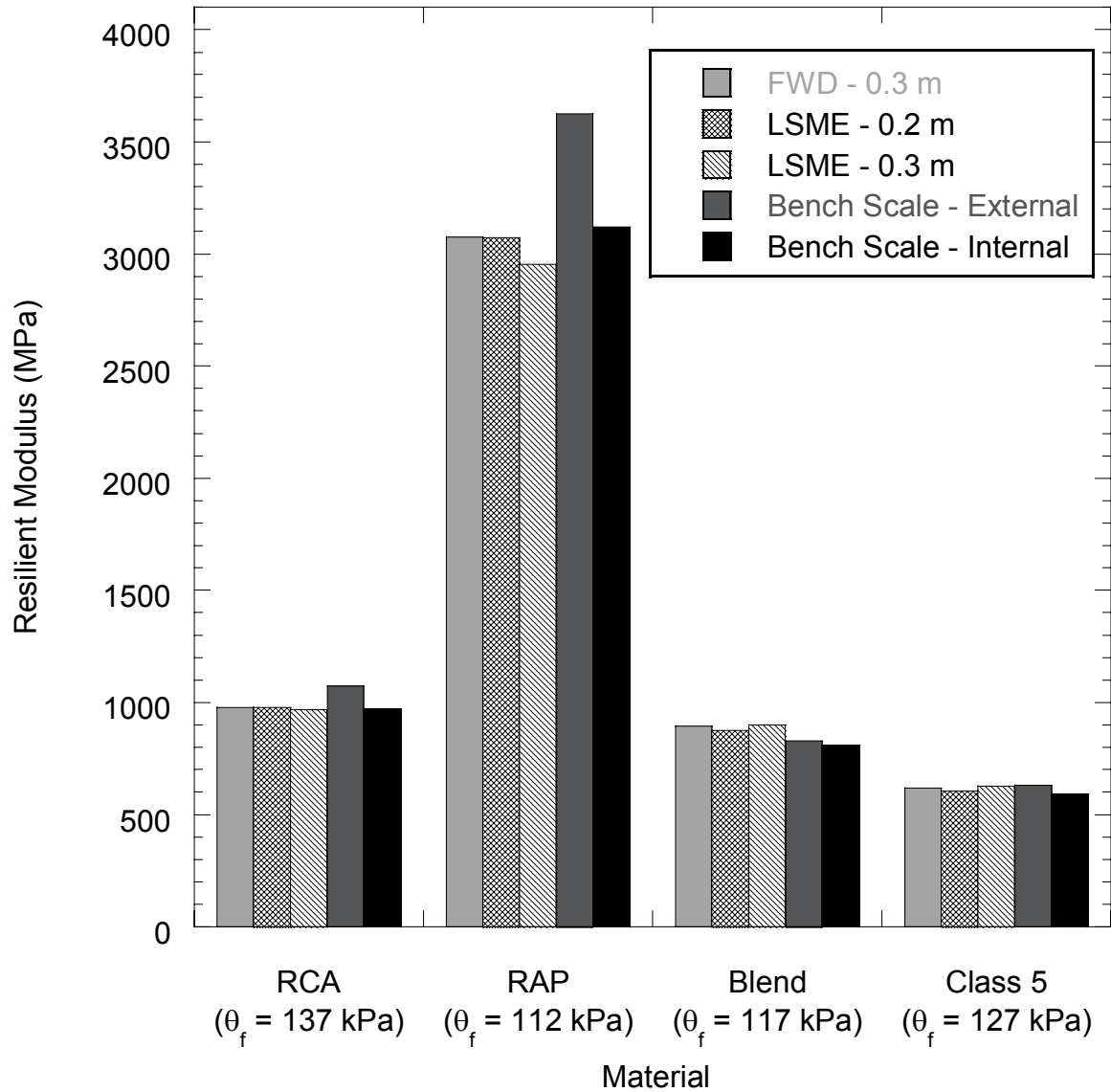


Fig. 4.30. Low-strain elastic modulus at field bulk stress ( $\theta_f$ ) for RAP, RCA, blended RCA/Class 5, and Class 5 as estimated from different test methods.

## 5. Summary and Conclusions

This laboratory investigation dealt with the determination of the resilient modulus of two recycled materials: recycled asphalt pavement (RAP) and recycled concrete aggregate (RCA). The investigation also dealt with the determination of the resilient modulus of one blended material consisting of approximately 50% RCA and 50% conventional base material (Class 5). The objectives were to assess the stiffness of recycled materials and to determine the scalability of laboratory results to field scale conditions. The objective was met by determining the resilient modulus of the recycled materials using large-scale model experiments (LSME) and comparing to the resilient modulus determined from bench-scale tests in accordance with NCHRP 1-28a and field scale tests using a falling weight deflectometer (FWD). The low-strain modulus of each material was also determined using seismic testing methods, and backbone curves (normalized modulus versus strain) were developed from the resulting stress-strain relationships. A conventional base course meeting the gradation standard of a Minnesota Department of Transportation Class 5 aggregate was used as a reference material in this study.

RAP experienced higher plastic deflections compared to the Class 5, while RCA experienced lower plastic deflections. The plastic deflection of RAP was approximately 211% and 402% greater than that of Class 5 for 0.2 m and 0.3 m layer thicknesses, respectively, and the plastic deformation of RCA was approximately 69% smaller than that of Class 5 for both layer thicknesses. Blended RCA/Class 5 experienced plastic deflections that were 39% and 20% smaller than Class 5 for layer thicknesses of 0.2 m and 0.3 m, respectively. For an increase in



layer thickness from 0.2 m to 0.3 m, base plastic deflections of RCA and Class 5 decreased 10% and 13%, respectively. Plastic deflection of RAP is 40% larger for 0.3-m layer thickness compared to 0.2-m layer thickness, which is attributed to the viscous nature of the asphalt coating the RAP particles. Plastic deformation of blended RCA/Class 5 is 13% larger for the same increase in layer thickness, which can most likely be attributed to experimental error. Conventional base course aggregate (Class 5) can be expected to contribute between 4 and 8% to an acceptable rutting depth of 13 mm. RCA and blended RCA/Class 5 can be expected to contribute 3 to 6% to the acceptable depth, and RAP can be expected to contribute 30 to 40%. Flexible pavements that incorporate RAP as a base course layer can be expected to encounter rutting problems. Flexible pavements that incorporate RCA and RCA/natural aggregate blends will experience rutting comparable to pavements that incorporate conventional base course aggregates.

The bench-scale resilient modulus tests with internally and externally measured deflections gave the highest and the lowest resilient moduli, respectively, the LSME tests with the 0.3 m and 0.2-m layer thicknesses having the second and third highest resilient moduli, respectively. The magnitudes of the tests are evenly spaced, and no direct correlation between the four methods can be discerned. The summary resilient modulus (SRM) of RCA was 42% to 77% higher than that of Class 5, whereas the SRM of RAP was 23% to 33% greater. The SRM of blended RCA/Class 5 was 18% greater than that of Class 5, which was comparable in magnitude to RAP. An increase in layer thickness from 0.2 m to 0.3 m had the effect of increasing the SRM of the materials from 130 MPa to 176 MPa. An increase in

RCA content increased the SRM at a rate that was non-linear, suggesting that the blended aggregate sample obtained in the field may have a composition other than the actual 50% RCA/50% Class 5.

Scaling was achieved by normalizing the resilient modulus of a material by the low-strain modulus and plotting the data as a function of the strain level at the corresponding stress state. The resulting plot for all four materials described a backbone curve which illustrates the stress-strain dependency of the given material. However, an uncharacteristically high low-strain modulus value for RAP greatly reduced the normalized resilient modulus and made the construction of a backbone curve difficult. This behavior is attributed to the bitumen coating the RAP particles causing the particles to adhere to each other, which leads to an increase in strain resistance at low stresses. Different test methods induce different strain levels at the same bulk stress, resulting in varying resilient modulus. Internally and externally measured bench-scale tests resulted in higher and lower resilient moduli, respectively, compared to FWD or LSME moduli. The LSME with 0.3 m-thick layer (the same as in the field) resulted in higher resilient modulus compared to the field moduli obtained from the FWD test. The LSME with 0.2-m thick layer resulted in resilient moduli which were close to the field FWD moduli. However, when properly scaled for the stress and strain levels, the low-strain modulus estimated from the different test methods are remarkably close to each other indicating the scalability of laboratory modulus to operating field modulus.

## REFERENCES

- ACPA (2009). "Recycling Concrete Pavements," *Bulletin B043P*, American Concrete Pavement Association, Skokie, IL.
- Barksdale, R. D., and Itani, S. Y. (1989). "Influence of Aggregate Shape on Base Behavior," *Transportation Research Record*, No. 1227, Transportation Research Board, Washington, D.C., pp. 173–182.
- Bejarano, M.O., Harvey, J. T., Lane, L. (2003). "In-Situ Recycling of Asphalt Concrete as Base Material in California", *Proc. 82nd Annual Meeting*, Transportation Research Board, Washington D.C. CD-Rom, 22 pp.
- Bennert, T., Papp Jr, W. J., Maher, A. and Gucunski, N. (2000). "Utilization of Construction and Demolition Debris under Traffic-Type Loading in Base and Subbase Applications," *Transportation Research Record*, No. 1714, pp. 33-39.
- Benson, C. H., Edil, T. B., Ebrahimi, A., Kootstra, R. B., Li, L., and Bloom, P. (2009). "Use of Fly Ash for Reconstruction of Bituminous Roads: Large-Scale Model Experiments," Minnesota Department of Transportation, St Paul, MN.
- Blankenagel, B. J. and Guthrie, W. S. (2006). "Laboratory Characterization of Recycled Concrete for Use as Pavement Base Material," *Geomaterials*, No. 1952, pp. 21-27.
- Brown, S. F., and Pell, P. S. (1967). "An Experimental Investigation of the Stresses, Strains and Deflections in a Layered Pavement Structure Subjected to Dynamic Loads," *Proc, 2nd Int. Conf. Struct. Des. of Asphalt Pavements*, pp 487–504.
- Burreglo, S. B., Yuan, D., Nazarian, S., (2009). "Cement Treated RAP Mixes for Roadway Base and Subbase: Evaluation of RAP Variability," *Technical Memorandum 0-6084-3*, Center for Transportation Infrastructure Systems, The University of Texas at El Paso, El Paso, TX.
- Bush, A. J. and Alexander, D. R. (1985). "Pavement Evaluation Using Deflection Basin Measurements and Layered Theory," *Transportation Research Record* 1022, Transportation Research Board, National Research Council, Washington DC, pp. 16-29.

- Camargo, F. F., Edil, T. B., Benson, C. H. (2009). "Strength and Stiffness of Recycled Base Materials Blended with Fly Ash," *Proc. 88th Annual Meeting*, CD-ROM, 09-1971, National Research Council, Washington DC.
- Chini, A. R., Kuo, S. S., Armaghani, J. M. and Duxbury, J. P. (2001). "Test of Recycled Concrete Aggregate in Accelerated Test Track," *Journal of Transportation Engineering*, Vol. 127, No. 6, pp. 486-492.
- Ebrahimi, A., Kootstra, B. R. , Edil, T. B., and Benson, C. H. (2010). "Equivalency-Based Design and Mechanical Properties of Recycled Roadway Materials With or Without Fly Ash Stabilization", *Proc. 89th Annual Meeting*, Transportation Research Board, Washington D.C, submitted.
- Edil, T.B. and Fratta, D. (2009). "Development of Testing Methods to Determine Interaction of Geogrid-Reinforced Granular Material for Mechanistic Pavement Analysis," *Wisconsin Highway Research Program #0092-07-05*, Wisconsin Department of Transportation, Madison, Wisconsin.
- Edil, T. B. and Luh, G. F. (1978). "Dynamic Modulus and Damping Relationships for Sands," *Proc. Geotechnical Engineering Specialty Conference on Earthquake Engineering and Soil Dynamics*, American Society of Civil Engineers, Pasadena, California, Vol. I, pp. 394-409.
- FHWA (2008). "User Guidelines for Byproducts and Secondary Use Materials in Pavement Construction," *FHWA Report FHWA-RD-97-148*, Federal Highway Administration, McLean, Virginia.
- Grogan, T. (1996). "Aggregate: Demand on a Roll," *ENR*, 237 (14), p 82.
- Guthrie, W. S., Cooley, D. and Eggett, D. L. (2007). "Effects of Reclaimed Asphalt Pavement on Mechanical Properties of Base Materials," *Transportation Research Record*, No. 2006, pp. 44-52.
- Hardin, B.O. and Drnevich, V.P. (1972). "Shear Modulus and Damping in Soils: Design Equations and Curves," *Journal of the Soil Mechanics and Foundation Division, Proceedings of the ASCE*, Vol. 98, No. SM7, pp. 667 – 692.
- Harichandran, R. S., Baladi, G. Y., Yeh, M. (1989). "Development of a Computer Program for Design of Pavement Systems Consisting of Bound and Unbound Materials," Dept. of Civil and Environmental Engineering, Michigan State University, Lansing, Michigan, 1989.
- Hicks, R. G. (1970). "Factors Influencing the Resilient Properties of Granular Materials," PhD Thesis, University of California, Berkeley, Berkeley, CA.

- Hicks, R. G., and Monismith, C. L. (1971). "Factors Influencing the Resilient Properties of Granular Materials," *Highway Research Record* 345, pp 15–31.
- Huang, Y. (2004). *Pavement Analysis and Design*, 2<sup>nd</sup> Ed., Prentice-Hall, Inc., Upper Saddle River, New Jersey.
- Johnson, A., Clyne, T. R., and Worel, B. J. (2009). "2008 MnROAD Phase II Construction Report," Minnesota Department of Transportation, Maplewood, Minnesota.
- Kim, W., Labuz, J. F. and Dai, S. (2007). "Resilient Modulus of Base Course Containing Recycled Asphalt Pavement," *Transportation Research Record*, No. 2006, Transportation Research Board, National Research Council, Washington, DC, pp. 27-35.
- Kim, D. S., and Stokoe II, K. H. (1992). "Characterization of Resilient Modulus of Compacted Subgrade Soils Using Resonant Column and Torsional Shear Tests," *Transportation Research Record*, No. 1369, Transportation Research Board, National Research Council, Washington, DC, pp. 83-91.
- Kolisoja, P. (1997). "Resilient Deformation Characteristics of Granular Materials," PhD Thesis, Tampere University of Technology, Pub. No. 223, Tampere, Finland.
- Kootstra, B. R., Ebrahimi, A., Edil, T. B., and Benson, C.H. (2010). "Plastic Deformation of Recycled Base Materials," *GeoFlorida'2010*, ASCE Geo Institute, submitted.
- Kramer, S.L. (1996). *Geotechnical Earthquake Engineering*. Prentice Hall. Upper Saddle River, NJ.
- Kuo S. S., Mahgoub, H. S. and Nazef, A. (2002). "Investigation of Recycled Concrete Made with Limestone Aggregate for a Base Course in Flexible Pavement", *Geomaterials*, No. 1787, pp. 99-108.
- Lekarp, F., Isacsson, U., and Dawson, A. (2000). "State of the Art. I: Resilient Response of Unbound Aggregates," *Journal of Transportation Engineering*, ASCE, 126(1), pp 66–75.
- Li, L., Benson, C. H., Edil, T. B., Hatipoglu, B., and Tastan, E. (2007). "Evaluation of Recycled Asphalt Pavement Material Stabilized with Fly Ash," *ASCE Geotechnical Special Publication* (CD-ROM), 169 pp.
- Molenaar, A. A. A. and Van Niekerk, A. A. (2002). "Effects of Gradation, Composition, and Degree of Compaction on the Mechanical Characteristics of

- Recycled Unbound Materials," *Transportation Research Record: Journal of the Transportation Research Board*, Transportation Research Board, Washington, D.C., No. 1787, pp. 73-82.
- Monismith, C. L., Seed, H. B., Mitry, F. G., and Chan, C. K. (1967). "Prediction of Pavement Deflections from Laboratory Tests," *Proc. 2<sup>nd</sup> Int. Conf. Struct. Des. of Asphalt Pavements*, pp 109–140.
- Morgan, J. R. (1966). "The Response of Granular Materials to Repeated Loading," *Proc. 3<sup>rd</sup> Conf.*, ARRB, pp 1178–1192.
- Nataatmadja, A. (1992). "Resilient Modulus of Granular Materials Under Repeated Loading," *Proc., 7th Int. Conf. on Asphalt Pavements*, Univ. of Nottingham, Nottingham, U.K., 1, pp 172–185.
- Nataatmadja, A. and Tan, Y. L. (2001). "Resilient Response of Concrete Road Aggregates," *Journal of Transportation Engineering*, Vol. 127, No. 5, pp 450-453.
- Plaistow, L. C. (1994). "Non-Linear Behavior of Some Pavement Un-bound Aggregates," MS Thesis, Dept. of Civil Engineering, University of Nottingham, Nottingham, England.
- Poon, C. S., Qiao, X. C. and Chan, D. X. (2006). "The Cause and Influence of Self-Cementing Properties of Fine Recycled Concrete Aggregates on the Properties of Unbound Sub-Base," *Waste Management*, Vol. 26, No. 10, pp. 1166-1172.
- Richart, F.E., Jr., Hall, J.R., and Woods, R.D. (1970). *Vibrations of Soils and Foundations*, Prentice Hall, Inc., Eaglewood Cliffs, NJ.
- Santamarina, J.C., Klein, K.A., and Fam, M.A. (2001). *Soils and Waves*. John Wiley & Sons Ltd., West Sussex, England, 488 pp.
- Schuettpelz, C. (2008). "Evaluation of the Influence of Geogrid Reinforcement on Stiffness in Compacted Base Course Material," MS Thesis, University of Wisconsin-Madison, Madison, WI.
- Seed, H. B., Mitry, F. G., Monismith, C. L., and Chan, C. K. (1967). "Prediction of Flexible Pavement Deflections from Laboratory Repeated Load Tests." *NCHRP Rep. No. 35*, National Cooperative Highway Research Program.
- Seed, H. B. and Idriss, I. M. (1970). "Soil Moduli and Damping Factors for Dynamic Response Analyses," *Report No. EERC 70-10*, University of California, Earthquake Engineering Research Center, Berkeley, CA, 1970.

- Son, Y. H., (2010). "Resilient Moduli of Recycled Materials," Personal Communication.
- Tanyu, B.F., Kim, W. H., Edil, T. B., and Benson, C. H., (2003). "Comparison of Laboratory Resilient Modulus with Back-Calculated Elastic Moduli from Large-Scale Model Experiments and FWD Tests on Granular Materials," *Resilient Modulus Testing for Pavement Components*, ASTM STP 1437, G. N. Durham, W. A. Marr, and W.L. De Groff, Eds., ASTM International, West Conshohocken, Pa.
- Thom, N. H., and Brown, S. F. (1988). "The Effect of Grading and Density on the Mechanical Properties of a Crushed Dolomitic Limestone," *Proc. 14<sup>th</sup> ARRB Conf.*, Vol.14, Part 7, pp 94–100.
- Thom, N. H., and Brown, S. F. (1989). "The Mechanical Properties of Unbound Aggregates from Various Sources," *Unbound Aggregates in Roads*, R. H. Jones and A. R. Dawson, eds., pp 130–142.
- Van Niekerk, A. A., Houben, L. J. M., and Molenaar, A. A. A. (1998). "Estimation of Mechanical Behavior of Unbound Road Building Materials from Physical Material Properties," *Proc., 5<sup>th</sup> Int. Conf. on the Bearing Capacity of Roads and Airfields*, R. S. Nordal and G. Rafsdal, eds., Vol.3, pp 1221–1233.
- Wen, H. and Edil, T. B. (2009). "Sustainable Reconstruction of Highways with In-situ Reclamation of Materials Stabilized for Heavier Loads," *Proc. 2nd Int. Conf. on Bearing Capacity of Roadway, Railways and Airfields*, Urbana-Champaign, IL, CD-ROM.
- WisDOT (2009). "Layer Coefficient Values for Cracked and Seated Concrete," *Transportation Synthesis Report*, Wisconsin Department of Transportation, Madison, Wisconsin.

**APPENDIX A**

**IMPLEMENTATION OF ABBREVIATED TEST PIT AREA**



## **A.1 Introduction**

Previous testing using the LSME incorporated the entire 3.0 m x 3.0 m test area to measure deflections and determine the resilient modulus for a given base course material under cyclical loading. However, limited amounts of base course material available for testing made it necessary to reduce the evaluated test area within the LSME to 1.0 m x 1.0 m. The remainder of the 3.0 m x 3.0 m test area was made up of recycled pavement material (RPM) to maintain the boundary stress that would otherwise be lost by a reduction in test area. The equivalency of the abbreviated LSME test area to the full LSME test area was determined by comparing the resilient modulus of RPM obtained using both test methods.

The RPM was compacted to a thickness of 0.3 m within the entire 3.0 m x 3.0 m LSME test area according to methods described in section 3.3.1. The abbreviated 1.0 m x 1.0 m test area was then excavated in the center of the LSME test area, leaving approximately 2.0 m of RPM around the LSME perimeter, as shown in Fig. A.1. The exposed subgrade was loosened and recompactd prior to placement of the specimen material to establish a consistent initial density that would be repeated for all subsequent tests. The circumference of the abbreviated test area was lined with nonwoven, heat bonded geotextile to separate the RPM from the test specimen and allow confinement of the test specimen from the surrounding RPM, as shown in Fig.A.2. RPM was recompactd within the abbreviated test area and the summary resilient modulus of the tested material was determined using methods described in section 3.3.4.



Fig. A.1. Overview of abbreviated test pit area prior to material placement.



Fig. A. 2. Placement of RPM within abbreviated test pit area.

The resilient modulus of the RPM determined for the abbreviated test area was measured to be 538 MPa. Benson et al. (2009) reported a summary resilient modulus of 505 MPa on LSME tests for the same material using the full 3.0 m x 3.0 m test area. Using the smaller test area increased the summary resilient modulus by approximately 6%. A comparison of the summary resilient modulus determined for the two specimen sizes is presented in Fig. A.3. The summary resilient moduli determined for the 0.3-m thick LSME tests on RAP, RCA, blended RCA/Class 5 and Class 5 as discussed in section 4.2 are also presented in Fig. A.3. for scale. The magnitude of the RPM resilient modulus is similar for both the full and abbreviated test pit areas. Boudreau (2003) tested the repeatability of bench-scale resilient modulus tests and found that the coefficient of variance was as high as 4.5% for specimens tested at the same stress level. The mean average and the standard deviation measured between the two tests were 522 MPa and 23 MPa respectively, indicating a coefficient of variance of 4.4%. Assuming a correlation between the bench-scale and LSME tests, the two test methods are within an acceptable amount of variance.

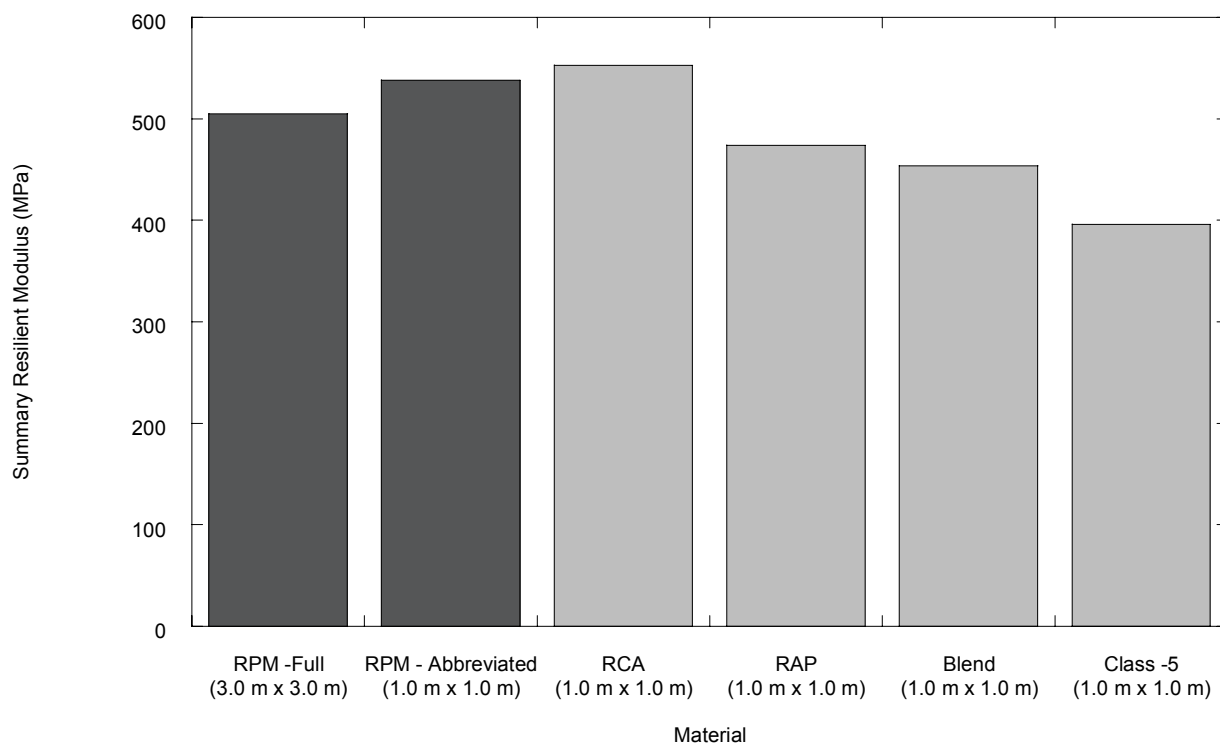


Fig. A.3. Comparison of resilient modulus of RPM obtained for full and abbreviated test pit areas with RCA, RAP, blended RCA/Class 5 and Class 5 obtained for abbreviated test pit area.

## **APPENDIX B**

### **DETERMINATION OF LAYER COEFFICIENTS**

### B.1 Determination of Layer Coefficients

The design of pavement structures is dependent on the determination of appropriate layer thicknesses based on the mechanical properties of the associated pavement layers. The AASHTO design procedure relates the structural capacity of a given layer to a structural number,  $SN_i$ , which is defined as the product of the layer thickness,  $D_i$ , and layer coefficient,  $a_i$ . The SN for the pavement structure as a whole is calculated according to Eqn. B.1.

$$SN = SN_1 + SN_2m_2 + SN_3m_3 = a_1D_1 + a_2D_2m_2 + a_3D_3m_3 \quad (B.1)$$

The variable  $m_i$  is the drainage modification factor, which is assumed to be 1.0 for the base materials used in this study. Design layer thicknesses are chosen in such a way that the resulting SN is greater than or equal to a required SN. The required SN is typically determined based on estimated traffic, serviceability loss, and effective roadbed resilient modulus (AASHTO 1993).

The layer coefficient measures the relative ability of a unit thickness of a given material to function as structural component in a pavement (Haung 2007). The layer coefficient for untreated base course can be estimated from the resilient modulus of the layer according to the relationship proposed by Rada and Witczak (1981) and presented in Eqn. B.2.

$$a_2 = 0.249(\log M_r) - 0.977 \quad (B.2)$$

where  $M_r$  is the resilient modulus measured in psi.

The layer coefficients were calculated for the 0.2-m and 0.3-m thick layers tested in the LSME using the SRM according to Eqn. B.2 for RAP, RCA, blended RCA/Class 5 and Class 5. The relationship between layer coefficient and layer

thickness for these materials is presented in Fig. B.1. The SN for each of the base course materials tested in the LSME was calculated as the product of the layer thickness (in inches) and the associated layer coefficient. The SN and layer coefficients for each LSME test are presented in Table B.1.

The magnitude of the layer coefficients follow the hierarchy seen previously for SRM, with RCA and Class 5 having the highest and lowest values, respectively, and RAP and blended RCA/Class 5 having the second and third highest values, respectively. The layer coefficients of RAP, blended RCA/Class 5, and Class 5 all increased at the same rate with an increase in layer thickness. The layer coefficient of RCA increased with increased layer thickness as well, albeit at a much slower rate. The Class 5 layer coefficients of 0.16 and 0.21 determined for the LSME layer thicknesses of 0.2 m and 0.3 m, respectively, are marginally higher than typical values for granular base course of 0.10 and 0.14 (Huang 2004). RCA had layer coefficients of 0.21 and 0.24 for layer thicknesses of 0.2 m and 0.3 m, which is within typical values for rubblized concrete as reported by WisDOT (2009).



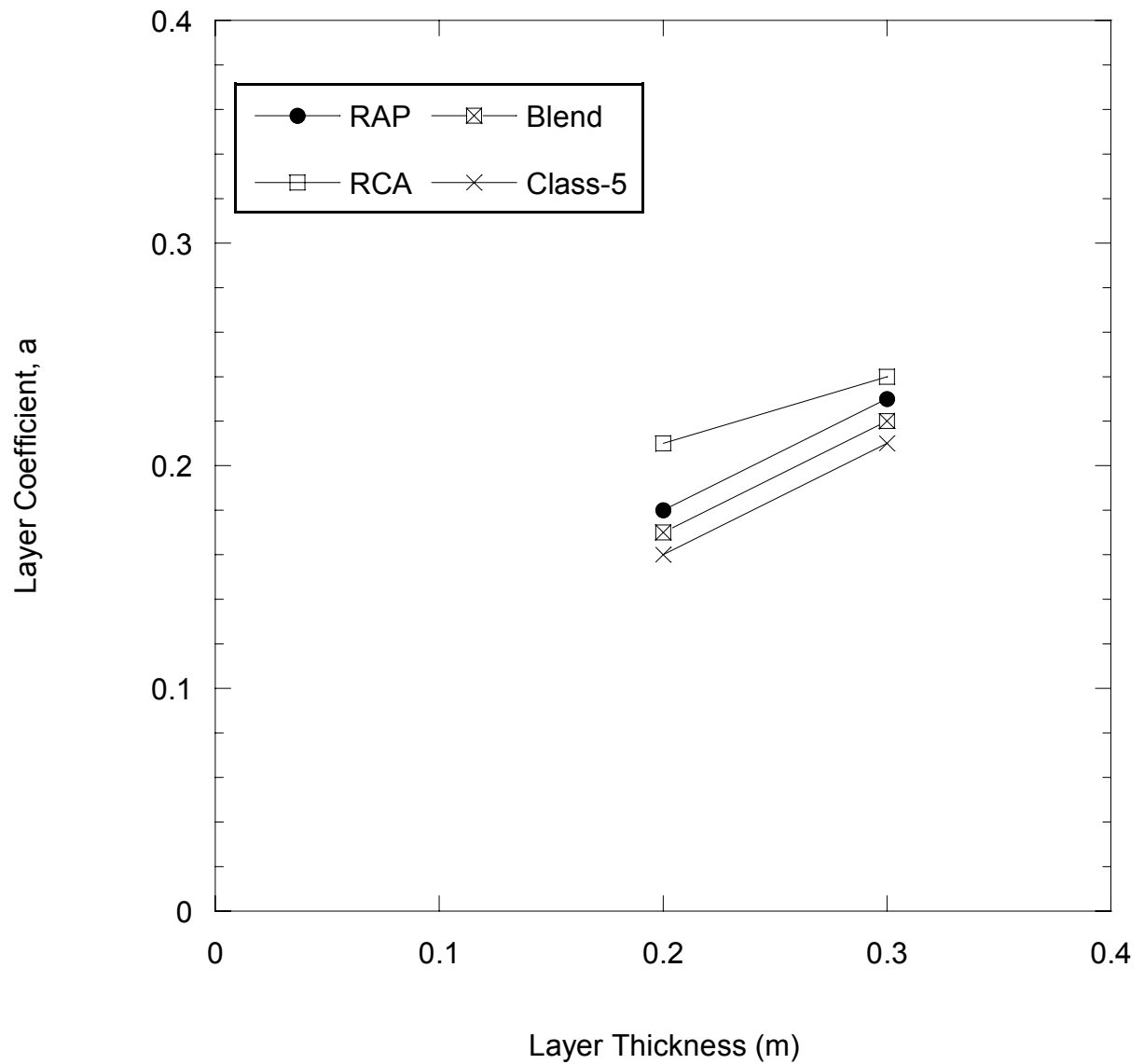


Fig. B.1. Layer coefficient vs. base layer thickness for RAP, RCA, blended RCA/Class 5, and Class 5.

Table B. 1. Layer coefficients and structural numbers for different LSME thicknesses.

Material	Layer thickness (m)	Summary Resilient Modulus (kPa)	Layer Coefficient, $a_2$	Structural Number, SN
RAP	0.2	314	0.18	1.44
	0.3	474	0.23	2.76
RCA	0.2	418	0.21	1.68
	0.3	553	0.24	2.88
Blended RCA/Class 5	0.2	278	0.17	1.36
	0.3	454	0.22	2.64
Class 5	0.2	243	0.15	1.2
	0.3	396	0.21	2.52

# **Recycled Unbound Materials**

## **TPF-5 (129) Recycled Unbound Materials**

Mn/DOT Contract No. 89264 Work Order No. 2

CFMS Contract No. B14513

### **Task I: Design**

#### **Task ID: Climate Effects ( Freeze-Thaw Cycles)**

**Ozlem Bozyurt, Tuncer B. Edil, James Tinjum, and Craig H. Benson**  
**University of Wisconsin- Madison**

**August, 2011**

## **1. INTRODUCTION**

## **2. BACKGROUND**

### **2.1. Recycled Unbound Base Materials**

Researchers have investigated the use of RCA in road base or subbase courses to provide a viable option for the reuse of this C&D waste (Poon and Chan 2005). RCA is used predominantly in pavement construction as replacement for natural aggregates and cement-treated subbase layers (Saeed et al. 2006). Molenaar and Niekerk (2007) investigated the engineering properties of RCA and suggested that good-quality road base or subbase can be built from these materials. The Federal Highway Administration (FHWA) (2008) reported that, when compared to natural aggregates, RCA has lower density, higher water absorption, higher soundness mass loss, and higher content of foreign material. In most cases, the properties of RCA are within the specifications for base course or concrete aggregate.

Park (2003) investigated the characteristics and performance of dry and wet RCA as road base and subbase for concrete pavement by comparing the engineering properties of RCA with those of crushed stone aggregate. The performance characteristics were evaluated based on compactibility, shear resistance, and stability of RCA; and the mechanical properties were evaluated in the field by using a falling weight deflectometer to determine deflection. RCA had the same compactibility as crushed stone aggregate and shear resistance equal to or better than crushed stone aggregate. Park (2003) concluded that the RCA can be used as base and subbase materials in place of crushed stone aggregate for supporting a concrete pavement system.

The National Asphalt Pavement Association (NAPA) (2009) reported that asphalt pavement is the most recycled material in the US. The US highway construction industry annually produces more than 100 million tons of RAP that is recycled into new pavements (NAPA 2009). According to FHWA (2011), RAP is a valuable and high-quality material that may demonstrate good performance as a granular road base and a replacement for more expensive virgin aggregate.

Guthri et al. (2007) conducted free-free resonant column tests on RAP and natural aggregate blends to evaluate the effects of percentage change of RAP on the stiffness of road base. Blends were prepared according to the following RAP and natural aggregate percentages: 100/0, 75/25, 50/50, 25/75, and 0/100. Stiffness was determined after compaction at OMC, after a 72-h period of heating at 60°C to simulate summer conditions; and after a 10-day period of capillary soaking followed by a 24-h period of submersion to simulate conditions of field saturations. At OMC, the stiffness decreased with the addition of 25% RAP, then increased with the addition of 50%, 75%, and 100% RAP. When the material was heated for 72 h, the stiffness increased with the addition of 25% RAP and then decreased with the addition of 50%, 75% and 100% RAP. According to Guthri et al. (2007), the decrease in stiffness is related to the softening behavior of asphalt due to heat. In the soaked condition, the stiffness of the material behaved similar to the samples in the dry condition, but with stiffness values between 40% and 90% lower.

Kim et al. (2007) investigated the stiffness of base course containing different ratios of RAP and natural aggregate. Resilient modulus tests were conducted on the recycled material in accordance with National Cooperative Highway Research Program testing protocol 1-28A (NCHRP 1-28a). The 50% aggregate-50% RAP specimens developed stiffness equivalent to the 100% aggregate specimens at lower confining pressures (~ 20 kPa); at higher confinement (~ 120 kPa), the RAP specimens were stiffer.

Bennert et al. (2000) compared the mechanical properties of two types of C&D waste, RCA and RAP, with dense-graded aggregate base course, used in roadway base applications in New Jersey. The RAP and RCA were mixed at varying percentages with the dense-graded aggregate base course. Bennert et al. (2000) found that the pure RAP and RCA samples had higher stiffness than the dense-graded aggregate base course, and the stiffness of the base course increased with an increase in RAP and RCA content. The pure RCA specimens accumulated the least amount of permanent strain. Even though pure RAP was found to be stiffer than the dense-graded aggregate base course, the RAP accumulated the greatest amount of permanent strain. Bennert et al. (2000) reported that the resulting contrast between the pure RAP resilient modulus and its permanent deformation might be due to the breakdown of asphalt binder under loading.

## 2.2. Freeze-Thaw Effect on RAP and RCA

Seasonal variation in moisture and temperature occurs in most areas of the US. The  $M_r$  of road base and subbase tends to change throughout the pavement's life due to these seasonal variations. The freeze–thaw (F-T) cycling of pavement profiles may significantly influence pavement performance. The  $M_r$  of an aggregate base/subbase is thought to increase during freezing and drying and decrease during thawing and wetting (Kootstra et al. 2009). Therefore, pavement design in regions where variations in temperature and moisture are appreciable should consider these factors (Zaman and Zhu 1999).

Rosa (2006) reported that when the air temperature at the surface is lower than the temperature of the soil, heat is extracted from the soil and removal of heat from the soil causes its temperature to drop. If the surface temperature is below 0°C, a freezing front advances into the soil and ice crystals begin to form along the freezing front. When pore water freezes within unbound base/subbase aggregate, the volume of the voids increases. This volume change causes degradation, and ultimately decreases the stiffness of road base layers. A study conducted by Rosa (2006) on the effect of F-T on the engineering properties of one RSG and four RPMs mixed with fly ash found that the  $M_r$  decreased with increasing F-T cycling, leveling off after 5 cycles.

Camargo (2008) investigated the effects of F-T on  $M_r$  of RPM, RSG, and Class 5 base with and without fly ash stabilization. Specimens without fly ash were compacted at OMC using modified Proctor, and no inflow or outflow was allowed during subjecting specimens to F-T cycles. The resilient modulus test was conducted according to NCHRP 1-28a. RPM had a higher summary resilient modulus (SRM), which is the  $M_r$  corresponding to the typical level of 208 kPa bulk stress in the base course layer and also exhibited smaller plastic strain accumulations during  $M_r$  testing than Class 5 aggregate (without subjecting to any F-T cycling). A reduction in SRM was observed in Class 5 base and RSG after subjecting materials to 5 F-T cycles. There was no consistent effect of F-T cycling on materials without fly ash; the SRM of Class 5 base decreased slightly (7%), whereas RPM and RSG increased slightly (14% and 1%). F-T cycling was found to have a small effect on SRM of Class 5 base without any additives. In this study, no net changes in the volume were observed for Class 5 base and RPM, whereas the volume change for RSG ranged from 0.4 to 0.6 %. The small effect of F-T cycling on the SRM is consistent with the

small volume changes recorded during freezing and thawing, which indicate little change in soil structure (Simonsen et al. 2002). Camargo (2008) concluded that freezing and thawing results in a looser soil structure, which causes a lower resilient modulus.

### 2.3. Resilient Modulus

The design of roadway pavement relies on proper characterization of the load-deformation response of the pavement layers (Tian et al. 1998). Base and subgrade deform when subjected to repeated loads from moving vehicular traffic. The  $M_r$  defines the nonlinear elastic response of pavement geomaterials, such as unbound aggregate base and subbase, under repeated traffic loading. The resilient behavior of unbound aggregate layers is affected by the stress state experienced because of wheel loading and the physical properties of aggregate (Pan et al. 2006). The  $M_r$  is a linear-elastic modulus obtained from dynamic loading, defined as the ratio of the cyclic deviator stress to the resilient (recoverable) strain, and is defined as:

$$M_r = (\sigma_d / \epsilon_r) \quad (1)$$

where  $\epsilon_r$  is the recoverable elastic strain and  $\sigma_d$  is the applied deviator stress.

Design of pavements and rehabilitation of layered pavement systems use  $M_r$  as an essential parameter in the design process (Heydinger et al. 2007). The  $M_r$  is a key input in NCHRP 1-37 (mechanistic-based pavement design approach), which is being evaluated for adoption by numerous state highway agencies (Pan et al. 2006). The performance of pavement is dependent on the stiffness of the pavement structure under specified traffic loads and environmental conditions. Generally, a high  $M_r$  for a base course infers a stiffer base course layer, which increases pavement life. The resilient response of granular material is important for the load-carrying ability of the pavement and the permanent strain response, which characterize the long-term performance of the pavement and rutting phenomenon (Lekarp et al. 2000).

## 3. MATERIALS

The recycled materials used in this study were obtained from various states in the US. Three RAPs and three RCAs were collected and named according to state of origin. The

materials represent coarser, medium, and finer gradations based on their grain size ( $D_{50}$ ,  $C_c$  and  $C_u$ ). The reference base course used as the control in this study was a gravel meeting Class 5 aggregate specifications for base course per the Minnesota Department of Transportation.

A summary of the index properties and soil classifications is shown in Table 1. The materials used in this study are classified as non-plastic per ASTM D 2487, the Unified Soil Classification System (USCS). The recycled materials (three RCAs and three RAPs) classified as A-1-a and Class 5 aggregate classified as A-1-b according to the AASHTO soil classification system (ASTM D 3282). Specific gravity ( $G_s$ ) and absorption tests were conducted according to AASHTO T 85. Asphalt content was determined by ASTM 6307. The modified Proctor compaction test (ASTM D 1557) was performed to determine the optimum moisture content ( $w_{opt}$ ) and maximum dry unit weight ( $\gamma_{dmax}$ ). The particle size distributions (PSD) for the investigated materials were determined according to ASTM D 422 and shown in Fig. 1, along with upper and lower bounds reported in literature (Bennert et al. 2000; Bejarano et al. 2003; Blankenagel and Guthrie 2006; Gutrie et al. 2007, Saeed 2008, Kuo et al. 2002 ).

## **4. METHODS**

### **4.1. Resilient Modulus**

Resilient modulus tests were performed on compacted specimens according to NCHRP 1-28a Procedure Ia, which applies to base and subbase materials. The materials used in this study classify as Type I material in NCHRP 1-28A, which requires a 152-mm-diameter and 305-mm-high specimen for resilient modulus testing (NCHRP 2004). Specimens were prepared at OMC and compacted to 95% of maximum modified Proctor density. Specimens were compacted in six lifts of equal mass within 1% of the target dry unit weight and 0.5% of target moisture content to ensure uniform compaction (NCHRP 2004).

Resilient modulus tests were conducted with internal and external linear variable displacement transducers (LVDT). External LVDTs have an accuracy of  $\pm 0.005$  mm, and internal LVDTs have an accuracy of  $\pm 0.0015$  mm. Clamps for the internal LVDTs were built in accordance with NCHRP 1-28A specifications. Internal LVDTs were placed at quarter points of the specimen to measure the deformations over the half-length of the specimen, whereas external LVDT



measured deformations of the entire specimen length. An MTS Systems Model 244.12 servo-hydraulic machine was used for loading the specimens. Loading sequences, confining pressures and data acquisition were controlled from a computer running LabView 8.5 software.

The  $M_r$  for each load sequence was obtained by averaging the  $M_r$  from the last 5 cycles of each test sequence. The  $M_r$  data were fitted with the power function model proposed by Moosazehd and Witzak (1981)

$$M_R = k_1 \times \theta^{k_2} \quad (2)$$

where  $M_r$  is resilient modulus,  $\theta$  is bulk stress and  $k_1$  and  $k_2$  are empirical fitting parameters. The constants  $k_1$  and  $k_2$  are unique to a given material and are independent of one another.  $k_1$  and  $k_2$  are material-dependent parameters. For a given material,  $k_2$  obtained from replicate tests were averaged and fixed for that material (Camargo 2008). Bulk stress is another means of quantifying confining pressure and deviator stress in a single term and is defined as the sum of the three principle stresses. Bulk stress is defined as

$$\theta = \sigma_1 + \sigma_2 + \sigma_3 \quad (3)$$

where  $\sigma_1$ ,  $\sigma_2$ , and  $\sigma_3$  are the principal stresses acting on the specimen.

For base course, the summary resilient modulus (SRM) corresponds to the  $M_r$  at a bulk stress of 208 kPa, as suggested by Section 10.3.3.9 of NCHRP 1-28a. SRM is used to determine the layer coefficient, which is a required input in the AASHTO pavement design equation (Tian et al 1998. ). The power function (Eq. 2) is a simple model widely used for granular material. The estimated SRM per the power function model was compared to the measured modulus. Statistical analysis indicated that results from the power function model are significant at a 95% confidence level, and the model represents the data reasonably well for RCA ( $R^2=0.85$ ) and for RAP ( $R^2=0.90$ ) (Bozyurt 2011).

## 4.2. Freeze-Thaw Cycling

The effect of F-T cycling on the engineering properties of the recycled materials was determined by measuring the  $M_r$  of specimens subjected to F-T cycles. A method that follows ASTM D 6035 for specimen conditioning was used at the University of Wisconsin-Madison (UW-Madison) for frost susceptibility (Camargo 2008). ASTM D 6035 describes a method to determine the F-T effects on hydraulic conductivity. Specimens conditioned in accordance with ASTM D 6035 were subjected to resilient modulus test.

Specimens for F-T testing were prepared in the same manner as for resilient modulus test. Test specimens were compacted in plastic molds at the specified moisture content and maximum dry unit weight. Specimens, instrumented with a thermocouple, were tested to insure that complete freezing occurred within 24 hours at  $-19^{\circ}\text{C}$ .

Accordingly, specimens were retained in their plastic mold, wrapped with plastic sheeting, and placed in a freezer for one day. The plastic molds were sealed carefully to prevent exposure to moisture during F-T cycling. Thus, the bulk water content was kept constant during F-T cycles.

After freezing, the height and weight of the specimens were measured to monitor the volume change during freezing. The specimens were then thawed at room temperature for 24 h. After the designated number of F-T cycle, specimens were extruded frozen and thawed inside the resilient modulus cell. Resilient modulus testing was then conducted, as described previously. In this study, the effect of 5, 10, and 20 F-T cycles was investigated.

## **5. RESULTS**

### **5.1. Recycled Asphalt Pavement**

SRM for recycled materials and Class 5 aggregate were summarized in Table 2, along with the parameters  $k_1$  and  $k_2$  for the power function model (Eq. 2) and the rate of decrease for F-T cycles (0, 5, 10 and 20). The effect of freeze-thaw (F-T) cycling on SRM for the representative RAP and Class 5 aggregate material is shown in Fig. 2.

F-T cycling has a relatively small effect (7% decrease over five F-T cycles) on the SRM of Class 5 aggregate in comparison to the RAP. Camargo (2008) also observed a 7 % of decrease in SRM for natural aggregate after five F-T cycles. However, the rate of decrease for Class 5 aggregate over 10 and 20 F-T cycles was 14% and 21%, respectively. The SRM of the RAPs showed the most reduction after the first five F-T cycles, with relatively small change thereafter. The differences in the effects of F-T cycles on a material can be attributed to the differences in material gradation, mechanical properties, and mineralogy and origin of aggregate.

For instance, RAP (TX) (coarser) exhibited the smallest rate of decrease (28%) in SRM after 20 (F-T) cycles compared with RAP (CA) (medium) (32%) and RAP (MN) (finer) (32%).

The rate of decrease of SRM for RAP ranged from 20 to 66%, which is similar to the range reported by Rosa (2006) for various coarse and fine grained soils. Even though the SRM of RAP decreases over 20 F-T cycles, the SRM of the RAP was still greater than that of Class 5 aggregate as revealed in Fig. 3.

In this study, the specimens were compacted in a PVC mold, and sealed very carefully to prevent water loss during the conditioning process. Due to the asphalt coating around the fine particles in RAP, water retention capacities are less than natural aggregates; therefore, the lubrication effect of water between RAP particles is higher. Consequently, RAP does not have the ability to retain moisture during F-T cycling.

The reduction in the stiffness over time may be related to the volume change of the water retained in the pores, the hydrophobicity of asphalt, and the weakness occurred in asphalt binders over time. Rosa (2006) reported that when pore water freezes within unbound base/subbase aggregates, the volume of the voids increases; and this resulting volume change causes degradation, and ultimately decreases the stiffness of road base layers. Arm (30) reported that degradation, owing to poor F-T resistance, occurs because the volume of water present in the pores expands upon freezing, thus generating considerable forces that break up the aggregate particles. Therefore, the pavement moduli change during F-T cycles might occur as result of changes in the phase of the pore water over time (Da-tong et al., 1998).

In this study, relatively low volume changes were observed because specimens underwent F-T cycles in a closed system (i.e., no external source of water), the only water present remained within the pores of the material; therefore, frost action was limited to change in volume of the post-compaction pore water upon freezing. No net volume changes were observed for Class 5 aggregate and RAP

An increase in the stiffness of RAP after F-T cycles has been reported in other studies. For instance, Attia and Abdelrahman (2010) reported that  $M_r$  of RAP increased after two F-T cycles for specimens were kept in latex membranes to keep moisture content constant during the test. However, during the conditioning process, a significant amount of water loss occurred, which may be a significant factor for the  $M_r$  increase over time. Camargo et al. (2009) found 14 % increase in SRM of RPM after five F-T cycles. This difference in SRM may be attributed to different mechanical properties of RPM as compared to RAP due to different recycling processes.

## 5.2. Recycled Concrete Aggregate

The effect of F-T cycling on the SRM for representative RCA and Class 5 aggregate is presented in Fig. 4. For RCA, SRM decreased after five F-T cycles, followed by a consistent increase. The rate of decrease during the first five F-T cycles varied according to the material geographical origin. As the source and origin of the RCA differ (i.e., the gradation, compaction characteristics, and mechanical properties differ), these variations affect the rate of change in SRM. This variation affects the rate of change in SRM, however a similar trend observed over time among the RCA material remained as seen in Fig. 5.

The SRM for RCA (TX) decreased 10 % over five F-T cycles followed by an increase over 20 F-T cycles back to 30 % of the initial SRM (at zero F-T cycle); RCA (MI) decreased 18 % over five F-T cycles followed by an increase back to 38 % of the initial SRM. The same trend was observed for RCA (CA) with an 11% decrease over five F-T cycles followed by an increase of 5% above the initial SRM over ten F-T cycles.

The self-cementing properties of RCA and fine content generation over time could explain why an increase in stiffness after five F-T cycles occurred. These trends are consistent with other research in which the strength of subbase prepared with RCA has been found to increase with time (Arm 2001). RCA particles typically have a coarser and more angular shape than natural aggregates as a result of material crushing and processing operations (Saeed et al. 2006), leaving a significant amount of mortar adhered to the surface of the particles (Saeed et al. 2006; Juan and Gutierrez 2009, Gokce et al. 2011). Processed RCA has hardened cement paste that holds smaller aggregate particles together (Saeed et al. 2006). The amount of cement paste attached to aggregate in RCA depends on the process used to produce RCA and the properties of the original concrete (Chini et al. 2001).

Poon et al. (2006) stated that unhydrated cement content retained within the adhered mortar was the cause of self-cementing in RCA used for unbound base. Arm (2001) conducted a field investigation over two years on the stiffness of unbound base layers made of crushed concrete from demolished structures. An increase in  $M_r$  with time was observed and attributed to the self-cementing properties of RCA. Arm (2001) conducted repeated load triaxial tests on crushed virgin aggregate and concrete specimens after certain storing periods (1, 3, 7, 28 and 90 days). An increase in modulus was observed for crushed concrete specimens, but not for natural

base layers, over time. Arm (2001) postulated that the self-cementing properties of crushed concrete were the reason behind the increase of stiffness, with time, in unbound base layers made with crushed demolished concrete.

There was an increased observed in the fine amount of the RCA specimens after 20 freeze-thaw cycles. Recent studies show that the fine percentage increased has an important effect in the stiffness of aggregates. Mishra et al. (2010) investigated the effect of fines on compaction for dolomite samples and they found that the MDU increased as the percentage of fines in the sample increase. Since the addition of fines gradually filled the voids, the aggregate matrix became denser. They also found that as the fines content increased beyond a certain point, all the voids in the uncrushed gravel matrix (rounded aggregate particles, had a lower amount of total voids than crushed samples) were filled, and the coarse particles started to float in the matrix. This resulted in a reduction in the dry density without a corresponding significant decrease in aggregate material matrix strength. This phenomenon was also observed by Ebrahimi et al. (2011) during the investigation of ballast void filling with fouling materials (i.e., fines and water content).

Increased density contributes to an increased stiffness for granular material; however, increased fines content and increased crushing efforts appear to diminish these effects (Hicks and Monismith, 1971). For example, fines content  $> 12\%$  may significantly decrease the  $M_r$  of unbound granular materials (Barksdale and Itani, 1989). The fines percentage in the soil matrix likely improves the  $M_r$  of unbound aggregates to a point, after which the matrix starts to be dominated by the fines in which the  $M_r$  starts to decrease. The increased in the SRM for RCA specimens could be also related to the change in the matrix of specimen due to the increase of fine amount. The increased fine content filled the voids in RCA specimens, and the specimen became stiffer over time.

Relatively low volume changes were observed for Class 5 aggregate and recycled materials, because specimens were freezing and thawing in a closed system (no external sources of water available), the only water present remained within the pores of the material; therefore, frost action was limited to change in volume of the in situ pore water upon freezing (Rosa 2006).

## 6. CONCLUSIONS

Freeze/thaw cycling was found to influence the stiffness properties of unbound recycled pavement and recycled concrete aggregates used for base course. Resilient modulus can be used to investigate the effect of freeze-thaw (F-T) cycles on unbound road base/subbase layers consisting of natural aggregate, RAP, and RCA.

The stiffness of RAP decreased over the first 5 F-T cycles, with smaller decrease recorded thereafter. This decrease in stiffness of RAP subjected to F-T cycles may be attributed to particle degradation and progressive asphalt-binder weakening. For RCA, the exposure to F-T cycles led first to a decrease in stiffness, followed by an increase, which may be attributed to progressive generation of fines and hydration of cement paste. The seismic modulus method confirmed the trends of changing stiffness of RCA during F-T cycling. Among the recycled materials evaluated in this study, quantitative differences in F-T response was observed, which was reflective of material grading and source. Exposure of the natural aggregate control (Class 5 base) to F-T cycles resulted in relatively small decreases in stiffness; however, the stiffness of the recycled materials was always greater than the natural aggregate, even after F-T induced decreases.

## REFERENCES

USGS. *Crushed Stone: Statistical Compendium U.S. Geological Survey*. U.S. Geological Survey, Reston, VA, 2010.

ACPA. *Recycling Concrete Pavements*. American Concrete Pavement Association, 2009.

Bennert, T., Jr. W. J. Papp, A. Maher, and N. Gucunski. Utilization of Construction and Demolition Debris Under Traffic-Type Loading in Base and Subbase Applications. In *Transportation Research Record: Journal of the Transportation Research Board*, No. 1714, Transportation Research Board of the National Academies, Washington, D.C., 2000, pp. 33-39.

Saeed, A., M. I. Hammons, D. R. Feldman, and T. Poole. *Evaluation, Design and Construction Techniques for Airfield Concrete Pavement Used as Recycled Material for Base*. Publication IPRF-07-g-002-03-5. IPRF, 2006.

Lee, J. C., T. B. Edil, C. H. Benson, and J. M. Tinjum. Use of BE<sup>2</sup>ST in-Highways for Green Highway Construction Rating in Wisconsin. *Proceeding of The 1<sup>st</sup> T&DI Green Streets & Highway Conference*, Denver, Colorado, 2010.

Kuo, S.-S., H. S. Mahgoub, and A. Nazef. Investigation of recycled concrete made with limestone aggregate for a base course in flexible pavement. In *Transportation Research Record: Journal of the Transportation Research Board*, No. 1787, Transportation Research Board of the National Academies, Washington, D.C., 2002, pp. 99-108.

Guthri, S. W., D. Cooley, and D. L. Eggett. Effects of Reclaimed Asphalt Pavement on Mechanical Properties of Base Materials. In *Transportation Research Record: Journal of the Transportation Research Board*, No. 2005, Transportation Research Board of the National Academies, Washington, D.C., 2007, pp. 44-52.

FHWA. *User Guideline for Byproducts and Secondary Use Materials in Pavement Construction*. Publication FHWA-RD-97-148. FHWA, U.S. Department of Transportation, 2008.

Schaertl, G. J. *Scaling and Equivalency of Bench-Scale Tests to Field Scale Condition*. MS thesis. Department of Civil and Environmental Engineering, University of Wisconsin, Madison, 2010.

ARA. *Guide for Mechanistic-Emprical Design on New and Rehabilitated Pavement Structures*. Publication NCHRP Project 1-37A, NCHRP, 2004.

NAPA. *How to Increase RAP Usage and Ensure Pavement Performance*. National Asphalt Pavement Association, 2009.

FHWA. *Reclaimed Asphalt Pavement in Asphalt Mixtures: State of the Practice*. Publication FHWA-HRT-11-021. FHWA, U.S. Department of Transportation, 2011.

Kim, W., J. F. Labuz, and S. Dai. Resilient Modulus of Base Course Containing Recycled Asphalt Pavement. In *Transportation Research Record: Journal of the Transportation Research Board*, No. 2005, Transportation Research Board of the National Academies, Washington, D.C., 2007, pp. 27-35.

Molenaar, A. A. A., and A. A. van Niekerk. Effects of Gradation, Composition, and Degree of Compaction on the Mechanical Characteristics of Recycled Unbound Materials. In *Transportation Research Record: Journal of the Transportation Research Board*, No. 1787, Transportation Research Board of the National Academies, Washington, D.C., 2007, pp. 73-82.

Park, T. Application of Construction and Building Debris as Base and Subbase Materials in Rigid Pavement. In *Transportation Research Record :Journal of Transportation*

*Engineering* , No. 129, Transportation Research Board of the National Academies, Washington, D.C. ,2003, pp. 558-563.

Rosa, M. *Effect of Freeze and Thaw Cycling on Soils Stabilized using Fly Ash*. MS thesis. Department of Civil and Environmental Engineering, University of Wisconsin, Madison, 2006.

Kootstra, B. R., A. Ebrahimi, T. B. Edil, and C. H. Benson. Plastic Deformation of Recycled Base Materials. *GeoFlorida 2010: Advances in Analysis, Modeling & Design*, 2010, pp.2682-2691.

Jong, D.-T., P. J. Bosscher, and C. H. Benson. Field Assessment of Changes in Pavement Moduli Caused by Freezing and Thawing. In *Transportation Research Record: Journal of the Transportation Research Board*, No.1615, Transportation Research Board of the National Academies, Washington, D.C.,1998, pp. 41-48.

Zaman, M. M., and J.-H. Laguros, J. G. Zhu. Durability Effects on Resilient Moduli of Stabilized Aggregate Base. In *Transportation Research Record: Journal of the Transportation Research Board*, No. 687, Transportation Research Board of the National Academies, Washington, D.C.,1999, pp. 29-39.

Tian, P., M. M. Zaman, and J. G. Laguros. Gradation and Moisture Effects on Resilient Moduli of Aggregate Bases. In *Transportation Research Record: Journal of the Transportation Research Board*, No.1619, Transportation Research Board of the National Academies, Washington, D.C.1998, pp.75-84.

Pan, T., E. Tutumluer, and J. Anochie-Boateng. Aggregate Morphology Affecting Resilient Behavior of Unbound Granular Materials. In *Transportation Research Record: Journal of the Transportation Research Board*, No.1952, Transportation Research Board of the National Academies, Washington, D.C., 2006, pp. 12-20.

Williams, R. R., and S. Nazarian. Correlation of Resilient and Seismic Modulus Test Results. *Journal of Materials in Civil Engineering*, Vol 19, No.12, ASCE, 2007, pp. 1026-1032.

Pucci, M. J. *Development of a Multi-Measurement Confined Free-Free Resonant Column Device and Initial Studies*. MS thesis, Department of Civil, Architectural and Environmental Engineering, University of Texas, Austin, 2010.

Toros, U., and D. R. Hiltunen. Effects of Moisture and Time on Stiffness of Unbound Aggregate Base Course Materials. In *Transportation Research Record: Journal of the Transportation Research Board* , No.2059, Transportation Research Board of the National Academies, Washington, D.C., 2008, pp. 41-51.

Bejarano, M.O, J. T Harvey, and L. Lane. In-Situ Recycling of Asphalt Concrete as Base Material in California. *Proc. 82nd Annual Meeting, Transportation Research Board*, Washigton, D.C, 2003, pp. 22.



Camargo, F. F., T. B. Edil, and C. H. Benson. Strength and Stiffness of Recycled Base Materials Blended with Fly Ash. *Transportation Research Board 88th Annual Meeting*, Washington, D.C., 2009.

NCHRP. *Laboratory Determination of Resilient Modulus for Flexible Pavement Design*. Publication NCHRP Research Results Digest, NCHRP, 2004.

Moosazedh, J., and M. W. Witzczak. Prediction of subgrade moduli for soil that exhibits nonlinear behavior. In *Transportation Research Record: Journal of the Transportation Research Board*, No.810, Transportation Research Board of the National Academies, Washington, D.C., 1981, pp. 9-17.

Bozyurt, O. *Behavior of Recycled Asphalt Pavement and Recycled Concrete Aggregate as Unbound Road Base*. MS thesis. Department of Civil and Environmental Engineering, University of Wisconsin, Madison, 2011.

Arm, M. Self-cementing Properties of Crushed Demolished Concrete in Unbound Layers: Results from Triaxial Tests and Field Tests. *Waste Management*, Vol. 21, No.3, 2001, pp. 235-239.

Attia, M., and M. Abdelrahman. Modeling the Effect of Moisture on Resilient Modulus of Untreated Reclaimed Asphalt Pavement. In *Transportation Research Record: Journal of the Transportation Research Board*, No. 2167, Transportation Research Board of the National Academies, Washington, D.C., 2010, pp. 30-40.

Nokkaew, K., J. M. Tinjum and C. H. Benson. Hydraulic Properties of Recycled Asphalt Pavement and Recycled Concrete Aggregate. GeoCongress, ASCE, 2011

Juan, M. S., and P. A. Gutierrez. Study on the Influence of Attached Mortar Content on the Properties of Recycled Concrete Aggregate. *Construction and Building Materials*, Vol. 23, 2009, pp.872-877.

Gokce, A., S. Nagataki, T. Saeki, and M. Hisada. Identification of Frost-susceptible Recycled Concrete Aggregates for Durability of Concrete. *Construction and Building Materials*, Vol. 25, 2011, pp. 2426-2431.

Chini, A. R., S.-S. Kuo, J. M. Armaghani, and J. P. Duxbury. Test of Recycled Concrete Aggregatenin Accelerated Test Track. In *Transportation Research Record : Journal of Transportation Engineering* , No. 6, Transportation Research Board of the National Academies, Washington, D.C., 2001, pp. 486-492.

Poon, C.-S., X.C. Qiao, and D. Chan. The Cause and Influence of Self-Cementing Properties of Fine Recycled Concrete Aggregates on the Properties of Unbound Sub-Base. *Waste Management*, Vol.26, No.10, 2006, pp. 1166-1172.

Mishra, D., E. Tutumluer, and A. A. Butt. Quantifying Effects of Particle Shape and Type and Amount of Fines on Unbound Aggregate Performance Through Controlled Gradation. In *Transportation Research Record: Journal of the Transportation Research Board*, No. 2167, Transportation Research Board of the National Academies, Washington, D.C. , 2010, pp 61-71.

Ebrahimi, A., J. M. Tinjum and T. B. Edil. Deformational Behavior of Fouled Railway Ballast, *Journal of Geotechnical and Geoenvironmental Engineering*, ASCE, 2011.

Barksdale, R. D., and S. Y. Itani. Influence of Aggregate Shape on Base Behavior. In *Transportation Research Record*, No.1227, Transportation Research Board of the National Academies, Washington, D.C., 1989, pp. 173-182.

Schuettpelz, C. C., D. Fratta, and T. B. Edil. Mechanistic method for determining the resilient modulus of base course materials based on elastic wave measurements. *Journal of Geotechnical and Geoenvironmental Engineering*. Vol. 136, No. 8, 2010, pp. 1086-1094

## **TABLES**

Table 1. Index Properties of recycled materials and Class 5 aggregate

Material	States	D <sub>50</sub> (mm)	C <sub>u</sub>	C <sub>c</sub>	G <sub>s</sub>	AB (%)	AC /MC (%)	w <sub>opt</sub> (%)	γ <sub>dmax</sub> (kN/m <sup>3</sup> )	Gravel (%)	Fines (%)	USCS
Class 5 Aggregate	MN	1.0	21	1.4	2.6	–	–	8.9	20.1	22.9	9.5	GW-GM
	CA	4.8	22	1.4	2.3	5.0	37	10.4	19.9	50.6	2.3	GW
RCA	MI	9.7	35	3.9	2.3	5.4	–	8.7	20.8	68.5	3.2	GP
	TX	13.3	38	6.0	2.3	5.5	45	9.2	19.7	76.3	2.1	GW
RAP	CA	3.0	13	1.2	2.4	2.0	5.7	6.1	20.7	36.8	1.8	SW
	MN	1.6	7	0.7	2.4	1.8	7.1	6.7	20.8	26.3	2.5	SP
	TX	5.4	11	1.1	2.3	1.3	4.7	8.1	20.3	54.2	1.0	GW

Note: AC=Asphalt Content, MC=mortar Content, AB=Absorption, MN=Minnesota, CA=California, MI=Michigan, TX=Texas

Table 2. SRM and power model fitting parameters  $k_1$  and  $k_2$  for base materials after 0, 5, 10 and 20 F-T cycles

Material	States	Freeze-Thaw Cycles	External			Internal			SRM <sub>0</sub> / SRM <sub>N</sub>
			$k_1$	$k_2$	SRM (MPa)	$k_1$	$k_2$	SRM (MPa)	
Class 5 Aggregate	MN	0	66.2	0.20	191	129.2	0.15	281	1.0
		5	59.1	0.21	186	59.1	0.28	261	0.9
		10	35.5	0.30	177	34.7	0.36	240	0.9
		20	24.8	0.34	153	24.7	0.41	223	0.8
RCA	CA	0	119.4	0.15	262	273.6	0.13	550	1.0
		5	74.8	0.21	227	113.4	0.27	489	0.9
		10	99.1	0.20	282	185.7	0.21	578	1.1
	MI	0	32.7	0.34	199	107.2	0.25	400	1.0
		5	22.8	0.39	191	55.3	0.35	361	0.9
		10	47.8	0.32	257	177.5	0.18	472	1.2
		20	83.6	0.22	268	388.7	0.07	553	1.4
	TX	0	74.6	0.23	258	236.1	0.13	464	1.0
		5	43.6	0.30	211	76.8	0.32	419	0.9
		10	44.6	0.31	236	120.8	0.26	471	1.0
		20	81.1	0.24	289	150.2	0.28	601	1.3
	RAP	CA	0	122.5	0.14	256	348.8	0.06	473
5			122.5	0.13	249	147.9	0.20	436	0.9
10			76.6	0.20	223	136.2	0.19	379	0.8
20			66.0	0.21	203	122.8	0.18	323	0.7
MN		0	93.9	0.174	238	236.1	0.127	464	1.0
		5	57.6	0.25	220	85.8	0.27	361	0.8
		10	54.0	0.25	200	80.2	0.27	344	0.7
		20	31.2	0.33	180	57.3	0.32	314	0.7
TX		0	156.6	0.14	334	358.7	0.12	686	1.0
		5	155.2	0.12	287	344.1	0.10	585	0.9
		10	88.6	0.24	272	250.4	0.15	566	0.8
		20	66.0	0.21	203	122.8	0.18	323	0.7

## **FIGURES**

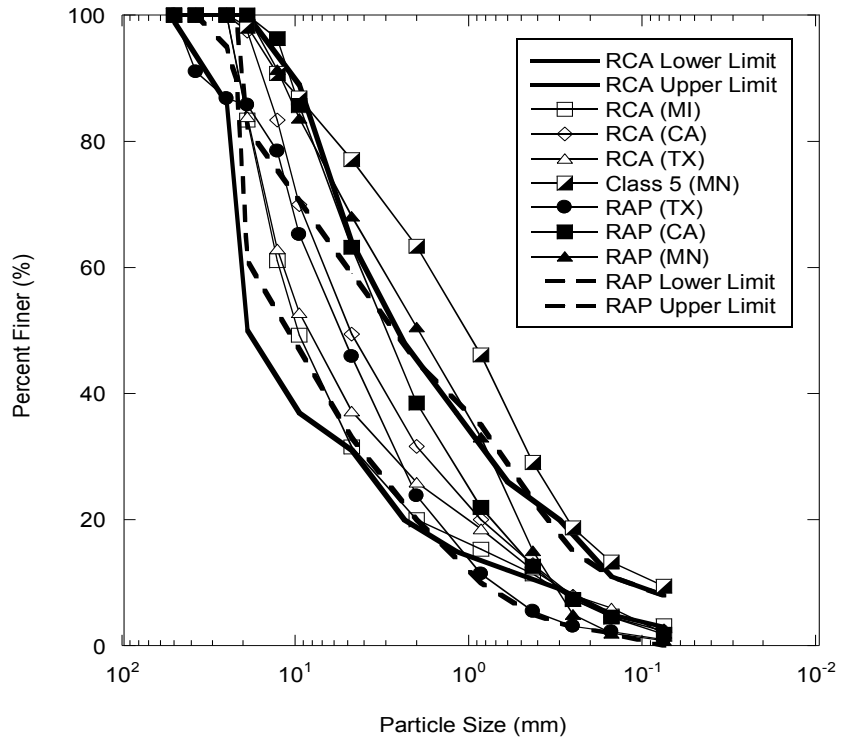


Fig. 1. Particle size distribution for RCA, RAP, and Class 5 aggregate and lower and upper limits of RAP/RCA from the literature.

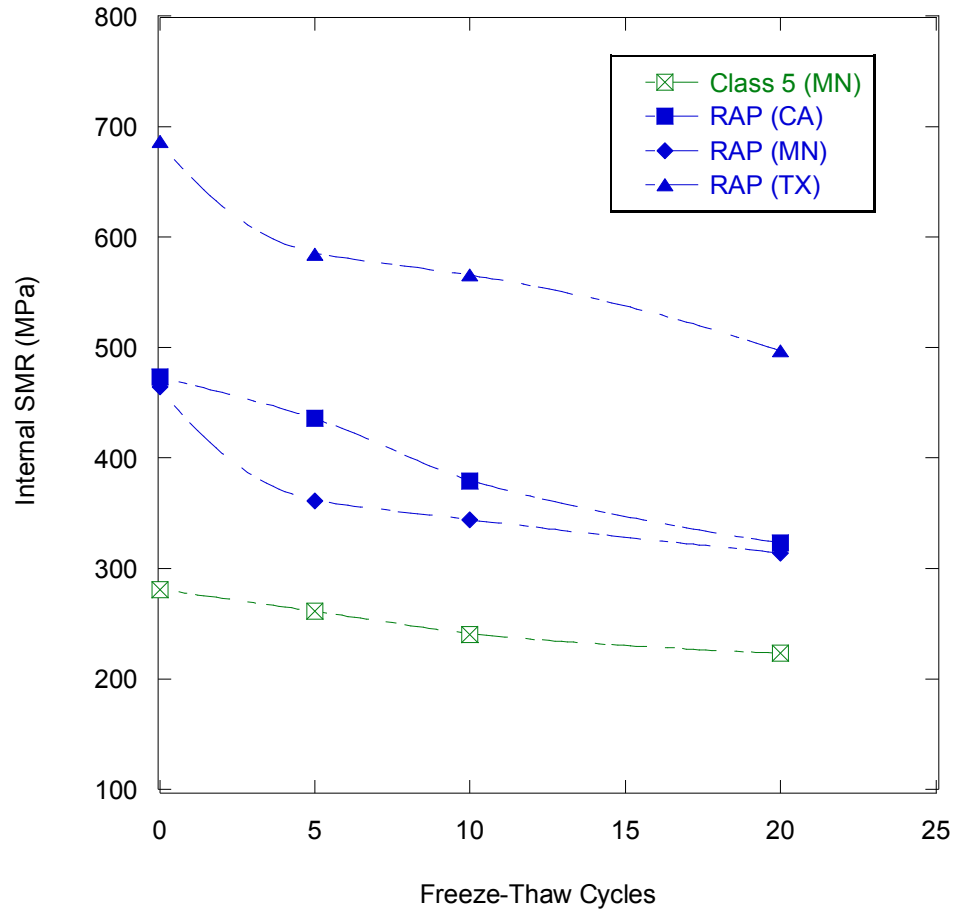


Fig. 2. Summary Resilient Modulus (SRM) of RAP and Class 5 aggregate after 0, 5, 10 and 20 freeze-thaw cycles



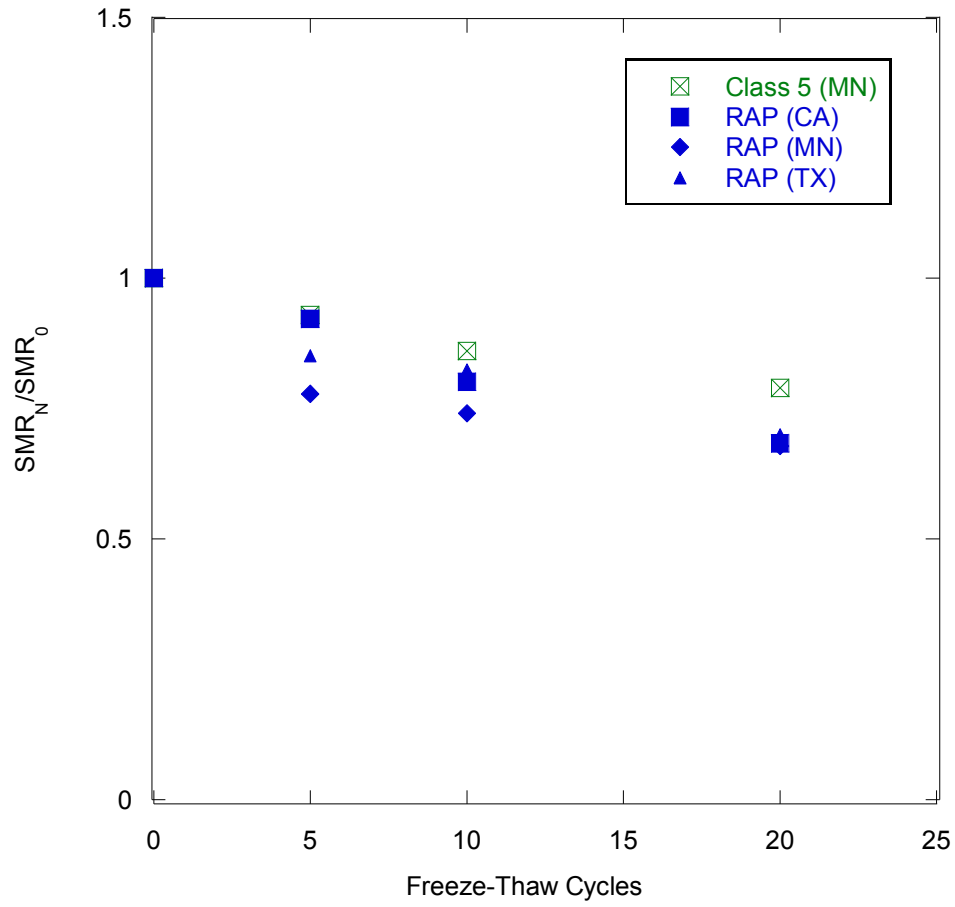


Fig. 3. Normalized Summary Resilient Modulus (SRM) of RAP and Class 5 aggregate after 0, 5, 10 and 20 freeze-thaw cycles

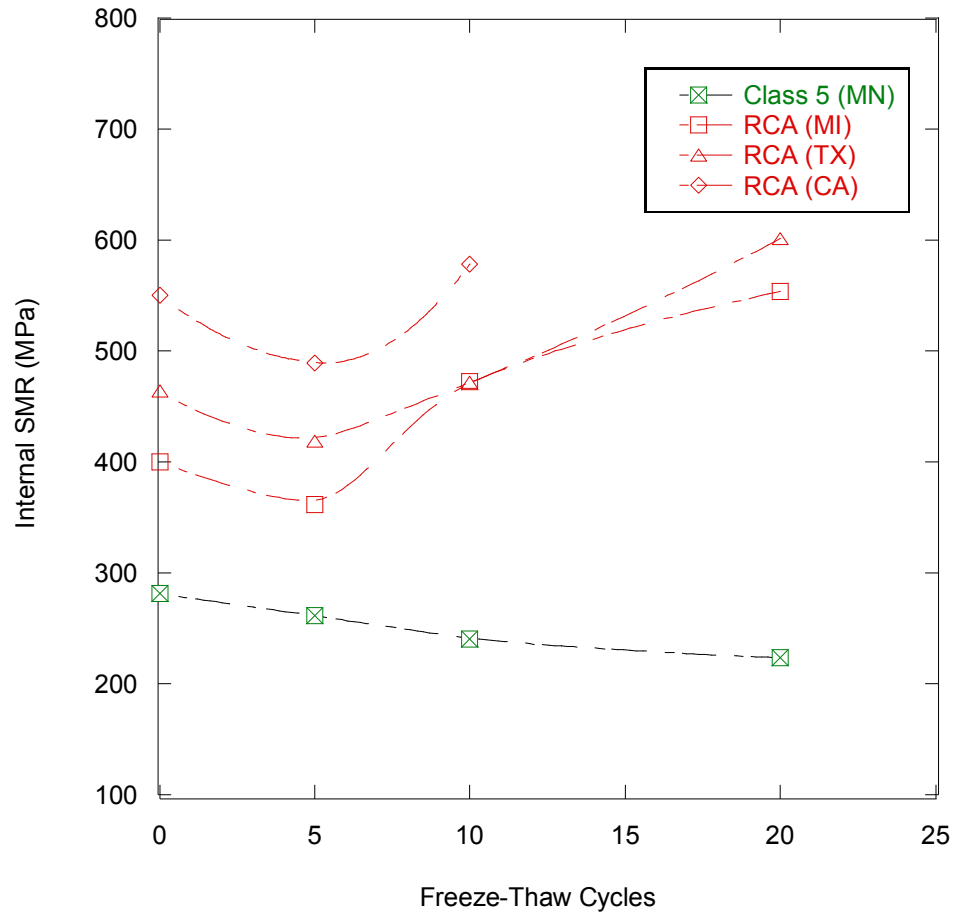


Fig. 4. Normalized Summary Resilient Modulus (SRM) of RCA and Class 5 aggregate after 0, 5, 10 and 20 freeze-thaw cycles

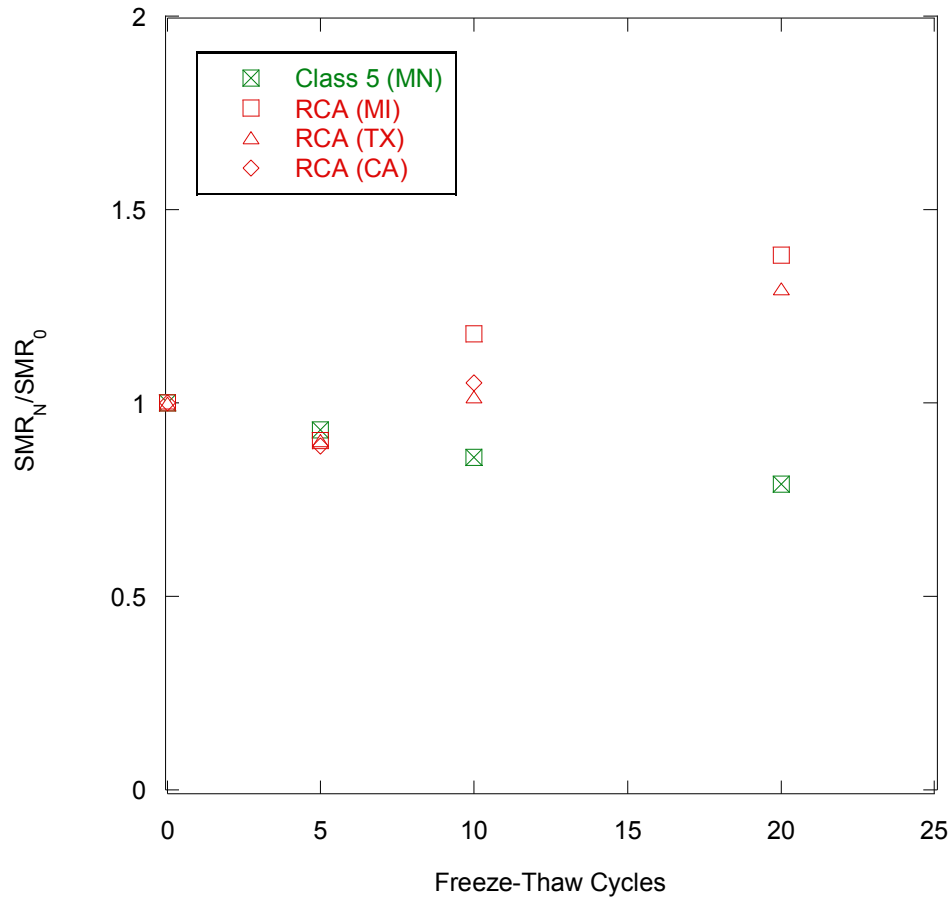


Fig. 5. Normalized Summary Resilient Modulus (SRM) of RCA and Class 5 aggregate after 0, 5, 10 and 20 freeze-thaw cycles

# **Recycled Unbound Materials**

## **TPF-5 (129) Recycled Unbound Materials**

Mn/DOT Contract No. 89264 Work Order No. 2

CFMS Contract No. B14513

### **Task I: Design**

#### **Task ID (Part 2): Climate Effects (Hydraulic Properties of Recycled Asphalt Pavement and Recycled Concrete Aggregate)**

**Kongrat Nokkaew, James M. Tinjum, and Craig H. Benson**

University of Wisconsin- Madison

December 2, 2011

## ABSTRACT

The saturated hydraulic conductivity ( $k_{\text{sat}}$ ) and water characteristic curves (WCCs) of three recycled asphalt pavements (RAPs) and three recycled concrete aggregates (RCAs) were measured. The  $k_{\text{sat}}$  was determined using a constant-head, rigid-wall, 152-mm-diameter permeameter. The specimens were prepared at 95% of maximum dry density based on modified Proctor testing. The  $k_{\text{sat}}$  of the RAPs varied from  $3.8 \times 10^{-5}$  to  $3.7 \times 10^{-4}$  m/s and from  $1.6 \times 10^{-5}$  to  $2.6 \times 10^{-5}$  m/s for the RCAs. Hazen's equation (1911) tends to over predict  $k_{\text{sat}}$  for RAPs and RCAs. Hanging columns with large-scale testing cells (305-mm inner diameter and 76-mm height) fitted with air aspirators were used to determine the WCCs. The WCC of each recycled material was fitted using the Fredlund and Xing (1994) model because this model is used in the Mechanistic-Empirical Pavement Design Guide (MEPDG). A hanging column test can measure suction lower than 1 kPa with high accuracy ( $\pm 0.02$  kPa). The slopes of the WCCs of RAPs were steeper than those of RCAs, although RAPs have higher densities. Compared to Rahardjo et al. (2010), RAPs and RCAs used in this study provided higher air entry suction because the specimens were prepared at higher, compacted density to replicate field conditions. To develop a WCC for RAPs and RCAs over a larger range of suctions, a device such as a pressure plate extractor is recommended.

## INTRODUCTION

The use of recycled material as a base course in pavement construction has widely increased over recent decades. Use of recycled material can reduce global warming potential, energy consumption, and hazard waste generation (Lee et al., 2010). The use of recycled material can provide cost and time savings because the material is generated and reincorporated on site (Bennert et al., 2000).

Among recycled materials, recycled asphalt pavement (RAP) and recycled concrete aggregate (RCA) are commonly used for pavement construction (FHWA, 2008). RAP is a coarse granular material derived from crushing existing asphalt surfaces. RCA is an aggregate material obtained from demolition of old concrete structures such as roads, runways, and buildings (Guthrie et al., 2007; FHWA, 2008). Studies have confirmed that recycled materials provide high strength and durability, either as a mixture or as a complete replacement for conventional aggregate (Blankenagel and Guthrie, 2006). However, the hydraulic properties of RAPs and RCAs, which affect long-term performance of base course (Cedergren, 1988), have not been thoroughly investigated.

The important hydraulic properties of base course include saturated hydraulic conductivity ( $k_{\text{sat}}$ ) and the water characteristic curve (WCC). The Mechanistic-

Empirical Pavement Design Guide (MEPDG) requires  $k_{sat}$  as an input for drainage design and the WCC for adjusting the modulus for base and subgrade for structural pavement design (NCHRP, 2004). However, the WCCs of RAP and RCA (typically, coarse aggregate) are difficult to obtain directly because the water content of coarse aggregate can change rapidly at low suction ( $< 1$  kPa), and few methods measure suction,  $\psi$ , accurately for  $\psi < 1$  kPa (Li et al., 2009). To accurately characterize the hydraulic properties of large aggregate, specimens should be prepared at field density, and the size should be large enough to represent field compaction condition. ASTM D2434-68 recommends that the minimum diameters of specimen cylinder for granular materials should be approximately 8 times of the maximum aggregate size for hydraulic conductivity test.

This study investigated the  $k_{sat}$  of three compacted RAPs and three RCAs used as a base course with constant-head, rigid-wall, compaction-mold permeameters. The WCCs were measured by hanging columns with large-scale testing cells (304-mm inner diameter and 76-mm height). The WCC of each recycled material was fit using the Fredlund and Xing (1994) model because this model is used in the Mechanistic-Empirical Pavement Design Guide (MEPDG). The hydraulic properties of RAP and RCA measured in this study are compared to results from the literature for similarly graded, coarse aggregate.

## **Hydraulic properties of coarse granular material**

### **Saturated hydraulic conductivity**

Saturated hydraulic conductivity ( $k_{sat}$ ) is the property that defines the ability of water to flow through saturated soil. The  $k_{sat}$  of granular material is mainly influenced by particle size and grain size distribution. Various empirical relationships have been proposed to predict  $k_{sat}$  of coarse-grained soil (e.g., Hazen, 1911; Kenny et al., 1984; Sherard et al., 1984). Hazen (1991) proposed the relationship between  $k_{sat}$  and effective diameter ( $D_{10}$ ) for uniformly graded, loose sand as:

$$k_{sat} = 0.01c_1D_{10}^2 \quad (1)$$

where the unit of  $k_{sat}$  is m/s,  $c_1$  is a constant related to particle shape (0.4 to 1.2), and  $D_{10}$  is the 10<sup>th</sup> percentile for particle size in units of mm.

### **Water characteristic curve**

A WCC describes the relationship between water content or degree of saturation and  $\psi$ , where  $\psi = u_a - u_w$  ( $u_a$  is pore air pressure and  $u_w$  is pore water pressure). The  $\psi$  corresponding to intersection between two sloping line at low suction of the WCC is defined as air-entry suction ( $\psi_a$ ) (Fredlund and Rahardjo,

1993). Although the drying path and wetting path of the WCC might be different due to hysteresis, measurement of the wetting path is difficult and only the drying curve is typically measured, especially for granular material (Hillel, 1980).

Numerous fitting equations have been proposed to describe the WCC (e.g., Brooks and Corey, 1964; van Genuchten, 1980; Fredlund and Xing, 1994). Among those models, the Fredlund and Xing equation provides a sigmoid curve suitable for different type of soil for matric suction from 0 to 1 GPa. The model requires four fitting parameters as defined by:

$$\theta = C(\psi) \frac{\theta_s}{\{ \ln[e + (\psi/a_f)^{b_f}] \}^{c_f}} \quad (2)$$

$$C(\psi) = \left[ 1 - \frac{\ln\left(1 + \frac{\psi}{h_{rf}}\right)}{\ln\left(1 + \frac{1000000}{h_{rf}}\right)} \right] \quad (3)$$

where  $\theta$  is volumetric water content,  $\theta_s$  is saturated volumetric water content,  $\psi$  is suction in kPa, and  $a_f$ ,  $b_f$ ,  $c_f$  and  $h_{rf}$  are fitting parameters.  $C(\psi)$  is the adjusting function used to force  $\theta$  to zero at 1 GPa.

## MATERIALS

Three RAPs and three RCAs were collected from different states across the US (Bozyurt, 2011). The RAPs and RCAs were named according to the source state. Index tests were conducted on each recycled material. Grain size distribution and classification were determined according to ASTM D422. Specific gravity ( $G_s$ ) and percent absorption were determined per AASHTO T85. Compaction tests were conducted using modified Proctor effort according to ASTM D1557.

Results of index tests on the RAPs and RCAs are summarized in Table 1. The RAPs and RCAs are broadly graded, including classifications of SM, SP, SW, and GM according to the Unified Soil Classification System (USCS). The  $G_s$  of RAPs are lower than conventional aggregates because RAPs are comprised of asphalt, which has low  $G_s$ . The grain size distributions of the tested materials are presented in Figure 1. RAPs have a lower percentage of fines than RCAs. RAPs are hydrophobic materials while RCAs are hydrophilic materials (Rahardjo et al., 2010). Thus, percent of absorption of RAPs tend to be higher than of RCAs. Percent absorption of RAPs ranged between 1.5 and 3.0, while RCAs had percent absorption ranging from 5.0 to 5.8. Compaction curves for RAPs and RCAs are presented in Figure 2. Both RAP and RCA materials are sensitive to the molding water content. RAP has higher maximum density than RCA and lower optimum water content.

**Table 1. Properties of RAPs and RCAs**

Properties	RAP			RCA		
	Colorado	New Jersey	Wisconsin	Colorado	California	MnROAD
USCS designation	SP	GW	SP	SM	SW	SP
Specific gravity, $G_s$	2.40	2.49	2.46	2.63	2.63	2.71
Maximum dry unit weight ( $kN/m^3$ )	20.6	20.3	20.2	18.9	19.8	19.7
Optimum water content (%)	5.7	6.4	7.7	9.3	10.9	11.2
Percent fines	0.7	0.7	0.5	12.82	3.05	2.32
Percent absorption	3.0	2.1	1.5	5.8	5.0	5.0

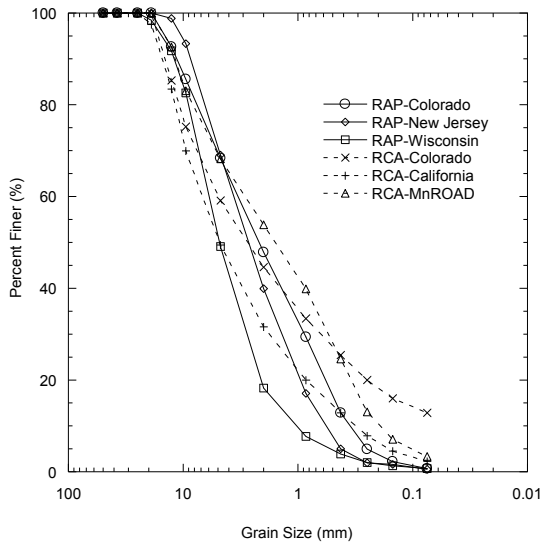


**Figure 1. Grain size distributions**

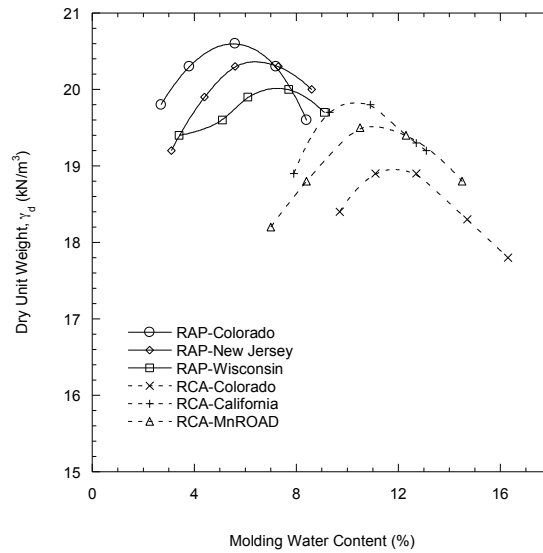


**Figure 2. Modified Proctor compaction curves**

## METHODS

### Hydraulic conductivity measurement

Hydraulic conductivity was conducted following ASTM D5856, measurement of hydraulic conductivity of porous material using a rigid-wall, compaction-mold permeameter. The specimens were compacted in 152-mm-diameter compaction molds at 95% of the maximum dry density as shown in Table 1. Tap water was used for all tests. The flow rate of an empty cell was checked for compliance in head loss. If the flow rate of an empty cell is lower than 10 times the flow rate of the cell with the specimen, the head loss from the specimens can be considered to be negligible (Daniel, 1994). The Different hydraulic gradients controlled to be less than 5 were applied to specimens. The ratio of outflow to inflow was measured to confirm saturation of the specimens.



### WCC measurement using large-scale hanging column test

A hanging column test combined with an air aspirator was used to determine the WCCs for the RAPs and RCAs. Figure 3 presents the schematic of the hanging column test. The test equipment includes four main parts: testing cell, outflow column, manometer, and the hanging column. The hanging column test can measure the WCC precisely at  $\psi < 1$  kPa with high accuracy ( $\pm 0.02$  kPa; i.e.,  $\approx 2$ -mm height of water). The lowest  $\psi$  which can be measured with this setup is 0.05 kPa. The highest  $\psi$  for the hanging column test is approximately 80 kPa due to the limitation of water cavitation. However, ceiling height also limits the  $\psi$  applied, or 25 kPa in this study. Suction higher than 25 kPa was supplied to the specimens using an air aspirator.

Testing followed ASTM D6836 method A. Large-scale cylinder specimens of 305-mm inner diameter and 76-mm height were prepared to simulate a base course layer in the field (Figure 4). A 1-bar porous ceramic plate was used in the testing cell. Rubber gaskets were installed to prevent air flow intrusion.

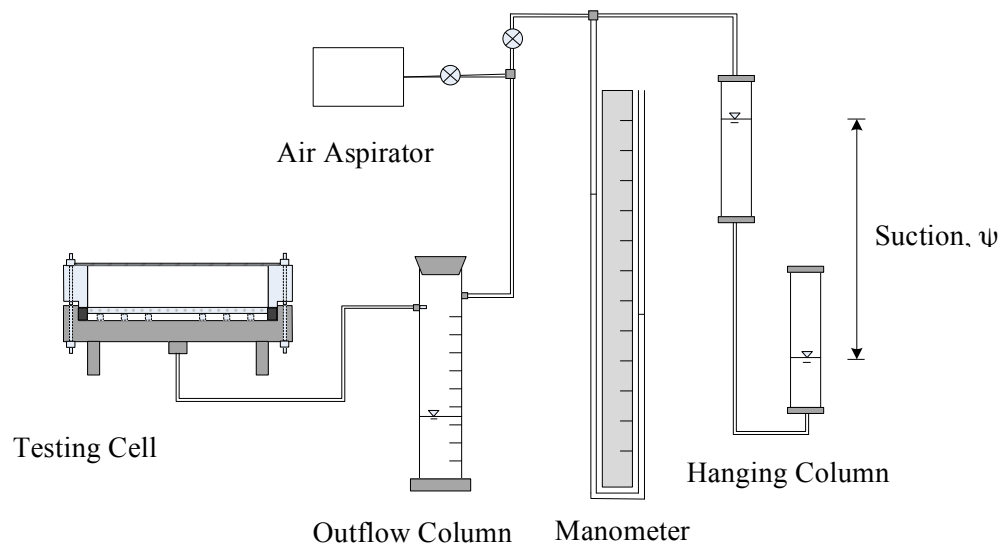


**Figure 3. Schematic of hanging column apparatus**

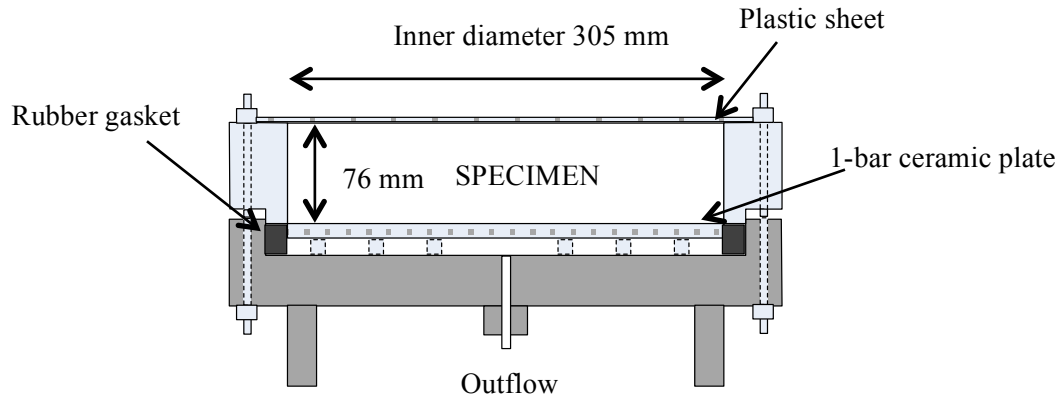


**Figure 4. Schematic of large-scale testing cell**

The specimens were prepared at  $\theta_s$  calculated from the desired dry unit weight and measured  $G_s$ . Specimens were compacted in the testing cell to 95% of maximum dry density. A shaking table was used during compaction to ensure the specimen reached the target density. De-aired, distilled water was used for specimen preparation.

## RESULTS

Average  $k_{sat}$  determined from five replicate tests are summarized in Table 2. The average  $k_{sat}$  of the RAPs ranged between  $3.8 \times 10^{-5}$  to  $3.7 \times 10^{-4}$  m/s, while  $k_{sat}$  of the RCAs ranged between  $1.6 \times 10^{-5}$  and  $2.6 \times 10^{-5}$  m/s. A statistical chart presenting the maximum and minimum values, and the percentiles at 75, 50 (median), and 25 for  $k_{sat}$  is depicted in Figure 5. The measured  $k_{sat}$  varied within a narrow range (maximum  $k_{sat}$ /minimum  $k_{sat} < 2$ ) for each replicate test for RAP and RCA, which indicates consistency of method. Figure 6 presents the relationship between effective diameter ( $D_{10}$ ) and  $k_{sat}$  for the recycled materials. Increasing  $D_{10}$  tends to increase  $k_{sat}$  for PAPs, but does not show significantly increasing  $k_{sat}$  for RCAs. The Hazen (1911) prediction for  $k_{sat}$  (Eqn. (1)) was developed by using  $c_1 = 0.4$  and 1.2 for the lower and upper bounds, respectively. RAPs and RCAs have lower  $k_{sat}$  for the same  $D_{10}$ . In comparison to the loose, uniformly graded aggregate for which the Hazen empirical equation was developed, the recycled materials of this study are compacted and more broadly graded; thus, this widely used predictor of  $k_{sat}$  is not applicable for these recycled materials.

**Table 2 Average ( $k_{sat}$ ) of RAPs and RCAs**

Description	RAP			RCA		
	Colorado	New Jersey	Wisconsin	Colorado	California	MnROAD
$D_{10}$ (mm)	0.35	1.00	0.56	0.073	0.31	0.08
Measured $k_{sat}$ (m/s)	$3.8 \times 10^{-5}$	$3.7 \times 10^{-4}$	$5.2 \times 10^{-5}$	$1.6 \times 10^{-5}$	$1.9 \times 10^{-5}$	$1.8 \times 10^{-5}$

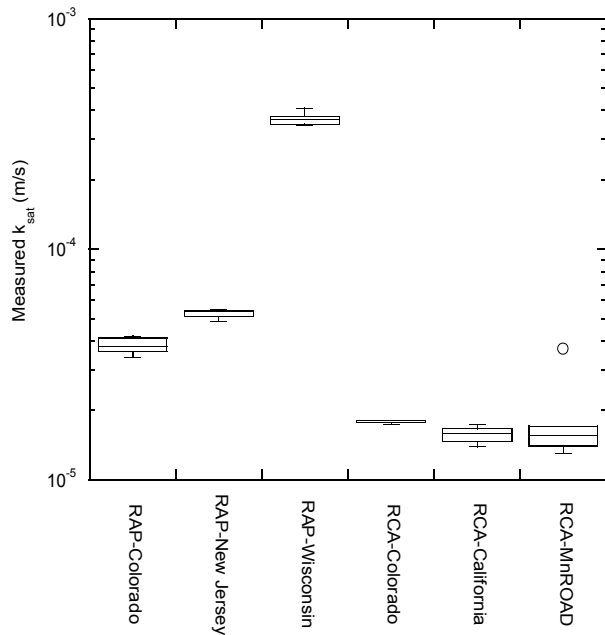


**Figure 5. Statistical chart for  $k_{sat}$  of RAPs and RCAs**

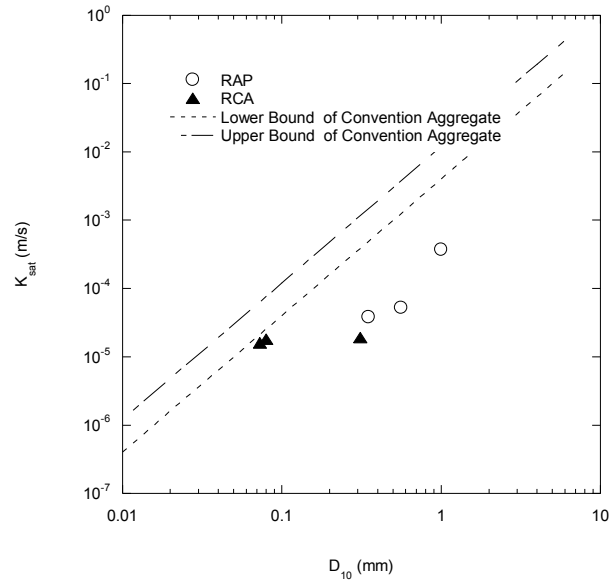


**Figure 6.  $K_{sat}$  versus  $D_{10}$  for RAPs and RCA**

The hanging column test combined with an air aspirator used in this study was able to measure suction between 0.05 and 75 kPa for RAP and RCA, with high accuracy for low suction measurements ( $\pm 0.02$  kPa). Measured WCCs of the RAPs and RCAs are presented as Figure 7. The  $\psi_a$  of the RAPs range from 0.1 to 1.1 kPa, and from 0.5 to 3.0 kPa for the RCAs. The slope at the desorption part of the WCC is greater for the RAPs in comparison to the RCAs. Residual water content ( $\theta_r$ ) represents the water content at the dry state of the WCC for which an increase in  $\psi$  does not correspond to an appreciable change in  $\theta$ . The  $\theta_r$  of RAPs was obtained for RAP-New Jersey and RAP-Wisconsin. However, the  $\theta_r$  of RAP-Colorado and the RCAs were indeterminate in this study. Extending the  $\psi$  measurement to a higher range ( $> 80$  kPa) from another test method (e.g., pressure plate extractor) is recommended if a full-range WCC of RAP and RCAs is desired or necessary.

The data from each measured WCC was fit to the Fredlund and Xing (1994) model as presented by Eqns (2) and (3) using least square methodology. As shown in Figure 7, the Fredlund and Xing model provides good fits for the recycled materials evaluated in this study. The  $a_f$  parameter might be related to  $\psi_a$  of the WCC, while the  $b_f$  and  $c_f$  parameters influence the slope of WCC at low and high  $\psi$ , respectively. The higher the  $b_f$ , the greater the slope on the desorption portion. The  $h_{rf}$  parameter used to adjust  $\theta$  became zero at 1 GPa. The fitting parameters for the Fredlund and Xing model are summarized in Table 3.

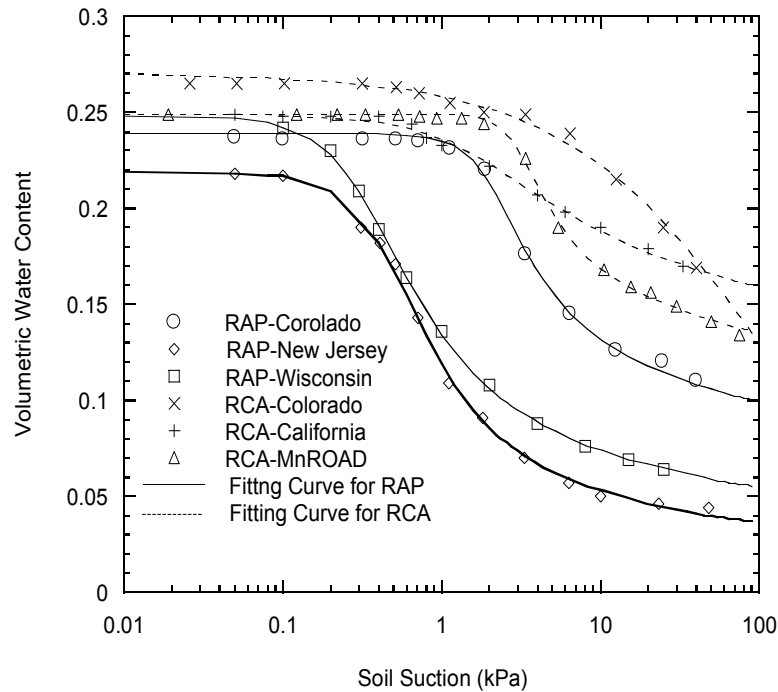


**Figure 7. Measured WCC data fitted to Fredlund and Xing (1994) model**

**Table 3 WCC parameters for RAPs and RCAs**

Description	Symbol	RAP			RCA		
		Colorado	New Jersey	Wisconsin	Colorado	California	MnROAD
Saturated $\theta$ , Porosity	$\theta_s, n$	0.24	0.22	0.25	0.27	0.25	0.25
Air Entry Suction, kPa	$\psi_a$	1.1	0.2	0.1	3.0	0.5	1.7
Fredlund and Xing fitting parameters							
Best fit	$a_f$ (kPa)	1.8	0.4	0.3	4.1	1.4	2.8
	$b_f$	3.5	2.4	2.1	1.2	1.2	4.7
	$c_f$	0.3	0.7	0.6	0.4	0.2	0.2
	$h_{rf}$ (kPa)	97	97	100	6197	5596	6047

**Table 4 Comparison of  $\psi_a$  of RAPs and RCAs to reference data**

Materials	USCS Classification	Dry Density (Mg/m <sup>3</sup> )	$\psi_a$ (kPa)	Reference
RAPs	GW, SP	1.94-1.97	0.1-1.1	This study
RCAs	SP, SP, SM	1.83-1.92	0.5-3.0	
RAPs	GP, SP	1.53-1.67	0.01-0.03	Rahardjo et al. (2010)
RCAs	GP, SP	1.55-1.71	0.042-22	

Air-entry suctions for RAPs and RCAs from this study were compared to those from Rahardjo et al. (2010) in Table 4. The  $\psi_a$  of the RAPs and RCAs measured in this study are greater than those of RAPs and RCAs conducted by Rahardjo (2010). The RAPs and RCAs used in this study were compacted to realistic field conditions and thus have higher density than the comparable reference data.

## SUMMARY AND CONCLUSIONS

This study presents the hydraulic properties ( $k_{sat}$  and WCC) of compacted RAPs and RCAs obtained from different states across the USA that have been used as base course for highway construction. The  $k_{sat}$  of the RAPs ranged from  $3.8 \times 10^{-5}$  to  $3.7 \times 10^{-4}$  m/s and from  $1.6 \times 10^{-5}$  to  $2.6 \times 10^{-5}$  m/s for the RCAs. The  $k_{sat}$  are proportional to the effective diameter ( $D_{10}$ ) for RAPs, but does not provide a strong relationship for RCAs. Hazen's (1911) equation for conventional aggregate tends to over predict  $k_{sat}$  for both RAPs and RCAs.

A hanging column test combined with an air aspirator can generate suction between 0.05 and 75 kPa for a recycled base, providing high accuracy for low suction measurements ( $\pm 0.02$  kPa). Fredlund and Xing's (1994) equation provides a good fit for the WCCs of RAPs and RCAs. Compared to Rahardjo et al. (2010), RAPs and RCAs used in this study provided higher  $\psi_a$  because the specimens were prepared at higher, compacted density. Extension of  $\psi$  measurements using devices such as a pressure plate extractor or sensors would be recommended if the full-range WCC for RAPs and RCAs is desired.

## ACKNOWLEDGEMENTS

The material evaluated in this study was provided from the TPF-5(129) Recycled Unbound Materials Pool Fund administered by the Minnesota Department of Transportation. We thank Professor Tuncer B. Edil for his input. The grain size analyses

were provided by Ozlem Bozyurt, a graduate student in the Department of Civil and Environmental Engineering (CEE). The compaction curves were prepared by Dr. Young-Hwan Son, Assistant Professor, Department of Rural Systems Engineering, College of Agriculture and Life Sciences, Seoul National University.

## REFERENCES

- AASHTO T85. (2010). "Standard method of test for specific gravity and absorption of coarse aggregate."
- ASTM D1557. (2009). "Standard method for laboratory compaction characteristics of soil using modified effort (56,000 ft-lb/ft<sup>3</sup> (2,700 kN-m/m<sup>3</sup>))."
- ASTM D2434-68. (2006). "Standard test method for permeability of granular soils (Constant Head)."
- ASTM D422. (2007). "Standard test method for particle-size analysis of soils."
- ASTM D5856. (2007). "Measurement of hydraulic conductivity of porous material using a rigid-wall, compaction-mold permeameter."
- ASTM D6836. (2008). "Standard test method for determination of the soil water characteristic curve for desorption using hanging column, pressure extractor, chilled mirror hygrometer, or centrifuge."
- Bennert, T., Papp, W.J., Maher, J.A., and Gucunski, N. (2000). "Utilization of construction and demolition debris under traffic-type loading in base and subbase applications." *Transport. Res. Rec.*, No. 1350, Washington, D.C., 33–39.
- Blankenagel, B.J., and Guthrie, W.S. (2006). "Laboratory characterization of recycled concrete for use as pavement base material." *Transport. Res. Rec.*, No. 1952, Washington, D.C., 2006, 21–27.
- Bozyurt, O. (2011). "Behavior of recycled pavement and concrete aggregate as unbound road base." MS Thesis, University of Wisconsin-Madison, WI
- Brooks, R.H. and Corey, A. T. (1964). "Hydraulic properties of porous media." Hydrology Paper No.3, Colorado State University.
- Cedergren, H. R. (1988). "Why all important pavement should be well drained." *Transport. Res. Rec.*, No. 1188, Washington, D.C., 56-62.
- Daniel, D. E. (1994). "State-of-the-art: Laboratory hydraulic conductivity tests for saturated soils." In: *Hydraulic conductivity and waste contaminant transport in soil*. Edited by Daniel, D.E. and Trautwein, S.J., Philadelphia: ASTM, 30-77.
- FHWA (2008). "User guidelines for byproducts and secondary use materials in pavement construction," *FHWA Report FHWA-RD-97-148*, FHWA, VA.
- Fredlund, D.G. and Rahardjo, H., (1993). *Soil mechanics for unsaturated soils*, Wiley, New York.
- Fredlund, D.G., and Xing, A.,(1994). "Equation for the soil-water characteristic curve." *Can. Geotech. J.*, 31(4), 521-532.
- Guthrie, W.E.S., Cooley, D., and Eggett, D.L. (2007). "Effects of reclaimed asphalt pavement on mechanical properties of base materials." *Transport. Res. Rec.*, No. 2005, Washington, D.C., 44–52.
- Hazen, A. (1911). "Discussion of "Dam foundations" by A.C. Koenig." *Trans. Am. Soc. Civ. Eng.*, 73, 199–203.
- Hillel, D. (1980). *Fundamental of soil physics*. Academic Press, Inc., San Diego, CA.
- Kenney, T., Lau, D., and Ofoegbu, G., (1984). "Permeability of compacted granular materials." *Can. Geotech. J.*, 21(4), 726-729.

- Lee, J.C., Edil, T.B., Tinjum, J.M., and Benson, C.H. (2010). "Qualitative assessment of environmental and economic benefits of recycled materials in highway construction." *Transport. Res. Rec.*, Washington, D.C., No. 1952, 138-142.
- Li, X., Zhang, L.M., and Li, J. H. (2009). "Development of a modified axis translation technique for measuring SWCCs for gravel soils at very low suctions," *Geotech. Test. J.*, 32(6), 1-11.
- NCHRP (2004). "Guide for Mechanistic-Empirical Design of pavement structures: part 2 – Design Inputs." *ARA, Inc.*, ERES Consultants Division, Champaign, IL.
- Rahardjo, H., Vialvong, K., and Leong, E.C. (2010). "Water characteristic curves of recycled materials" *Geotech. Test. J.*, 34(1), 1-8.
- Schlicht, P.D., Benson, C.H., Tinjum, J.M., and Albright, W.H. (2010). "In-service hydraulic properties of two landfill final covers in northern California." *Proceeding of GeoFlorida 2010*, ASCE, FL, Feb, 20-24, 2867-2877.
- Sherard, J.-L., Dunnigan, L.-P., and Talbot, J.-R. (1984). "Basic properties of sand and gravel filters." *J. Geotech. Eng.*, ASCE, 110(6), 684-700.
- van Genuchten, M. (1980), "A close-form equation for predicting the hydraulic conductivity of Unsaturated soils," *Soil. Sci. Am. J.*, 44, 892-898.

# **Recycled Unbound Materials**

## **TPF-5 (129) Recycled Unbound Materials**

Mn/DOT Contract No. 89264 Work Order No. 2

CFMS Contract No. B14513

### **Task II: Construction and Maintenance**

#### **Task IIA: Compaction Level and Assessment**

**Ozlem Bozyurt, Tuncer B. Edil, James Tinjum, and Craig H. Benson**  
**University of Wisconsin- Madison**

**August, 2011**



## 1. INTRODUCTION

The most common C&D materials used as unbound base course in pavement construction are recycled concrete aggregate (RCA) and recycled asphalt pavement aggregate (RAP). RCA is the product of the demolition of concrete structures such as buildings, roads, and runways. RAP is produced by removing and reprocessing existing asphalt pavement (Kuo et al., 2002; Guthri et al., 2007; FHWA 2008). By beneficially reusing concrete and asphalt, a waste product is converted to a resource for pavement construction (Langer 1988). An increase in the amount of RCA used to replace natural aggregates in pavement construction has economic and environmental benefits, while extending the supply of traditional construction materials (Saeed et al. 2006).

RAP and RCA compete with natural aggregates that are currently used in roadway base applications (Guthri et al. 2007; FHWA 2008). Despite the increased acceptance of recycled base material in construction, research concerning the mechanical properties and durability of such materials is limited (Bennert et al. 2000; Nataatmadja and Tan 2001; Guthri et al. 2007). Recycled materials should perform well under the intended use in pavement design; therefore, the mechanical properties of recycled materials need to be investigated thoroughly such that appropriate design procedures and specifications can be established.

Schaertl (2010) indicates that RCA and RAP used alone or in blends with natural aggregates can have different resilient modulus ( $M_r$ ), sensitivity to stress state, and rutting performance compared to natural aggregates. The durability and toughness of recycled materials can also be different than that of natural aggregates (Weyers et al. 2005).

The objective of this study is to characterize the properties of RCA and RAP as unbound base or subbase material without treatment or stabilization, to assess their behavior under laboratory conditions. Variability in material properties, homogeneity of material, and the identification and control of material quality are addressed in this study.

The impacts of compactive effort on the stiffness of the unbound base layer constructed from RCA and RAP were investigated to determine how the compaction level is influential on properties and varies by composition of materials. The compaction moisture effect on the stiffness of RCA and RAP were also assessed. RAP and RCA may contain impurities that affect their mechanical properties and long-term performance, the impurity type and content affecting the stiffness of RAP and RCA were investigated.

## **2. BACKGROUND**

### **2.1. Recycled Material as Unbound Base Material**

The advanced age of transportation infrastructure in the US, coupled with increasing traffic loads, has accelerated deterioration of this network of roads, necessitating considerable maintenance expenditures. On a parallel path, the road construction industry is being encouraged, through political and societal pressures, to incorporate recycled material and by-products in pavement structures as alternatives to diminishing aggregate resources (Lekarp et al. 2000). Recycling of pavement material is a viable alternative to use of natural aggregates in road maintenance and rehabilitation activities. Conservation of resources, preservation of the environment, and retention of existing highway geometrics are some of the benefits obtained by reusing pavement material.

Pavement systems are designed to withstand, for a given lifespan, the stresses imposed by traffic and the damaging effects of environmental factors (Warner 2007). Pavement is a multi-layered structure, composed of a concrete or asphalt slab resting on a foundation system that may include base, subbase and subgrade (Poon and Chan 2005). Conventionally, natural material including crushed stone, gravel, and stabilized soil are used in road base and subbase.

Researchers have investigated the use of RCA in road base or subbase courses to provide a viable option for the reuse of this C&D waste (Poon and Chan 2005). RCA is used predominantly in pavement construction as replacement for natural aggregates and cement-treated subbase layers (Saeed et al. 2006). Molenaar and Niekerk (2007) investigated the engineering properties of RCA and suggested that good-quality road base or subbase can be built from these materials. The Federal Highway Administration (FHWA) (2008) reported that, when compared to natural aggregates, RCA has lower density, higher water absorption, higher soundness mass loss, and higher content of foreign material. In most cases, the properties of RCA are within the specifications for base course or concrete aggregate.

Park (2003) investigated the characteristics and performance of dry and wet RCA as road base and subbase for concrete pavement by comparing the engineering properties of RCA with those of crushed stone aggregate. The performance characteristics were evaluated based on compactibility, shear resistance, and stability of RCA; and the mechanical properties were evaluated in the field by using a falling weight deflectometer to determine deflection. RCA had the same compactibility as crushed stone aggregate and shear resistance equal to or better than

crushed stone aggregate. Park (2003) concluded that the RCA can be used as base and subbase materials in place of crushed stone aggregate for supporting a concrete pavement system.

The National Asphalt Pavement Association (NAPA) (2009) reported that asphalt pavement is the most recycled material in the US. The US highway construction industry annually produces more than 100 million tons of RAP that is recycled into new pavements (NAPA 2009). According to FHWA (2011), RAP is a valuable and high-quality material that may demonstrate good performance as a granular road base and a replacement for more expensive virgin aggregate.

Guthri et al. (2007) conducted free-free resonant column tests on RAP and natural aggregate blends to evaluate the effects of percentage change of RAP on the stiffness of road base. Blends were prepared according to the following RAP and natural aggregate percentages: 100/0, 75/25, 50/50, 25/75, and 0/100. Stiffness was determined after compaction at OMC, after a 72-h period of heating at 60°C to simulate summer conditions; and after a 10-day period of capillary soaking followed by a 24-h period of submersion to simulate conditions of field saturations. At OMC, the stiffness decreased with the addition of 25% RAP, then increased with the addition of 50%, 75%, and 100% RAP. When the material was heated for 72 h, the stiffness increased with the addition of 25% RAP and then decreased with the addition of 50%, 75% and 100% RAP. According to Guthri et al. (2007), the decrease in stiffness is related to the softening behavior of asphalt due to heat. In the soaked condition, the stiffness of the material behaved similar to the samples in the dry condition, but with stiffness values between 40% and 90% lower.

Bennert et al. (2000) compared the mechanical properties of two types of C&D waste, RCA and RAP, with dense-graded aggregate base course, used in roadway base applications in New Jersey. The RAP and RCA were mixed at varying percentages with the dense-graded aggregate base course. Bennert et al. (2000) found that the pure RAP and RCA samples had higher stiffness than the dense-graded aggregate base course, and the stiffness of the base course increased with an increase in RAP and RCA content. The pure RCA specimens accumulated the least amount of permanent strain. Even though pure RAP was found to be stiffer than the dense-graded aggregate base course, the RAP accumulated the greatest amount of permanent strain. Bennert et al. (2000) reported that the resulting contrast between the pure RAP resilient modulus and its permanent deformation might be due to the breakdown of asphalt binder under loading.

## 2.2. Definition of Resilient Modulus

The design of roadway pavement relies on proper characterization of the load-deformation response of the pavement layers (Tian et al. 1998). Base and subgrade deform when subjected to repeated loads from moving vehicular traffic. The  $M_r$  defines the nonlinear elastic response of pavement geomaterials, such as unbound aggregate base and subbase, under repeated traffic loading. The resilient behavior of unbound aggregate layers is affected by the stress state experienced because of wheel loading and the physical properties of aggregate (Pan et al. 2006). The  $M_r$  is a linear-elastic modulus obtained from dynamic loading, defined as the ratio of the cyclic deviator stress to the resilient (recoverable) strain, and is defined as:

$$M_r = (\sigma_d / \varepsilon_r) \quad (1)$$

where  $\varepsilon_r$  is the recoverable elastic strain and  $\sigma_d$  is the applied deviator stress.

Design of pavements and rehabilitation of layered pavement systems use  $M_r$  as an essential parameter in the design process (Heydinger et al. 2007). The  $M_r$  is a key input in NCHRP 1-37 (mechanistic-based pavement design approach), which is being evaluated for adoption by numerous state highway agencies (Pan et al. 2006). The performance of pavement is dependent on the stiffness of the pavement structure under specified traffic loads and environmental conditions. Generally, a high  $M_r$  for a base course infers a stiffer base course layer, which increases pavement life. The resilient response of granular material is important for the load-carrying ability of the pavement and the permanent strain response, which characterize the long-term performance of the pavement and rutting phenomenon (Lekarp et al. 2000).

## 2.3. Factors affecting the Resilient Modulus of Unbound Aggregate

The  $M_r$  of unbound granular material is dependent on loading stress states, material characteristics (e.g., material type, gradation, particle shape and angularity), dry density, moisture condition. For unbound pavement layer design, the resilient response of aggregate is affected by these influencing factors (Lekarp et al 2000). Although several different factors can influence the resilient behavior of a granular base course, stress state has the greatest overall

effect (Lekarp et al. 2000). The  $M_r$  of untreated granular material has shown primary dependency on confining pressure and sum of principal stresses. The  $M_r$  of RAP and RCA increases significantly with an increase in confining stress and decreases somewhat with an increase in deviator stress (Bennert et al. 2000; Bejarano et al., 2003; Molenaar and Niekerk 2007; Kim et al. 2007). Kim et al. (2007) found that increasing deviator stress decreased the  $M_r$  of RAP, but had less of an effect than the confining stress.

Compaction is the process of densifying soil by the application of mechanical energy due to which the strength characteristics of the soil improves. Through compaction, soil strength can be increased, bearing capacity of pavement layers can be improved, and undesirable volume changes (e.g., caused by frost action, swelling, and shrinkage) may be controlled (Holtz 1990). Most construction specifications for unbound aggregate layers reference the maximum dry unit weight (MDU) and optimum moisture content (OMC) as determined from Proctor (standard or modified) testing. Density is used in pavement construction as a quality control measure to help to determine the compaction level of the constructed layers (Mishra et al. 2010). Generally, increasing the density of granular material results in a stiffer layer while reducing the magnitude of the resilient modulus and the permanent deformation under static and dynamic loads (Seyhan 2001).

The degree of compaction (DOC) of a soil is measured in terms of the dry unit weight and is affected by compaction effort (energy per unit volume), soil type (i.e., grain-size distribution, shape of soil grains, specific gravity of soil solids), moisture content, and dry density of soil. According to Molenaar and Niekerk (2007), DOC is the most important factor affecting the mechanical characteristics of recycled, unbound material.

Molenaar and Niekerk (2007) reported that the mechanical characteristics of an unbound base course made with recycled concrete and masonry rubble were mainly governed by the degree of compaction. Gradation had the smallest influence on the  $M_r$  of the recycled material. Bejarano et al. (2003) also concluded that increasing density increased the stiffness of RAP and RCA.

Taha et al. (1999) conducted the modified Proctor compaction and the CBR tests on RAP and virgin aggregate blends with the following percentages: 100/0, 80/20, 60/40, 40/60, 30/80, and 0/100. They found that RAP might be suitable for replacement of virgin aggregate in the pavement subbase if RAP is mixed with virgin aggregate. RAP is highly permeable and the

moisture retention capacity of RAP is almost negligible due to asphalt coating and the low amount of fines (Nokkaew et al. 2011). Therefore, water may drain during compaction. All RAP/virgin aggregate mixtures, with the exception of the 100/0 and 80/20 blends, qualified for use in road base. As more RAP is added to a blend, the maximum dry unit weight tends to decrease. The maximum dry density (MDD) of pure RAP was about 83% of the maximum density of pure virgin aggregate, the addition of more virgin aggregate made compaction and handling easier, decreased the OMC, and increased the MDD. Poon and Chan (2005) also investigated the possibility of using RCA as unbound subbase, finding that the use of pure RCA increased OMC and decreased the MDD of the subbase compared to those of natural subbase.

The degree of saturation or water content affects the resilient response characteristics of most untreated granular materials (Lekarp et al. 2000). Water content is a primary factor affecting the stiffness characteristics of granular materials (Zaman and Zhu 1999). An increase in moisture content commonly leads to a decrease in  $M_r$  (Pan et al. 2006). The stiffness of typical granular specimens is nearly constant at lower saturation levels, but decreases significantly as degree of saturation rises (Hicks and Monismith 1971). Heydinger et al. (1996) studied the behavior of granular materials at high degrees of saturation and reported that  $M_r$  decreased with increasing saturation level. According to Lekarp et al. (2000) the excess pore water pressures developed during cyclical loading decreases the effective stress in the material at high degree of saturation. Consequently, the decrease in effective stress causes a subsequent decrease in both the strength and stiffness of the material. The effect of moisture content on the  $M_r$  of unbound granular materials also depends on the applied stress levels and material types (Pan et al. 2006). A study conducted by Kim et al. (2007) on RAP found that specimens tested at 65% OMC had higher  $M_r$  when compared to specimens prepared at 100% OMC at all confining pressures.

Mishra et al. (2010) evaluated aggregate properties (e.g., aggregate type, amount of fines, moisture content) that affect the strength and deformation behavior of crushed limestone and dolomite and uncrushed gravel used for road subgrade replacement and subbase. The aggregate type (i.e., crushed or uncrushed particle) that controls the angularity and the amount and plasticity of fines was the most important parameter in controlling the aggregate performance. Mishra et al. (2010) concluded that the performance of crushed aggregates used as unbound layers was better than uncrushed aggregates. Several studies about the effects of surface characteristics of unbound aggregates were also analyzed by Mishra et al. (2010). They reported

that angular materials resist permanent deformation better than rounded particles because of improved particle interlock and higher angle of shear resistance between particles. An increase in the proportion of crushed particles beyond 50% increased the friction angle significantly, indicating resistance to the accumulation of permanent deformation (Mishra et al. 2010).

Heydinger et al. (2007) explored the effects of aggregate type, gradation, and moisture condition on  $M_r$ . Three aggregate sources (crushed lime-stone, natural stone, and slag) at five gradations and three moisture conditions (dry, moist, and saturated) were used. The effect of material source was more significant on the  $M_r$  of aggregates than the effect of gradation and moisture condition. The natural stone consistently has the highest  $M_r$ , followed by limestone and then slag. Even though, there was no strong variation of the  $M_r$  of gravel aggregates (natural stone and crushed lime-stone) with respect to gradation, the  $M_r$  of open-graded limestone aggregate was higher than the dense-graded specification. The moduli obtained from moist samples were lower than those from the dry samples, particularly at the lower stress levels.

### **3. MATERIALS AND METHODS**

#### **3.1. MATERIALS**

The recycled materials used in this study were obtained from various states in the US and named according to state of origin. The reference base course was a gravel meeting the Class 5 specifications for base course in Minnesota per the Minnesota Department of Transportation (MnDOT). The blended material was a mix of approximately equal parts (by mass) RCA from MnDOT (50%) and Class 5 (50%). The Class 5 gravel was used as the control material in this study.

To evaluate the effects of compaction effort on stiffness of unbound recycled materials three RAPs (RAP (TX), RAP (CA), RAP (MN)), three RCA (RCA (TX), RCA (MI), RCA (CA)), one blend ( 50% RCA-50% Class 5 aggregate )material and Class 5 aggregate used. The materials represent coarser, medium, and finer gradations based on their grain size.

The particle size distribution (PSD) curves for the investigated materials were determined according to ASTM D 422. Samples were wet-sieved through a No. 200 (75- $\mu$ m opening) sieve to separate the fine particles attached to the coarser aggregates. The PSDs for the RCA and the RAP samples are shown in Fig. 1, along with the upper and lower bounds from the literature

(Bennert et al. 2000; Bejarano et al. 2003; Blankenagel and Guthrie 2006; Gutrie et al. 2007, Saeed 2008, Kuo et al. 2002 )

To evaluate the effects of compaction moisture effect on  $M_r$ , RAP (TX), RAP (OH), RCA (CO) and RCA (OH) were selected. These materials represent medium and finer gradations for RCAs and coarser and finer gradations for RAPs based on their grain size ( $D_{10}$ ,  $D_{30}$ ,  $D_{50}$  and  $D_{60}$ ). The PSDs for the RCA and the RAP samples are shown in Fig. 2, along with the upper and lower bounds from the literature (Bennert et al. 2000; Bejarano et al. 2003; Blankenagel and Guthrie 2006; Gutrie et al. 2007, Saeed 2008, Kuo et al. 2002 ).

A summary of the index properties and soil classifications is shown in Table 1. The materials used in this study are classified as non-plastic per ASTM D 2487, the Unified Soil Classification System (USCS). Specific gravity ( $G_s$ ) and absorption tests were conducted according to AASHTO T 85. Asphalt content was determined by ASTM 6307. The modified Proctor compaction test (ASTM D 1557) was performed to determine the optimum moisture content ( $w_{opt}$ ) and maximum dry unit weight ( $\gamma_{dmax}$ ).

## **2.4. METHODS**

### **2.4.1. Compaction**

The modified Proctor compaction test was performed on each material in accordance with ASTM D 1557, and the OMC and maximum dry unit weight were determined. Before running the compaction test, the samples were screened through a 25-mm sieve.

### **2.4.2. Resilient Modulus Test**

Resilient modulus tests were performed on compacted specimens according to NCHRP 1-28a Procedure Ia, which applies to base and subbase materials. The materials used in this study classify as Type I material in NCHRP 1-28A, which requires a 152-mm-diameter and 305-mm-high specimen for resilient modulus testing (NCHRP 2004). Specimens were prepared at OMC and compacted to 95% of maximum modified Proctor density. Specimens were compacted in six lifts of equal mass within 1% of the target dry unit weight and 0.5% of target moisture content to ensure uniform compaction (NCHRP 2004).

Resilient modulus tests were conducted with internal and external linear variable displacement transducers (LVDT). External LVDTs have an accuracy of  $\pm 0.005$  mm, and internal LVDTs have an accuracy of  $\pm 0.0015$  mm. Clamps for the internal LVDTs were built in



accordance with NCHRP 1-28A specifications. Internal LVDTs were placed at quarter points of the specimen to measure the deformations over the half-length of the specimen, whereas external LVDT measured deformations of the entire specimen length. An MTS Systems Model 244.12 servo-hydraulic machine was used for loading the specimens. Loading sequences, confining pressures and data acquisition were controlled from a computer running LabView 8.5 software.

The resilient modulus ( $M_r$ ) for each load sequence was obtained by averaging the  $M_r$  from the last 5 cycles of each test sequence. The  $M_r$  data were fitted with the power function model proposed by Moosazedh and Witczak (1981)

$$M_R = k_1 \times \theta^{k_2} \quad (2)$$

where  $\theta$  is bulk stress and  $k_1$  and  $k_2$  are empirical fitting parameters. The constants  $k_1$  and  $k_2$  are unique to a given material and are independent of one another. For a given material,  $k_2$  obtained from replicate tests were averaged and fixed for that material (Camargo 2008). Bulk stress is another means of quantifying confining pressure and deviator stress in a single term and is defined as the sum of the three principle stresses. Bulk stress is defined as

$$\theta = \sigma_1 + \sigma_2 + \sigma_3 \quad (3)$$

where  $\sigma_1$ ,  $\sigma_2$ , and  $\sigma_3$  are the principal stresses acting on the specimen.

For base course, the summary resilient modulus (SRM) corresponds to the  $M_r$  at a bulk stress of 208 kPa, as suggested by Section 10.3.3.9 of NCHRP 1-28a. SRM is a primary pavement design variable used directly in the empirical-mechanistic pavement design. It is also used to determine the layer coefficient, which is a required input in the older AASHTO pavement design (Tian et al. 1998).

#### **2.4.3. Compacted Moisture Effect on Stiffness of Recycled Materials**

Three moisture contents (OMC, 2% dry of OMC, 2% wet of OMC) were selected to evaluate the as-compacted moisture content on the stiffness of RCA and RAP. Resilient modulus tests were performed on compacted specimens according to NCHRP 1-28a Procedure Ia. Specimens were prepared at OMC, OMC +2% and OMC-2% and compacted to 95% of maximum modified Proctor density. Specimens were compacted in six lifts with equal mass per layer, and different moisture content levels were achieved by controlling the amount of compacted mass per layer for each test.

#### **2.4.4. Compaction Effort Effect on Stiffness of Recycled Materials**

Maximum dry unit weight was controlled at three different compaction levels, 95% of MDU (modified), 90% MDU (standard) and 85% MDU (reduced) for the same OMC. Resilient modulus tests were performed on compacted specimens according to NCHRP 1-28a Procedure Ia. Different compaction levels were achieved by controlling the amount of compacted mass and the sample height during the compaction process.

### **3. RESULTS**

#### **3.1. Effect of Compaction Effort on Stiffness of Unbound Base/Subbase Layers**

Camargo (2008) reported that deformations measured with internal LVDTs more accurately described deformation of the specimens for computation of resilient modulus. External LVDT measurements are affected by bedding errors, sample end effects, and machine compliance (Bejarano et al. 2002). Therefore, the resilient modulus presented herein is based on deformations measured with internal LVDTs. Variability in determining  $M_r$  was assessed by performing duplicate tests.

The increase in fines content as a result of compaction is evaluated by conducting dry PSD tests after compacting the specimens to modified Proctor compaction at OMC. The resulting gradations (pre-compaction and post-compaction) are compared (Appendix D). The increase in fines was more pronounced for RCA (ranging from 2.5 to 7.8%) than RAP (ranging from 1.9 to 4.9 %) and Class 5 aggregate (4.6 %), details are in Bozyurt 2011. Degradation during compaction for RCA may be related to breaking of cementitious materials from the particles. For RAP, it was not as pronounced but the aged asphalt coating may be more prone to break away from the particles.

The SRM along with the parameters  $k_1$  and  $k_2$  for the resilient modulus power function model summarized in Table 2 for Class 5 aggregate, Blend (MN), and representative recycled materials at three different compaction levels. (Eq. 2), are. These SRM and parameters correspond to modified, standard, and reduced Proctor efforts (95%, 90%, and 80% of MDU) at OMC.

The rate of decrease of SRM for Class 5 aggregate for standard and reduced compaction levels was 28% and 47%, respectively. RAP (TX) exhibited the smallest rate of decrease (22%)

of SRM after reduced compaction effort compared with RAP (CA) (32%) and RAP (MN) (40%). The different rates of decrease for RAP from different sources could be related to the gradation of the RAPs before compaction. RAP (TX) has coarser, RAP (CA) medium, and RAP (MN) finer gradations. As seen from Fig. 3, the highest decreased of SRM observed for the finer gradation.

For the RCA samples, the highest rate of decrease in SRM are observed in RCA (CA) (48%), followed by RCA (TX) (42%) and RCA (MI) (36%) after reduced compaction effort. The effects of different compaction levels on SRM of materials varied amongst recycled materials could be attributed to their differences in mechanical properties and the sources of the materials.

Leite et al. (2011) investigated the compactive effort influence on the physical characteristics of the recycled construction and demolition waste (RCDW) aggregates used in pavement applications. The effect of compaction effort on the RCDW aggregate properties was evaluated by using intermediate (50% of the modified effort) and modified Proctor energies. CBR for the modified effort was 60% higher compared to the intermediate effort and the resilient modulus as well increased with the increment of the Proctor energy. Leite et al. (2011) concluded that the use of high compaction effort could reduce the resilient displacement of the RCDW aggregate from 10% to 20 % by increasing the stiffness of the base layer.

Bejarano et al. (2003) evaluated the stiffness of RAP compared to typical base course aggregate using the resilient modulus tests by compacting samples to optimum moisture content (OMC) at 95% and 100% maximum density. Bejarano et al. (2003) found that when the compaction density increased from 95% to 100% of maximum density, the stiffness of RAP and typical base course increased.

Since the density of the materials decreased through the change of compaction effort, the decrease in stiffness is expected (Bejarano et al. 2003). Trend of decreasing SRM observed for all materials as seen from Fig. 4. Even though the rate of decrease is higher for RCA and RAP, the SRM of RCA and RAP remained higher as revealed in Fig. 5. The lower compaction effort has significant influence on the stiffness of any kind of materials. However the decrease in the amount of stiffness varied upon material sources and gradations.

### 3.2. Effect of Compaction Moisture Content on Stiffness of Unbound Base/Subbase Layers

Recent studies show that the  $M_r$  of unbound conventional road base layers is dependent on the moisture content (Hicks and Monismith 1971; Heydinger et al. 1996; Zaman and Zhu 1999; Lekarp et al. 2000). The SRM of the RCA (CO), RCA (OH), and RAP (OH), and RAP (TX) are summarized in Table 3, along with the parameters  $k_1$  and  $k_2$  from varying compaction moisture contents. These SRM and parameters correspond to OMC-2%, OMC, OMC+2% at 95 % of MDU.

Fig. 6 represents the effect of compaction moisture content on the stiffness of recycled materials. Even though specimens are prepared at the same MDU, the SRM is higher at dry of OMC and lower at wet of OMC. A decrease in moisture content leads to increase the SRM values of RAP and RCA compacted at the same MDU. This increase in the stiffness could be attributed to the increase in matric suction with decreasing moisture content. (Tian et al. 1998)

The moisture contents of recycled materials before and after resilient modulus test at OMC-2% and wet of OMC+2% are presented in Table 4. As shown in Table 4, the water drained from the RAP samples during compaction and  $M_r$  testing, especially for the samples compacted at wet of OMC. Even though the materials were kept in sealed plastic bags after adding water for 24 h before testing, the excess water (OMC+2%) was not absorbed by the fines in RAP and drained freely. The rate of decrease observed in SRM for RAP (OH) (4%) and RAP (TX) (11%) is less than RCA (CO) (21%) and RCA (OH) (38%) as seen from Fig. 7. The rate of decrease in SRM for RAP is lower than RCA, since the moisture holding capabilities of RAP fractions were reduced due to asphalt coating (Attia and Abdelrahman 2010). For RAP materials, the percent material passing No.200 sieve was less than 3%. The lack of fines in RAP could be another reason that explains why the materials did not hold the extra moisture (Alam et al. 2010).

Researches have shown that  $M_r$  typically decreases with an increase in moisture content (Pan et al. 2006). The stiffness of typical granular specimens is nearly constant at lower saturation levels, but decreases significantly as degree of saturation rises (Hicks and Monismith 1971). This decrease could be attributed to the decrease in matric suction, and increase in the lubricating effect of water with increasing moisture content. A study conducted by Kim et al. (2007) on RAP found that specimens tested at 65% OMC had higher  $M_r$  when compared to samples prepared at 100% OMC at all confining pressures. .

Attia and Abdelrahman (2010) investigated the effect of moisture content on  $M_r$  of base layer containing RAP (from rehabilitation projects in MN) and Class 5 aggregate (conventional base aggregate) at varying MC between OMC-3% and OMC+2%. The  $M_r$  test was conducted in accordance with NCHRP 1-28A test protocol, by compacting the samples with gyratory compactor. The  $M_r$  of Class 5 aggregate exhibited an increase by 150-300% at low and high confining pressures comparing for samples compacted at OMC-3% versus compacted at OMC+2%. RAP showed an increase in the  $M_r$  by 250-320% comparing samples compacted at OMC-3% versus compacted at OMC+2%.

In this study, the rate of increase in SRM for RAP (OH) and RAP (TX) was 113% and 121%, respectively; comparing samples compacted at OMC+2% and OMC-2%. The results are differed from Attia and Abdrahman (2010) due to the difference in the compaction process of materials during  $M_r$  test and the percent change in OMC.

#### **4. CONCLUSION**

This laboratory investigation dealt with the characterization of the engineering properties of the recycled materials (recycled asphalt pavement (RAP) and recycled concrete aggregate (RCA), as well as one field blended materials consisting of 50% RCA and 50% conventional base material used as unbound base/subbase layer without treatment. These recycled materials were collected from a wide geographical area, covering six states in the U.S: California, Colorado, Michigan, Minnesota, Ohio, Texas. A conventional base material meeting the gradation standard of Minnesota Department of Transportation Class 5 aggregate used as a reference material. The investigation also dealt with the determination of the influence of compaction effort and compaction moisture content, and freeze-thaw cycling on the engineering properties of unbound recycled materials, and the behavior of RAP or RCA blended to Class 5 aggregate used as unbound base/subbase layer.

The objectives of this investigation were to evaluate the impacts of compactive effort on the stiffness of the unbound base layer constructed from RCA and RAP were investigated to determine how the compaction level is influential on properties and varies by composition of materials. The compaction moisture effect on the stiffness of RCA and RAP were also assessed. RAP and RCA may contain impurities that affect their mechanical properties and long-term

performance, the impurity type and content affecting the stiffness of RAP and RCA were investigated. The objectives were met by determining the resilient modulus of the recycled materials in accordance with NCHRP 1-28a protocol measuring deflections both externally and internally on the specimens.

Compaction effort has an impact on resilient modulus of recycled materials greater than observed for natural aggregate. Compaction moisture effect has an impact on resilient modulus greater for RCA than RAP. The  $M_r$  decreases with an increase in moisture content for RAP and RCA. The rate of decrease in SRM for RAP is lower than RCA, since the moisture holding capabilities of RAP fractions were reduced due to asphalt coating. This decrease could be attributed to the decrease in matric suction, and increase in the lubricating effect of water with increasing moisture content.

## REFERENCES

- Bejarano, M. O., Harvey, J. T. and Lane, L. (2003). "In-Situ Recycling of Asphalt Concrete as Base Material in California." *Proc. 82nd Annual Meeting*, Transportation Research Board, Washington, D.C., 22.
- Bennert, T., Papp Jr. W., Maher, A. and Gucunski, N. (2000). "Utilization of Construction and Demolition Debris Under Traffic-Type Loading in Base and Subbase Applications." *Transportation Research Record*, No. 1714, Washington, D.C., 33-39.
- Blankenagel, B. J. and Guthrie, W. S. (2006). "Laboratory Characterization of Recycled Concrete for Use as Pavement Base Material." *Geomaterials 2006*, No.1952, 21-27.
- Camargo, F. F. (2008). "Strength and Stiffness of Recycled Base Materials Blended with Fly Ash." MS Thesis, University of Wisconsin-Madison, WI
- Camargo, F. F., Edil, T. B. and Benson, C. H. (2009). "Strength and Stiffness of Recycled Base Materials Blended with Fly Ash." *Transportation Research Board 88th Annual Meeting*. Washington, D.C.
- FHWA. (2008). "User Guideline for Byproducts and Secondary Use Materials in Pavement Construction". *FHWA Report FHWA-RD-97-148*, FHWA, VA.
- FHWA. (2011). "Reclaimed Asphalt Pavement in Asphalt Mixtures: State of the Practice." FHWA-HRT-11-021.,FHWA, McLean:

- Guthri, S. W., Cooley, D., and Eggett, D. L. (2007). "Effects of Reclaimed Asphalt Pavement on Mechanical Properties of Base Materials." *Journal of the Transportation Research Board*, No.2005, Washington, D.C., 44-52.
- Heydinger, A. G., Xie, Q. L., Randolph, B. W. and Gupta, J. D. (1996). "Analysis of Resilient Modulus of dense and Open-graded Aggregates." *Transportation Research Board*, Washington, D.C., No.1547, 1-6.
- Hicks, R. G. and Monismith, C. L. (1971). "Factors Influencing the Resilient Properties of Granular Materials." *Highway Research Record*, No.345, 15-31.
- Holtz, R. (1990). "Compaction Concepts. Chapter3. In *Guide to Earthwork Compaction. In State of the Art Report 8* (pp. 9-23). Washington, D.C.: TRB, National Research Council.
- Kim, W., Labuz, J. F. and Dai, S. (2007). "Resilient Modulus of Base Course Containing Recycled Asphalt Pavement." *Journal of the Transportation Research Board* , No.2005, Washington, D.C., 27-35.
- Kuo, S.-S., Mahgoub, H. S., & Nazef, A. (2002). "Investigation of recycled concrete made with limestone aggregate for a base course in flexible pavement." *Transportation Research Record*, No.1787, Washington, D.C., 99-108.
- Langer, W. H. (1988). "Natural aggregates of the conterminous, United States." *Geological Survey Bulletin*, No.1594, 33.
- Lee, J., Edil, T. B., Benson, C. H. and Tinjum, J. M. (2010). "Use of BE<sup>2</sup>ST in Highways for Green Highway Construction Rating in Wisconsin." *Proceeding of The 1<sup>st</sup> T&DI Green Streets and Highway Conference*, Denver, CO.
- Leite, F. d., Motta, R. d., Vasconcelos, K. L. and Bernucci, L. (2011). "Laboratory Evaluation of Recycled Construction and Demolition Waste for Pavements." *Construction and Building Materials*, 2972-2979.
- Lekarp, F., Isacsson, U. and Dawson, A. (2000). "State of the Art.II: Permanent Strain Response of Unbound Aggregates." *Journal of Transportation Engineering* , No.126, Washington, D.C., 76-83.
- Mishra, D., Tutumluer, E. and Butt, A. A. (2010). "Quantifying Effects of Particle Shape and Type and Amount of Fines on Unbound Aggregate Performance Through Controlled Gradation." *Transportation Research Record: Journal of the Transportation Research Board*, No.2167, Washington, D.C., 61-71.
- Molenaar, A. A. and Niekerk, A. A. (2007). "Effects of Gradation, Composition, and Degree of Compaction on the Mechanical Characteristics of Recycled Unbound Materials."

*Transportation Research Record: Journal of the Transportation Research Board*, No.187, Washington, D.C., 73-82.

Moosazedh, J. and Witczak, M. (1981). "Prediction of Subgrade Moduli for Soil that Exhibits Nonlinear Behavior." *Journal of Transportation Research Board*, No.810, Washington, D.C., 10-17.

NAPA. (2009). "*How to Increase RAP Usage and Ensure Pavement Performance.*" NAPA.

Nataatmadja, A. and Tan, Y. L. (2001). "Resilient Reponse of Recycled Concrete Road Aggregates." *Journal of Transportation Engineering*, No.127, Washington, D.C., 450-453.

NCHRP. (2004). "Laboratory Determination of Resilient Modulus for Flexible Pavement Design." NCHRP Research Results Digest.

Nokkaew, K., Tinjum, J. M., Benson, C. H. and Edil, T. (2011). "Hydraulic Properties of Recycled Asphalt Pavement and Recycled Concrete Aggregate", GeoCongress, FL.

Pan, T., Tutumluer, E. and Anochie-Boateng, J. (2006). "Aggregate Morphology Affecting Resilient Behavior of Unbound Granular Materials." *Transportation Research Record: Journal of the Transportation Research Board*, No.1952, Washington, D.C., 12-20.

Park, T. (2003). "Application of Construction and Building Debris as Base and Subbase Materials in Rigid Pavement." *Journal of Transportation Engineering*, No.129, Washington, D.C., 558-563.

Poon, C.-S., Qiao, X., and Chan, D. (2006). "The Cause and Influence of Self-Cementing Properties of Fine Recycled Concrete Aggregates on the Properties of Unbound Sub-Base" *Waste Management*, No.26, 1166-1172.

Rosa, M. (2006). "*Effect of Freeze and Thaw Cycling on Soils Stabilized using Fly Ash.*" MS Thesis, University of Wisconsin-Madison, WI.

Saeed, A. (2008). "Performance-Related Tests of Recycled Aggregates for Use in Unbound Pavement Layers." Transportation Research Board of the National Academies. Washington, D.C.

Saeed, A., Hammons, M. I., Feldman, D. R. and Poole, T. (2006). "Evaluation, Design and Construction Techniques for Airfield Concrete Pavement Used as Recycled Material for Base". Innovative Pavement Research Dpindation Airport Concrete Pavement Technology Program, Skokie, IL:.

Schaertl, G. J. (2010). "*Scaling and Equivalency of Bench-scale Tests to Field Scale Conditions.*" MS Thesis, University of Wisconsin-Madison, WI



- Seyhan, U. (2001). "Characterization of Anisotropic Granular Layer Behavior in Flexible Pavements." Doctoral Thesis, University of Illinois, Urbana, IL.
- Taha, R., Ali, G., Basma, A. and Al-turk, O. (1999). "Evaluation of Reclaimed Asphalt Pavement Aggregate in Road Bases and Subbase." *Transportation Research Record: Journal of the Transportation Research Board*, No.1652, Washington, D.C., 264-269.
- Tian, P., Zaman, M. M. and Laguros, J. G. (1998). "Gradation and Moisture Effects on Resilient Moduli of Aggregate Bases." *Transportation Research Record*, No.1619, Washington, D.C., 75-84.
- Warner, J. D. (2007). "The Beneficial Reuse of Asphalt Shingles in Roadway Construction." MS Thesis, University of Wisconsin-Madison, WI
- Weyers, R. E., Gregory, S. W., David, W. M., S, L. D. and Cady, P. D. (2005). "Testing Methods to Determine Long Term Durability of Wisconsin Aggregate Resources." Virginia Polytechnic Institute.
- Zaman, M. M., & Zhu, J.-H. L. (1999). "Durability Effects on Resilient Moduli of Stabilized Aggregate Base." *Transportation Research Record*, No.1687, Washington, D.C., 29-39.

## **TABLES**

Table 1. Index properties for Recycled Materials , Blend and Class 5 aggregate

Material	States	D <sub>10</sub> (mm)	D <sub>30</sub> (mm)	D <sub>50</sub> (mm)	D <sub>60</sub> (mm)	C <sub>u</sub>	C <sub>c</sub>	G <sub>s</sub>	Absorption (%)	Asphalt Content /Mortar Content (%)	Impurities (%)	Gravel (%)	Sand (%)	Fines (%)	USCS	AASHTO
Class 5 Aggregate	MN	0.1	0.4	1.0	1.7	21	1.4	2.57	–	–	0.25	22.9	67.6	9.5	GW-GM	A-1-b
Blend	MN	0.2	0.6	1.5	2.8	13	0.5	–	–	–	0.36	32.7	63.8	3.4	SP	A-1-b
RCA	MI	0.4	4.1	9.7	12.3	35	3.9	2.37	5.4	–	0.35	68.5	28.3	3.2	GP	A-1-a
	CO	0.1	0.6	2.8	4.9	66	1.1	2.28	5.8	47	0.26	40.9	46.3	12.8	SC	A-1-b
	CA	0.3	1.7	4.8	6.8	22	1.4	2.32	5.0	37	0.26	50.6	47.1	2.3	GW	A-1-a
	TX	0.4	6.5	13.3	16.3	38	6.0	2.27	5.5	45	0.86	76.3	21.6	2.1	GW	A-1-a
	OH	0.2	1.2	3.4	5.3	34	1.7	2.24	6.5	65	0.16	43.2	49.5	7.3	SW-SM	A-1-a
RAP	MN	0.3	0.7	1.6	2.3	7	0.7	2.41	1.8	7.1	0.06	26.3	71.2	2.5	SP	A-1-a
	CA	0.3	1.3	3.0	4.2	13	1.2	2.56	2.0	5.7	0.33	36.8	61.4	1.8	SW	A-1-a
	TX	0.7	2.5	5.4	7.9	11	1.1	2.34	1.3	4.7	0.05	41.0	44.9	1.0	SW	A-1-a
	OH	0.5	1.6	2.9	3.8	7	1.3	2.43	0.6	6.2	0.06	32.1	66.2	1.7	SW	A-1-a

Note: Asphalt Content found for RAP/RPM and Mortar Content found for available RCA

D<sub>10</sub> = effective size, D<sub>30</sub> = particle size for 30% finer, D<sub>50</sub> = median particle size, D<sub>60</sub> = particle size for 60% finer, C<sub>u</sub> = coefficient of uniformity, C<sub>c</sub> = coefficient of curvature, G<sub>s</sub> = Specific Gravity, AC= Asphalt Content, Abs=Absorption, Note: Particle size analysis conducted following ASTM D 422, G<sub>s</sub> determined by ASTM D 854, Absorption of coarse aggregate were determined by ASTM C127-07, USCS classification determined by ASTM D 2487, AASHTO classification determined by ASTM D 3282, asphalt content determined by ASTM D 6307

Table 2. Summary resilient modulus (SRM) and power model fitting parameters  $k_1$  and  $k_2$  (Eq. 4.1) for base materials for different compaction efforts (Modified (95%), Standard (90%) and Reduced (85%))

Material	States	Compaction Effort (%)	External			Internal			SRMSRM <sub>CE*%/</sub> SRMSRM <sub>95%</sub>
			$k_1$	$k_2$	SRM (MPa)	$k_1$	$k_2$	SRM (MPa)	
Class 5 Aggregate	MN	95%	66.2	0.198	191	129.2	0.146	281	1.0
		90%	29.0	0.310	152	34.7	0.328	200	0.7
		80%	10.7	0.446	116	8.6	0.536	150	0.5
Blend	MN	95%	90.71	0.174	229	116.8	0.206	350	1.0
		90%	47.30	0.281	212	95.9	0.221	311	0.9
		80%	39.4	0.285	181	61.6	0.284	280	0.8
RCA	CA	95%	119.4	0.148	262	273.6	0.131	550	1.0
		90%	61.9	0.227	208	199.4	0.151	447	0.8
		80%	33.8	0.320	187	55.8	0.305	285	0.5
	MI	95%	49.6	0.278	219	107.2	0.134	400	1.0
		90%	43.7	0.272	188	88.2	0.203	352	0.9
		80%	34.0	0.314	182	50.4	0.306	258	0.6
	TX	95%	74.6	0.233	258	236.1	0.126	464	1.0
		90%	67.2	0.223	220	62.9	0.319	345	0.7
		80%	47.1	0.275	205	46.7	0.329	271	0.6
RAP	CA	95%	122.5	0.138	256	348.8	0.057	473	1.0
		90%	94.8	0.157	219	177.8	0.152	400	0.8
		80%	35.0	0.330	203	112.9	0.197	322	0.7
	MN	95%	93.9	0.174	238	236.1	0.127	464	1.0
		90%	87.8	0.168	215	113.1	0.220	366	0.8
		80%	42.2	0.289	197	53.1	0.312	280	0.6
	TX	95%	156.6	0.142	334	358.7	0.122	686	1.0
		90%	101.8	0.194	287	261.8	0.153	592	0.9
		80%	75.5	0.245	280	226.0	0.163	540	0.8

Table 3. Summary resilient modulus (SRM) and power model fitting parameters  $k_1$  and  $k_2$  (Eq. 4.1) for recycled materials for different optimum moisture contents (OMC), (+2% OMC, OMC, -2% OMC)

Specimens	Water Content	External			Internal			SRM <sub>wc</sub> /SMR <sub>OMC</sub>
		$k_1$	$k_2$	SRM (MPa)	$k_1$	$k_2$	SRM (MPa)	
RCA (CO)	2% Dry	150.33	0.11	268	100.47	0.28	440	1.3
	OMC	98.01	0.17	247	118.30	0.20	350	1.0
	2% Wet	58.66	0.22	193	38.37	0.37	275	0.8
RCA (OH)	2% Dry	94.09	0.17	239	127.50	0.22	404	1.3
	OMC	48.94	0.28	222	49.20	0.34	310	1.0
	2% Wet	11.93	0.47	148	10.66	0.54	193	0.6
RAP (OH)	2% Dry	133.97	0.15	297	191.41	0.17	485	1.1
	OMC	83.43	0.23	287	158.62	0.19	429	1.0
	2% Wet	75.32	0.22	243	131.79	0.21	411	1.0
RAP (TX)	2% Dry	168.66	0.13	341	307.49	0.17	758	1.2
	OMC	156.58	0.14	334	269.07	0.16	625	1.0
	2% Wet	113.60	0.19	317	202.55	0.19	557	0.9

Table 4. The change in water content before and after resilient modulus test for recycled materials

Specimens	Water Content	Before Test (%)	After Test (%)	Difference (%)
RCA (CO)	2% Wet	13.0	12.9	0.2
	OMC	10.9	10.9	0.1
	2% Dry	9.0	8.2	0.8
RCA (OH)	2% Wet	13.4	12.3	1.1
	OMC	11.8	11.5	0.3
	2% Dry	9.5	9.4	0.0
RAP (OH)	2% Wet	11.1	9.0	2.2
	OMC	8.9	8.8	0.0
	2% Dry	7.1	7.0	0.1
RAP (TX)	2% Wet	10.8	6.8	4.0
	OMC	8.3	6.1	2.2
	2% Dry	6.3	6.0	0.4

## **FIGURES**

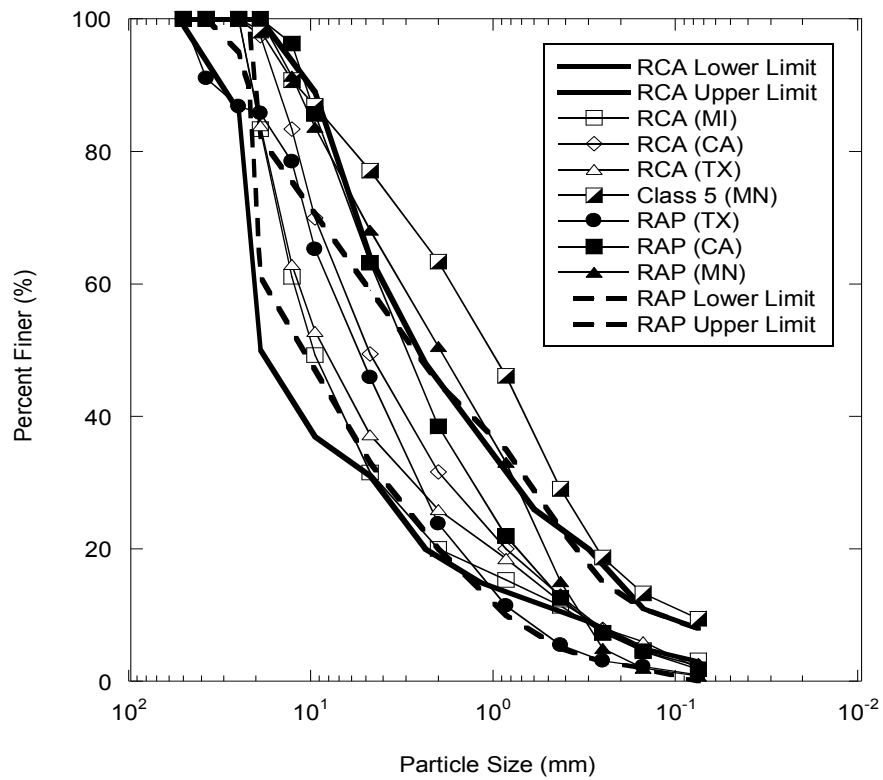


Fig. 1. Particle size distribution for RCA, RAP, and Class 5 aggregate and lower and upper limits of RAP/RCA from the literature.



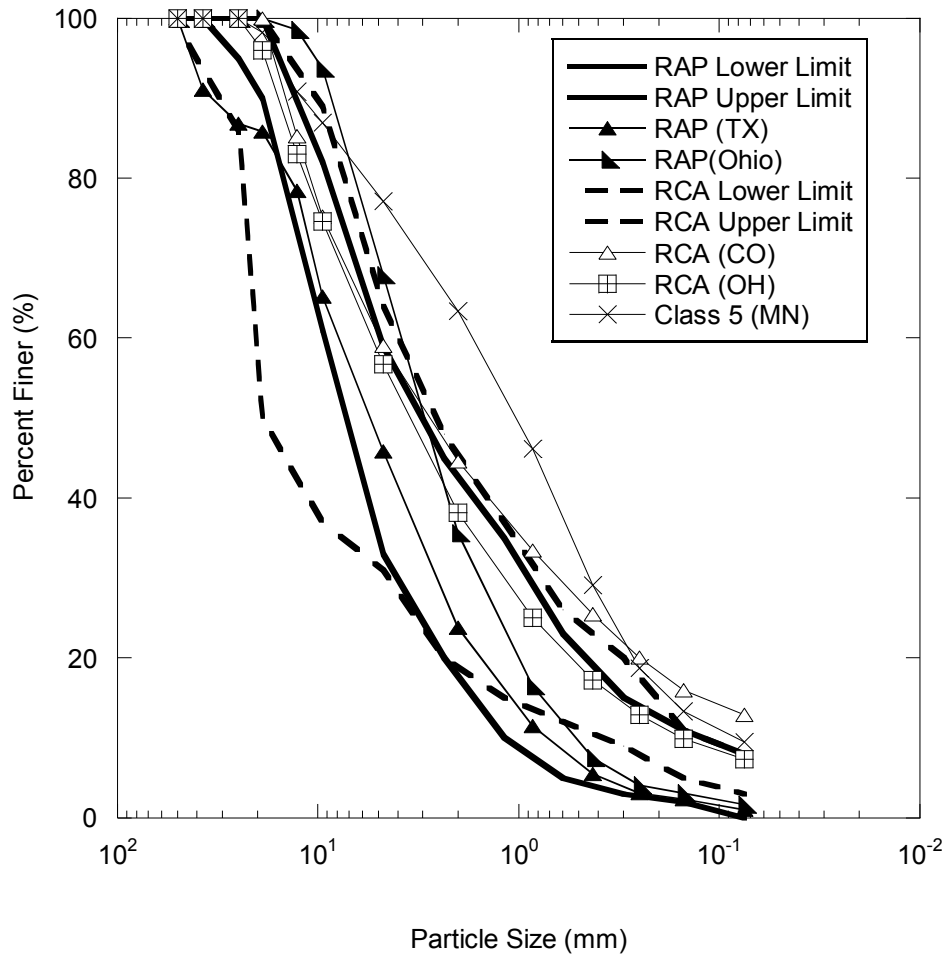


Fig. 2. Particle size distributions for RCA (CO), RCA (OH) and RAP (TX), RAP (OH) and Class 5, and RAPs and RCAs reported lower and upper limits from literature

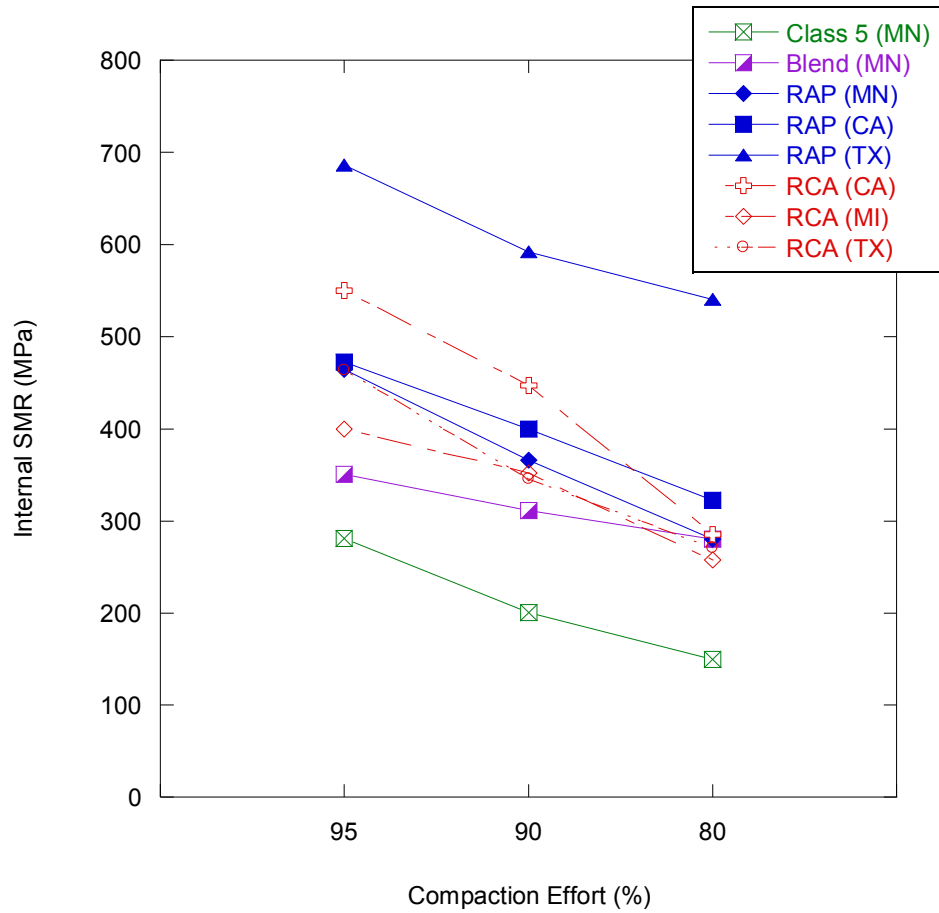


Fig. 3. Internal summary resilient modulus (SRM) for different compaction efforts for RAP, RCA, Blend and Class 5 aggregate

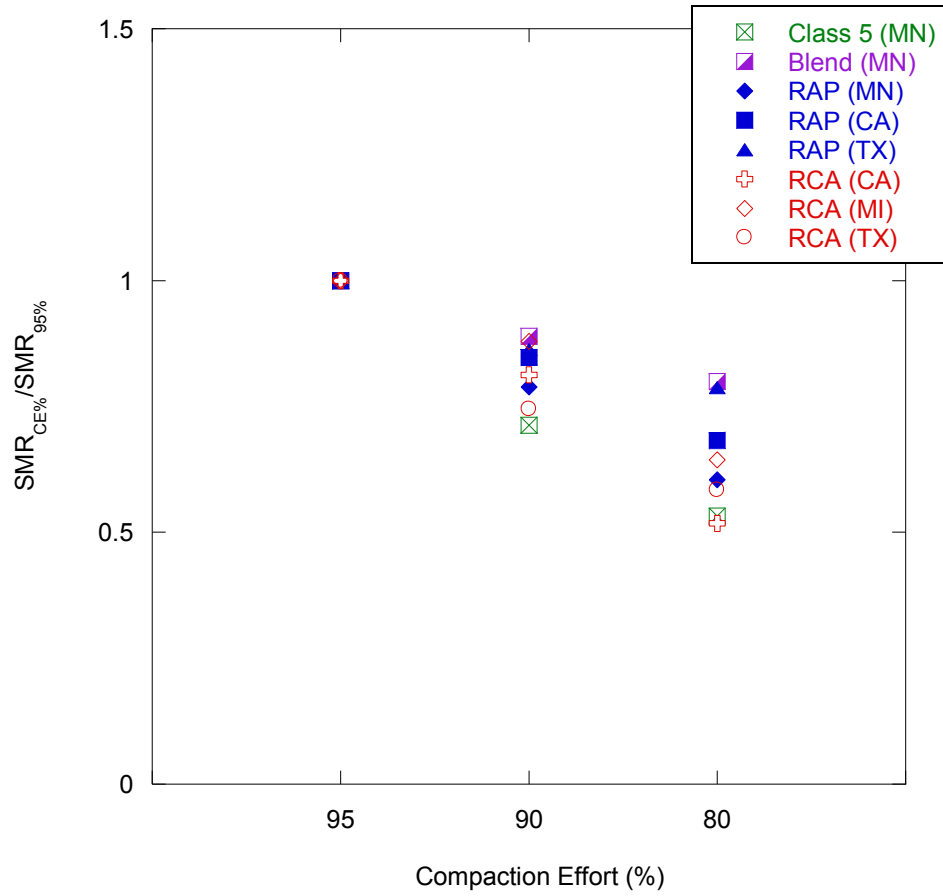


Fig. 4. Normalized value of summary resilient modulus (SRM) for different compaction efforts for RAP, RCA, Blend and Class 5 aggregate

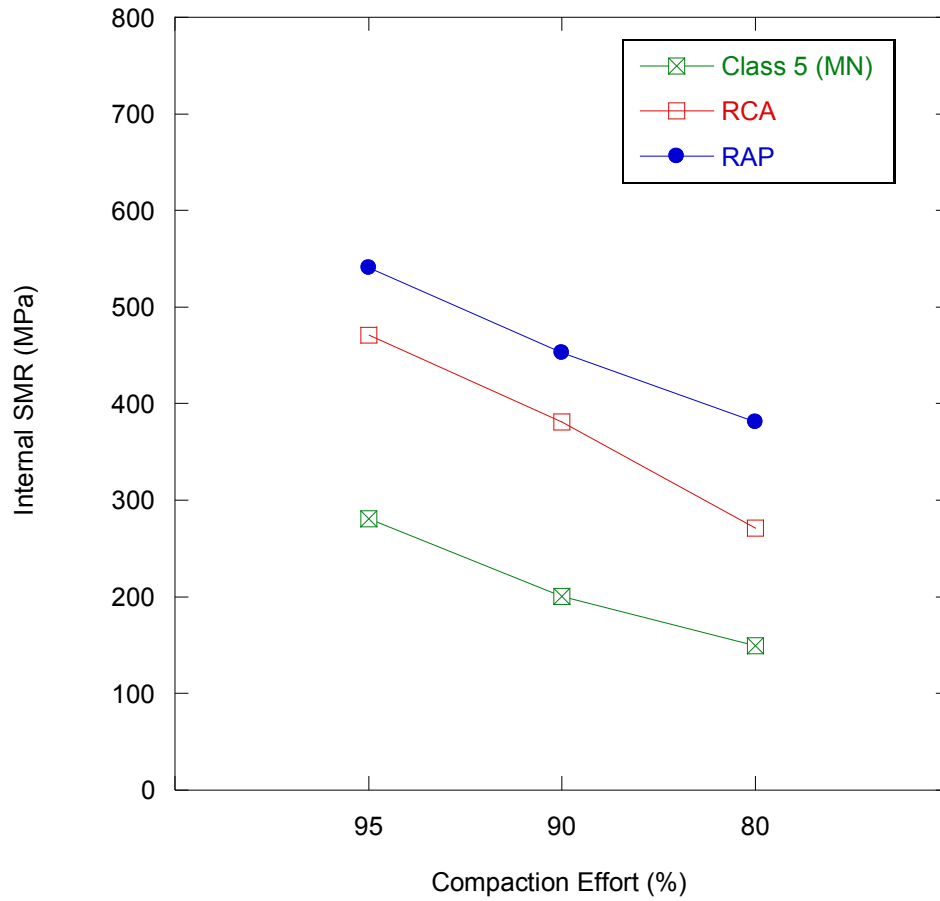


Fig. 5. Average Internal summary resilient modulus (SRM) for RCA, RAP and Class 5 aggregate at different compaction effort

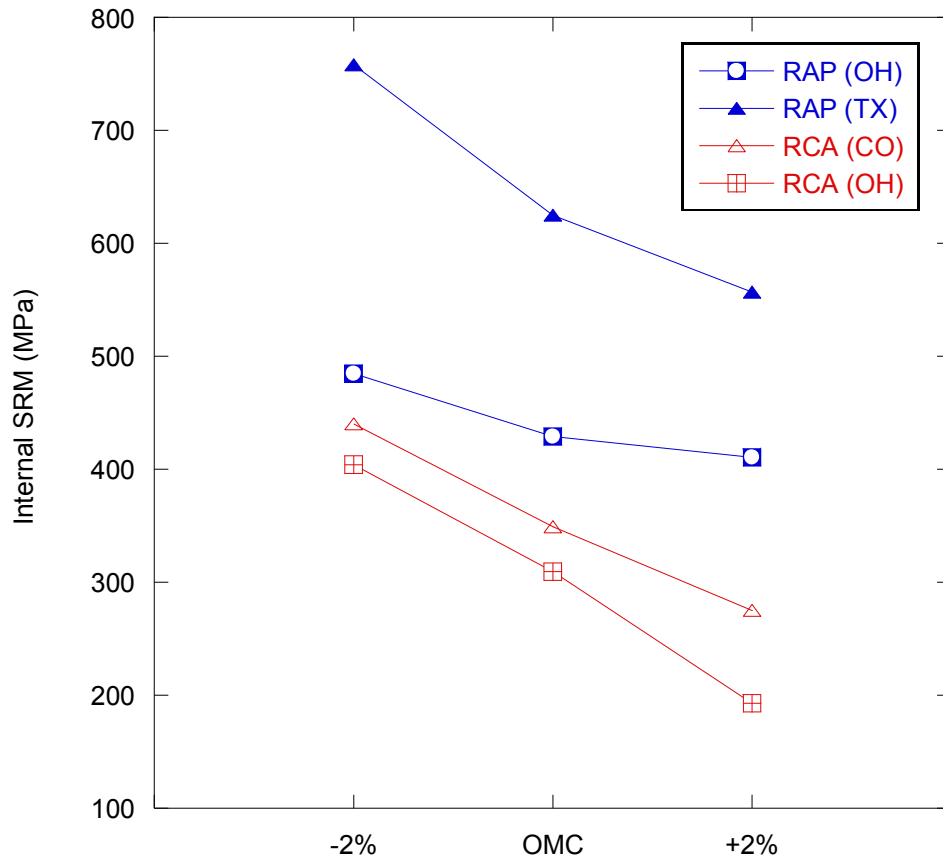


Fig. 6. Internal Summary Resilient Modulus (SRM) for RAP and RCA at 2% dry of optimum moisture content (OMC), OMC and 2% wet of OMC.

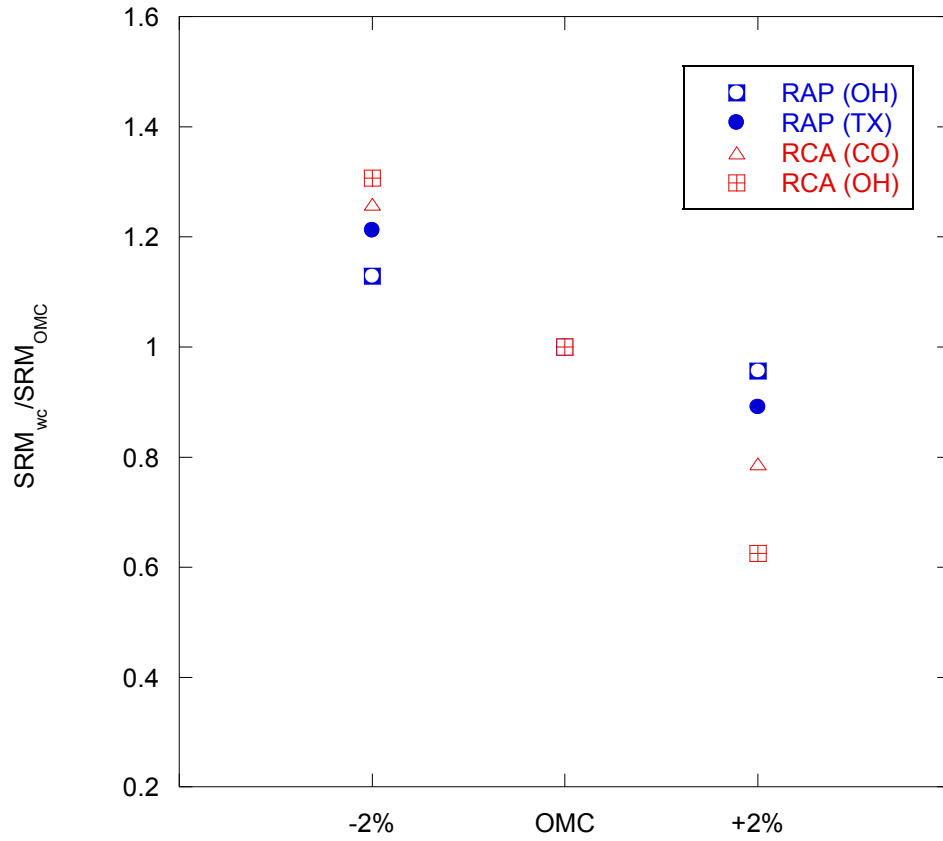


Fig. 7. Normalized Summary Resilient Modulus for RAP and RCA at 2% dry of optimum moisture content (OMC), OMC and 2% wet of OMC.

**FIELD PERFORMANCE**  
**Falling Weight Deflectometer Data**  
**Analysis**

**Recycled Asphalt Pavement and**  
**Recycled Concrete Aggregate**

**TPF-5 (129) Recycled Unbound Materials**

Mn/DOT Contract No. 89264 Work Order No. 2

CFMS Contract No. B14513

Task IIBa: Field Performance and Maintenance: FWD Survey

**Gregory J. Schaertl, Tuncer B. Edil, and Craig H. Benson**

**University of Wisconsin- Madison**

**August 21, 2010**

## INTRODUCTION

The objectives of this study were (1) to determine the maximum deflection of each pavement section under simulated loading by the FWD and (2) to determine the resilient modulus of the pavement layers, focusing on the performance of base course layers composed of recycled asphalt pavement (RAP), recycled concrete aggregate (RCA) and a 50-50 blend of RCA with conventional base course aggregate (Class 5). RAP refers the removal and reuse of the hot mix asphalt (HMA) layer of an existing roadway, and RCA refers to the reuse of materials reclaimed from roadways as well as from other structures such as old buildings and airport runways. A conventional base course meeting the gradation standard of a Minnesota Department of Transportation Class 5 aggregate was used as a reference material in this study.

## MATERIALS AND METHODS

Index properties and compaction data for RAP, RCA, blended RCA/Class 5, and Class 5 are presented in Table 1, with particle size distribution graphs presented in Fig. 1. Each of the four materials is classified as non-plastic, poorly graded gravel, with the RAP specimen having an asphalt content of 4.8%.

Table 1. Index properties for RAP, RCA, Blended RCA/Class 5, and Class 5.

Sample	$W_{opt}$ (%)	$\gamma_{d max}$ (kN/m <sup>3</sup> )	LL (%)	PL (%)	Gravel Content (%)	Sand Content (%)	Fine Content (%)	USCS Symbol
RAP	6.7	20.8	NP	NP	31.8	67.4	0.8	SP
RCA	11.2	19.5	NP	NP	31.8	64.9	3.3	SP
Blend	8.9	20.1	NP	NP	32.7	63.9	3.4	SP
Class 5	8.0	20.7	NP	NP	28.1	64.2	7.7	SP



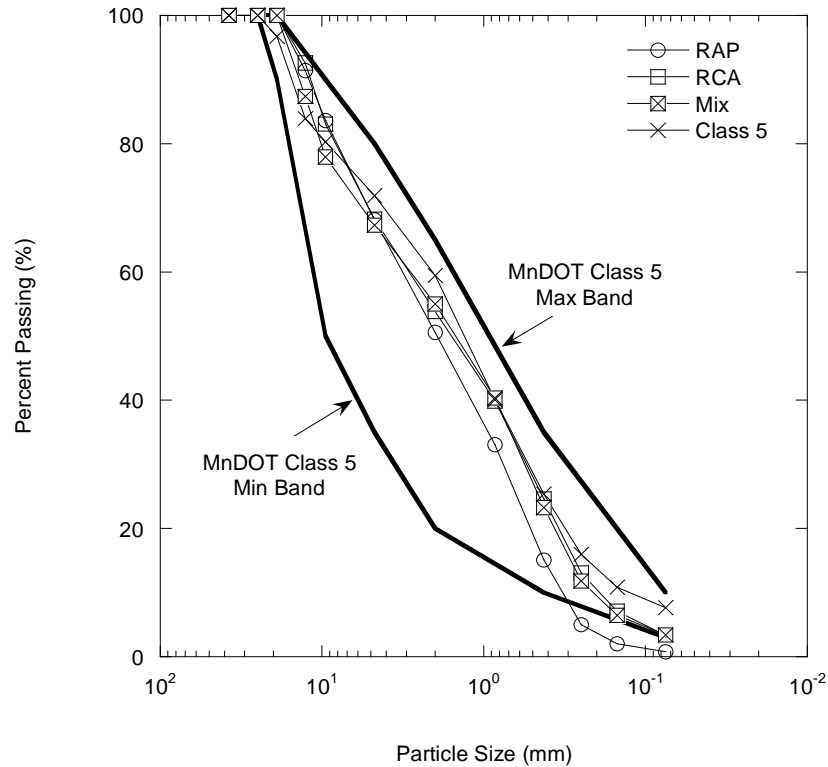


Fig.1. Particle size distributions for RAP, RCA, Blended RCA/Class 5 and Class 5 with MnDOT specifications.

Field-scale in-situ moduli of the materials were obtained from Falling Weight Deflectometer (FWD) tests performed at the MnROAD testing facility near Albertville, Minnesota. Traffic is diverted from westbound I-94 and onto the MnROAD mainline, which is 3.5 miles long by 2 lanes wide. Four test cells were constructed for each of the four base materials tested; the pavement profiles are shown in Fig.2. FWD analysis is performed on different dates throughout the year, and the modulus of each base course can be determined over time.

<b>Cell 16: Recycled Concrete Aggregate (RCA)</b>	<b>Cell 17: Blended 50% / 50% RCA/Class 5 (Blend)</b>	<b>Cell 18: Recycled Asphalt Pavement (RAP)</b>	<b>Cell 19: Mn/DOT Class 5 Aggregate (Class 5)</b>
<b>127 mm Asphalt Concrete</b>	<b>127 mm Asphalt Concrete</b>	<b>127 mm Asphalt Concrete</b>	<b>127 mm Asphalt Concrete</b>
<b>305 mm RCA</b>	<b>305 mm Blend</b>	<b>305 mm RAP</b>	<b>305 mm Class 5</b>
<b>305 mm Class 3 Aggregate</b>	<b>305 mm Class 3 Aggregate</b>	<b>305 mm Class 3 Aggregate</b>	<b>305 mm Class 3 Aggregate</b>
<b>178 mm Select Granular Material</b>	<b>178 mm Select Granular Material</b>	<b>178 mm Select Granular Material</b>	<b>178 mm Select Granular Material</b>
<b>Clay</b>	<b>Clay</b>	<b>Clay</b>	<b>Clay</b>

Fig. 2. Pavement profiles of cells tested using FWD at MnROAD testing facility. (Adapted from Johnson et al. 2009)

Testing was performed using a trailer-mounted Dynatest model 1000 FWD. The FWD was controlled by an on-site computer that recorded and stored load and deflection data. A 40 kN load was applied by the FWD to a 300-mm-diameter plate in contact with the pavement surface. Surface deflections were measured by nine load transducers located at distances of 0, 0.30, 0.61, 0.91, 1.22, 1.52, and 1.83 meters from the center of the load. FWD tests at each cell were conducted at 200 feet intervals along the mainline alignment, as well as at lateral intervals corresponding to the mid-lane and outer-wheel paths of both the driving and passing lanes.

The measured deflections were used to back-calculate the elastic modulus of the pavement layers using the MODULUS program developed at the Texas Transportation Institute. MODULUS uses linear-elastic theory to back-calculate elastic moduli from FWD data. The back-calculation was based on a four-layer model consisting of asphalt concrete, base course, sub-base and subgrade layers. For the purposes of this analysis, the Class 3 aggregate and select granular material indicated in Fig. 2 were combined as one layer. The Pavement profile and deflection data were provided by the Minnesota Department of Transportation (Mn/DOT). The asphalt surface, base course, and sub-base layers were assigned a Poisson's ratio of 0.35, and the subgrade layer was assigned a Poisson's ratio of 0.40 (Huang 2004).

## RESULTS AND DISCUSSION

### Maximum Deflection of Test Cells

The average maximum elastic deflection and 1-standard deviation of all tests at a given time experienced by each of the four test cells is presented in Fig.3 as a function of time. As the air temperature warms during spring 2009, the gradual increase in deflection can be attributed to an increase in viscosity in the HMA layer and a gradual thawing of the subgrade and subbase layers. The maximum deflection occurs during summer 2009 when air temperature is highest and HMA viscosity is the greatest. The deflection gradually decreases through the fall season as the air temperature drops and the viscosity of the HMA decreases. The deflection recorded during February 2010 is less than 0.1 mm for all test cells, and most likely reflects frozen conditions at the time of testing. Warming temperatures cause the deflection to once again increase during spring 2010 to levels that are comparable in magnitude to deflections experienced during the same time period in 2009.

Overall, Class 5 experienced the greatest elastic maximum deflections, followed by blended RCA/Class 5, RAP, and RCA, respectively. Similar results were reported for small-scale and large-scale tests performed on the same materials by Schaertl (2010) and Son (2010), respectively.

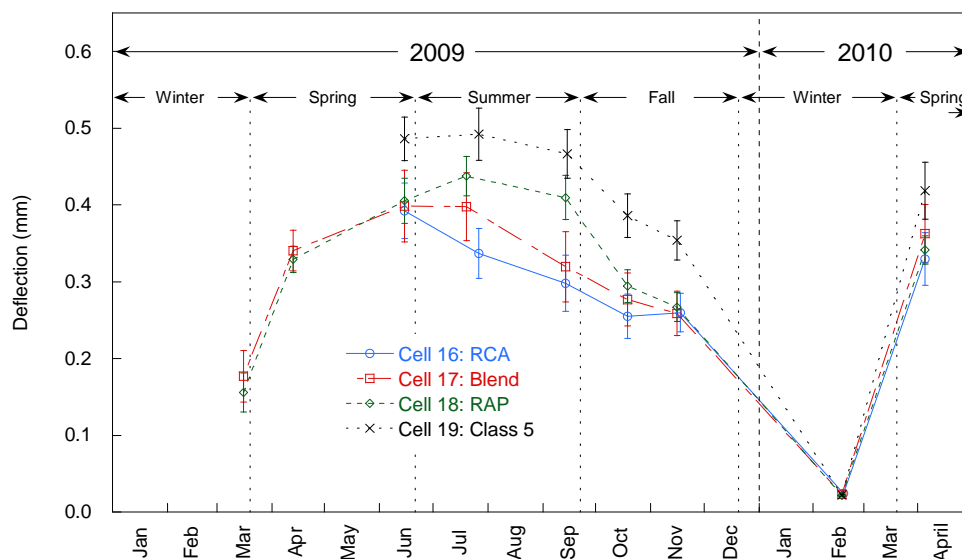


Fig.3. Average center deflection as a function of time for test cells constructed with RAP, RCA, blended RCA/Class 5, and Class 5 base course (error bars represent one standard deviation).

### Resilient Modulus of All Layers

The average resilient moduli of the HMA, base course, subbase and subgrade layers for each of the four test cells is presented in Fig.4 as a function of time. The error

bars represent 1-standard deviation of the resilient modulus data for the given layer and time. The broken line between November 2009 and April 2010 represents a non-continuous transition through a frost-penetration period. Modulus 6.0 was not able to analyze deflection data recorded during March 2009 and February 2010 due to very small deflections recorded, most likely due to frozen conditions. The magnitude of the resilient modulus experienced by the HMA is inversely proportional to the air temperature, gradually decreasing from spring to summer, and gradually increasing from summer to fall. The increased viscosity allows the layer to deflect to a greater degree, resulting in a decrease in stiffness. The base, subbase, and subgrade are not as sensitive to temperature and therefore the resilient moduli of these layers remain relatively constant compared to that of the HMA.

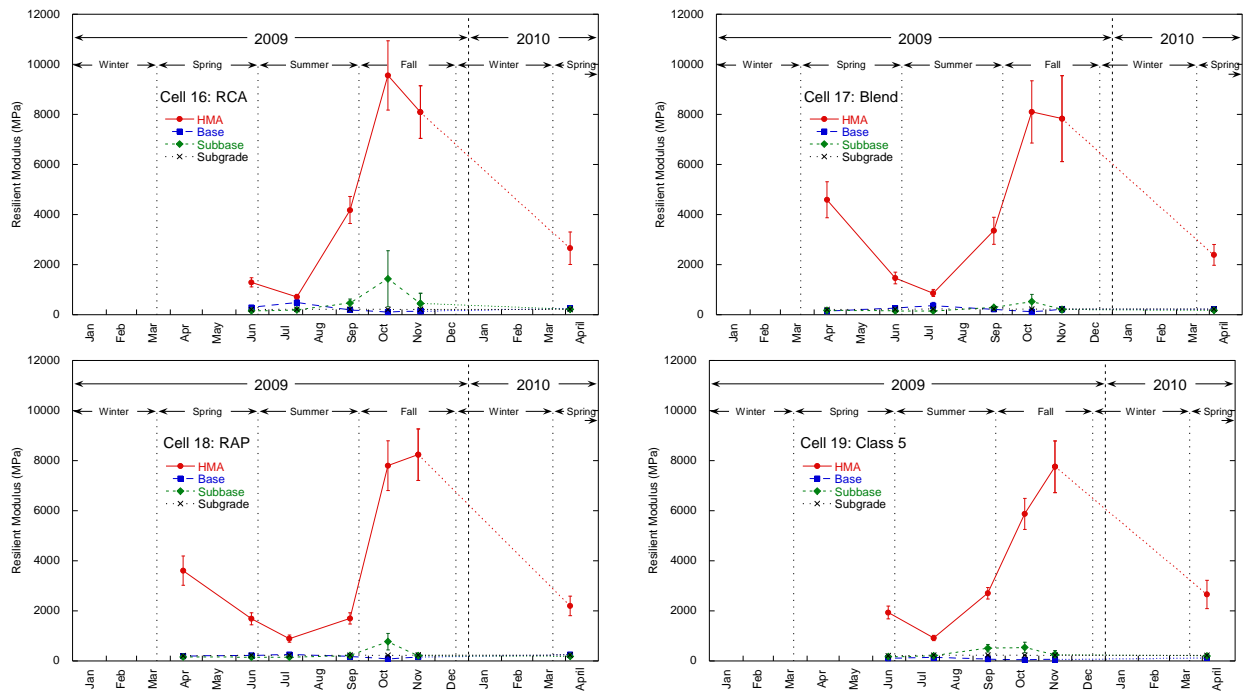


Fig.4. Resilient modulus of HMA, base course, subbase and subgrade as a function of time for test cells constructed with (a) RCA, (b) blended RCA/Class 5, (c) RAP, and (d) Class 5 base course.

### Resilient Modulus of Base Course Layers

The resilient modulus of the base course at the midlane and outer wheel paths of both the driving and passing lanes for the four test cells is presented in Fig.5 as a function of time. The data points represent the average of the resilient moduli calculated along each of the measurement alignments. The dotted line connecting November 2009 to April 2010 represents a non-continuous transition through a frost-penetration period. The resilient modulus was greater at the midlane compared to the outer wheel path. The outer wheel path of both lanes encounters a greater amount of wheel loading, and as a consequence experiences a greater degree of compaction. The increased compaction contributes to a denser particle matrix which increases the

overall stiffness of the material. The trend of the base course resilient modulus over time is the opposite of the trend of the HMA: the base course resilient modulus increases with a decrease in HMA modulus, and the decreases with an increase in HMA modulus. As the HMA becomes stiffer, the underlying base course is exposed to less translated stress and, as a result, less strain.

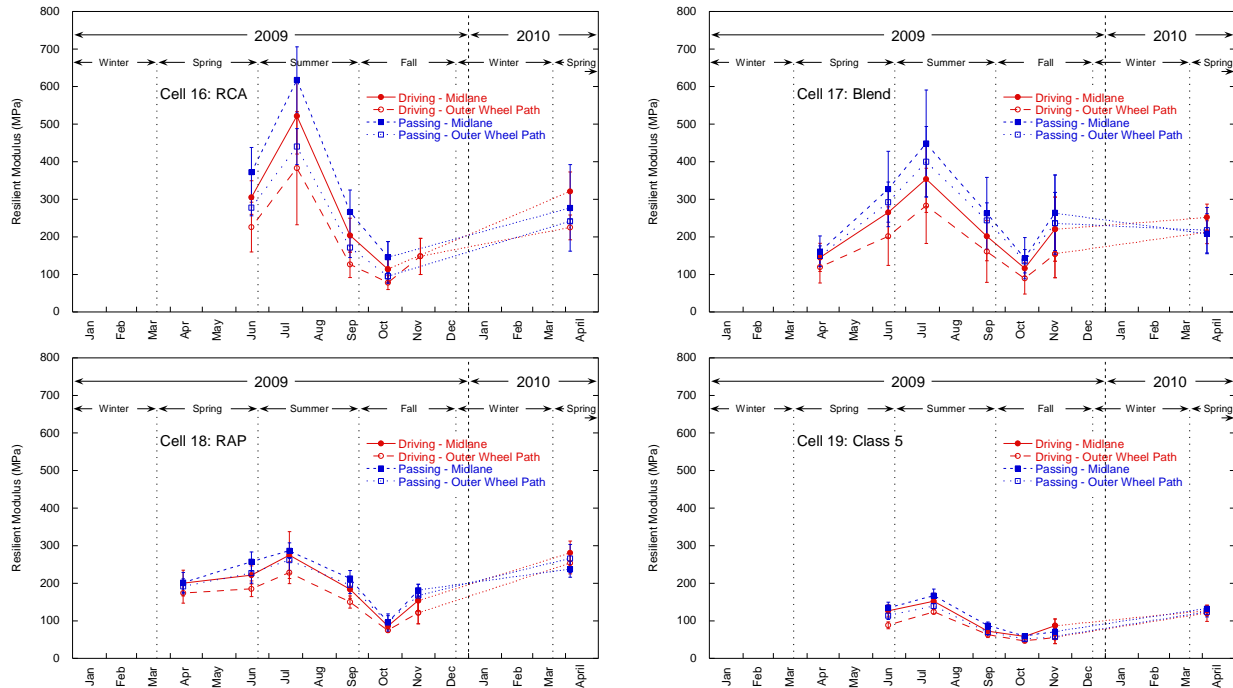


Fig.5. Resilient modulus of base course at the mid-lane and outer-wheel paths of the driving and passing lanes as a function of time for test cells constructed with (a) RCA, (b) blended RCA/Class 5, (c) RAP, and (d) Class 5 base course.

The resilient modulus of the base course at each cell is presented in Fig.6 as a function of time. The resilient modulus from all FWD tests conducted at each cell (varying spatially and temporally) is presented as a box plot in Fig.7. Class 5 had the lowest resilient modulus of the four base course materials tested. Although there was a significant amount of overlap, RCA had the greatest resilient modulus, with blended RCA/Class 5 and RAP having resilient moduli that were comparable in magnitude. The relationship between the magnitudes of the four materials are consistent with the results of small and large-scale laboratory testing conducted by Son (2010) and Schaertl (2010).

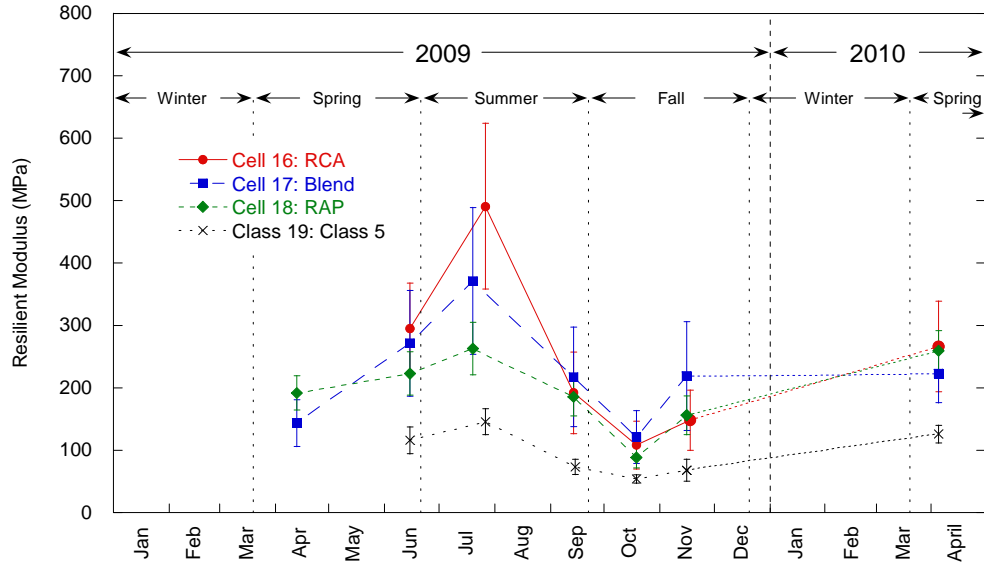


Fig.6. Resilient modulus of base course as a function of time for test cells constructed with RAP, RCA, blended RCA/Class 5, and Class 5 base course (error bars represent one standard deviation).

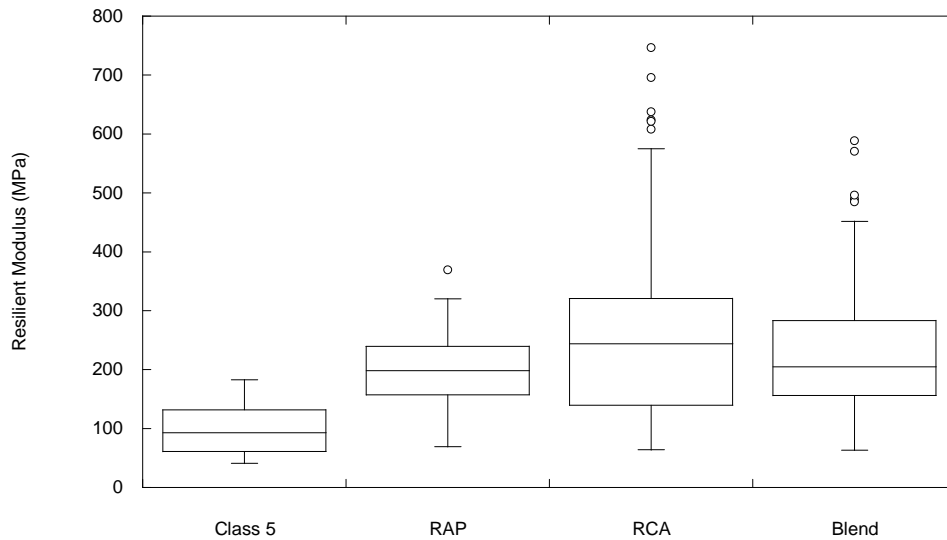


Fig.7. Comprehensive resilient modulus of all tests for cells constructed with RAP, RCA, blended RCA/Class 5, and Class 5 base course.

## CONCLUSION

1. Test cells that incorporated Class 5 as a base course experienced the greatest elastic maximum deflections, followed by blended RCA/Class 5, RAP, and RCA, respectively. An increase in air temperature increases the viscosity of the overlying HMA layers and allows a greater amount of deflection to occur to the

system as a whole. Frozen subgrade contributes to a decrease in deflection during the winter months.

2. The stiffness of the HMA layers decreases during periods of increased temperature due to increased viscosity in the bituminous material. The stiffness of the base, subbase, and subgrade are relatively constant compared to that of the HMA.
3. The resilient modulus was greater at the midlane compared to the outer wheel path due to greater overall loading in these areas. The base course resilient modulus increases with a decrease in HMA modulus and decreases with an increase in HMA modulus. As the HMA becomes stiffer, the underlying base course is exposed to less translated stress and, as a result, less strain.
4. RCA and Class 5 had the highest and lowest resilient moduli, respectively. Blended RCA/Class 5 and RAP had resilient moduli that were comparable in magnitude.

## BIBLIOGRAPHY

- FHWA (2008). "User Guidelines for Byproducts and Secondary Use Materials in Pavement Construction," *FHWA Report FHWA-RD-97-148*, Federal Highway Administration, McLean, Virginia.
- Guthrie, W. S., Cooley, D. and Eggett, D. L. (2007). "Effects of Reclaimed Asphalt Pavement on Mechanical Properties of Base Materials," *Transportation Research Record*, No. 2006, pp. 44-52.
- Johnson, A., Clyne, T. R., and Worel, B. J. (2009). "2008 MnROAD Phase II Construction Report," Minnesota Department of Transportation, Maplewood, Minnesota.
- Kuo S. S., Mahgoub, H. S. and Nazef, A. (2002). "Investigation of Recycled Concrete Made with Limestone Aggregate for a Base Course in Flexible Pavement", *Geomaterials*, No. 1787, pp. 99-108.
- Schaertl, G. J. (2010). "Scaling and Equivalency of Bench-Scale Tests to Field-Scale Conditions," MS Thesis, University of Wisconsin-Madison, Madison, WI.
- Son, Y. H., (2010). "Resilient Moduli of Recycled Materials," Personal Communication.

# **Recycled Unbound Materials**

## **TPF-5 (129) Recycled Unbound Materials**

Mn/DOT Contract No. 89264 Work Order No. 2

CFMS Contract No: B14513

### **Task III: Materials Control**

**Ozlem Bozyurt, Tuncer B. Edil, James Tinjum, and Craig H. Benson**  
**University of Wisconsin- Madison**

**August 2011**



## **1. Introduction**

RCA and RAP/RPM are known to contain impurities that may affect their mechanical properties and long-term performance. These impurities often include soft bituminous materials such as crack sealants as well as pavement markings, metallic objects and other potentially deleterious materials. Thus, a testing program is conducted to assess how impurity type and content affect the resilient modulus and plastic strain of RAP and RCA. This program will be conducted in two parts.

The first part of the testing program consists of identifying the types and amounts of impurities present in RCA and RAP/RPM. This is accomplished by carefully segregating and identifying the components of each of the samples of RCA and RAP/RPM collected. Each component impurity is weighed and described.

The second part of the testing program will consist of a systematic evaluation of the impact of impurities on the properties of RCA and RAP/RPM. Specimens of RCA and RAP/RPM containing varying amounts of impurities will be prepared at optimum compaction conditions and tested using the resilient modulus procedure. Data from these tests will be evaluated to determine how the resilient modulus and plastic strain vary with the type and amount of each impurity. Equations will be developed that describe how the resilient modulus varies with the fraction of each impurity and thresholds will be recommended regarding acceptable levels of each type impurity. Results of this evaluation will be checked by comparison to the field data from the MnROAD test sections.

## **2. Background**

### **2.1. Deleterious Materials (Impurities) in Recycled Materials**

Kuo et al. (2002) reported that impurities (foreign material) present in RCA are one of the biggest concerns surrounding the use of this material in construction. Kuo et al. (2002) investigated the impurities in RCA made with limestone aggregate for a base course in flexible pavement. The amount of impurities was identified by means of visual inspection. Impurities were classified into different categories such as wood chips and paper, plastics, steel, asphalt, and brick. Asphalt was found to be the most predominant type of impurity in the samples. The

average impurity content was 3.67% for RCA and 1.99% for lime stone aggregates, and both of these percentages are considered to be a negligible amount.

RCA for unbound base course shall be free of all materials that fall into the category of solid waste or hazardous materials defined by AASHTO (AASHTO Designation M 319-02) (2006). Additionally, RCA should not contain more than 5% bituminous concrete materials by mass and 5% brick by mass. AASHTO (2006) also suggests that the engineer might select stockpiling as an approach to assist in qualitatively identifying the presence of deleterious materials. Stockpiling conditions of recycled materials plays an important role in qualitatively assessing the uniformity of the materials. Even though AASHTO (2006) defines mean percentages of impurities, they still mentioned that during the construction, the engineers may make some adjustments on the amount of impurities without impacting the performance of the base course. However, visual examination of the material may not be helpful in determining the detrimental amount of wood chips or brick materials in recycled materials. Therefore, additional research or study will be important in establishing the acceptable amount of deleterious materials for recycled materials.

The Greenbook specification for construction materials (CMB) allows 3% brick by weight (GREENBOOK, 2009). The deleterious material content should not comprise a detrimental quantity as defined in section 200-1.1. Various deleterious materials have different weights (i.e., wood chips are lighter than brick, plastic are lighter than small piece of wire meshes etc.). Wire mesh, plastics, brick would be degraded less than sticks or pieces of wood, which would than leave voids in the base layer causing possible failures in the pavement. For the concrete production, the amount of deleterious material is defined with many different specifications, but for unbound recycled base materials, there is not enough specification defining the effect of impurities.

The impact of impurities on the properties of RAP and RCA should be evaluated to determine how the resilient modulus and plastic strain vary with the type and amount of each impurity. After finding the variation of resilient modulus with the fraction of each impurity, thresholds could be recommended regarding acceptable levels of each type of impurity.

### 3. Materials and Methods:

#### 3.1. Materials

Sixteen recycled materials, one conventional base course, and one blended recycled/conventional material were used in this investigation. Seven of the recycled materials were recycled asphalt pavement (RAP), six were recycled concrete aggregate (RCA), and two were recycled pavement materials (RPM). The recycled materials used in this study were obtained from a wide geographical area, covering eight different states: California, Colorado, Michigan, Minnesota, New Jersey, Ohio, Texas and Wisconsin (**Error! Reference source not found.**). The materials named according to the origin of the materials. The reference base course was a gravel meeting the Class 5 aggregate specifications for base course in Minnesota per the Minnesota Department of Transportation (MnDOT). Class 5 aggregate is formed by quartz, granite and carbonates (limestone and dolomite). The ratio of quartz/granite to carbonates is 2.1. The percentage of mineral type in Class 5 aggregate is 68 % for Quartz/Granite and 32 % for Carbonates. Percent quartz/granite (aggregate and concrete) and percent carbonate of gravel (aggregate and concrete) of gravel are 43% and 20%, respectively. The blend (MN) was a mix of approximately equal parts (by mass) RCA from MnDOT (50%) and Class 5 aggregate (50%). The Class 5 aggregate was used as the control in this study.

The material from MnDOT was obtained during construction of roadway cells at the MnROAD test facility in Maplewood, Minnesota for investigation of the field behavior. The RAP was milled from the surface of roadway cells that were previously constructed at the MnROAD test facility. The RCA was obtained from a stockpile maintained by the Knife River Corporation at their pit located at 7979 State Highway 25 NE in Monticello, Minnesota.

The RAP from the Ohio Department of Transportation (ODOT) came from an existing asphalt pavement, processed through a portable plant, and stored in approximately 2268 Mg stockpiles. The Ohio RCA is from a 1.2-m-high barrier wall that existed between the north- and south-bound lanes of State Route 315 in downtown Columbus, Ohio. The broken-up concrete was taken from the project to a portable processing plant, crushed, sized, and stockpiled. The material for this project came from stockpiles of approximately 9071 Mg. The RCA samples provided were 100% RCA.

The material received from the Colorado DOT was collected from over 500 demolition sites from curb, gutter, sidewalk, highways, high-rise buildings, and housing foundations.

Although the concrete came from varied sources, the aggregates for the production of the concrete originated from rock in Colorado, most from the quarries in Morrison and Golden and some aggregates were sourced from the Platte River.

The material provided by the New Jersey DOT (NJ DOT) is from stockpiles for demolition projects, primarily in New Jersey. The material in the stockpiles is in flux since NJ DOT constantly adds new loads and removes content for different purposes.

The RAP from California DOT is a combination of roadway millings and waste from an HMA plant (discharge from warm up and cleaning processes). The RCA is broken concrete rubble from the demolition of structures. Stockpiling in California is usually done three times a year. These stockpiles are not added to throughout their life-cycle. If stockpiled material is still unavailable during visits from subcontractors, new material is used to create a new stockpile.

The RCA sent by the Texas DOT is from a commercial source; therefore, the individual sources of aggregate or material characteristics included in the RCA are not known. The Texas RAP is from a highway project where the contractor milled the "binder" course after approximately 1.5 years of service. The RAP 1 from Michigan was provided by the Michigan DOT and is from highway reconstruction projects.

A summary of the grain characteristics and classifications for the seventeen materials is shown in **Error! Reference source not found.** The materials used in this study are classified as non-plastic per the Unified Soil Classification System (USCS). The Class 5 aggregate is classified as well-graded gravel (GW-GM) per the USCS (ASTM D 2487) and A-1-b per the AASHTO Soil Classification System (ASTM D 3282). The blended RCA/Class 5 is classified as A-1-b according to ASTM D 3282 and as poorly graded sand (SP) according to ASTM D 2487. The samples of RCA range from an SP to a well-graded gravel (GW) classification via USCS and A-1-a or b for AASHTO. The various RAPs and RPMs classify as SP, SW, or GW, whereas their AASHTO classifications are A-1-a or b. All materials are coarse-grained granular materials with fines contents mostly less than 7% except Class 5 aggregate and one RCA sample.

The particle size distribution (PSD) curves were determined according to ASTM D 422. Samples were wet-sieved through a No. 200 (75- $\mu\text{m}$  opening) sieve to separate the fine particles attached to the coarser aggregates. The PSDs for the RCA and the RAP/RPM samples are shown in Fig. 2 and Fig. 3 respectively, along with the upper and lower bounds from the literature.

### **3.2. Methods:**

#### **3.2.1. Impurity Test:**

Impurities are one of the biggest concerns surrounding the use of the recycled materials in construction (Kuo et al., 2002). To determine the amount of impurities, 15 kg from each sample defined in Section 3.1 were air dried and passed through sieves to separate the aggregates into different sizes to facilitate the removal of impurities. Impurities collected visually from each sieve were weighed and described. Impurities were classified into different categories. For RAP, the types of impurities are pavement markings, metallic objects, wood chips, plastic objects and glass materials and for RCA, metallic objects, wood chips, asphalt aggregates, aggregates with plastic fibers, plastic objects, and glass and geotextile materials.

### **4. Results and Analysis:**

#### **4.1. Impurity Test:**

Deleterious materials were classified into different categories such as wood chips, glass, geotextiles, steel, and asphalt aggregate, aggregate with plastic fibers, and sea shells, and the percentage by weight of the deleterious materials present in RCA, RAP/RPM and Class 5 aggregate is summarized in Table 1 and plotted in Fig. 4. Asphalt aggregates and aggregate with plastic fibers are heavier than the wood chips, sea shells and geotextile materials; therefore their percentage by weight is high.

The amount of deleterious materials present in RCA and RAP/RPM varied amongst the source of the materials (Fig. 5). Even though, RCA had higher amount of deleterious materials compared to RAP/RPM, the source of RCA affected the occurrence of deleterious materials. These differences may be related to the production process or stockpiling conditions of RCA. Generally, asphalt aggregate, aggregate with plastic fibers, and wood chips were the most predominant type of impurities for RCA (Fig. 6). As shown in Fig. 7, the average impurity content was 1% for RCAs obtained from different states (CO, OH, TX, MN, CA, MI, WI, and NJ). Kuo et al. (2002) investigated the impurities in RCA made with limestone aggregate for a base course in flexible pavement. The amount of impurities was identified by means of visual inspection. Impurities were classified into different categories such as wood chips and paper,

plastic, steel, asphalt, and brick. Asphalt was found to be the most predominant type of impurity in the samples. The average impurity content was 3.67% for RCA and 1.99% for limestone aggregate, which are higher than determined in this study covering a larger range of RCA covering a broader geographic distribution. This may be reflective of the improvements in recycling processes in more recent years minimizing the impurities. Kuo et al. (2002) considered their percentages to be negligible.

Geotextiles and pavement markings were the predominant type of impurities for RAP/RPM (Appendix C). The average impurity amount was 2% for all RAP/RPM samples from different states (CO, OH, TX, MN, CA, MI, WI, and NJ) (Fig. 8). During the production of RAP/RPM, some extraneous content may be mixed into the recycled material, such as pavement markings or wood chips from the environment around the road. The stockpiling conditions of the recycled material also could create additional impurities (Bozyurt 2011).

## **5. Summary and Conclusions:**

The amount of deleterious materials present in RCA and RAP/RPM varied amongst the source of the materials. Generally, asphalt aggregate, aggregate with plastic fibers, and wood chips were the most predominant type of impurities for RCA. The average impurity content was 1% for RCAs obtained from different states (CO, OH, TX, MN, CA, MI, WI, and NJ). Geotextiles and pavement markings were the predominant type of impurities for RAP/RPM. The average impurity amount was 2% for all RAP/RPM samples from different states (CO, OH, TX, MN, CA, MI, WI, and NJ).

The production of RCA and RAP/RPM involves the removal and reprocessing of existing asphalt pavement from roadway structures. During the removable process of asphalt pavement, some additional materials were mixing to the recycling materials, such as wood chips from the nature around the road or the pavement markings. Even though the majority of the recycled materials is recycled and used in the same year, some of them were stockpiled in order to use in long terms. The stockpiling conditions of the recycled materials also could create additional impurities. The second part for this testing program, mentioned in the introduction, will be finalized to find the allowable limit of impurities in RCA and RAP/RPM materials.

**TABLES**

Table 1. Index properties for Recycled Materials and Class 5 aggregate

Material	States	D <sub>10</sub> (mm)	D <sub>30</sub> (mm)	D <sub>50</sub> (mm)	D <sub>60</sub> (mm)	C <sub>u</sub>	C <sub>c</sub>	G <sub>s</sub>	Absorption (%)	Asphalt Content /Mortar Content (%)	Impurities (%)	Gravel (%)	Sand (%)	Fines (%)	USCS	AASHTO
Class 5 Aggregate	MN	0.1	0.4	1.0	1.7	21	1.4	2.57	—	—	0.25	22.9	67.6	9.5	GW-GM	A-1-b
Blend	MN	0.2	0.6	1.5	2.8	13	0.5	—	—	—	0.36	32.7	63.8	3.4	SP	A-1-b
RCA	MN	0.1	0.4	1.0	1.7	21	1.4	2.39	5.0	55	0.87	31.8	64.9	3.3	SW	A-1-a
	MI	0.4	4.1	9.7	12.3	35	3.9	2.37	5.4	—	0.35	68.5	28.3	3.2	GP	A-1-a
	CO	0.1	0.6	2.8	4.9	66	1.1	2.28	5.8	47	0.26	40.9	46.3	12.8	SC	A-1-b
	CA	0.3	1.7	4.8	6.8	22	1.4	2.32	5.0	37	0.26	50.6	47.1	2.3	GW	A-1-a
	TX	0.4	6.5	13.3	16.3	38	6.0	2.27	5.5	45	0.86	76.3	21.6	2.1	GW	A-1-a
	OH	0.2	1.2	3.4	5.3	34	1.7	2.24	6.5	65	0.16	43.2	49.5	7.3	SW-SM	A-1-a
	NJ	0.2	0.5	2.0	5.1	28	0.3	2.31	5.4	—	1.67	41.2	54.6	4.3	SP	A-1-b
RAP	MN	0.3	0.7	1.6	2.3	7	0.7	2.41	1.8	7.1	0.06	26.3	71.2	2.5	SP	A-1-a
	CO	0.4	0.9	2.2	3.3	9	0.7	2.23	3.0	5.9	0.09	31.7	67.7	0.7	SP	A-1-a
	CA	0.3	1.3	3.0	4.2	13	1.2	2.56	2.0	5.7	0.33	36.8	61.4	1.8	SW	A-1-a
	TX	0.7	2.5	5.4	7.9	11	1.1	2.34	1.3	4.7	0.05	41.0	44.9	1.0	SW	A-1-a
	OH	0.5	1.6	2.9	3.8	7	1.3	2.43	0.6	6.2	0.06	32.1	66.2	1.7	SW	A-1-a
	NJ	1.0	2.8	4.9	5.9	6	1.3	2.37	2.1	5.2	0.48	50.9	48.4	0.7	GW	A-1-a
	WI	0.6	1.4	2.7	3.6	6	0.9	2.37	1.5	6.2	0.08	30.9	68.5	0.5	SP	A-1-b
RPM	NJ	0.5	2.1	5.8	8.7	18	1.0	2.35	2.6	4.3	0.04	55.7	43.6	0.6	GW	A-1-b
	MI	0.4	1.7	4.6	6.5	17	1.1	2.39	1.7	5.3	0.13	49.3	50.4	0.4	SW	A-1-b

Note: Asphalt Content found for RAP/RPM and Mortar Content found for available RCA

C<sub>u</sub> = coefficient of uniformity, C<sub>c</sub> = coefficient of curvature, G<sub>s</sub> = Specific Gravity, AC = Asphalt Content, Abs = Absorption, Note: Particle size analysis conducted following ASTM D 422, G<sub>s</sub> determined by ASTM D 854, Absorption of coarse aggregate were determined by ASTM C127-07, USCS classification determined by ASTM D 2487, AASHTO classification determined by ASTM D 3282, asphalt content determined by ASTM D 6307



## FIGURES

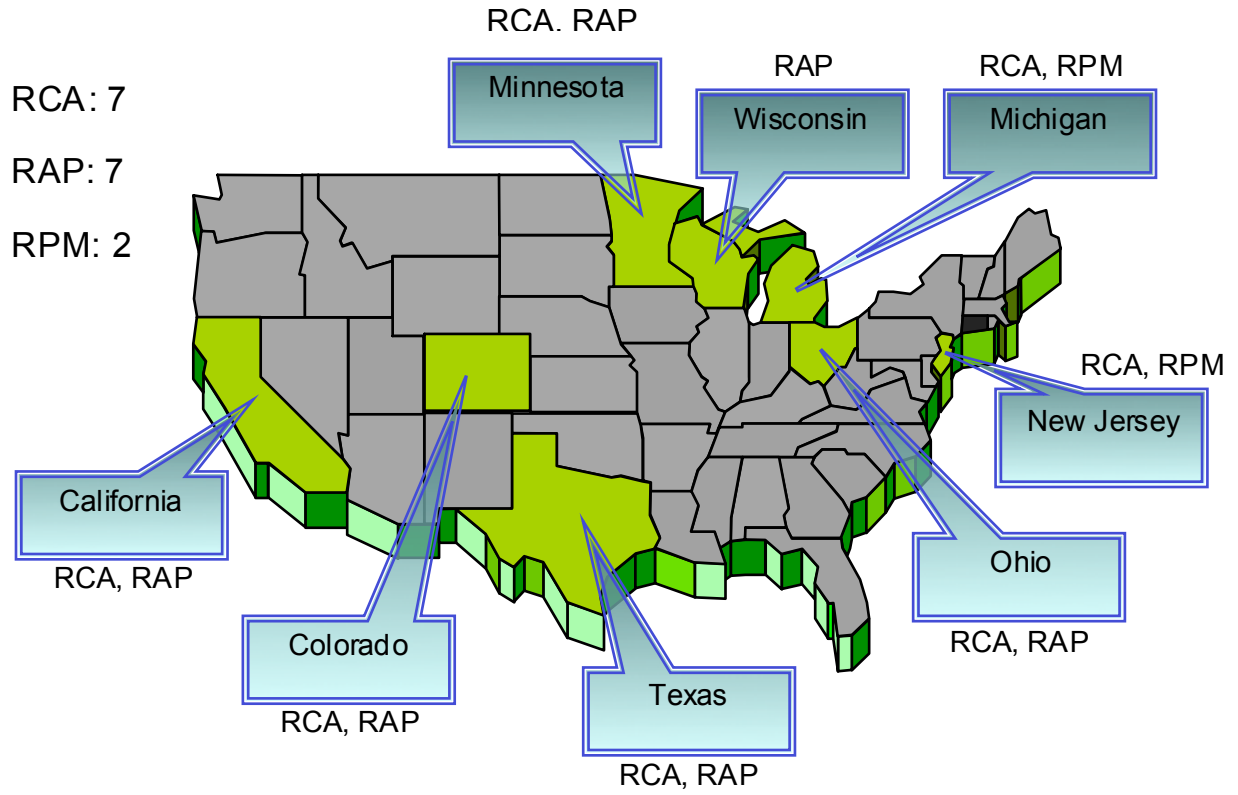


Fig. 1. Locations of recycled material used in this study

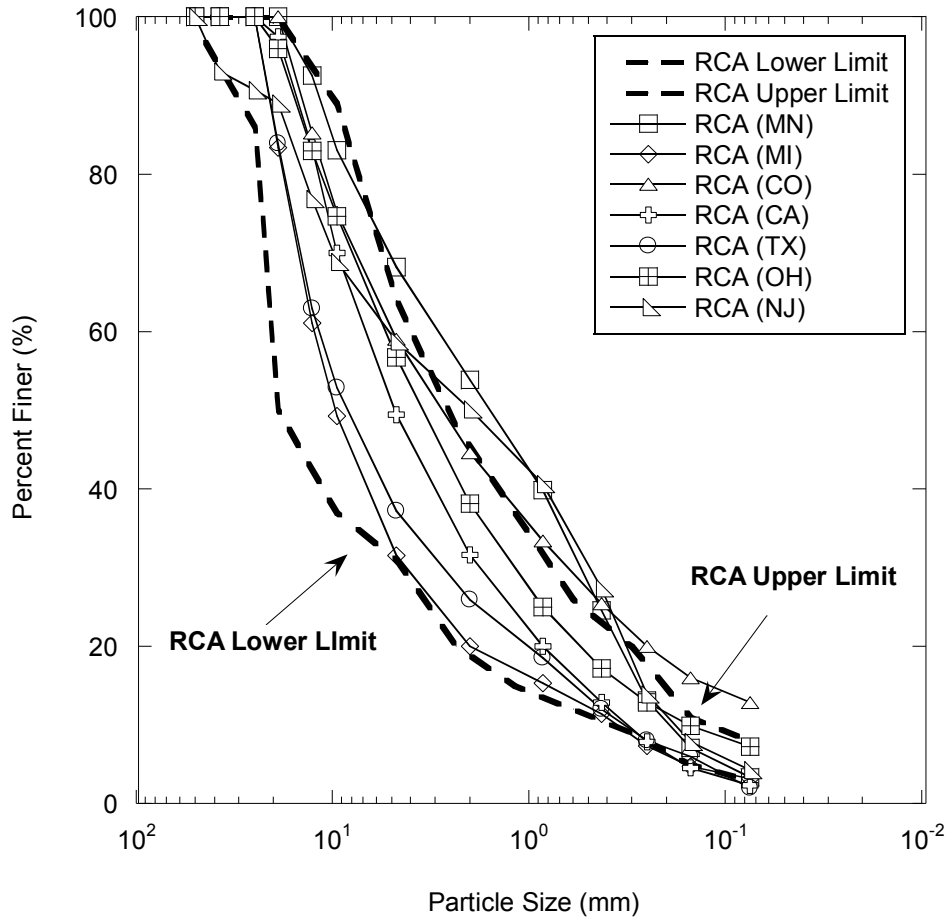


Fig. 2. Particle Size Distribution for RCA and RCAs reported lower and upper limits from literature

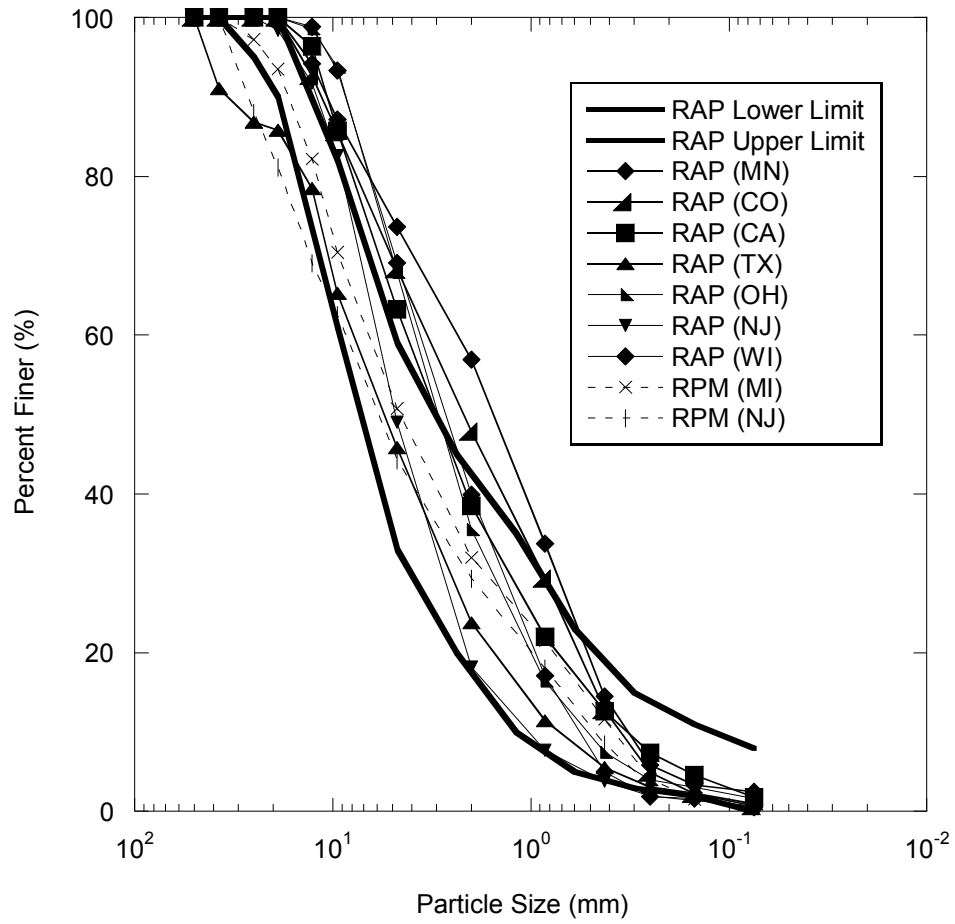
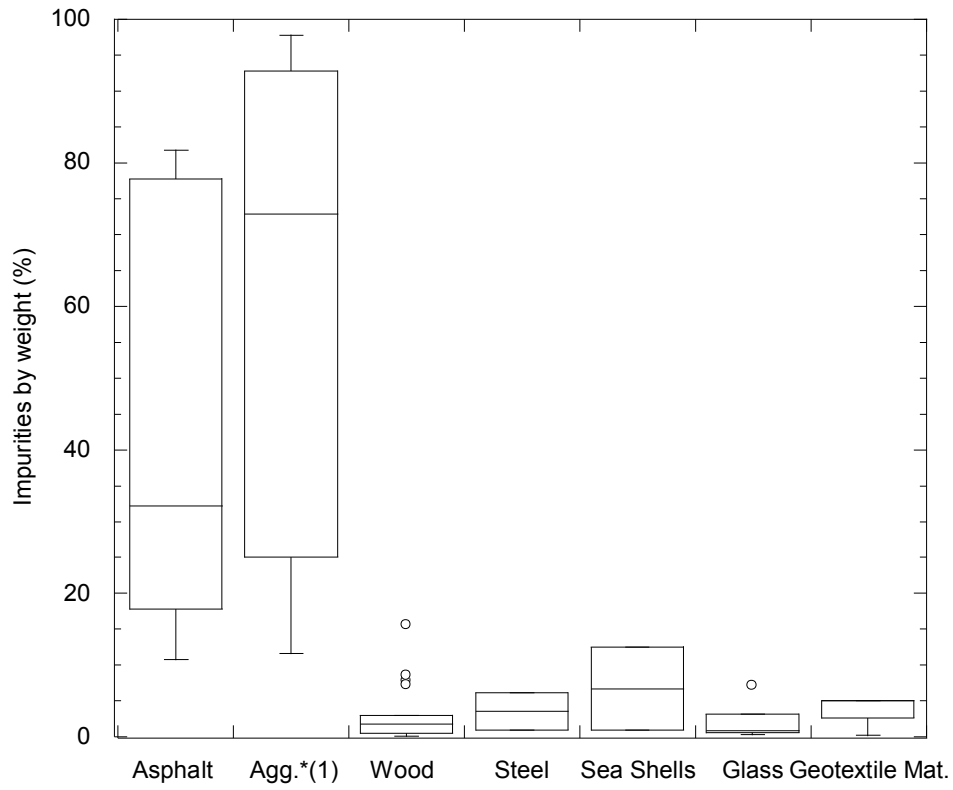


Fig. 3. Particle Size Distribution for RAP/RPM and RAPs reported lower and upper limits from literature



\*(1): Aggregates with plastic fibers

Fig. 4. Distribution of impurities by weight percentage

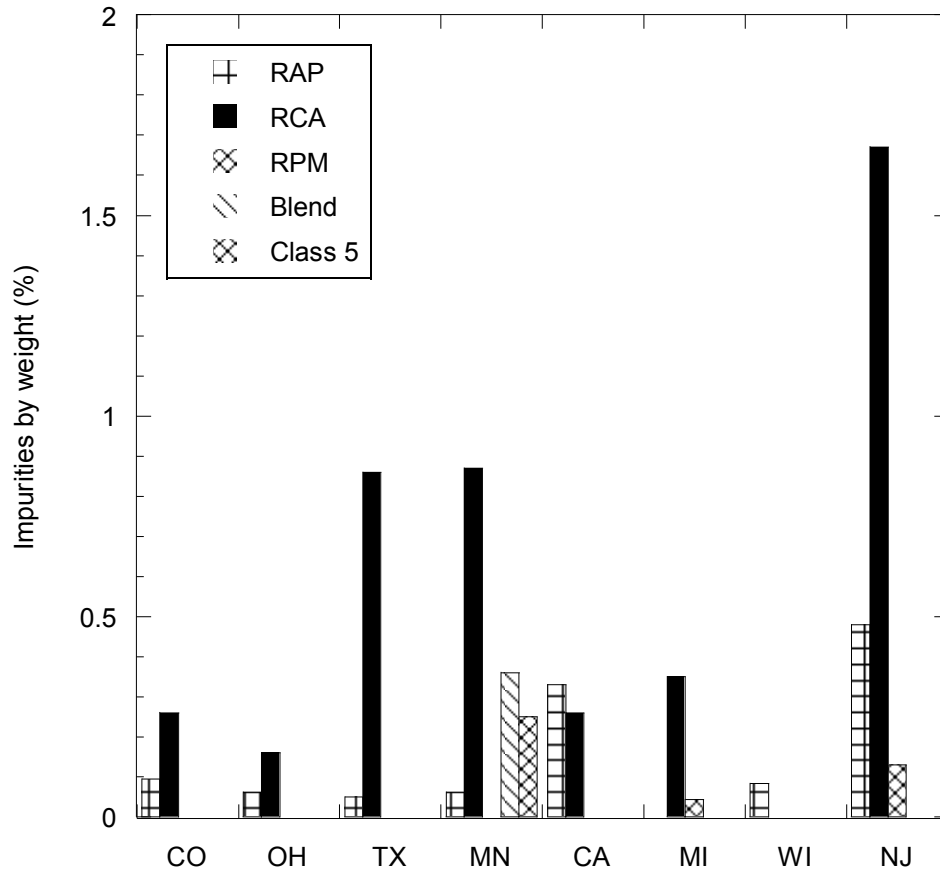


Fig. 5. Percent impurities found in recycled materials from different states



Fig. 6. Deleterious materials found in RCA: Sea shells and Steel

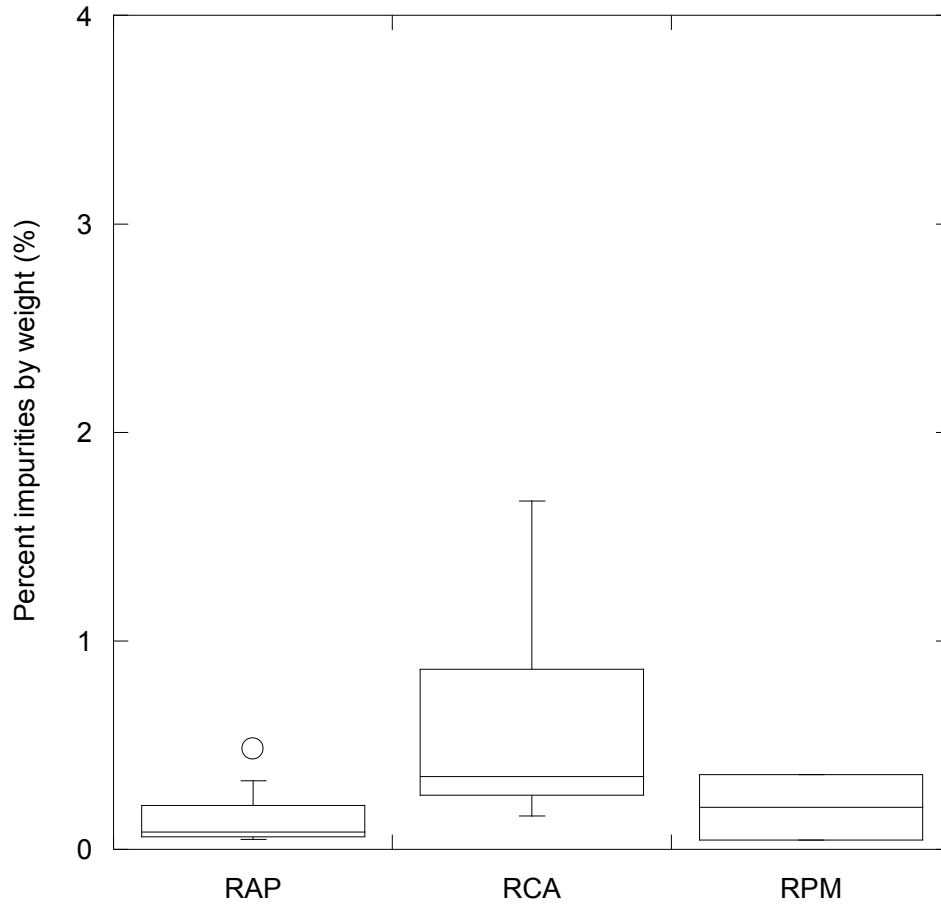


Fig. 7. Average percentage impurities by weight for recycled materials





Fig. 8. Deleterious materials found in RAP: Pavement markings and wood chips

## REFERENCES

- AASHTO (2006). "Standard Specification for Reclaimed Concrete Aggregate for Unbound Soil-Aggregate Base Course." Washington, D.C.
- Bozyurt (2011). "Behavior of Recycled Asphalt Pavement and Recycled Concrete Aggregate as Unbound Road Base." MS thesis, University of Wisconsin, Madison, WI.
- GREENBOOK (2009). "Construction Materials, Section 200-Rock Materials." *Greenbook Standard Specifications for Public Works Construction*.
- Kuo, S.-S., Mahgoub, H. S., & Nazef, A. (2002). "Investigation of recycled concrete made with limestone aggregate for a base course in flexible pavement." *Transportation Research Record*, No.1787, Washington, D.C., 99-108.

# **Recycled Unbound Materials**

## **TPF-5 (129) Recycled Unbound Materials**

Mn/DOT Contract No. 89264 Work Order No. 2

CFMS Contract No. B14513

### **Task IV: Leaching Characteristics (pH-dependent Leaching of Trace Elements from Recycled Concrete Aggregate)**

**Jiannan Chen, Sabrina Bradshaw, Craig H. Benson, James M Tinjum,  
and Tuncer B. Edil**

**University of Wisconsin- Madison**

**December 2, 2011**

**ABSTRACT:** Recycled concrete aggregate (RCA) has excellent mechanical properties and is often used as base course in pavement construction. However, highly alkaline leachate from RCA has been observed in laboratory studies. The associated high-pH leaching patterns can be of concern, especially when compared to the neutral pH environment observed in actual road sections using RCA as base course. In this study, the pH-dependent leaching concentrations of trace elements copper (Cu) and zinc (Zn) and the oxyanion chromium (Cr) were investigated on unfractionated RCA samples and fractionated RCA samples (i.e., fine particles <0.075 mm, sand-sized particles <4.75 mm and >0.075 mm, and gravel-sized particles <75 mm and >4.75 mm). A pH-buffering plateau was observed between pH 4.9 and 7.0 in the acid neutralization capacity curve. Cu and Zn showed the highest levels of leaching at  $\text{pH} \approx 2$ , and the lowest leaching at  $\text{pH} > 7.5$ . Cr showed the lowest level of leaching between pH 5.0 and 6.5, and higher leaching concentrations towards the acid and alkali directions. The fine particles tended to leach more Cu and Zn than sand- and gravel-sized particles at  $2 < \text{pH} < 13$ , while leaching of Cr from the fine fraction was not elevated except at  $\text{pH} < 2$ .

## INTRODUCTION

Ever-increasing road reconstruction due to aging infrastructure in the United States (U.S.) is causing increased demand for virgin aggregate. The production of virgin aggregate constitutes one of the greatest costs in highway construction. The demand for aggregate in the U.S. increased from 58 million tons in 1900 to 2.3 billion tons in 1996, and is estimated to reach 3.0 billion tons by 2020 (USGS 1997). Additionally, approximately 123 million tons of waste is generated annually from building demolition (FHWA 2004), which adds to the cost of waste handling and disposal. Currently, the construction industry is moving towards beneficial use of recycled waste materials in construction in lieu of virgin aggregate. Specifically, recycled concrete aggregate (RCA) provides excellent mechanical properties (e.g., lower specific gravity, higher resilient modulus, and freeze-thaw durability) for use as base course aggregate in pavement structures (ACPA 2009). Moreover, use of RCA has significant life-cycle benefits, such as reducing greenhouse gas emissions, energy and virgin aggregate consumption, and costs of pavement construction. In the U.S., an average of 140 million tons of RCA is produced annually (ACPA 2008), and at least 41 states recycle concrete pavements (FHWA 2004). However, wise use of recycled materials also requires their safe use. Since RCA is a cement-based material, there are concerns related to potentially elevated leaching patterns due to the inherent high alkalinity of RCA. In practical applications using cement-based material, wide pH ranges  $7.5 \leq \text{pH} \leq 12$  due to both weathering of material and material alkalinity have been observed (Van der Sloot et al. 2008). pH-dependent leaching patterns from contaminated soil and waste materials also have been reported (Dijkstra et al. 2006, Dijkstra et al. 2004 and Engelsen et al. 2010).

In this study, the pH-dependent leaching characteristics of trace metals and minor elements from four samples of RCA collected from a wide geographic area (California, Colorado, Minnesota and Texas) were investigated. The effect of grain size of the RCA on leaching was also considered. Since the chemical constituency and exposed surface area of finer and coarser particles may be different, grain size is expected to strongly influence the leaching of trace metals from RCA. pH-dependent testing along with consideration of grain size is considered to be a more realistic approach for the prediction of metal leaching in a field scenario.

## MATERIALS AND METHODS

pH-dependent batch tests were conducted according to methods outlined in Kosson et al. (2002) using four RCA sources: California (CA), Colorado (CO), Minnesota (MN) and Texas (TX). Physical properties and chemical compositions of the four RCAs are shown in Table 1. One representative sample was taken from each source and homogenized by hand mixing. The representative samples were separated into two specimens: one used to represent the entire sample and the other for grain-size fractioning. The fractionated samples were sieved into three grain-size fractions: fine particles ( $<0.075$  mm), sand-sized particles ( $<4.75$  mm,  $>0.075$  mm), and gravel-sized particles ( $<75$  mm,  $>4.75$  mm). All fractions were then reduced to less than 2 mm-size with a steel jaw crusher (50 mm  $\times$  152 mm opening high Mn-steel jaw crusher by Sturtevant Inc., MA, USA).

The total elemental composition of each RCA specimen was determined by acid digestion according to ASTM D 5198-09. A 1:1 nitric acid digestion of 5 g of solid sample was performed at 90 to 95°C for 2 h. The total carbon (TC), total inorganic carbon (TIC), and total organic carbon (TOC) were determined with a SC144 DR sulfur and carbon analyzer (LECO Inc., St. Joseph, MO, USA). The batch tests were performed with unfractionated (entire) samples and fractionated samples at a liquid to solid ratio of 10:1 by weight. Samples were agitated in an end-over-end tumbler at a speed of 30±2 revolutions per min (rpm). A pH range of 2 to 13 was used for the pH-dependent leaching tests, with target pH of 13, 12, 10.5, 9, 8, 7, 5.5, 4 and 2. A pre-test titration was conducted to determine the contact time to equilibrium and the acid/base addition required for each batch. pH, electrical conductivity (EC), and oxidation-reduction potential (Eh) were determined after testing. The acid neutralization capacity (ANC) curve of each material was also derived from the pH-dependent batch test by the quantity of acid/base addition to each batch and the corresponding final pH reading of the eluate. Development of the ANC is an important step in conducting pH-dependent leaching tests on cement-based materials, since the acid buffering ability of the material will affect the leaching characteristics of the contaminants by both controlling the pH condition and maintaining the integrity of solid matrix when acid attacking (Giampaolo and Mastro 2001).

**Table 1. Physical properties and chemical compositions of RCAs**

<b>Location (State)</b>		CA <sup>1</sup>	CO <sup>2</sup>	MN <sup>1</sup>	TX <sup>3</sup>
<b>Physical properties</b>		<b>Method</b>			
Moisture Content (%)	ASTM D2216	4.5	3.9	3.0	2.1
Optimum Water Content (%)	ASTM D1557	10.9	11.9	11.2	9.2
Max Dry Unit Weight (kN/m <sup>3</sup> )	ASTM D1557	19.8	18.9	19.5	19.7
Specific Gravity	AASHTO T85	2.6	2.6	2.7	2.6
Absorption (%)	AASHTO T85	5.0	5.8	4.9	5.5
<b>Particle size distribution</b>					
75-4.75 mm (wt%)		50.6	40.9	31.8	76.3
4.75-0.075 mm (wt%)	ASTM D2487	47.1	46.3	64.9	21.6
<0.075 mm (wt%)		2.3	12.8	3.3	2.1
<b>Hydraulic Properties</b>					
Hydraulic Conductivity (m/s)	ASTM D5856	1.9×10 <sup>-5</sup>	1.6×10 <sup>-5</sup>	1.8×10 <sup>-5</sup>	7.7×10 <sup>-6</sup>
<b>Chemical composition</b>					
Total Carbon (%)	LECO carbon analyzer	1.9	1.9	1.6	3.2
Total Organic Carbon (%)		1.4	0.3	0.4	0.4
Total Inorganic Carbon (%)		0.5	1.5	1.2	2.8
Copper (Cu) (mg/kg)	ASTM D5198	16.5	10.0	13.6	6.1
Zinc (Zn) (mg/kg)		32.4	58.8	30.4	20.4
Chromium (Cr ) (mg/kg)		20.2	7.5	11.5	8.9
<b>Material pH</b>					
Entire Sample	Accumet	12.1	12.1	11.3	12.0
Gravel-sized Particles	AR50	12.1	12.1	11.6	12.1
Sand-sized Particles	pH meter	11.9	11.9	11.2	11.7
Fines Particles		11.9	11.8	10.9	11.1

Note: <sup>1</sup>Stockpile of single demolition, <sup>2</sup>Various demolitions, <sup>3</sup>Commercial source with special aggregate and material characteristics.

All Samples were then filtered using 0.45- $\mu$ m filter paper, preserved with nitric acid, and stored at 4°C. Trace elemental concentrations and oxyanion concentrations in the eluate were determined with inductively coupled plasma optical emission spectrometry (ICP-OES, Vista-MPX CCD Simultaneous ICP-OES, Varian Inc., CA, US). Two trace elements, Cu and Zn, were chosen to be evaluated in this study because acid digestion showed Cu and Zn to be the most concentrated trace elements in the RCAs (Table 1). One oxyanion, Cr, was chosen for analysis because previous leaching studies (Sadecki et al. 1996, Engelsen et al. 2006) showed relatively high Cr released concentration from RCA.

## RESULTS AND DISCUSSIONS

### Acid Neutralization Capacity – Acid/Base Addition and pH

Figure 1 shows the ANC curve of the unfractionated (entire) RCA samples and their fractionated subsets. Negative values in Figure 1 represent base additions. pH data from the ANC for fractionated RCA and unfractionated RCA are shown in Table 1. The material pH (no acid or base added) of the RCAs ranged from 11.3 to 12.1, with CA, CO, and TX RCA having similar pH, and relatively low pH from MN RCA. Similar ANC curves were observed for CO, TX, and MN RCA – rapid drop of pH followed by a plateau around pH 4.9 to 7.0. Garrabrants et al. (2004) concluded that the plateau in the ANC can be explained by dissolution of calcium carbonate (carbonation) in concrete, which is caused by a reaction between portlandite and calcium silicate hydrate with carbon dioxide from the environment. Carbonation conditions may occur during the concrete service life and in stockpile storage. In comparison, the CA RCA showed a pH plateau that was less obvious. The TIC results showed that the CA RCA had much less inorganic carbon (0.4% of mass) compared with the CO RCA (1.5% by mass), TX RCA (2.7% by mass), and MN RCA (1.2% by mass).

The gravel-sized and sand-sized particles (87.2% to 97.8% of total RCA mass fraction) presented an ANC curve similar to the unfractionated RCA. Moreover, the gravel-sized particles had higher material pH (11.5 to 12.1) than sand particles (11.1 to 11.9) and fine particles (10.9 to 11.8), and likely control the pH of the bulk (unfractionated) pH (11.3 to 12.1). Carbonation is the most probable reason for this pH difference among fractions, since all fractions are sourced from the same monolithic concrete and treated using the same procedure. Carbonation begins on the surface of the concrete and slowly penetrates the interior of the concrete (Houst and Wittmann 2002 and Garrabrants et al. 2004). After crushing, the fines have a much higher surface area than gravel-sized particles, which results in more reactive surface for carbonation, consuming more cement and leading to a lower material pH. The higher carbonation degree in the fines can also be shown by comparing the ANC curve of the fine fraction with the other fractions. The fines fraction had a higher resistance of acid attack than other fractions. In general, the acid neutralization capacity decreased as the particle size increased.

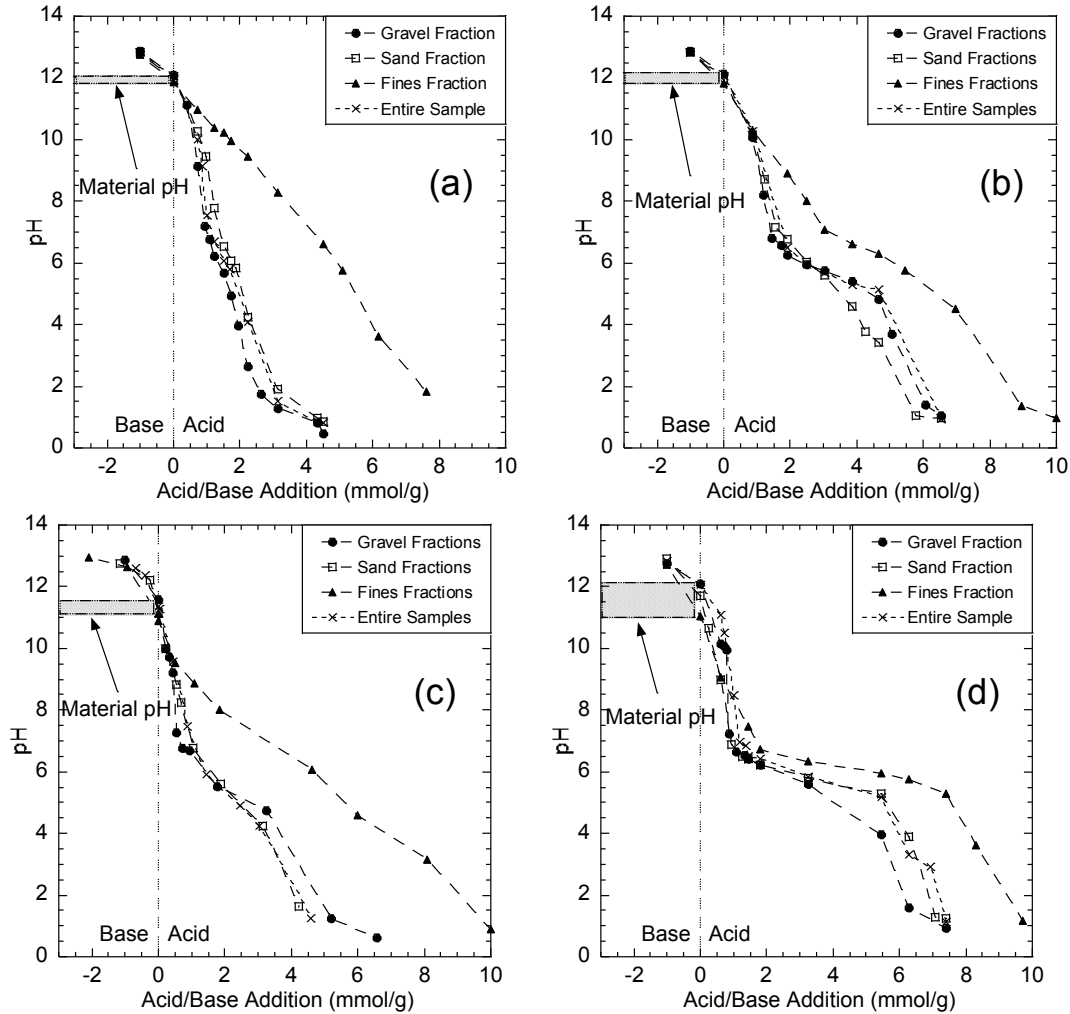


Figure 1 ANC curves of (a) CA RCA (b) CO RCA (c) MN RCA (d) TX RCA

### Leaching of Trace Elements Cu and Zn from Recycled Concrete Aggregate

Figure 2 shows pH-dependent leaching of Cu and Zn from the unfractionated RCAs. Cu and Zn showed similar leaching trends, with maximum leached concentrations at  $\text{pH} \approx 2.0$  and minimum leached concentrations at alkaline or near-neutral pH (7.5–13.0). An increase in leaching concentration with decreasing pH was observed for each element, with Cu starting at  $\text{pH} \approx 6.5$  and Zn at  $\text{pH} \approx 7.5$ .

The concentrations of leached Cu and Zn were not directly related to the total elemental content of the RCA (Table 1). CO RCA tended to leach more Cu and Zn than the other RCAs within the pH range of 2.0 to 13.0, even though the total elemental composition had lower quantities of Cu and Zn available to leach compared to the other three RCAs tested. This trend in leaching behavior was also observed in waste material leaching studies performed by Van der Sloot et al. (1997) and Kosson et al. (2002).

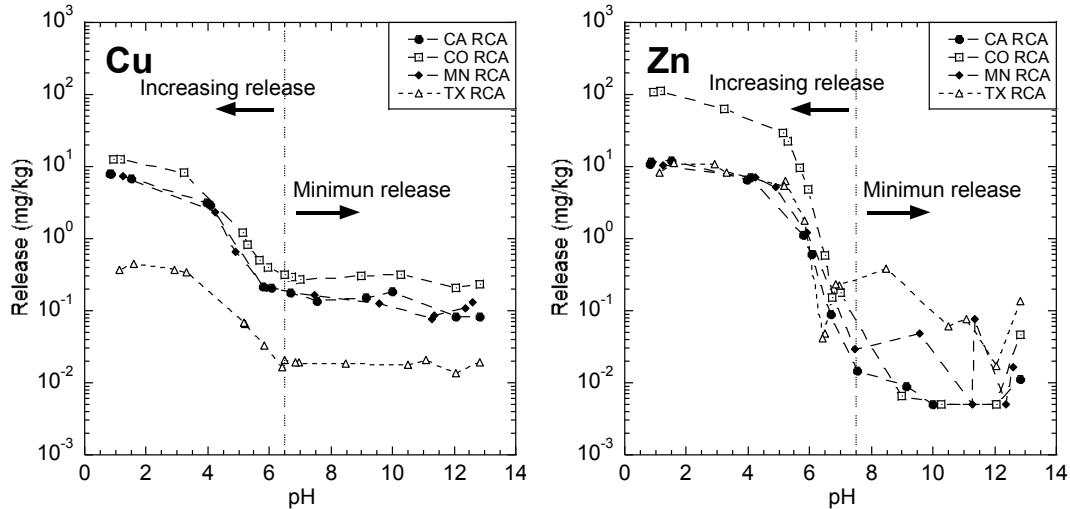


Figure 2 pH-dependent leaching of Cu and Zn from unfractionated RCAs

Figure 3 shows the pH-dependent leaching patterns of Cu and Zn from three fractions. The grain-size specific fractions showed a similar leaching trend for all RCA sources. In the pH range of 2 to 13, fine particles showed a higher leaching concentration than coarser-sized particles, and the leaching was enhanced as particle size decreased. At pH>12, slightly enhanced leaching of Cu and Zn were observed from fines, while gravel-sized particles showed no obvious difference in leaching behavior. Previous studies with field road base have shown that this alkaline effluent usually occurs in the first few flushes from field road base and has been observed in previous studies (Sadecki et al. 1996, Engelsen et al. 2006). At pH typical of field-scale studies (6.5~8.0), leaching of Cu and Zn from smaller sized fractions increased, with the fine fraction having leached concentrations of Cu and Zn up to an order of magnitude higher (MnDOT 2010).

### Leaching of Oxyanion Cr from Recycled Concrete Aggregate

Chromium, which usually forms negative-charge oxyanions (e.g.,  $\text{CrO}_4^{2-}$ ), showed a V-shaped pH leaching pattern. The minimum release of Cr occurred between pH 5.0 and 6.5, and increasing concentrations were observed towards both pH=2 and pH=13. The most acidic region (pH $\approx$ 2) showed higher leaching levels (3.2 to 6.1 mg/kg) relative to the most alkaline region (pH $\approx$ 12) where concentrations were between 0.9 and 1.2 mg/kg (Figure 4). The leaching amount was also independent from the total elemental content. All RCAs showed similar Cr levels at pH $\approx$ 2 and pH $\approx$ 13, while Cr contents in solid samples showed notable differences, ranging from 7.5 to 20.2 mg/kg. Figure 5 shows the various Cr species across the range of pH and Eh conditions (Cornelis et al. 2008). The Eh data of the unfractionated RCAs are also plotted in Figure 5. At high pH (pH>11.0),  $\text{CrO}_4^{2-}$  (hexavalent chromium) is the dominant form of Cr, whereas various tri-valent chromium forms occur at pH<11.0.

A similar V-shaped leaching pattern was also observed among each grain-size fraction (Figure 6). There is no obvious differences in Cr leaching among the three fractions at pH 2.0 to 13.0. Finer particles showed a slightly higher leaching ability than gravel-sized and sand-sized particles at pH<2.



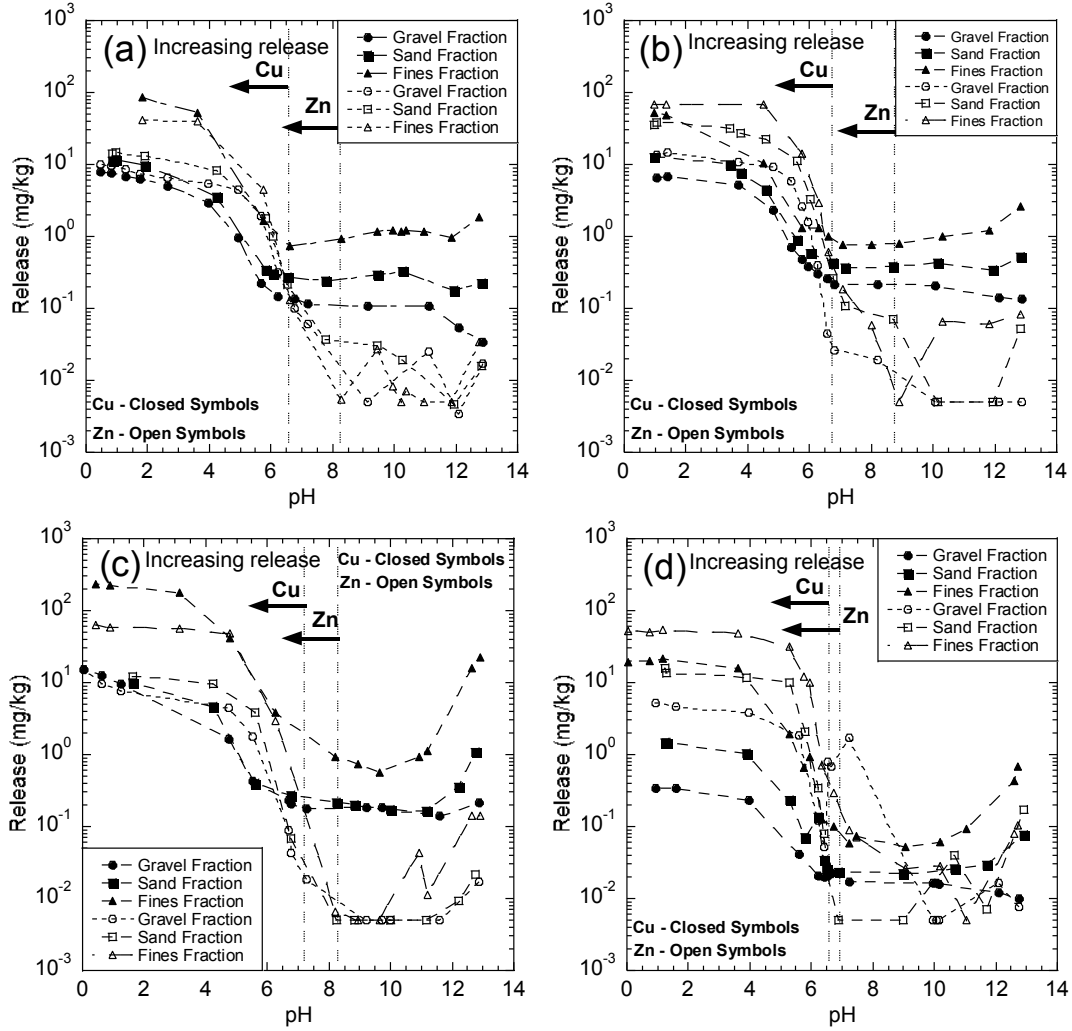


Figure 3 pH-dependent leaching of Cu (closed symbol) and Zn (open symbol) from (a) CA RCA (b) CO RCA (c) MN RCA (d) TX RCA

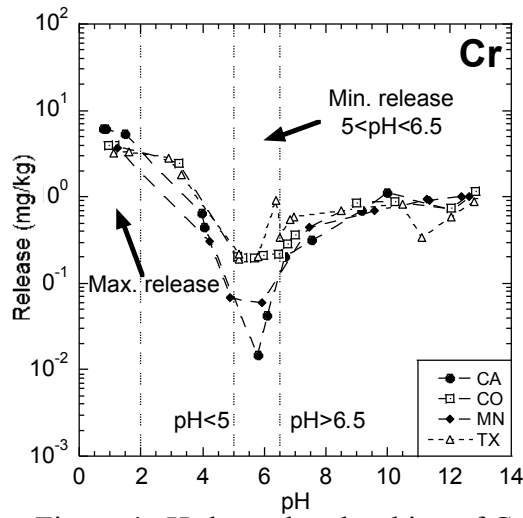


Figure 4 pH-dependent leaching of Cr from four unfractured RCAs

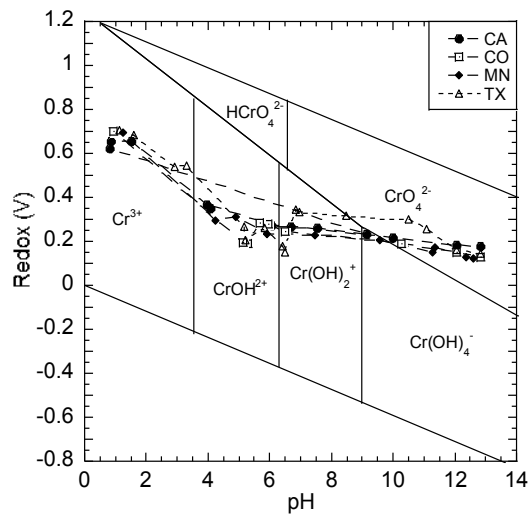


Figure 5 Cr species as a function of pH and Eh (Cornelis et al. 2008)

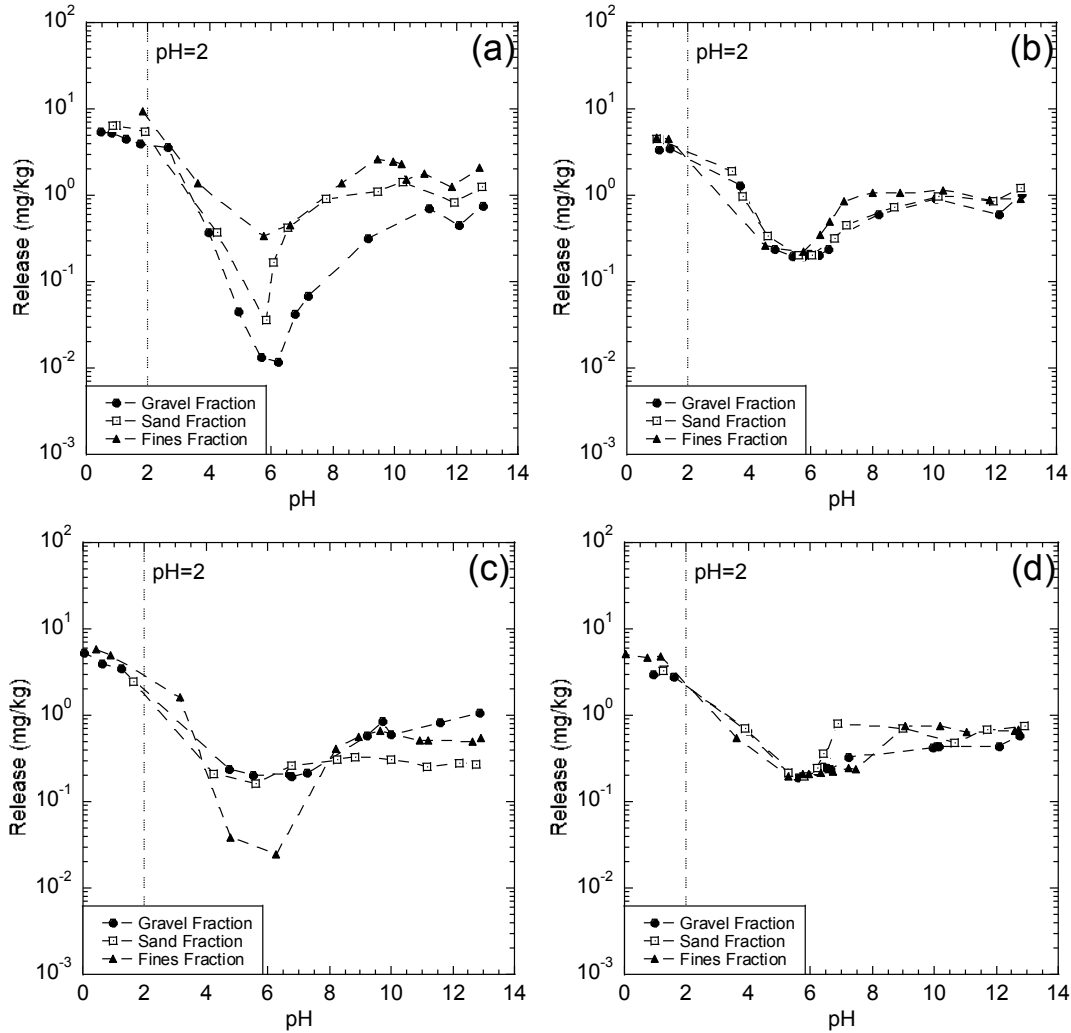


Figure 6 pH-dependent leaching of Cr from fractionated (a) CA RCA (b) CO RCA (c) MN RCA (d) TX RCA

## Discussion

As background to this study, leaching observations were made from both field and lab tests. A field road section using MN RCA as the base course was constructed in a separate, ongoing study, and parallel column tests that used all four RCA sources were conducted. Leachate pH and metal concentrations from the laboratory column tests have been noticeably different from leachate samples collected from a pan lysimeter installed under the RCA base course layer in the field. The column tests and field test results indicate that pH-dependent leaching behavior can occur and be used to interpret the leaching differences. pH from column leaching tests ranged between 11.0 and 12.5 and showed no decline over 100 pore volumes of flow (PVF), while pH of field samples decreased to near neutral and remained between 6.5 and 8.0 after 1.2 PVF and 7 months. Trace elements (Cu and Zn) in the field leachate peaked at 10.3 and 73.3  $\mu\text{g/L}$ , respectively, whereas column test leachate had a maximum Cu and Zn concentration of 10.8  $\mu\text{g/L}$  and 2.4  $\mu\text{g/L}$ . Oxyanion Cr in the field leachate peaked at

16.7 µg/L, compared with oxyanion concentrations of 80.8 µg/L from the column leaching tests (MnDOT 2010).

Finer particle sizes have higher trace metal leaching potential and ANC than gravel-size particles, even though all particles are sourced from the same monolithic concrete. However, given the duration of stockpiled conditions or other exposures to the environment, the chemical composition of each fraction is likely to change. Carbon dioxide exposure and carbonation change the cement hydrate phase, enhancing the leaching of trace elements. Enhanced trace element leaching may be avoided if fine particles of RCA can be minimized along with avoiding exposure to carbon dioxide in stockpile conditions. Moreover, at high pH (pH>12), leaching of Cr(VI) is pronounced and the impact to the environment should be considered.

## CONCLUSIONS

Acid neutralization capacity curves of Colorado, Minnesota and Texas RCA showed significant acid neutralization capacity, while RCA sourced from California had an lower acid neutralization capacity. When RCAs were fractionated (i.e., fine particles <0.075 mm, sand-sized particles <4.75 mm and >0.075 mm, and gravel-sized particles <75 mm and >4.75 mm) finer particles showed a higher acid neutralization capacity than coarser particles. Different leaching patterns of trace elements (Cu and Zn) and the oxyanion (Cr) were observed from the pH-dependent batch tests. Cu and Zn showed highest leaching concentrations at pH≈2 and lowest leaching at pH>7.5. An elevated leaching concentration was also observed for each element at pH 6 to 7.5. Cr showed a V-shaped leaching pattern, with the lowest leaching concentrations occurring between pH 5.0 and 6.5, and higher leaching concentrations in the more acidic and alkaline regions (pH<5 and pH>6.5). Fine particles leached more Cu and Zn than coarser grains at pH 2 to 13. However, the difference in leaching based on grain size alone is relatively small for Cr at pH 2 to 13. When pH<2, finer particles tended to leach more Cr than coarser grains, but this extremely low pH environment is unlikely in any field scenario. pH-dependent tests along with consideration of grain size and leachate pH-Eh states can be used to assess metal leaching in a field scenario.

## REFERENCES

- ACPA (2008). "Concrete - The Environment & Recycling." <http://www.acpa-southwest.org/environ.htm>.
- ACPA (2009). "Recycling Concrete Pavements." American Concrete Pavement Association.
- Cornelis, G., Johnson C. A., Gerven, T. V., Vandecasteele, C. (2008). "Leaching mechanisms of Oxyanionic metalloids and metal species in alkaline solid wastes: a review." *Applied Geochemistry*, 23, 955–975.
- Dijkstra, J. J., Meeussen, J. C. L., Comans, R. N. J. (2004). "Leaching of heavy metals from contaminated soils: an experimental and modeling study." *Environmental Science & Technology*, 38 (16), 4390–4395.

- Dijkstra, J. J., Van der Sloot, H. A., Comans, R. N. J. (2006). "The leaching of major and trace elements from MSWI bottom ash as a function of pH and time." *Applied Geochemistry*, v 21, n 2, 335-351.
- Engelsen, C. J., Van der Sloot, H. A., Petkovic, G., Wibetoe, G., Stoltenberg-Hansson, E., Lund, W. (2006). "Constituent release predictions for recycled aggregates at field site in Norway." *WASCON 2006*, 6th International Conference on the Environmental and Technical Implications of Construction with Alternative Materials, Beograd, Serbia and Montenegro, June 2006.
- Engelsen, C. J., Van der Sloot, H. A., Wibetoe, G., Justnes, H., Lund, W., Stoltenberg - Hansson, E. (2010). "Leaching characterization and geochemical modeling of minor and trace elements released from recycled concrete aggregates." *Cement and Concrete Res.*, 40 (12), 1639-49.
- FHWA (2004). "Recycled Concrete Aggregate – Federal Highway Administration National Review." Federal Highway Administration. Washington, D.C.
- Garrabrants, A. C., Sanchez, F., Kosson, D. S. (2004). "Changes in constituent equilibrium leaching and pore water characteristics of a Portland cement mortar as a result of Carbonation." *Waste Manage.* 24(1), 19–36.
- Giampaolo, C., Mastro, S. Lo. (2000). "Acid neutralization capacity and hydration Behavior of incineration bottom ash-Portland cement mixtures." *Cement Concrete Research.* 32, 769–775.
- Houst, Y. F., Wittmann, F. H. (2002). "Depth profiles of carbonates formed during natural carbonation Original Research Article." *Cement and Concrete Research*, 32 (12), 1923-1930.
- Kosson, D. S., Van der Sloot, H. A., Sanchez, F., Garrabrants, A. C. (2002). "An integrated frame work for reevaluating leaching in waste management and utilization of secondary materials." *Environmental Eng. Sci.* 19, 159–204.
- MnDOT (2010). "Recycled Unbound Materials." Report MN/ No.TPF-5(129), Minnesota DOT, Maplewood.
- Sadecki, R. W., Busacker, G. P., Moxness, K. L., Faruq, K. C., Allen, L. G. (1996). "An Investigation of Water Quality in Runoff from Stockpiles of Salvaged Concrete and Bituminous Paving." Report MN/PR-96/3. Minnesota DOT.
- USGS (1997). "Natural Aggregates – Foundation of America's Future." *USGS Fact Sheet FS*. United States Geological Survey, U.S. Department of the Interior, Washington, D.C. 144-97.
- Van der Sloot, H. A., Heasman, L., Quevauviller, P. (1997). "Harmonisation of leaching/extraction tests." *Elsevier Science B.V.*, Amsterdam.
- Van der Sloot, H. A., Van Zomeren, A., Stenger, R., Schneider, M., Spanka, G., Stoltenberg- Hansson, E., Dath, P. (2008). "Environmental CRiteria for CEMENT based products, Phase I: Ordinary Portland Cements, Phase II: Blended Cement." *ECN-E--08-011*, the Netherlands.